

Selection of Norovirus Aptamers for Food Analytical Applications

Dissertation

zur Erlangung des Doktorgrades

an der Fakultät für Mathematik, Informatik und Naturwissenschaften

Fachbereich Chemie

der Universität Hamburg

Vorgelegt von

Katja Schilling

Hamburg, 2018

Gutachter: Prof. Dr. Ulrich Hahn
Prof. Dr. Bernward Bisping

Datum der Disputation: 22. Februar 2019

Datum der Freigabe zur
Veröffentlichung: 29. März 2019

Prüfungskomitee: Prof. Dr. Ulrich Hahn (Vorsitz)
Prof. Dr. Markus Fischer
Dr. Angelika Paschke-Kratzin

Der praktische Teil dieser Arbeit wurde von Februar 2013 bis Juni 2017 am Gulf Coast Seafood Laboratory der Food and Drug Administration auf Dauphin Island, Alabama, USA absolviert und die Dissertation im folgenden Jahr in Hamburg verfasst. Die Arbeit wurde von Prof. Dr. Ulrich Hahn am Institut für Biochemie und Molekularbiologie des Fachbereichs Chemie der Fakultät für Mathematik, Informatik und Naturwissenschaften der Universität Hamburg betreut.

List of Publications

Published Manuscript

Schilling K., DeGrasse J., Woods J. **The Influence of Food Matrices on Aptamer Selection by SELEX (Systematic Evolution of Ligands by Exponential Enrichment) targeting the Norovirus P-domain.** *Food Chemistry* **2018**, *258*, 129-136.

Manuscript in Preparation

Schilling K., Rodriguez R., Woods J. **Norovirus Aptamers: Target Affinity and Food Analytical Application Suitability.**

First Author Posters

Schilling K., Woods J. (August, 2016) **The Influence of Four Food Matrices on Aptamer Enrichment Targeting the P-domain of Norovirus.** International Association of Food Protection Annual Meeting, St Louis Missouri USA

Schilling K., Woods J. (June, 2016) **Selection of Aptamers against the Norovirus Protruding Domain in Presence of Four Different Food Matrices.** Aptamers in Bordeaux Meeting 2016, Bordeaux France

Schilling K., DeGrasse J., Woods J. (June, 2015) **Aptamer Selection for Extraction of Norovirus from Foods.** American Society of Microbiology Annual Meeting 2015, New Orleans Louisiana USA

Schilling K., DeGrasse J., Woods J. (July, 2014) **Aptamer Selection for Extraction of Norovirus from Foods.** FDA Research Conference, Silver Spring Maryland USA

Second Author Posters

Rodriguez R., Schilling K., Woods J. (July, 2017) **Comparative Study: Extraction and Detection of Enteric Viruses in Soft Fruit.** International Association of Food Protection Annual Meeting, Tampa Florida USA

Woods, J. W., T. Nguyen, K. Schilling, K. R. Calci, and R. Rodriguez. **Multiple enteric viruses detected in breaded oysters associated with illnesses.** Biannual Calicivirus Meeting. Savannah, GA October 2016.

Oral Presentations

Schilling K. (February 18. 2016) **Aptamers for the Norovirus Surface.** CDC in Atlanta, USA

Schilling K. (June 21. 2016) **Aptamers Binding to the Norovirus Surface.** Ifremer in Nantes, France

Table of Content

Table of Content

List of Publications	I
Table of Content	II
Abbreviation List	VIII
Zusammenfassung	XI
Abstract	XIII
1 Theoretical Section	1
1.1 Norovirus.....	1
1.1.1 An Introduction to Norovirus.....	1
1.1.2 Norovirus Genome Organization and Viral Capsid Structure	3
1.1.3 Production of Norovirus Capsid and Capsid Proteins	4
1.1.4 Norovirus Classification and Epidemiology.....	6
1.1.5 Norovirus Environmental Stability and Transmission	8
1.1.6 Norovirus in Oysters.....	9
1.1.7 Current Norovirus Diagnostic Tools, Virus Extraction and Future Challenges.....	11
1.2 Aptamers.....	14
1.2.1 Aptamers and Their Selection by Systematic Evolution of Ligands by Exponential Enrichment (SELEX)	14
1.2.2 Specialized Aptamers and Aptamer Modification	17
1.2.3 Aptamer Structures.....	18
1.2.4 Aptamer Applications	20
1.2.5 Aptamers for Norovirus	22
2 Objective	24
3 Results.....	25
3.1 Production of Aptamer Target for SELEX.....	25
3.1.1 Amplification, Cloning, and Sequencing of P-domain Gene	25
3.1.2 Production, Purification and Identification of P-domain and Control Protein	25
3.2 <i>In vitro</i> Selection of Aptamers for the NoV P-domain	29

Table of Content

3.2.1	SELEX.....	29
3.2.2	Affinity of Enriched Nucleic Acid Pools for the P-domain	33
3.2.3	Sequence Analysis	34
3.3	Identification of P-domain Binding Oligonucleotides	37
3.3.1	Affinity of Selected Oligonucleotides for the Control Protein	37
3.3.2	Affinity of Selected Oligonucleotides for the NoV P-domain.....	37
3.4	Characterization of Aptamer Candidates	39
3.4.1	Determination of Aptamer-Target Selectivity, Affinity and Specificity	39
3.4.2	Structure Analysis of Aptamer Buf-2.....	41
3.5	Aptamer P-domain Binding in Presence of Food Matrices	44
3.6	NoV Aptamers in Comparison	46
3.6.1	Motif Search Between Published Sequences	46
3.6.2	Aptamer Affinity for a Variety of NoV VLPs.....	49
3.6.3	Structure Analysis of Biotinylated and Non-Biotinylated Oligonucleotides Using Circular Dichroism Spectroscopy.....	53
3.7	Aptamer-mediated Dot-Blot for the Detection of NoV VLPs	55
3.8	Aptamer-mediated NoV Pull-down	57
3.8.1	Aptamer-mediated Pull-down for the Extraction of NoV From Buffer	57
3.8.2	Aptamer-mediated Pull-down for the Extraction of NoV From Oyster.....	59
4	Discussion	62
4.1	Aptamer Selection for the Norovirus P-domain.....	62
4.1.1	Negative Selection and Target Suitability.....	62
4.1.2	SELEX Strategy for Comparative Study	63
4.1.3	SELEX in Presence of Food Matrices.....	65
4.1.4	PCR-Bias during SELEX	66
4.1.5	Aptamer Selection for the P-domain in Presence of Oyster Matrix.....	68
4.2	Aptamer Identification and Characterization.....	68
4.2.1	Oligonucleotide Screening and Identification of Aptamer Candidates	68

Table of Content

4.2.2	Structure of Aptamer Buf-2	70
4.3	Aptamer P-domain Binding in the Presence of Food Matrices.....	73
4.4	NoV Aptamers in Comparison.....	76
4.4.1	Motif Search Among Published Norovirus Aptamer Candidates.....	76
4.4.2	Aptamer Affinity for a Variety of NoV VLPs	76
4.4.3	Aptamer Structure Investigation Using Circular Dichroism Spectroscopy	80
4.5	Aptamer-mediated Dot-blot	81
4.6	Aptamer-mediated Norovirus Pull-Down	83
5	Conclusion and Outlook.....	86
6	Experimental Section	89
6.1	Virus Concentration and Extraction.....	89
6.1.1	Virus Concentration and Extraction from Shellfish including Viral RNA Extraction: FDA-Shellfish Method	89
6.1.2	Virus Extraction and RNA Extraction from Clinical Stool Samples.....	90
6.2	Purification of DNA, RNA, and Oligonucleotides Using Commercial Kits	91
6.2.1	DNA Isolation from Agarose Gels.....	91
6.2.2	Purification of PCR Products	91
6.2.3	Purification of Oligonucleotides.....	91
6.2.4	Purification of Single-Stranded Nucleic Acid.....	91
6.2.5	Purification of DNA Post-Cycle-Sequencing Reaction.....	91
6.2.6	Purification of Plasmids from Overnight Culture.....	91
6.3	Nucleic Acid Separation and Detection	92
6.3.1	Agarose Gel Electrophoresis and In-Gel Nucleic Acid Detection with Ethidium Bromide	92
6.3.2	Nucleic Acid Detection Using Autoradiography.....	93
6.4	Nucleic Acid Quantification.....	93
6.4.1	Nucleic Acid Quantification using the NanoDrop	93
6.4.2	Nucleic Acid Quantification using the Qubit [®] -Fluorometer.	93

Table of Content

6.5	Nucleic Acid Amplification, Modification, and Sequencing.....	94
6.5.1	Amplification of VP1 Gene by Reverse Transcriptase PCR.....	94
6.5.2	Amplification of P-domain Gene by PCR	94
6.5.3	Amplification of Nucleic Acid Library During SELEX	95
6.5.4	Multiplex Reverse Transcriptase Real Time PCR Assay for Norovirus.....	95
6.5.5	Amplification of plasmid DNA from Bacterial Colony by PCR	95
6.5.6	Sequencing of VP1 gene PCR product	96
6.5.7	Generation of Single-Stranded Nucleic Acid by Lambda Exonuclease Digestion...	96
6.5.8	Radionuclide End-Labeling of Oligonucleotides	96
6.6	Molecular Cloning and Transformation	97
6.6.1	Cloning and Transformation Using the Champion™ pET Directional TOPO® Kit ...	97
6.6.2	Cloning of PCR Products and Transformation	97
6.6.3	Identification of Colonies Carrying the Recombinant Vector.....	97
6.7	Protein Analytical Methods.....	97
6.7.1	Protein Separation Techniques	97
6.7.2	Protein Separation by SDS PAGE and Subsequent In-Gel Detection.....	98
6.7.3	Protein Separation Using the 2200 Tape Stations.....	98
6.7.4	Dot-blot for Protein Identification.....	98
6.7.5	Protein Identification After In-Gel Trypsin Digestion by LC MS	99
6.7.6	Protein Quantification Using the Qubit Fluorometer.....	99
6.8	Protein Production and Purification.....	99
6.8.1	Production of P-domain in <i>E. coli</i>	99
6.8.2	Production of Control Protein	100
6.8.3	Cell Lysis and Protein Purification	100
6.8.4	Purification of Recombinant Protein.....	100
6.8.5	Protein Dialysis	101
6.9	<i>In vitro</i> Selection of Aptamers for the Norovirus P-domain Produced in <i>E. coli</i>	101
6.9.1	Preparations of Food Matrices for SELEX.....	101

Table of Content

6.9.2	Protein Immobilization on Paramagnetic Particles.....	101
6.9.3	SELEX.....	102
6.10	Identification and Characterization of Aptamers and Oligonucleotides	103
6.10.1	Sequence Abundance and Motif Search.....	103
6.10.2	FRAs to Investigate DNA Protein Interaction.....	104
6.10.3	FRAs to Investigate DNA Protein Interaction in Presence of Food Matrices	104
6.10.4	FRAs to Investigate DNA Protein Interaction in Presence of Competitors	105
6.10.5	FRAs to Investigate Target Binding of Selected NoV Aptamers.....	105
6.11	Analysis of Oligonucleotides Using Circular Dichroism Spectroscopy	106
6.12	Aptamer-mediated Dot-blot Detecting Norovirus Virus Like Particles.....	107
6.13	Aptamer-mediated Pull-down of Norovirus GII.4.....	108
6.13.1	Preparation of the Paramagnetic Beads.....	108
6.13.2	Preparation of BSA-Blocked Streptavidin Coated Paramagnetic Beads.....	108
6.13.3	Preparation of Aptamers	108
6.13.4	Aptamer-mediated Virus Pull-down From Buffer.....	109
6.13.5	Aptamer-mediated Virus Pull-Down in Presence of Oyster Food Matrix.....	109
6.13.6	NoV RNA Extraction and Detection Post Pull-Down	109
7	Experiment Materials.....	111
7.1	Chemicals	111
7.2	Buffers, Solutions and Media.....	111
7.3	Commercial Kits	113
7.4	Nucleotides and Radionuclides.....	114
7.5	Oligonucleotides and Nucleic Acid Library.....	114
7.6	Enzymes and Enzyme Reagents	115
7.7	Plasmids and Bacteria	116
7.8	Viruses and Virus Like Particles (VLPs).....	116
7.9	Antibodies and Other Proteins	117
7.10	Other Materials.....	117

Table of Content

7.11	List of Software.....	118
8	Literature.....	119
9	Annex.....	134
9.1	Register of Figures.....	134
9.2	Register of Tables.....	136
9.3	List of Hazardous Components in Accordance with GHS.....	138
9.3.1	Pictogram description in accordance with the GHS.....	140
9.3.2	Lists of P and H phrases in accordance with the GHS.....	142
9.4	List of Chemicals classified as CMR Substances.....	151
9.5	List of Instrumentation.....	151
9.6	Pipetting Schemes for PCR Master Mixes.....	154
9.7	Pipetting Schemes for 10 % SDS PAGE Gel.....	156
9.8	Full Sequences of P-Domain, and VP1 Gene.....	157
9.8.1	Sequence P-Domain (5'-3').....	157
9.8.2	Sequence of the VLP gene (5'-3').....	157
9.9	List of Sequences Identified in the Last SELEX-rounds of the five parallel SELEX-experiments.....	158
9.10	Plasmid Map of Vector pET 100/D-TOPO.....	165
10	Curriculum Vitae.....	XV
11	Acknowledgements.....	XVII
12	Eidesstaatliche Erklärung.....	XVIII

Abbreviation List

Abbreviation List

The Abbreviation list does not include SI units as well as abbreviations for chemical formulas or chemical elements. It also does not include names for oligonucleotides given in this thesis.

A	Adenine (nucleobase of DNA/RNA)	DE3	Designation indicating that an <i>E. coli</i> strain carries the lambda DE3 lysogen gen
ASM	American Society of Microbiology	Div	Diverticular
BAM	Bacteriological Analytical Manual	dNTP	Deoxynucleotide triphosphate
BNAs	Bridge nucleic acids	dUTP	Deoxyuridine triphosphate
bp	Base pair	<i>E. coli</i>	<i>Escherichia coli</i>
BSA	Bovine Serum Albumin	ELASA	Enzyme linked aptamer sorbent assay
Bmax	Concentration of available binding partners in saturation binding	ESI	Electron spray ionization
C	Cytosine (nucleobase of DNA/RNA)	FRA	Filter retention assay
CD	Circular Dichroism	G	Guanine (nucleobase of DNA/RNA)
CE	Capillary Electrophoresis	g	Gravitational force
Cfu	Colony forming unit	GI-VI	Norovirus genogroup I-VI
CP	Cedar Point	HBGA	Human blood group antigen
CTP	Cytidine triphosphate	His-tag	Polyhistidine-tag with at least six histidine residues
Cy3	Orange fluorescent dye	HID 50	50 % human infectious dose
Cy5	Far-red fluorescent dye	IBRQ	Iowa Black® Dark Quenchers
DNA	Deoxyribonucleic acid		

Abbreviation List

IDT	Integrated DNA Technologies	Nola	New Orleans
		NoV	Norovirus
IPTG	Isopropyl- β -D-thiogalactopyranosid	nt	Nucleotide
		OD 600	Optical density at 600 nm
IQF	Individually quick frozen	ORF	Open reading frame
ITC	Isothermal Titration Calorimetry	OTA	Ochratoxin A
JB	Just Beads	PAGE	Polyacrylamide gel electrophoresis
K_d	Equilibrium dissociation constant	PCR	Polymerase chain reaction
K_{off}	Dissociation constants	P-Domain	Protruding domain
K_{on}	Association constants	PEG	Polyethylene glycol
LB	Luria-Bertani (term for bacterial growth media)	pET	Plasmid Expression vector T7 bacteriophage
LC	Liquid chromatography	PMC	Pub Med Central
LNAs	Locked nucleic acids	R^2	Coefficient of determination
MedCTP	5-methyl-dCTP	RNA	Ribonucleic acid
MEME	Multiple Em for Motif Elicitation	Rpm	Revolution per minute
MNV	Murine norovirus	RT	Reverse Transcription
MS	Mass spectrometry	SB	Selection buffer
NGS	Next Generation Sequencing	SDS	Sodium dodecyl sulfate
		SELEX	Systematic Evolution of Ligands by Exponential Enrichment
NIH	National Institutes of Health		
NMR	Nuclear magnetic resonance	SMV	Snow mountain virus

Abbreviation List

<i>SOM</i> Amer	Slow Off Rate Modified Aptamer	T	Thymidine (nucleobase of DNA/RNA)
SPE	Solid phase extraction	TEMED	N,N,N',N'-Tetramethyl- ethylendiamin
SPR	Surface plasmon resonance		
SRSV	Small Round Structure	UV	Ultraviolet
viruses		VEGF	Vascular endothelial growth factor
Syd	Sydney		

Zusammenfassung

Das Norovirus (NoV) ist ein humanpathogenes Virus, welches zu Krankheit in allen Altersgruppen führen kann. Eine NoV Infektion verursacht vornehmlich Symptome der Gastroenteritis, einschließlich starken Erbrechens und Diarrhoe, sowie gelegentlich Fieber, Kopfschmerz und andere systemische Symptome. NoV Infektionen werden oft durch Einnahme von mit NoV kontaminierten Lebensmitteln verursacht. Die hohe Kontagiosität des Virus und die Vielfalt an Lebensmitteln, welche mit dem Virus kontaminiert sein können, stellen eine Herausforderung für die analytische Lebensmittelchemie, speziell für die Extraktion und Detektion von Viren dar. Gegenwärtige Extraktionsmethoden beruhen auf der Verwendung von speziellem Equipment zur Viruskonzentration oder der Viruspräzipitation. Im Zuge der Präzipitationsmethode verliert die Virushülle ihre Integrität und freigesetzte virale RNA wird mittels Polymerasekettenreaktion detektiert.

Der Bedarf an schnellen und unkomplizierten Norovirus Extraktionsmethoden für Vorort-Untersuchungen bei Krankheitsausbrüchen begründet die immerwährende Notwendigkeit der Entwicklung neuer Methoden die einen einfachen Nachweis des NoV in kurzer Zeit ermöglichen. Darüber hinaus sind Virusextraktionsmethoden welche eine intakte Virushülle extrahieren für bestimmte Anwendungen von Interesse, zum Beispiel für das Next Generation Sequencing. Ein Ansatz um die genannten Anforderungen zu erfüllen ist der Einsatz von sogenannten Aptameren als Extraktionsinstrument. Aptamere sind Oligonukleotid-Moleküle, welche ein Zielmolekül mit hoher Affinität und Spezifität binden. Sie werden in einem iterativen Prozess *in vitro* mit der Methode Systematic Evolution of Ligands by EXponential Enrichment (SELEX) selektiert. Aptamere können in einer Vielzahl von Assays und anderen analytischen Methoden benutzt werden. Als Fängermoleküle können sie an eine stationäre Phase oder an bewegliche paramagnetische Partikel gekoppelt und in Extraktionsmechanismen eingesetzt werden. Auf Basis dieser Sachverhalte ergab sich die Zielsetzung dieser Arbeit: die Evaluierung der Zweckdienlichkeit von DNA-Aptameren als Norovirus Extraktionsmoleküle in Gegenwart von Lebensmittelmatrices sowie die Entwicklung eines Aptamer-vermittelten Norovirus Extraktionsverfahren.

Einer der Vorteile der SELEX Methode ist die freie Wahl der Pufferbedingungen während der *in vitro* Selektion von Aptameren. Die Aptamerselektion kann daher an die nachfolgenden analytischen Parameter angepasst werden, um eine Aptamer-vermittelte Extraktion von Norovirus aus Lebensmitteln unter geeigneten Bedingungen zu erreichen. Zunächst wurde daher der Einfluss von Lebensmitteln auf die Anreicherung von Aptameren während der SELEX untersucht. Zu diesem Zweck wurde eine SELEX Parallelstudie mit vier Lebensmittelmatrices

Zusammenfassung

durchgeführt. Als Zielmolekül für dieses SELEX diente die Norovirus P-Domäne, die am weitesten vorstehende Domäne der Norovirus Hülle. Hierfür wurde die P-Domäne in *Escherichia coli* rekombinant mit einem pET Expressionssystem produziert. Die Bindung zwischen selektierten Oligonukleotiden und dem SELEX Zielmolekül wurde in Gegenwart von Salzpuffer und Lebensmittelmatrices ermittelt. Die Ergebnisse dieser Vergleichsstudie suggerierten, dass eine Anreicherung von Aptameren in Gegenwart von komplexen Matrices während der SELEX nicht erfolgte. Stattdessen wurde in Gegenwart der Lebensmittelmatrices eine Anreicherung von Oligonukleotiden erreicht, welche keine spezifische Bindung zur P-Domäne aufwiesen. Darüber hinaus ließen die erhaltenen Ergebnisse den Schluss zu, dass eine Aptamerselektion nicht in Gegenwart von Lebensmitteln durchgeführt werden muss, selbst wenn das resultierende Aptamer in lebensmittelanalytischen Verfahren eingesetzt werden soll. Es ließ sich weiterhin erschließen, dass ein Aptamer welches in Gegenwart von unverdünnten Lebensmittelmatrices angewendet werden soll, Eigenschaften bedarf, welche über hohe Selektivität und Affinität hinausgehen. Zu diesen Eigenschaften können vorteilhafte kinetische Bedingungen für die Bindung des Zielmoleküls, sowie die Art der Aptamer Faltung in Gegenwart des SELEX Zielmoleküls gehören.

In der *in vitro* Selektion in Abwesenheit von Lebensmitteln wurde das DNA-Aptamer mit dem Namen „Buf-2“ selektiert, welches eine Bindung zur Norovirus P-Domäne mit hoher Affinität (K_d : 17 ± 7 nM) und Selektivität aufwies. Die Struktur von Buf-2 wurde mittels Zirkulärer-Dichroismus-Spektroskopie abgeschätzt. Es wurde angenommen, dass es sich bei der Struktur von Buf-2 um eine parallele und antiparallele G-Quadruplex-Hybrid-Struktur handelte.

Zusätzlich wurde die Norovirus Affinität von Aptameren geprüft, welche aus publizierten SELEX Experimenten der Jahre 2013-2018, unter anderem aus dieser Arbeit hervorgegangen sind. Hierfür wurde die Bindung von sieben ausgewählten Aptameren an Virushüllen von fünf Norovirus Genotypen mittels Filterretentions-Assays, unter der Anwendung von radioaktiv markierten Aptameren evaluiert. Die Ergebnisse zeigten, dass die Mehrheit der getesteten Aptamere eine Affinität zum Norovirus vom Genotyp GII.4 aufwiesen. Ein Aptamer wies zusätzlich ein breites Bindungsspektrum zu anderen Genotypen auf. Die Selektivität der Virusbindung dieses Aptamers muss jedoch in weiteren Untersuchungen bestimmt werden. Nachdem die Bindung der Aptamere an die Virushüllen bestätigt wurde, konnten die Aptamere in nachfolgenden Experimenten erfolgreich in Aptamer-vermittelten „Pull-Down“ und „Dot-Blot“ Verfahren angewendet werden.

Abstract

Norovirus (NoV) is a human pathogenic virus causing gastroenteritis and vomiting in individuals of all age groups; norovirus illness is often associated with foodborne transmission. Low viral load and the variety of food matrices which can be contaminated with the virus pose a challenge to norovirus extraction and detection. Current extraction methods are time consuming, involve specialty equipment or employ precipitation methods, breaking the viral capsid in the process. Still there is a perpetual need for rapid extraction methods that can be used in onsite outbreak investigations with low equipment requirements, where laboratory facilities are not available. Additionally, extraction methods providing intact viral particles are of interest for certain downstream applications such as next generation sequencing. The above requirements can be met by using aptamers as an extraction or detection tool. Aptamers are single-stranded nucleic acid molecules, that bind to a target, with high affinity and specificity and are selected *in vitro* by an iterative method called **S**ystematic **E**volution of **L**igands by **EX**ponential Enrichment (SELEX). They can be used in a variety of assay designs and can also be utilized in extraction settings if attached to a solid phase or paramagnetic particles. Hence, the fundamental objective of this study was to select, characterize and assess the utility of DNA aptamers for norovirus and its application for food analytical methods.

SELEX allows the selection of an aptamer in custom parameters, which can be tailored to inherent assay or extraction conditions. The aptamer selection conditions can therefore be adapted to the subsequent analytical parameters to achieve aptamer-mediated extraction of NoV from food. That being the case, a parallel study was conducted, investigating the influence of food matrices on aptamer enrichment during SELEX. The intention of the parallel *in vitro* selection, was to explore whether and how the presence of food alters aptamer selection. The norovirus protruding domain, the most extended capsid protein domain was used as SELEX target and for that purpose produced in *Escherichia coli* using a pET expression system. After SELEX completion, target binding of the enriched oligonucleotides in presence of food matrices was evaluated. Results of the comparative study suggest that the introduction of food to SELEX was either detrimental to enrichment of oligonucleotides with target-specific binding or facilitates enrichment of non-target-specific oligonucleotides. Moreover, a relationship between target binding of enriched oligonucleotides in presence of food and the selection condition was not observed. Results also suggest that a norovirus specific aptamer with application in food does not need to be selected in presence of the particular food but may require certain kinetic or three-dimensional properties beyond high affinity and selectivity to be applied for pathogen extraction and detection in undiluted food matrices.

Abstract

The *in vitro* selection completed in absence of food matrices resulted in the selection of the norovirus DNA aptamer termed 'Buf-2' which bound the norovirus P-domain with high affinity (K_d : 17 ± 7 nM) and selectivity. The structure of aptamer Buf-2, was estimated to be a hybrid of parallel and antiparallel G-quadruplex, based on recorded circular dichroism-spectra.

Prior to investigating the utility of Buf-2 as an extraction and detection tool in aptamer-mediated pull-down and dot-blot methods, the norovirus affinity of a variety of previously identified aptamers, published between 2013 and 2015, was assessed. Additionally, NoV binding of aptamer Buf-2, generated during this work and published in 2018, was evaluated. In a comparative study, the binding of seven aptamers to the norovirus capsid protein of five norovirus genotypes was assessed by filter retention assay. The majority of these aptamers showed affinity for norovirus genotype GII.4, with the exception of one aptamer which exhibited a broad reactivity to most norovirus genotypes included in this study. The aptamers were subsequently utilized successfully in an aptamer-mediated dot-blot and pull-down assay.

1 Theoretical Section

1.1 Norovirus

1.1.1 An Introduction to Norovirus

Noroviruses (NoVs), first described as winter vomiting disease², are the leading cause of acute gastroenteritis worldwide³, and the main cause for foodborne illness in the United States (US)⁴. In 1968 a 27 nm viral particle was discovered by electron microscopy in stool filtrate¹ (Figure 1), and later identified as NoV. The samples were collected from patients that had fallen ill at an elementary school in Norwalk Ohio and suffered from symptoms including gastroenteritis, vomiting, and diarrhea. The name “Norovirus” was assigned to the genus in 2002 by the International Committee on Taxonomy of Viruses, NoV was previously referred to as Norwalk virus based on the geographical location of its first

occurrence⁵. As one of five genera of the *Caliciviridae* family, along with Lagovirus, Sapovirus, Vesivivirus, and Nebovirus⁶⁻⁷, NoVs infect not only humans but also swine⁸⁻⁹, bovine¹⁰, ovine¹¹, murine¹², canine¹³, and feline¹⁴ species. NoV infections of humans with animal infecting NoV strains have not yet been reported¹⁵. Yet, human infecting NoVs have been detected in stool of pigs, cattle, and dogs¹⁶⁻¹⁷. Additionally, studies have uncovered an existing canine seroprevalence for different human infectious NoV genotypes that resembles the seroprevalence in the human population¹⁸. These findings indicate zoonotic potential for human NoV.

Norovirus infection causes severe gastroenteritis with symptoms including, diarrhea, vomiting, headache, and fever. Nevertheless, NoV illness is usually self-limiting, but can lead to serious complications or even death, among children, elderly, and immunocompromised individuals¹⁹⁻²¹. The individuals infected with NoV shed high virus loads; the shedding of viruses can start 3-14 hours before onset of clinical symptoms, which usually subside within 72 h. However, viral shedding usually continues for four weeks (median value) after virus inoculation with peak virus titers being shed after symptom resolution²². The shedding can last up to eight weeks depending on the infected individual. Viral shedding was also observed in infected people who did not show typical symptoms of norovirus infection²². The NoV 50 % human infectious dose (HID 50) was originally estimated to be in a range of 18-1015 genome equivalents²³. A recent study suggested

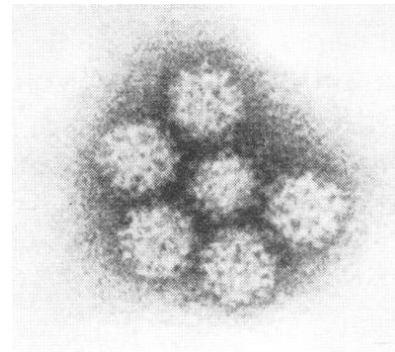


Figure 1. An electron microscopic picture of NoV particles from stool filtrate in PBS buffer¹ (the use of this figure is in agreement with the American Society of Microbiology (ASM), publisher of this figure, who authorizes advanced degree candidates to republish material for their dissertation).

Theoretical Section

a higher HID 50 of 1320 to 2800 genome equivalents, which is similar to the HID 50 of other RNA viruses²⁴. Both studies were completed using the prototype NoV 'Norwalk virus'.

It has been shown, that not all people are equally susceptible to NoV infection, which has been associated with an individual's ABO histo-blood group type²⁵. The ABO blood group of an individual is determined based on histo-blood group antigens (HBGA), which are presented on the surface of many cell types. It was found that individuals with A, B, or AB phenotype were less susceptible to NoV infection than those with an O phenotype²⁵. Individuals referred to as 'non-secretors' have also been shown to be less susceptible to infection with certain NoV strains. These non-secreting individuals lack the α -(1,2)-fucosyltransferase 2 (FUT 2) enzyme, which adds a fucose group to HBGA precursors. As a result, the A, B and H antigens are not present in bodily secretions of 'non-secretors'. The decreased susceptibility of 'non-secretors' to NoV infection has been linked to varying affinities of the virus surface proteins to HBGA, depending on the NoV strain²⁶⁻²⁷. Further investigation of the relationship between HBGA and the NoV capsid can be expected soon, as a NoV culture model has been developed in 2016²⁸. The development of a cell culture model for NoV replication is a recent accomplishment, but has been attempted numerously in the past fifteen years²⁹⁻³⁰. Nevertheless a culture model for murine NoV (MNV) had already been established in 2004³¹. Therefore, MNV has frequently been used as a surrogate for human NoV in infectivity studies. MNV replicates in macrophages, dendritic cells and B cells *in vivo* as well as in mouse macrophages and B cells *in vitro*. Additional studies involving immunocompromised mice, chimpanzees and pigs, have detected viruses in B cells, duodenal lamina, and in duodenal and jejunal enterocytes after animal infection. All of the mentioned cells are involved in the human immune response³²⁻³⁴.

1.1.2 Norovirus Genome Organization and Viral Capsid Structure

NoV is a non-enveloped virus with a single-stranded positive sense RNA genome of approximately 7.6 kb³⁵⁻³⁷. The NoV genome, except for murine NoV, is divided into three open reading frames (ORFs)³⁶. The first and second ORF overlap as shown below (Figure 2).

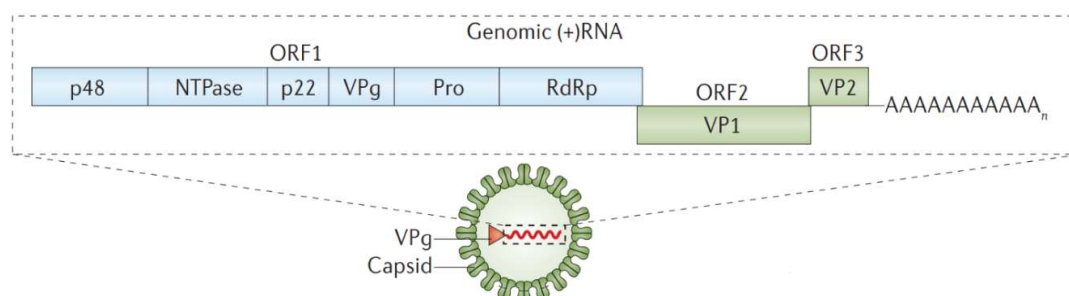


Figure 2. The organization of the norovirus genome, which is divided in three ORFs. ORF 1 encodes a large non-structural polyprotein, including the RNA dependent RNA Polymerase (RdRp), ORF 2 encodes the major structural protein VP1, and ORF 3 encodes a minor structural protein. This figure was modified from its original¹⁵ (the reuse of this figure is in agreement with Springer Nature and Copyright Clearance Center).

The first ORF encodes a polyprotein that results in at least six mature proteins after cleavage of the intermediate protein. The mature proteins have been defined as N-terminal protein (p48), a nucleoside triphosphatase (NTPase), a picornavirus like 3A protein (p22), the non-structural virus protein (VPg), which binds to the 5' end of the NoV genome, a proteinase with a chymotrypsin-like fold (Pro), and the RNA-dependent RNA polymerase (RdRp) in N- to C terminal order, respectively³⁸. The second ORF encodes the major structural capsid protein of NoV, designated as VP1³⁶. The third open reading frame encodes a minor structural protein (VP2)³⁹. Recently published research demonstrates that VP2 associates with the VP1 protein inside of the viral capsid and assists in the virus capsid assembly⁴⁰.

The VP1 protein is defined by two regions: the contiguous shell (S) domain and the protruding domain (P-domain). The P-domain is further divided into two subdomains: P1 and P2⁴¹. The P2 subdomain is the most exposed and genetically variable region of the VP1 protein. The NoV capsid consists of 90 dimers of the VP1 protein, resulting in 180 copies of the major capsid protein³⁶ (Figure 3). The X-ray crystal structure of the fully assembled capsid revealed that the VP1 dimers assemble into a T=3 icosahedral viral capsid. The radius of the shell region in the assembled capsid measures between 100 and 145 Å, whereas the combined S- and P-domains result in a larger capsid radius, measuring ~190 Å at the outer rim. The P-domain on the assembled capsid leaves large depressions at the icosahedral axes⁴¹. These 'cup-like' depressions are a unique feature of the *Caliciviridae* and inspired the name of the entire virus family (calici (greek) = cup; calyx (lat) = cup).

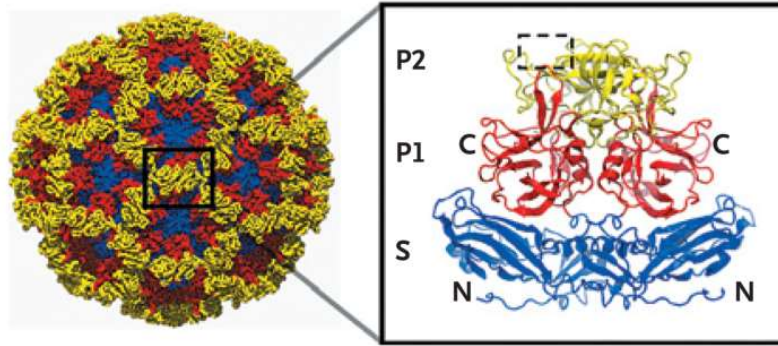


Figure 3. The structure of the NoV surface. The icosahedral structure of NoV formed by 180 molecules (90 dimers) of the VP1 protein. A VP1 dimer is shown in the frame to the right of the assembled capsid. The shell (S), protruding subdomain 1 (P1) and protruding subdomain 2 (P2) are shown in blue, red, and yellow, respectively. The dashed box at the top left side of the P2 domain indicates the binding side for HBGA. This figure has been modified from its original⁴² (the reuse this figure published by Massachusetts Medical Society for dissertation work is permitted without formal permission of New England Journal of Medicine).

1.1.3 Production of Norovirus Capsid and Capsid Proteins

The production of the NoV capsid was first described in 1992³⁶. It was found that the NoV major capsid protein VP1, produced in baculovirus recombinants, self-assembles into virus-like particles (VLPs) without requiring genomic RNA or the minor capsid protein VP2³⁶. However, more recent studies have shown that the minor VP2 protein associates with the S-domain inside the viral capsid, suggesting an assisting role in capsid assembly of the native virion⁴⁰. VLPs display authentic, morphologic, and antigenic characteristics consistent with native virus particles, and are of similar size as the norovirus itself. The VLPs have therefore been used successfully as intact NoV particles in vaccine development efforts^{36-37, 43-44}. Forming the virus like capsid, recombinant NoV VP1 characteristically self-assembles into 38 nm particles with T=3 symmetry composed of 180 VP1 copies⁴¹. Formation of smaller assemblies (23nm) with T=1 symmetry composed of 60 copies have been reported as well⁴⁵. The biochemical and antigenic properties of both particles were found to be conserved, and particles of different sizes have been shown to reassemble into the other particle sizes after alkaline treatment and subsequent dialysis⁴⁵. The P-domain, produced in a baculovirus system, does not self-assemble into VLPs. However, the S-domain of the VP1 protein forms small thin layered smooth particles which did not share antigenic properties with the native virion⁴⁶. The recombinant P-domain produced in *E. coli* forms a dimer⁴⁷, suggesting that the P-domain is the driving force to facilitate dimer formation of the VP1 protein⁴¹. Additionally, the P-domain produced in *E. coli* strain BL21 Star™(DE3) displays the typical binding pattern to A, B and H antigens compared to the intact viral capsid. This was confirmed for three different NoV strains and suggests that the P-domain contains elements responsible for NoV capsid binding to viral receptors⁴⁷⁻⁴⁸. More recently it has been shown that the recombinant P-domain with C-terminal modification results in the assembly of 12 modified P-domain dimers

Theoretical Section

forming the highly immunogenic 'P-particle' with T=1 symmetry⁴⁹⁻⁵⁰. Surface models have been applied to predict the structure of the different types of particles (Figure 4).

To date, VLPs have been produced for a wide variety of NoV strains and have been produced in expression systems beyond the baculovirus system including eukaryotic expression systems using yeast⁵¹, the human endothelial kidney cell line 293T⁵² as well as plant viral expression systems⁵³. They have not only been used for vaccine development, but also serve as NoV surrogates for studies involving adsorption and aggregation studies to investigate NoV binding to oyster tissue, and even for the characterization of NoV aptamers, among many other applications⁵⁴⁻⁵⁶.

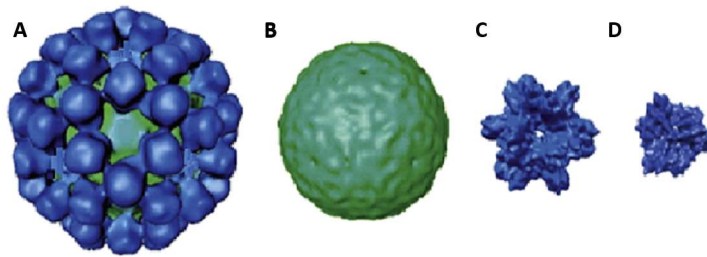


Figure 4. Structural surface models of five particles as resulting from assembly of VP1 protein or truncated VP1 proteins. The S-domain is shown in green and the P-domain shown in blue. (A) Complete VP1 protein assembled to a 37 nm VLP (180mer with, 37 nm diameter), (B) shell domain of the VP1 protein assembled to a particle (180mer with, 20 nm diameter), (C) P-particle (24mer with, 20 nm diameter), (D) small P-particle (12mer with, 14 nm diameter). This figure was modified from its original⁴⁹ (this figure was used for this thesis in agreement with Elsevier and Copyright Clearance Publishing Centre).

1.1.4 Norovirus Classification and Epidemiology

NoVs are classified based on the amino acid sequence of the complete VP1 protein⁵⁷. For NoV, six genogroups have been identified, of which genogroup I, II, and IV (GI, GII, and GIV) are pathogenic to humans. These genogroups are subdivided into 9, 21, and 3 genotypes, respectively. The genotypes are further divided into strains, which are named after city of first discovery⁵⁷. A new classification into seven genogroups has recently been proposed⁵⁸ (Figure 5).

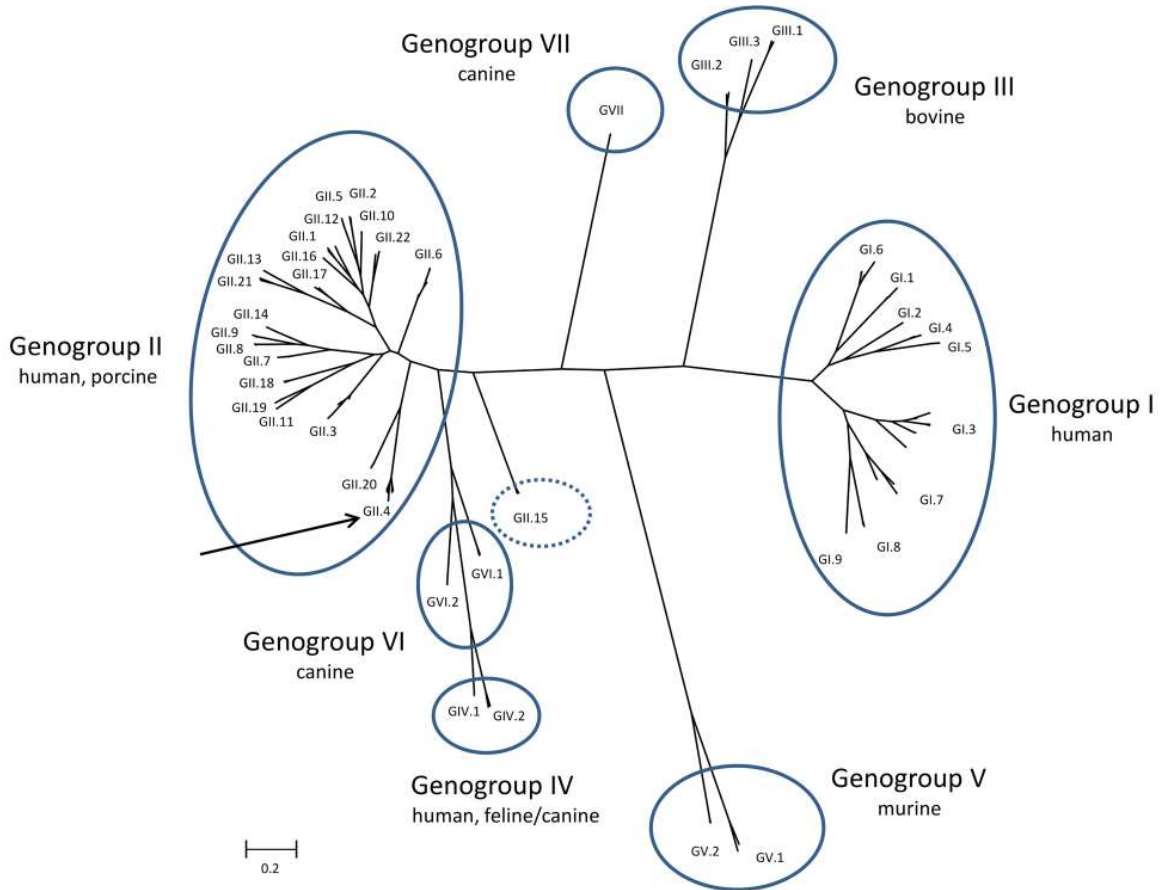


Figure 5. Phylogenetic tree, based on the NoV major capsid protein sequences. The tree was built using NoV capsid sequences from 105 strains that occurred in geographically disperse regions to create a phylogenetic tree reflecting NoV strains on a global scale. NoV genogroups I, II and IV infect humans, except for GII.11, GII.18, and GII.19, which infect porcine species and GIV.2 viruses which infect canines. GV.1 and GV.2 infect mice and rats, respectively. Genogroups GVI, and GVII infect canine species⁵⁸ (this figure was used with permission from the publisher ASM, who authorizes an advanced degree candidate to republish the requested material in her doctoral thesis or dissertation).

Theoretical Section

NoV is responsible for 18 % of all cases involving acute gastroenteritis worldwide; this was the result of a systematic review and meta-analysis of studies published between January 2008 and March 2014, using Polymerase Chain Reaction (PCR) as diagnostic tool⁵⁹. NoV has been the major etiological agent of nonbacterial gastroenteritis in Western societies, with 93 % and 85 % of nonbacterial gastroenteritis attributed to NoV in the US and Europe, respectively⁶⁰⁻⁶². Aside from NoV causing illness and death among humans and especially among children under the age of 5 years (70,000 norovirus-associated deaths among children worldwide for the year of 2011 were estimated), NoV illness poses a significant economic burden⁶³. A recent study estimated the global economic burden of NoV using a developed simulation model including a total of 233 countries and areas stratified by the world health organization (WHO). The estimated annual median number of illnesses and death across all age groups was 700 million and 219 thousand, respectively. The combined number of cases lead to an estimated median value of \$4.2 billion in direct health system costs and \$56.2 billion due to productivity losses caused by NoV illness⁶⁴.

Additionally, NoV's nosocomial transmission poses a major problem for health care facilities⁶⁵, especially if immunocompromised patients are present. These patients can act as NoV reservoirs and be a constant origin for NoV transmission⁶⁶⁻⁶⁷. Moreover, NoV is a major foodborne pathogen with 14 % of all NoV outbreaks being attributed to food⁶⁸, making NoV the leading cause of foodborne illness in the US. NoV was responsible for 58 % of all reported outbreaks in 2011, causing more foodborne associated illness than common bacterial pathogens such as *Salmonella* (nontyphoidal), *Clostridium perfringens*, *Campylobacter* spp. and *Staphylococcus aureus*⁴.

In the US, NoV GII.4 was the most predominant outbreak-causing genotype in the years of 2009 to 2013⁶⁹⁻⁷⁰, as it was the case for the entire northern hemisphere between 2003-2009. In Europe, NoV GII.4 was detected in 65 % of samples associated with NoV gastroenteritis outbreaks (n=2,256) over an 11 year period (2000-2011), and NoV GII was detected in 90 % of all samples, which tested positive for NoV⁵⁷. The role of genotype of GII.4 in outbreaks implicating food has recently been investigated. It was estimated that 10 % of all GII.4 outbreaks, 27 % of all other genotype outbreaks, and 37 % of outbreaks with multiple genotypes including GII.4 were attributed to foodborne NoV transmission worldwide⁶⁸. Results of a study investigating genotype distributions in outbreaks caused by NoV in the US between 2009 and 2013 suggested potential limitations of GII.4 in foodborne transmission. Although most foodborne outbreaks were caused by NoV GII.4, the ratio from outbreaks with person to person transmission to foodborne transmission was low compared to non GII.4 genotypes. These findings raise the question whether or not the predominance of this strain is attributed to foodborne transmission, or whether the

high occurrence of GII.4 in foodborne outbreaks is mainly due to the already existing high abundance of NoV GII.4⁷⁰. The high incidence rate of GII strains may be related to mutation of these strains to accommodate host factors. As host factors and outbreak settings vary in accordance to the infected population, these factors could have an effect on NoV epidemiology and influence the genotype evolution^{15, 71}. Recently NoV GII.17 has become a predominant strain in certain parts of Asia⁷² and has the potential to gain importance in the US and Europe, as this NoV strain quickly spreads globally⁷³.

1.1.5 Norovirus Environmental Stability and Transmission

The remarkable stability of NoV against environmental factors has been observed shortly after NoV discovery. The virus remained infectious post exposure to low pH, ether solution and incubation at elevated temperatures for prolonged periods of time (3 h at pH 2.7 at room temperature, 20 % ether solution at 4°C for 18 h, and incubation at 60 °C for 30 min)⁷⁴. The high stability of NoV in groundwater has since been confirmed for NoV GI.1, which stayed infectious for at least 61 days and had been detectable in ground, tap, and reagent water for at least 3 years⁷⁵. These findings are consistent with results of previous studies looking at long-term infectivity of poliovirus 3 (at least 140 days), adenovirus 2 (at least 364 days) and astrovirus Yuc8 (at least 120 days)⁷⁶⁻⁷⁷. Additionally, NoV stability in freezing and thawing processes was assessed, showing that GII.4 capsid integrity and genomic RNA titers were not affected by freezing and thawing for 14 times over the course of 17 weeks⁷⁸. NoV has also proved to be infectious after at least 12 days exposure on a carpeted surface⁷⁹ and exhibits high resistance to commonly used disinfectants, such as chlorhexidine and certain ethanol and triclosan based disinfectants⁸⁰. Moreover, the physical size of waterborne viruses, such as NoV, results in ineffective viral removal from sewage using common mechanical techniques such as filtration⁸¹. In general, waterborne viruses commonly remain in effluent water of waste water treatment plants, albeit at reduced levels and thereby enter the environment and recreational areas⁸². The contact of foods with NoV contaminated recreational waters is a common route of viral transmission (Figure 6)⁸³.

Theoretical Section

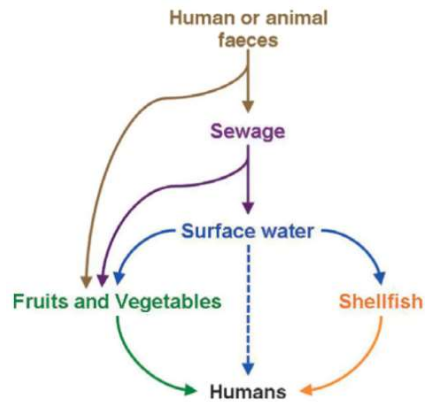


Figure 6. Routes of environmental virus transmission. This figure shows multiple routes of viruses to enter the food chain. This figure is adapted from its original⁸³ (the reuse of this figure is in agreement with the publisher, the Oxford University Press and Copyright Clearance Center).

NoV can also be transmitted by person to person contact through the fecal oral route, or by human exposure to virus aerosols that result from vomiting incidences⁸⁴. However, person to person contact can lead to foodborne transmission and has previously been confirmed in investigations, linking a foodborne outbreak to NoV illness in food handlers⁸⁵. This issue becomes more complex in asymptomatic food handlers, or in cases of NoV illness of a food handler that is accompanied by prolonged virus shedding after symptoms have resolved. In both scenarios, the food handler will continue his occupation while shedding virus, and thereby potentially infect customers through food contact. Both scenarios have led to NoV outbreaks in the past⁸⁶⁻⁸⁷.

As previously mentioned NoV caused illnesses is a global issue⁸⁸, which will likely stay current, as the globalization of the food chain progresses, and the trade of food increases. These factors contribute to the spreading of foodborne pathogens including NoV. The route of foodborne transmission can lead to a NoV contamination of a wide variety of foods. However, foods widely reported as virus vectors in Europe and the US are fresh and frozen berries⁸⁹⁻⁹², leafy greens⁹³ and molluscan shellfish, especially oysters⁹⁴⁻⁹⁷. An epidemiological study about seafood related illness, studying confirmed outbreaks between 1973 and 2006, showed that NoV was the third most common pathogen associated with seafood and the most common viral agent in the US during the study period⁹⁸.

1.1.6 Norovirus in Oysters

Oysters are edible bivalve mollusks of the class *pelecypoda*, which are characterized by two shell valves hinged together, and an abductor muscle opposite of the hinge. They are filter feeders, sieving suspended food particles from surrounding water. A recent study estimated a maximum filtration rate of about 170 L per 1 gram of oyster dry weight⁹⁹. The exact filtration rate according

to that study is depending on several environmental factors such as salinity, temperature, and biomass in the water surrounding the oyster. By filtering water, oysters can concentrate waterborne viruses. Therefore the viral titer in oysters can be 100-1000-fold higher compared to the surrounding water⁸². Commercially available oysters on the US west coast, and in parts of France are of the species *Crassostrea gigas*. On the US south- and east coasts the commonly grown oyster species is *Crassostrea virginica*. Oysters enter the market in various ways: raw, frozen, shucked, or unshucked, with or without its shells, and are being sold in a variety of preparations. During the work completed for this thesis, freshly harvested and shucked oysters were used primarily, but individually quick frozen (IQF) oysters were used sporadically as well. These IQF oysters used here, were presented on one shell after a quick-freezing method.

Although virus infections have been linked to oyster consumption since the 1960s¹⁰⁰, the association of NoV illness with oyster consumption has not been documented until the early 1980s through the 1990s¹⁰¹⁻¹⁰². In 2000, a three-year study was conducted in France to assess the presence of human enteric viruses in shellfish¹⁰³. Oysters (*Crassostrea gigas*) and mussels were collected in southern France monthly from 1995-1998 and samples analyzed by RT-PCR. NoV was found in 23 % of all samples. This number does however not represent NoV contamination of commercially available oysters, as some of the collection sites were predicted to be heavily contaminated with sewage and not designated commercial growing areas. The study also showed a higher incidence of shellfish containing NoV in the colder winter months from October to March. An additional study demonstrated that a correlation between winter epidemic of acute gastroenteritis in the French coastal population and the presence of NoV in oysters exists¹⁰⁴. Although the cause of illness was not confirmed to be due to oyster consumption, the findings show that incidences such as NoV epidemics are reflected in the presence of NoV in shellfish if both are in close proximity.

In efforts to test the depuration of NoV from oysters, it was found that viral numbers were not significantly reduced following 48 h of depuration, compared to a decrease of 95 % in bacterial titers over the same time period¹⁰⁵. Binding studies using NoV VLPs later revealed that the NoV capsid specifically binds to the diverticulum (div.) of oysters of the species *Crassostrea gigas* and *Crassostrea virginica* via a carbohydrate molecule^{55, 106}. Additional studies revealed that VLPs of the NoV GI.1 prototype bound almost exclusively in the diverticulum through an oyster HBGA A-like carbohydrate antigen¹⁰⁶. NoV VLPs of genogroup II bound the oyster's diverticulum, the oysters' gills, and mantle through a sialic acid containing ligand¹⁰⁷. It was also discovered that NoV of genogroup I accumulated in oysters with a seasonal pattern, showing highest accumulation in

the months of January through April. This was in contrary to the NoV genogroup II strains tested, which appeared to be accumulated with the same efficiency year round¹⁰⁷. These important discoveries verified that oysters do not passively retain NoV as filter feeders, but actively accumulate the virus via selective ligands. The strain specific differences in oyster tissue binding could explain why the NoV GI/GII ratio in shellfish outbreaks is higher, compared to non-shellfish related food outbreaks¹⁰⁸. NoV associated outbreaks originating from oysters have frequently been confirmed to involve multiple NoV strains^{95, 109}. As it has been shown, that NoV intergenotype and intragenotype recombination does occur¹¹⁰, the presence of multiple strains in an outbreak-associated oyster can increase the risk of viral recombination.

1.1.7 Current Norovirus Diagnostic Tools, Virus Extraction and Future Challenges

Until the 1990s, NoV was diagnosed in fecal samples by means of electron microscopy and referred to as small round structured viruses (SRSV) according its shape, and given a name based on the location in which these viruses were identified in relation to gastroenteritis associated symptoms (e.g., Norwalk)⁴². After the NoV genome was first cloned and sequenced, the virus could be characterized and later diagnosed using molecular methods³⁵. Prior to the establishment of quantitative polymerase chain reaction (qPCR) systems, NoV was detected using conventional reverse transcription-PCR assays (RT-PCR). Particular conventional PCR assays for the detection of NoV are still current¹¹¹, and are being used in reference laboratories in combination with sequencing for confirmation⁵⁸. In up-to-date NoV diagnostics, reverse transcription quantitative polymerase chain reaction (RT-qPCR) assays are the gold standard⁵⁸. The RT-qPCR assays used today are completed in one step, requiring only one reaction set up for the reverse transcription step and the subsequent PCR. Hydrolysis probes, also referred to as TaqMan[®] probes are used in the majority of the assays and are preferred over end point PCR protocols and SYBR Green assays, as they provide a real-time detection and increased specificity over intercalation dyes.

The genomic variety among NoV within one genogroup is extremely high, posing a challenge for primer and probe design. The most conserved region, which still allows the distinction of the genogroups I and II on the NoV genome is located at the ORF1/ORF2 junction¹¹², and therefore targeted in primer design. Additionally, this issue is addressed by using degenerate primers, which contribute to broadening the genomic spectrum of NoV genotypes detected by an assay. Multiplex RT-qPCR assays have been developed targeting the ORF1/ORF2 junction using degenerate primers, to identify NoV GI and GII simultaneously¹¹³⁻¹¹⁴. In addition, there are multiplex assays for the detection of GI, GII, and GIV¹¹⁵. In this work, NoV was detected by means of a multiplex assay for the most prevalent human pathogenic genogroups I and II using primers which anneal to a

Theoretical Section

NoV genome location that has been shown to be best suited for genotyping¹¹⁶. The primers used for both genogroups, carry the name 'COG' and were first described in 2003¹¹⁷. In this assay, both primers and probe oligonucleotides are degenerate. Additionally, primers and probes for an internal amplification control are being used to estimate PCR inhibition of the sample extract. The method is currently used in-house at the US Food and Drug Administration (FDA) and has been published previously, when it was utilized to determine NoV levels in oysters as part of a market survey in 2007 and to identify NoV genogroup I and II from oysters implicated in US outbreaks (the method will be referred to as the FDA-shellfish method in this manuscript)^{109, 113}.

Although at this point, RT-qPCR is the only reliable approach to NoV detection, there are three major approaches to virus extraction from foods. The approach utilized by FDA is virus concentration by ultracentrifugation. Additionally, virus concentration can be accomplished using polyethylene glycol (PEG), which is the most common method for virus concentration and has been used for virus extraction from shellfish since the late 1980s¹¹⁸. The third approach is a direct extraction of the viral RNA after virus lysis, taking advantage of the serine protease Proteinase K or other reagents (such as TriReagent®, or TRizol). Proteinase K was first used in combination with the PEG precipitation for NoV extraction from shellfish over 20 years ago¹¹⁹. However, for the scope of this work, the methods used in-house by the US FDA are of most importance. The FDA methods for viral extraction from shellfish and leafy greens are multi-laboratory validated methods used for surveillance by all state and federal laboratories in the US. The extraction of viruses from leafy greens has been published in FDA's Bacteriological Analytical Handbook (BAM) as BAM Chapter 26 B and is publicly available. Currently, virus extraction from berries is being validated, and the virus extraction method from oyster matrices has been submitted to be published in the BAM by the US FDA Gulf Coast Seafood Laboratory. The three methods for virus extraction from foods, described above and outlined in Figure 7 are based on the virus-elution off the food matrix, followed by viral concentration using the ultracentrifuge and different purification steps.

Theoretical Section

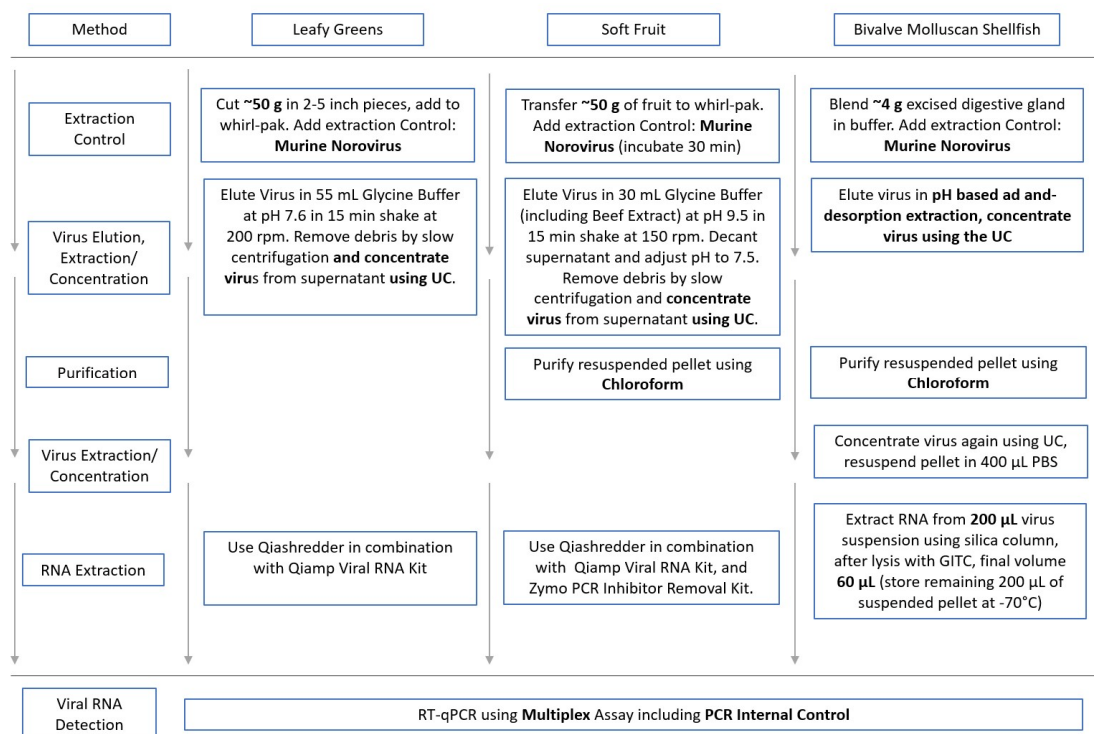


Figure 7. Schematic depiction of virus extraction methods for different food matrices used at the FDA laboratories.

One of the greatest challenges in food related NoV diagnostics has been the inability to culture the virus. Viral numbers in foods are usually low, and propagation without a host system is impossible; therefore, high sample numbers and high sample volumes/weights are necessary to accomplish reliable NoV analytics.

The concentration and extraction of NoV is usually labor intensive and in part requires expensive and immobile equipment. The continuous improvement of dependable NoV extraction methods is required to provide reliable data, which is comparable on a global scale. Additionally, further studies are needed to investigate which virus extraction method is best suited for each individual food, since it has been shown that viral extraction recovery of different extraction methods vary based on the food item from which the virus was to be extracted¹²⁰. Furthermore, there is a need for extraction methods to be used for onsite outbreak investigations, where robust laboratory facilities are not available⁵⁸. These methods need to be independent from heavy and expensive equipment and provide a simple, fast workflow resulting in reliable, and comparable data.

1.2 Aptamers

1.2.1 Aptamers and Their Selection by Systematic Evolution of Ligands by Exponential Enrichment (SELEX)

Aptamers are oligonucleotides that specifically bind a molecular target with high affinity. In 1990, an RNA molecule was identified to specifically bind a variety of organic dyes. The RNA molecule was selected *in vitro* from a large pool of roughly 10^{10} RNA oligonucleotides which exhibited a random region of 100 bp. The resulting specifically target binding oligonucleotide was called an aptamer, derived from the Latin word 'aptus' which means 'to fit'¹²¹. Simultaneously, RNA aptamers were selected for the T4 DNA polymerase utilizing nitrocellulose filters. The process by which the aptamers were derived was called Systematic Evolution of Ligands by EXponential enrichment (SELEX)¹²². The concept of *in vitro* selection of molecules however, had first been described for catalytic RNA molecules in early 1990¹²³. Although it was originally assumed that RNA would be better suited for ligand binding due to the natural pucker in the ribose ring, DNA aptamers have shown to be structurally diverse enough to bind a variety of ligands¹²⁴. The first DNA aptamer was generated for the protease thrombin using the SELEX method¹²⁵. This aptamer inhibited the thrombin-catalyzed fibrin-clot formation *in vitro* using either purified fibrinogen or human plasma, indicating the great therapeutic potential of aptamers. Four years later, peptide aptamers were generated from an *E. coli* produced peptide library¹²⁶.

To-date aptamers in general have been selected for an assortment of targets, reflected in the large number of manuscripts produced on this topic: an internet search using the keyword 'aptamers' with the U.S. National Institutes of Health (NIH) digital archive of biomedical and life sciences journal literature: PubMed Central (PMC) in January 2018 resulted in 9633 papers related to aptamers¹²⁷.

SELEX is an iterative process in which aptamers are selected from a diverse synthetic library of oligonucleotides¹²². This library consists of 20-100 randomized oligonucleotides flanked by two constant primer annealing regions. In each SELEX-round, the single-stranded nucleic acid library is exposed to the SELEX target. The time for this binding step is usually selected based on intended application of the selected aptamer. Subsequent to the binding step, unbound nucleic acid molecules are separated from target binding molecules. To accomplish this task, the target molecule is commonly immobilized on a medium to facilitate the partitioning. The binding molecules are recovered and amplified by PCR, completing one SELEX-round. For the next SELEX-round, complementary DNA strands from the previous SELEX-round's PCR product are being separated, to generate the nucleic acid library for the next SELEX-round. With increasing number

of SELEX-rounds, stringency is increased and selection conditions adjusted to continuously apply more selection pressure, facilitating the selection of molecules with high target affinity. The SELEX is completed when target specific enrichment of the derived nucleic acid library is confirmed, and no further enrichment is possible. Aptamers are then identified from the pool of enriched molecules. This is commonly accomplished by cloning the final SELEX-round's PCR product. Resulting single colonies are then isolated and sequences obtained by Sanger sequencing. Sequences which are represented multiple times in the last SELEX-round's nucleic acid pool are defined as 'enriched'. The target affinity of enriched molecules is subsequently assessed.

Shortly after SELEX had been introduced, the first optimized SELEX variants were presented and by 2011, more than 25 SELEX variations had been described¹²⁸. One of these variations is the 'Negative SELEX', which accounts for oligonucleotides that bind to the immobilization medium during the binding step. It thereby reduces the amount of oligonucleotides with non-target specific affinity during SELEX¹²⁹. The 'Negative SELEX' can occur before every binding step, or less frequently, and depends on the individual SELEX strategy. An additional, important SELEX variation is the 'Counter SELEX'¹³⁰, during which the library is not only exposed to the immobilization medium, but also to non-target molecules to reduce the occurrence of non-target specific oligonucleotides in the library even further. A full schematic depiction of the SELEX method with paramagnetic beads as immobilization medium including a negative selection is shown in Figure 8.

The partitioning of target binding and non-target binding oligonucleotides after the binding step is the most challenging and the most critical step in SELEX to facilitate aptamer enrichment. Therefore, many SELEX variations have been developed, suggesting enhanced separation techniques. One of these modified SELEX methods is the Capillary Electrophoresis SELEX (CE-SELEX), used to select a DNA aptamer for IgE with an estimated dissociation constant of 29 nM¹³¹⁻¹³². The CE-SELEX very efficiently separated the target-bound from non-target-bound oligonucleotides, as both groups exhibit different electrophoretic mobility. Using CE-SELEX the number of SELEX-rounds (commonly around 15) was reduced to 1-4 SELEX-rounds.

Theoretical Section

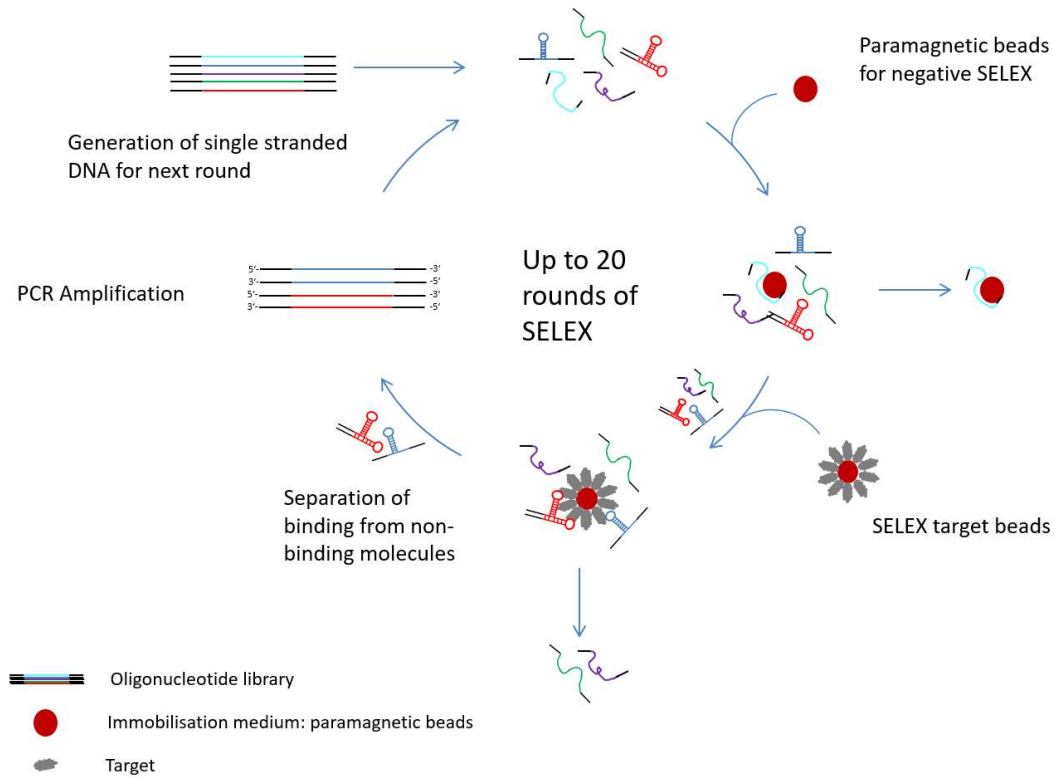


Figure 8. Schematic depiction of SELEX process using paramagnetic beads as immobilization medium to separate target binding from non-binding oligonucleotides.

In addition to optimizing the partitioning of target-bound from non-target-bound oligonucleotides during SELEX, the aptamer identification and isolation was improved in recent years by the introduction of Next Generation Sequencing (NGS). NGS was first used to identify aptamers in combination with 'Microfluidic SELEX' which had first been proposed in 2006, implementing microfluidic systems in SELEX in an effort to automate the aptamer selection process¹³³. Combining Microfluidic-SELEX and NGS resulted in the selection of aptamers for the platelet-derived growth factor with K_d values below 3 nM in three rounds of SELEX¹³⁴. The PCR product of every SELEX-round was sequenced, which allowed for tracing of molecule enrichment throughout SELEX, using NGS as a monitoring tool. The use of NGS in combination with SELEX allows for an early identification of enriched molecules, leading to fewer SELEX-rounds. Additionally, SELEX-rounds can be compared and SELEX conditions adjusted to facilitate increased stringency or the selection of aptamers with specific properties¹³⁵.

After aptamers had successfully been selected for a variety of pure entities, SELEX was completed using whole cells of the glioblastoma cell line U251¹³⁶. One of the selected aptamers was later identified to bind to an extracellular protein of U251 cells, the tenascin-c¹³⁶. Using cell-SELEX, aptamers were selected to targets in their natural states (e.g. on the cell surface, instead of a

target recombinantly produced in an expression system), increasing the chance of the selected aptamer to retain its function in the inherent analytical or therapeutic application. For aptamers to be used *in vivo*, this would require aptamer selection within an organism. In 2010 the idea of selecting an aptamer *in vivo* was put into practice. For the first-time, aptamer selection was accomplished within an animal model inside a tumor of a living organism and called '*in vivo* selection'¹³⁷.

Further SELEX variations have been introduced over time, each proposing a SELEX method targeted to enhance aptamer selection, streamline the SELEX process, and help obtain aptamers that keep their function in their intended application system. However, depending on the SELEX target, and the intended use of the aptamer, the selection of an aptamer has remained a challenge and further progress in molecular biology is necessary to facilitate a continuous improvement of the SELEX process.

After SELEX is completed, the target affinity of enriched oligonucleotides has to be determined. This can be accomplished, by means of saturation binding experiments to determine the equilibrium dissociation constant (K_d) as a measure of aptamer-target affinity. Saturation binding can be assessed with a wide variety of methods. Ultrafiltration in combination with ³²P labeled aptamers is one of the most commonly used techniques due to its low cost, and high sensitivity; it was also employed during this project. The interpretation of saturation binding assays was completed based on a previously published guide¹³⁸.

However, more modern methods like surface plasmon resonance (SPR), and isothermal titration calorimetry (ITC) both offer label free detection, and a faster workflow. Aptamers usually exhibit K_d values in the picomolar to low micromolar range. For the FDA approved aptamer Pegaptanib, the K_d for interaction with vascular endothelial growth factor (VEGF) ranged from as low as 49 pM to 130 pM¹³⁹. K_d values assessed for the thrombin binding aptamer and the target protease ranged from 25-200 nM¹²⁵. For the aptamer for adenosine/ATP a K_d of about 6 μ M was determined¹⁴⁰. In addition to a high target-affinity, an aptamer needs to bind its target selectively and specifically, which has to be confirmed in additional experiments.

1.2.2 Specialized Aptamers and Aptamer Modification

The susceptibility of RNA and DNA aptamers to nuclease degradation can complicate the inherent aptamer application; especially in biological settings or food matrix applications, where nucleases are abundant. To reduce the nuclease susceptibility of aptamers they can be modified. The most common modifications target the 2'-hydroxyl group of the RNA ribose moiety, substituting it with

fluoro-, amino-, or a methoxy group¹⁴¹. Another group of modified nucleic acids are called locked nucleic acids (LNAs), or bridge nucleic acid (BNAs). They are nucleic acid analogs with a modified sugar moiety¹⁴², where the 2' oxygen is connected to the 4' carbon atom of the ribose. The insertion of a LNA modified nucleotide is a post SELEX modification and can stabilize the aptamer and decrease its susceptibility to nuclease degradation and improve an aptamer's potential for *in vivo* application¹⁴³. Increase stability of DNA aptamers, as well as improved resistance against nuclease degradation has been accomplished by adding 2'-deoxy-2'-fluoro-D-arabinonucleic acid residues to different G-quadruplex aptamers (termed 2'F-ANA modification)¹⁴⁴. However, the most common DNA aptamer modification is the biotinylation. Biotinylated aptamers are used for immobilization and detection techniques.

There are two aptamer modifications that have contributed greatly to the aptamer field: the Spiegelmers, and the 'Slow Off-rate Modified Aptamers' (SOMAmers). Aptamers that consist of nucleotides with an L-ribose sugar, the enantiomer of the natural occurring D-ribose, are Spiegelmers. The name is derived from the German Word 'Spiegel' for mirror. Spiegelmers are selected using a D-ribose oligonucleotide library, but the target used for SELEX is a chemically synthesized enantiomer of the natural target protein. Once an aptamer is selected and characterized, it is synthesized with L-ribose nucleotides and used as affinity ligand for the natural target protein¹⁴⁵. Mixed RNA/DNA Spiegelmers have shown to be effective in *in vivo* application¹⁴⁶. However, Spiegelmer selection requires chemical synthesis of the target, which is costly and difficult especially for large proteins. Moreover, the protein folding of the chemically derived enantiomer can vary from that of the natural protein¹⁴⁷. SOMAmers are aptamers with modified dUTP and 5-methyl-dCTP (MedCTP) bases¹⁴⁸. A peptide like bond connects the benzyl, naphthyl, tryptamino, or isobutyl modifications to dUTP, increasing the chemical diversity of these oligonucleotides. SOMAmers have been selected for targets, for which conventional SELEX approaches did not facilitate aptamer enrichment, improving the SELEX success rate. However, the amplification of these modified aptamers requires particular, expensive enzymes and the availability of these oligonucleotides is limited due to existing patents¹⁴⁷. To generate SOMAmers with slow dissociation constants, the SELEX-target is immobilized on Co²⁺-NTA paramagnetic beads and the SELEX partially completed in presence of an excess of the polyanionic competitor dextran sulfate¹⁴⁸.

1.2.3 Aptamer Structures

Contrary to DNA, which most common tertiary structure is the double helix as postulated in 1953¹⁴⁹, single-stranded nucleic acid molecules fold intramolecularly and can adopt a variety of

Parallel quadruplexes, containing four strands of nucleic acids with the same direction, and anti-parallel quadruplexes, containing four nucleic acid strands with opposing directions. Since G-quadruplex structures have been shown to be remarkably resistant to nuclease degradation¹⁶¹⁻¹⁶², the identification of a G-quadruplex structure can be a crucial characteristic of an aptamer, especially for therapeutic or food analytical application. Although a high abundance of G in an oligonucleotide sequence can be an indicator for a G-quadruplex structure, this is not always the case. The G-quadruplex structure of an oligonucleotide can be confirmed by a variety of analytical techniques like ultra violet (UV) melting curves, polyacrylamide gel electrophoresis, fluorescent resonance energy transfer, sedimentation velocity analysis, crosslinking experiments, electron microscopy, and atomic force microscopy. However, most commonly circular dichroism (CD), X-Ray diffraction and nuclear magnetic resonance (NMR) are being used.

1.2.4 Aptamer Applications

Aptamers are often compared to antibodies, as both molecules specifically bind their target with high affinity. However, there are certain advantages of aptamers over antibodies, such as their size. An aptamers molecular weight is usually between 6-30 kDa, while antibodies have a molecular weight of 150-180 kDa. Aptamers might therefore have advantages in binding small targets or small domains that antibodies cannot access due to fewer steric hinderances owed to the small size of the aptamer compared to antibodies. Additionally, an aptamer's selection environment can be chosen based on inherent application and be accomplished *in vitro* in 2-9 weeks, whereas antibodies are limited to physiological conditions and are generated *in vivo* in about 6 months with higher costs involved. Aptamers can also be selected for a wide range of targets, whereas antibodies are limited to immunogenic molecules. Moreover, aptamers do not exhibit batch to batch variation and are very stable, exhibiting a long shelf life in comparison to antibodies. Aptamer advantages over antibodies have been pointed out in numerous review articles^{147, 163-164}. However, a gap in clinical application between the two affinity ligands is noticeable. Currently, over 30 antibodies are used in clinical applications¹⁶⁵, yet only one aptamer drug has been approved by the FDA. This aptamer is called pegaptanib (Macugen; Pfizer/Eyetech)¹⁶⁶, an aptamer which blocks the VEGF. Nevertheless, this aptamer-based drug has since been surpassed by antibody-based therapeutics such as bevacizumab (Avastin; Genentech) and ranibizumab (Lucentis; Genentech)¹⁶⁷⁻¹⁶⁸. A barrier preventing the selection of aptamers with clinical application might be the low success rate of SELEX and the fact that most aptamers are still generated by *in vitro* selection, not implementing inherent physiological or assay conditions neither in the SELEX process, nor in the aptamer characterization. However, the progress made in

the field and the continuous optimization of the SELEX process, encourages the continuous pursuit of aptamer selection for therapeutic applications and beyond¹⁶³.

With increasing global trade and growing consumer interest and demand to food safety, the development for rapid food analytical methods becomes increasingly important. As mentioned, aptamers offer a variety of well-known advantages over antibodies¹⁶⁹ including: high stability, high cost efficiency, they can be easily modified, and can be selected for toxic and nonimmunogenic substances in inherent assay conditions. Hence, the continuous interest in using aptamers for food analytical applications is not surprising. Aptamers have recently been described as an important emerging tool for food analytical applications¹⁷⁰ and they have indeed been selected for a wide variety of targets important to the food industry; for example: bacteria¹⁷¹⁻¹⁷⁴, toxins¹⁷⁵⁻¹⁷⁶, pesticide residue¹⁷⁷, allergens¹⁷⁸, metal ions¹⁷⁹, antibiotics residues in foods¹⁸⁰, and gluten¹⁸¹. These aptamers have been used for the development of assays utilizing a variety of analytical techniques, such as nanoparticle colorimetry¹⁷⁹, SPR¹⁸², or surface enhanced Raman scattering¹⁸³.

Remarkable accomplishments have been made with aptamers selected for *Salmonella* sp. and the OTA aptamer, which exhibits a K_d value of 360 nM. Its application been tested in a solid phase extraction (SPE) method in a variety of food matrices including wheat flour, cereal, and coffee^{159, 184}. Compared to reference samples the OTA contents estimated with the aptamer based method were slightly lower, yet not statistically different than the values provided for the reference method¹⁸⁴. Aptamers for *Salmonella* have been selected by various groups; among these aptamers, one was used to detect *Salmonella* in an eluate obtained by rinsing an entire chicken, using a magnetic capture apparatus in combination with a PCR assay¹⁷³. A different aptamer for *Salmonella* (specifically *Salmonella* Enteritidis) bound the serovar exclusively, suggesting potential for application in screening methods or for serotyping¹⁸⁵. Additionally, an aptamer biosensor had been developed with a detection limit of 3 colony forming units per mL. Aptamers for *Campylobacter* detection in chicken juice among other food matrices have recently been described in a sensor application¹⁷². However, the detection limit of bacteria in buffer (2.5 bacteria cells/mL) was considerably lower than in chicken juice (100 bacteria cells/mL).

Most aptamers selected for food analytical methods and assays focus on detection and have been implemented in a variety of biosensors used in food analytical methods¹⁸⁶. However, the complexity in composition and the wide variety of food matrices still poses a problem to streamlining food analytical assays. Most aptamer applications are accomplished using diluted food matrices, rinse solutions, or culture media for bacteria. One of SELEX's advantages is the choice of selection environment based on inherent assay development, which has been taken

advantage of in the field of therapeutics where SELEX is continuously adapted to generate versatile aptamers that can be used in clinical functions and has finally been completed in an organism during *in vivo* selection¹³⁷. On the contrary, food matrices have not yet been integrated into the SELEX process.

1.2.5 Aptamers for Norovirus

Since late 2013, several efforts have been published on aptamer selection for NoV. To generate NoV aptamers, multiple SELEX targets have been used, among those were: NoV VP1 protein with a polyhistidine-tag (His-tag)¹⁸⁷, the whole virus using NoV genotype GII.3 from stool filtrate⁵⁶, the mice infecting MNV¹⁸⁸, and *E. coli* produced P-Domain with a GST fusion tag¹⁸⁹.

As shown in Table 1 K_d values were only determined for two aptamer candidates with NoV GII.2 VLPs. The K_d value for the aptamer AG3 was assessed to be in the low picomolar range using MNV particles. The AG3 aptamer was selected for development of an aptasensor. Using the selected AG3 aptamer MNV was detected in diluted meat juice filtrate solution in picomolar concentrations using fluorescein labeled aptamer in a polycarbonate filter retention assay format. When used in an aptasensor application, a limit of detection of MNV concentration of 10 atto M was reported¹⁸⁸.

Theoretical Section

Table 1. Summary of selected, previously published NoV aptamers, their SELEX target and determined K_d .

Candidate	Sequence 5'-3'	Target protein	K_d
Beier ¹⁸⁷	GTCTGTAGTAGGGAGGATGGTCCGGGGCCCCGAGACGACGTTATCAGGC	His-Tag VP1	n.d.*
SMV 19 ⁵⁶	CACCAGTGTGTTGAGGTTTGAGCACACTGATAGAGTGTCA	Whole virus	191nM **
SMV 21 ⁵⁶	CCATGTTTTGTAGGTGTAATAGGTCATGTTAGGGTTTCTG	GII.2	101nM**
M 6-2 ¹⁸⁹	TGGGAAGAGGTCCGGTAAATGCAGGGTCAGCCCGGAGAG	P- Domain	n.d.*
M 1 ¹⁸⁹	TGTTTATGGGGATAAACGTATCTAATTCGTGTACTAATCA	with GST fusion protein	n.d.*
AG3 ¹⁸⁸	GCTAGCGAATTCGGTACGAAGGGCGAATTCACATTGGGCTGCAGCCCGGGGGAT CC	MNV	pM range***

* n.d.: not determined

** K_d was determined using GII.2 VLPs, not the SELEX target

*** no definitive K_d was published, but K_d determined to be in the picomolar range based on binding studies

Aptamers obtained by SELEX using NoV GII.2, or Snow Mountain Virus (SMV), resulted in multiple aptamer candidates, of which SMV 19 and SMV 21 exhibited the lowest determined K_d values. Multiple aptamers were tested in an enzyme linked aptamer sorbent assay (ELASA) and showed comparable performance to a GII.3 commercial antibody. Additionally, authors suggested potential for NoV capture using aptamers in combination with paramagnetic beads after using one of their aptamer candidates (SMV 25) in a capture assay followed by RT-qPCR, concentrating virus from artificially contaminated lettuce samples⁵⁶. Aptamers M 1 and M 6-2 were tested as capture molecule in a pull-down approach using paramagnetic beads followed by RT-qPCR. In this setting both aptamers showed potential as capture molecules for NoV GII.4 purified from diluted stool suspension. Aptamer target binding of M 1 and M 6-2 in food matrices was not investigated¹⁸⁹. Aptamer Beier was not tested for application in food matrices. It was however suggested, that this aptamer candidate would bind the VP1 protein at the Shell-domain-P-domain junction¹⁸⁷. This could be important, as the genomic region coding the shell domain is the most conserved among all NoV genotypes- an aptamer binding to this conserved region could bind a broad range of NoV genotypes.

2 Objective

NoV is a gastrointestinal virus with high environmental stability, posing a food safety hazard. It is an especially problematic foodborne pathogen, as low virus titers are sufficient to cause illness, and low-level contamination in food is difficult to detect. Aptamers, which are small nucleic acids that bind their target specifically, could be beneficial for the extraction of intact NoV particles without using specialized equipment and provide ease-of-use. Aptamers with specific affinity to NoV could be used in food related outbreak investigations and for extraction and detection of viral particles, which need to be intact for downstream application. The primary objective of this work was the selection and characterization of an aptamer specifically binding the NoV surface, and the use of this NoV aptamer in the development of an aptamer-mediated NoV extraction from foods. Although the use of aptamers in food analysis has been suggested, and aptamers have been selected for a variety of foodborne pathogens, including NoV¹⁸⁷⁻¹⁹⁰, the incorporation of food matrix into SELEX has yet to be evaluated. Therefore the objective for a part of this study, was to investigate the influence of four food matrices that are highly associated with NoV outbreaks (frozen strawberries, lettuce, whole oyster, and oyster digestive diverticula) on the enrichment of aptamers targeting the NoV GII.4 P-domain. The fundamental hypothesis of this study is that *in vitro* selection of aptamers in presence of food matrices will lead to the enrichment of oligonucleotides that can be used as an analytical tool in the food matrices in which presence they were selected. It is anticipated that successful aptamer target binding will be dependent on the presence of the food matrix used during selection, as each food matrix will influence aptamer folding and its ability to interact with its target. Aptamers resulting from the SELEX study were to be characterized and used in extraction and detection applications. Additionally, the functionality of these aptamer-mediated extraction and detection techniques, was to be assessed in the presence of food matrices.

In light of fast advances in NoV related aptamer research during the time of this work, NoV aptamers published in the timeframe 2013-2015, were to be partially characterized. This was a critical step to reach the objective, as the aptamer with most favorable binding properties would be best suited as molecular tool for detection and extraction. Furthermore, these NoV aptamers were to be included in the development of aptamer-mediated detection and extraction techniques, if appropriate binding characteristics towards the NoV surface protein were to be determined.

3 Results

3.1 Production of Aptamer Target for SELEX

3.1.1 Amplification, Cloning, and Sequencing of P-domain Gene

To accomplish P-domain production in a pET *E. coli* expression system, the VP1 gene needed to be amplified from viral RNA. For that purpose, NoV RNA was extracted from a stool sample which had previously tested positive for NoV GII.4 Den Haag. The stool sample was partially purified using chloroform, and viral RNA subsequently extracted (for experimental details, see section 6.1.2). After the VP1 gene was amplified from genomic RNA by RT-PCR, as described in section 6.5.1, the VP1 gene was cloned into pCR™4-TOPO vector and the recombinant vector used for transformation of chemically competent *E. coli* cells (TOP10). Colonies presumably containing recombinant plasmids were screened by colony PCR using M13 primers and positive clones isolated, amplified, and recombinant plasmid extracted (see section 6.6). The VP1 gene DNA was obtained by double restriction digestion of the recombinant plasmid and used as template for amplification of the P-domain gene which was subsequently cloned into the expression vector pet100. Approximately 100 of the resulting colonies were screened using T7 primers. After successful recombination was confirmed (for experimental detail, refer to sections 6.2.6, 6.5.5, and 6.6), glycerol stocks of bacteria carrying the recombinant vector were generated. The proper orientation of the gene in the expression vector was confirmed by sequencing the PCR product of a T7 colony screen (see section 6.5.5). Full sequences obtained for the P-domain and VP1 gene are shown in the annex (section 9.8).

3.1.2 Production, Purification and Identification of P-domain and Control Protein

The *E. coli* strain BL21 Star™(DE3) was used for protein production after cell transformation using the recombinant expression vector. The conditions during protein production were optimized by testing soluble and insoluble fraction of the cell lysate, after completion of protein production in different media conditions (with and without glucose) and at different times and temperatures. It was noted that the P-domain production resulted in large quantities of the protein in the insoluble fraction of the cell lysate, regardless of protein production conditions. Efforts to extract the P-domain from the insoluble fraction under denaturing conditions were not successful. However, an increase of soluble P-domain was accomplished, by inducing and conducting protein production at lower temperatures and in presence of low amounts of glucose in Luria-Bertani (LB) media. The optimized P-domain production conditions are summarized in Table 2 (for experimental detail, refer to section 6.8).

Results

Table 2. Optimal conditions of P-domain production in BL21 Star™(DE3). P-domain production was optimized regarding media, concentration of Isopropyl- β -D-thiogalacto-pyranosid (IPTG), time of harvest and production temperature.

Factor	Concentration/ time/condition during protein production
Media	LB-broth with 100 μ g/mL ampicillin and 0.1 % glucose
Final concentration of IPTG in media	0.1 mM
Time of harvest after induction	18 h
Temperature	16°C
OD ₆₀₀ at time of induction	1

The P-domain was purified from cell lysate by affinity chromatography using a cobalt resin. For purification, the clarified cell lysate was applied to a manually packed column, as described in section 6.8.4. Subsequently, the resin-bed was washed with lysis buffer, and protein wash buffer containing imidazole concentrations of 10 mM to 75 mM (for buffer composition refer to Table 15 in section 7.2). Finally, the P-domain was eluted with protein elution buffer containing 100-250 mM imidazole. To determine which imidazole concentration resulted in optimal P-domain elution off the cobalt resin, the different imidazole concentration fractions were analyzed by sodium dodecyl sulfate (SDS) polyacrylamide gel electrophoresis (PAGE), as described in section 6.7.2 (Figure 10 (A)).

The protein expression kit used for this work (Champion™ pET Directional TOPO® Expression Kit) provided an expression vector that served as a control for the expression experiment. The protein produced with this expression control experiment is the β -galactosidase, which is a 121 kDa protein when produced as a fusion protein with a 6xHis-tag. This protein was later used for negative selection in SELEX. During this work it will be referred to as 'control protein'. The control protein was produced in *E. coli*, as described in section 6.8.2 and purified by affinity chromatography using a cobalt resin. Solubility issues, as described above for the P-domain were not observed. The ideal imidazole concentration for control protein elution off the cobalt resin was determined by analyzing different imidazole concentration fractions by SDS-PAGE (Figure 10 (B)). It is notable that the elution of the control protein required less imidazole than elution of the P-domain. Eluted control protein was observed in the 25 mM imidazole protein wash buffer fraction and bands of greatest intensity were detected in the 50 mM and 75 mM imidazole protein wash buffer fractions.

Results

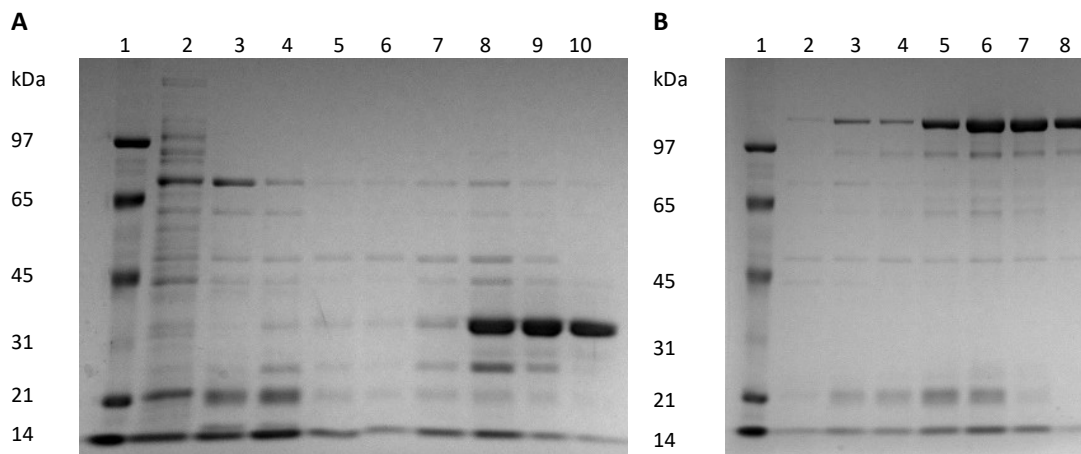


Figure 10. SDS Page Gels (10%) showing protein fractions collected during P-domain and control protein purification. Proteins were separated on 10 % SDS polyacrylamide gel. (A) P-domain, lane 1: SDS PAGE molecular weight marker-low range, lane 2: wash fraction with 10 mM imidazole, lanes 3 and 4: wash fractions with 25 mM imidazole, lane 5: wash fraction with 50 mM imidazole, lanes 6 and 7 : wash fraction with 75 mM imidazole, lane 8: eluate fraction with 100 mM imidazole, lanes 9 and 10: eluate fraction with 250 mM imidazole; (B) Control protein, lane 1: low range molecular weight marker, lane 2: wash fraction with 10 mM imidazole, lanes 3 and 4: wash fractions with 25 mM imidazole, lane 5: wash fraction with 50 mM imidazole, lane 6: wash fraction with 75 mM imidazole, lane 7: eluate fraction with 100 mM imidazole, lane 8: eluate fraction with 250 mM imidazole.

The P-domain was eluted in three fractions of approximately 1.7 mL each, with a determined protein concentration of 60-80 $\mu\text{g}/\text{mL}$ (for experimental details see sections 6.7.3 and 6.7.6). Efforts to increase the P-domain concentration by eluting the protein with higher concentration of imidazole in a smaller buffer volume were not successful, as the protein precipitated during dialysis to facilitate the removal of excess salt and imidazole. The P-domain purity of the eluate fractions was determined using the Tape Station 2200, as described in section 6.7.3. An average purity of 94-98 % was obtained for the P-domain (Figure 11).

The control protein was produced in higher quantities compared to the P-domain, as protein solubility during production was not an issue for this protein. The control protein concentrations obtained were as high as 160 $\mu\text{g}/\text{mL}$. The control protein was produced simply to be used for counter selection, to prevent the enrichment of oligonucleotides binding the 6xHis-tag. Therefore, the expression of this protein was not further optimized. The purity determined for the control protein was between 65-80 %. Selected purified fractions of the control protein and the P-domain and the according purities, which were calculated using the Tape Station software (Figure 11).

Results

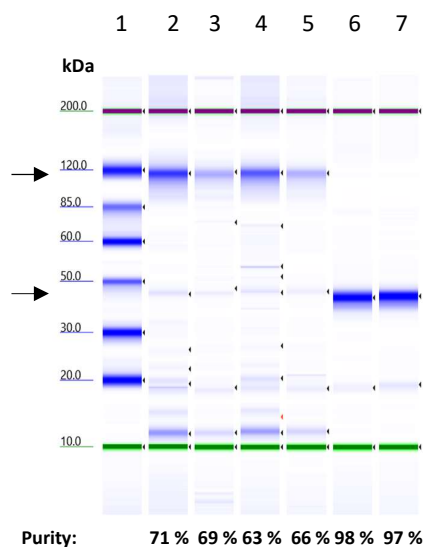


Figure 11. Tape Station 2200 Image of purified control protein and P-domain after electrophoresis. The arrow under the molecular weight marker 120 kDa is pointing at the control protein, and the arrow under the 50 kDa marker is pointing out the band of the P-domain. Lane 1: molecular weight marker, lanes 2 to 5: purified fractions of control protein, lane 6 and lane 7: purified fractions of P-domain. The purities calculated using the Tape Station 2200 Software are shown for the proteins in each fraction under the green line.

The identity of the P-domain was confirmed by LC-ESI-MS/MS (using an Orbitrap) after the protein digestion was accomplished in the gel using trypsin as described in section 6.7.5. The purified P-domain was also recognized by norovirus GII.4 antibody (abcam, ab167024) in a dot-blot as described in section 6.7.4. The identity of the control protein was not further investigated, as the expression vector with the gene was provided in the expression kit and the molecular weight of the protein was detected at the expected size.

The P-domain was produced, purified, and dialyzed against the selection buffer (SB) (buffer composition shown in the material section Table 16) and the P-domain purity of each batch determined using the Agilent Tape Station 2200. The P-domain was produced as needed in 3-4-day intervals for all applications. Freezing of the P-domain protein was observed to lead to precipitation which occurred during storage. Degradation was also noted after several weeks of storage, seen as multiple smaller protein bands in the SDS PAGE gel (data not shown). The control protein did not precipitate upon freezing and was stable when frozen for several weeks; therefore, it was produced less frequently.

3.2 *In vitro* Selection of Aptamers for the NoV P-domain

3.2.1 SELEX

The selection of aptamers for the NoV GII.4 Den Haag P-domain was accomplished by combining the classic SELEX strategy with a combination of negative and counter SELEX (referred to as negative SELEX in the following), as described in section 6.9. Additionally, food matrix-extracts and -suspensions were included in the SELEX process to simulate the aptamer's inherent assay conditions during NoV extraction. The negative SELEX was started in SELEX-round three using the control protein immobilized on cobalt coated paramagnetic particles and conducted as part of every round of SELEX until completion. After the fourth SELEX-round the pre-enriched oligonucleotide library was divided into five parallel SELEX-experiments and the different food matrices introduced to four of these SELEX-experiments by washing the aptamer-target complex with food matrix-extract or -suspension, prepared as described in section 6.9.1. One SELEX-experiment was completed using buffer only. The simplified outline of the study showing the five parallel SELEX-experiments is shown in Figure 12.

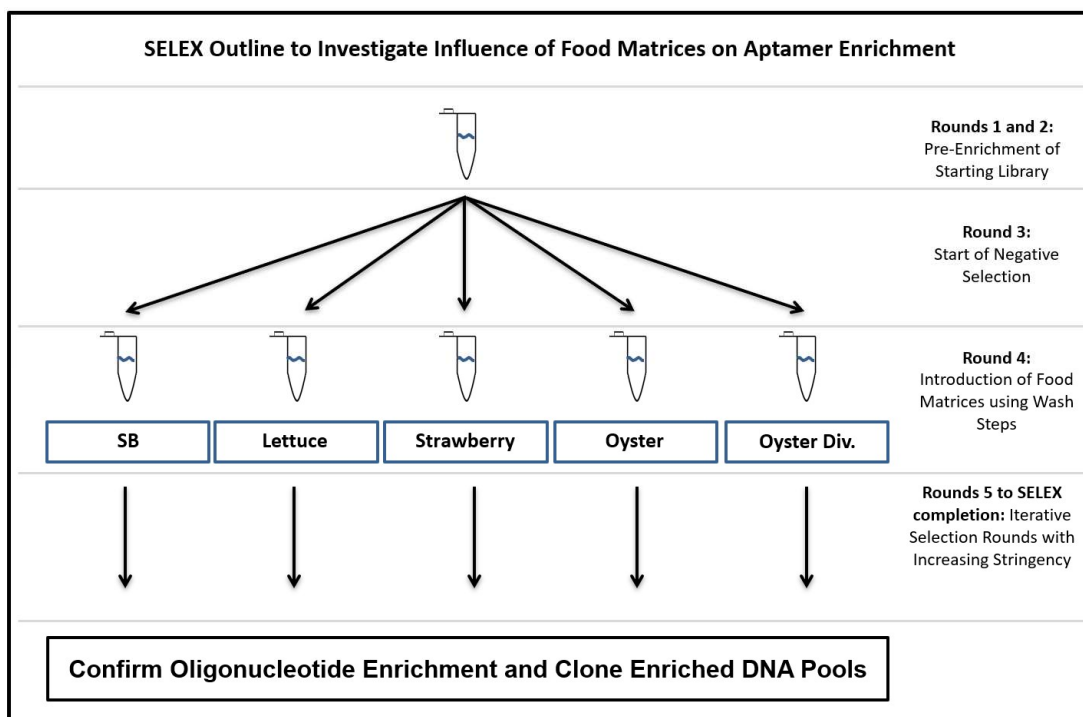


Figure 12. Outline to investigate the influence of food matrix on aptamer enrichment during SELEX.

Results

To increase stringency, the number of washing steps exposing the aptamer-target complex with the food matrices and buffer was gradually increased as the SELEX-experiments proceeded. Throughout the entire study, each SELEX-experiment was handled equally regarding target amount, negative selections, and washing steps with the food matrix for every SELEX-round. The five SELEX-experiments were termed, relative to the food matrix treatment of the aptamer-target complex, as follows:

- **buffer-SELEX-experiment;**
- **lettuce-SELEX-experiment;**
- **strawberry-SELEX-experiment;**
- **oyster-SELEX-experiment;**
- **oyster div.-SELEX-experiment.**

After elution of the target binding oligonucleotides, these were amplified by PCR. For every SELEX-round the number of PCR cycles needed to be determined independently for each SELEX-experiment to accomplish amplification, but avoid the plateau phase during PCR (see section 6.9.3). The PCR products of different numbers of PCR cycles needed for amplification of the eluted P-domain-binding nucleic acid molecules after the seventh SELEX-round are shown below for the five parallel SELEX-experiments (Figure 13). The PCR experiments conducted to amplify nucleic acids during SELEX included a positive control (unselected nucleic acid library) and a negative control using an aliquot of the SB, to monitor possible DNA contamination of SB (Figure 13 (A) and (B)). For the negative control the highest number of PCR cycles was used. The expected size of the PCR product of the oligonucleotide library in the agarose gel was 78 bp including the 40 bp randomized region flanked by the primer annealing sites (18 and 20 bp).

Results

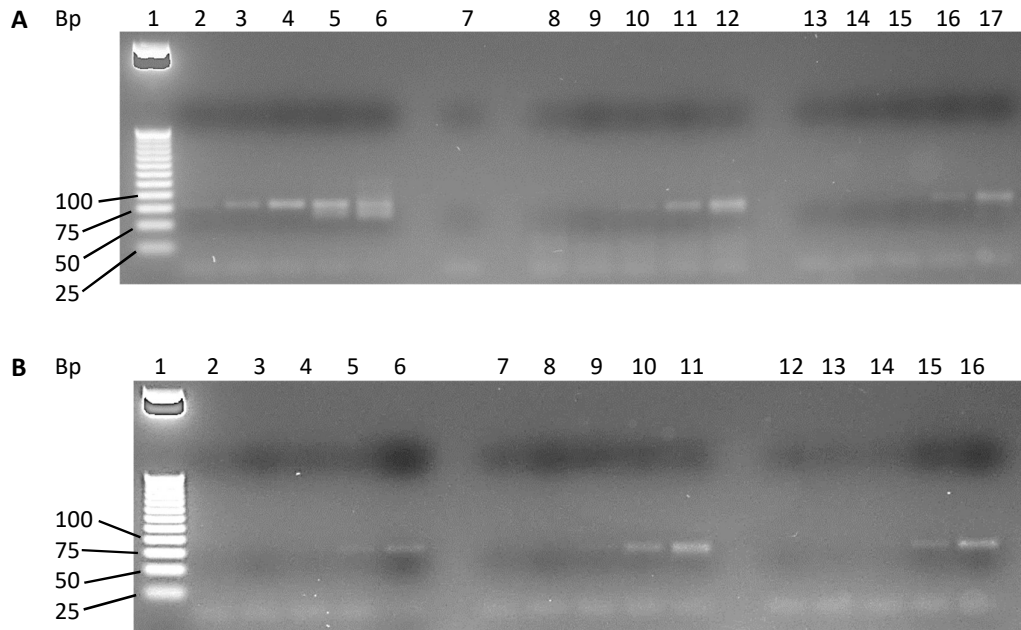


Figure 13. Agarose gel (3%) showing PCR amplicons to determine number of PCR cycles of SELEX-round 7. DNA fragments were separated on a 3 % Agarose gel. (A) Lane 1: 25 bp benchmarker Promega, lane 2, 3, 4, 5, 6: PCR product after cycle 9, 11, 13, 15, 17 respectively for the positive control (1:100000 dilution of unselected library); lane 7: PCR negative control using SB after 17 PCR cycles; lane 8, 9, 10, 11, 12: PCR product after cycle 9, 11, 13, 15, 17 respectively for the oyster-SELEX-experiment; lane 13, 14, 15, 16, 17: PCR product after cycle 9, 11, 13, 15, 17 respectively for the buffer-SELEX-experiment. (B) Lane 1: 25 bp benchmarker Promega, lane 2, 3, 4, 5, 6: PCR product after cycle 9, 11, 13, 15, 17 respectively for the oyster div.-SELEX-experiment; lane 7, 8, 9, 10, 11: PCR product after cycle 9, 11, 13, 15, 17 respectively for the strawberry-SELEX-experiment; lane 12, 13, 14, 15, 16: PCR product after cycle 9, 11, 13, 15, 17 respectively for the lettuce-SELEX-experiment.

For the oyster-, oyster div.-, strawberry- and lettuce-SELEX-experiments, PCR by-product formation throughout all SELEX-rounds was avoided. However, for the buffer-SELEX-experiment a short DNA fragment (about 40 bp) was observed in the agarose gel of the PCR product of SELEX-round 10 (data not shown). Despite efforts taken to avoid the by-product formation, such as reducing PCR cycles, the short PCR by-product was observed in the agarose gels for the remaining SELEX-rounds of the buffer-SELEX-experiment. Oligonucleotides of shorter length were also observed after cloning and sequencing of the enriched oligonucleotide pool after completion of the buffer-SELEX-experiment. The P-domain affinity of these shorter oligonucleotides was assessed in binding studies (see section 3.3.2).

A summary of the experiment conditions during the individual SELEX-rounds including PCR cycles completed for each round for each SELEX-experiment is given in Table 3. For the strawberry-SELEX-experiment no DNA was recovered beyond SELEX-round 9. Therefore, PCR cycles are not indicated for SELEX-rounds 10-16 of the strawberry-SELEX-experiment.

Results

Table 3. Conditions of individual SELEX-rounds including protein amounts, number, and volume of washing steps and PCR cycles for the five parallel SELEX-experiments.

SELEX Round	Amount of target protein (P-domain)	Time Binding step	Number of Wash steps* and volume	PCR Cycles for each SELEX-experiment				
				Buffer	Lettuce	Strawberry	Oyster	Oyster div.
1	370 pmol	30 min	1x300 µL	9	9	9	9	9
2	67 pmol	30 min	2x300 µL	15	15	15	15	15
3	67 pmol	30 min	2x300 µL	15	15	15	15	15
4	77 pmol	30 min	3x300 µL	14	10	10	10	10
5	77 pmol	30 min	3x500 µL	13	9	10	10	10
6	55 pmol	30 min	4x500 µL	15	13	12	12	12
7	55 pmol	25 min	4x500 µL	16	16	15	15	16
8	55 pmol	25 min	4x500 µL	16	16	25	16	16
9	55 pmol	25 min	5x500 µL	16	16	16	15	16
10	55 pmol	25 min	5x500 µL	16	13	-	13	13
11	55 pmol	20 min	5x500 µL	16	13	-	11	13
12	55 pmol	20 min	6x500 µL	21	19	-	19	19
13	55 pmol	20 min	6x500 µL	18	18	-	16	18
14	55 pmol	20 min	6x500 µL	16	14	-	14	14
15	55 pmol	20 min	6x500 µL	15	13	-	14	14
16	55 pmol	20 min	6x500 µL	13	12	-	13	13

* In regard to the washing steps, please note that the number of washing steps given in the table, after the introduction of food matrices in SELEX-round 4, includes the total number of washes including one wash with SB before oligonucleotide elution. Therefore, the number of washing steps with food matrix is represented by the number given minus one.

For all SELEX-experiments, an increase of necessary PCR cycles was observed in the first three SELEX-rounds, until the negative selection was started to rid the oligonucleotide pool of nucleic acids exhibiting non-specific affinity for the SELEX target. Subsequently, a decrease of PCR cycles was observed until SELEX-round 6. However, after the sixth SELEX-round the number of necessary PCR cycles increased again and stagnated until SELEX-round 9 for all five SELEX-experiments. To ensure increasing selection pressure and thereby facilitate a decrease in PCR cycles, the amount

of control protein and paramagnetic beads for the negative SELEX was increased in SELEX-round 9. This led to a decrease in necessary PCR cycles for an additional two SELEX-rounds. In SELEX-round 12 an increase in the number of PCR cycles was observed, following the implementation of an additional washing step with food matrix. However, the number of PCR cycles continued to gradually decrease after SELEX-round 12.

Sixteen rounds of SELEX were completed for the buffer-, lettuce-, oyster-, and oyster div.-SELEX-experiments. Nine rounds of SELEX were completed for the strawberry-SELEX-experiment, as DNA recovery beyond SELEX-round 9 could not be accomplished (see Table 3). In efforts to continue the strawberry-SELEX-experiment beyond the ninth SELEX-round, different approaches were taken: the ninth round of the strawberry-SELEX-experiment was repeated twice using recovered oligonucleotides from the eighth round of the strawberry-SELEX-experiment; for one of these attempts 35 PCR cycles were completed to recover eluted oligonucleotides after the binding step. As these repeated efforts did not lead to successful DNA recovery past SELEX-round 9, the strawberry-SELEX-experiment was terminated.

3.2.2 Affinity of Enriched Nucleic Acid Pools for the P-domain

The target binding of the oligonucleotide pools of the final SELEX-round of each SELEX-experiment were tested by filter retention assay (FRA). For that purpose, single-stranded nucleic acid pools were generated from PCR products of the final SELEX-rounds of each SELEX-experiment by exonuclease digestion. The DNA concentrations were measured after purification post exonuclease digestion and standardized to ensure that all oligonucleotide pools had equal DNA concentrations ensuing comparable results of the FRA. An aliquot of each oligonucleotide pool was subsequently labeled with ^{32}P and the P-domain affinity of the enriched oligonucleotide pools assessed by FRA. To obtain saturation binding curves, target binding was tested in a molar range of 0-600 nM P-domain. For the enriched oligonucleotide pools of the buffer-, lettuce-, oyster-, oyster div.-, and strawberry-SELEX-experiments, maximum P-domain binding of 78 %, 65 %, 43 %, 34 %, and 19 % was assessed, respectively. The unselected oligonucleotide library showed maximum P-domain binding of 6 % at the same concentration (Figure 14).

Results

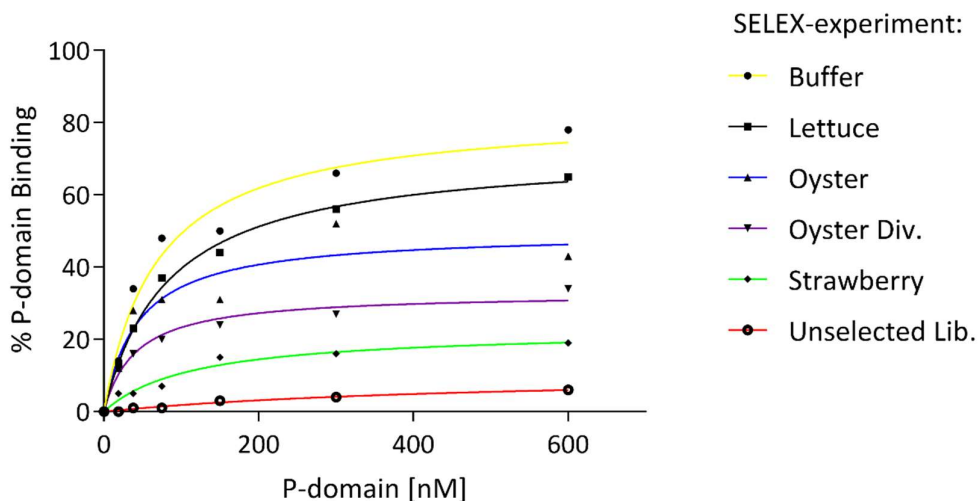


Figure 14. P-domain binding of enriched nucleic acid pools of the final round of each SELEX-experiment. P-domain-binding of final SELEX-round oligonucleotide pools of the five SELEX-experiments and the unselected library was assessed in a molar range of 0-600 nM P-domain.

After target binding of the oligonucleotide pools of each final SELEX-round was confirmed, the enriched pools were cloned and each fifty clones per SELEX-experiment were randomly chosen for sequencing through the company Genewiz®, as described in sections 6.6.2 and 6.9.3.

3.2.3 Sequence Analysis

For each of the five SELEX-experiment 50 clones were analyzed, resulting in a total number of 250 clones, which were randomly selected for sequence analysis of the insert DNA of the recombinant vector. For each SELEX-experiment 40-50 sequences of acceptable quality were obtained (determined by the Genewiz® quality control measures), which are shown in the annex section 9.9 (Table 40-Table 44). The sequences of the most abundant oligonucleotides enriched during the buffer-, lettuce- and strawberry-SELEX-experiments are shown in Table 4 with the according oligonucleotide names and the calculated relative abundances of the oligonucleotides in the enriched oligonucleotide pools of the according SELEX-experiment.

Results

Table 4. Oligonucleotides enriched during the parallel SELEX-experiments with their relative abundances in each oligonucleotide pool of the last SELEX-round. The relative abundances of the oligonucleotides in the last SELEX-round oligonucleotide pools were determined for each SELEX experiment, as indicated in the third and fourth column from the left.

Name of Oligonucleotide	Sequence 5'-3'	SELEX-experiment	Rel. Abundance [%]
Buf-1	GGGTAGAACTAGGCTGTTAACCATGCCCGCACCGACGTA	Buffer	53
		Lettuce	38
Buf-2	GAAATTGGGTTCTGGGTTTGGGTTGGGATTACTTAGCGATG	Buffer	13
		Oyster	4
		Oyster Div.	4
Buf-3	TTTGGTTTGGTTGGTCTGGTATC	Buffer	11
Buf-4	GGTGGGTGGGGGTTTGG	Buffer	15
		Lettuce	3
Buf-5	CATTTTTAGGTTGGGTAGGTTGGTAAAAATTTGTCTCTCT	Buffer	2
Buf-6	CTGGGTTGGGGGCTTATTTAATTTCTACTTTGGGGCGGGG	Buffer	2
Buf-7	AAGGGCGAATTCGCCCT	Buffer	2
Buf-8	GAGGGTCGCATC TTTGGTTTGGTTGGTCTGGTATG	Buffer	2
Let-1	GGACCAACTGATAAATGTTGGCCCCGTCTGAAGGCTAC	Lettuce	20
Let-2	AACGTATAACGCATTGACGTTCTCTTGAAGCTCAGATCGG	Lettuce	18
Let-3	ATAGTCGCTTGACGAGCTTTTTGCCACGCATGCTTGGGTC	Lettuce	8
Let-4	CAACGGATTCTAAAATGTTAGTCCCTCCCCGTCTGAGGGTAGA	Lettuce	8
Let-5	GTCCGGTATCGTGGTGGCTTAGACCAAGCAGTAATGTCTCGA	Lettuce	3
Let-6	CGGGGTGGGGTCTTTTACTGTGCTGCTAATGGGTGGGGGA	Lettuce	3
Straw-1	ACTTGAGGTAAAAAGCGTTTGGGTCGGTGGCGGGGTTTG	Strawberry	7
Straw-2	CATAACCTTCCTTCCATCCCTCCTCCCCACTTCCGCTGTC	Strawberry	5
Straw-3	CCCTTCTCTGTCCCCCTTCCTTCGACCCGTGTTAACC GCA	Strawberry	5
Straw-4	GGCGTGGTATTTTGTGTGTTTCTGTGTAGTGTGTAAAT	Strawberry	5

Results

The enrichment of oligonucleotides in SELEX can be represented by a loss of sequence diversity in the oligonucleotide pool over the course of a SELEX experiment¹⁹¹. This was observed for the buffer- and lettuce-SELEX-experiments. The analysis of sequences obtained from both experiments showed multiple sequences occurring repeatedly, resulting in a formation of eight sequence groups, representing each one oligonucleotide. The most dominating sequence group identified for both the SELEX-experiments was that representing oligonucleotide Buf-1. For Buf-1 a relative abundance of 53 % and 38 % was determined in the oligonucleotide pool of the final SELEX-round of the lettuce- and the buffer-SELEX-experiments, respectively. The additional three predominant sequence groups identified from the buffer-SELEX-experiment were represented by the oligonucleotides Buf-2, Buf-3, and Buf-4 with relative abundances of 13 %, 11 %, and 15 % in the oligonucleotide pool of the last SELEX-round, respectively. Buf-4 was also identified among the obtained sequences of the lettuce-SELEX-experiment and represented by one copy, resulting in a relative abundance in the oligonucleotide pool of the last round of the lettuce-SELEX-experiment of 3 %. Of the remaining sequence groups identified from the lettuce-SELEX-experiment, those representing the oligonucleotides Let-1, Let-2, Let-3, and Let-4 exhibited the highest relative abundances in the last SELEX-round of this experiment (see Table 4).

A loss of sequence diversity in the last SELEX-round nucleic acid pool could not be observed for the strawberry-, oyster- and oyster div.-SELEX-experiments. However, the enriched nucleic acid pools of the oyster- and oyster div.-SELEX-experiments each exhibited two copies of oligonucleotide Buf-2. The obtained sequences for the strawberry-SELEX-experiment showed four oligonucleotides that were represented by two to three copies each (Straw-1 through Straw-4).

In addition to the difference of sequence diversity in the last SELEX-round nucleic acid pools of the five parallel SELEX-experiments, differences in sequence length were observed, in comparison to the starting library (40 nt). Sequences of both Buf-3 and Buf-4 appeared truncated, each consisting of 23 nt and 17 nt, respectively. The sequence of oligonucleotide Buf-3 shared partial identity with the sequence of oligonucleotide Buf-8 (as it is highlighted in bold letters in the sequence of Buf-8 in Table 4). Oligonucleotide Buf-3 also occurred in the last SELEX-round's oligonucleotide pool of the lettuce-SELEX-experiment with relative abundances of 3 %.

3.3 Identification of P-domain Binding Oligonucleotides

3.3.1 Affinity of Selected Oligonucleotides for the Control Protein

The affinity of oligonucleotides Buf-1, Buf-2, Buf-3 and Buf-4 for the P-domain and to the control protein was assessed in a single determination. For that purpose, binding reactions were prepared with Buf-1, Buf-2, Buf-3 and Buf-4 using the P-domain and the control protein in a concentration range of 0-500 nM. To visualize the differences between oligonucleotide-P-domain binding and oligonucleotide-control protein binding at a protein concentration of 250 nM, oligonucleotide-protein-binding was plotted in a bar graph. The oligonucleotide binding to the P-domain was normalized to 100 % and oligonucleotide binding to the control protein was calculated in relation to P-domain binding for each oligonucleotide (Figure 15).

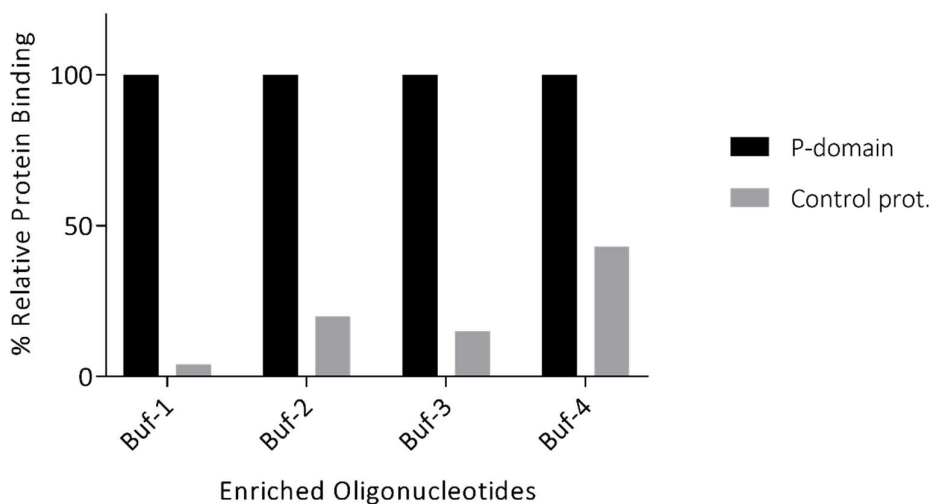


Figure 15. Binding of selected enriched oligonucleotides to the P-domain and the control protein. Protein binding was calculated at a concentration of 250 nM. P-domain binding was normalized to 100 % and binding to control protein calculated in relation.

3.3.2 Affinity of Selected Oligonucleotides for the NoV P-domain

In accordance to their abundance in the enriched oligonucleotide pools of the buffer-, lettuce- and strawberry-SELEX-experiments, the P-domain-affinities of various aptamer candidates were evaluated by FRA (Figure 16). P-domain binding of oligonucleotides from the nucleic acid pool of the last SELEX-rounds of both the oyster- and the oyster div.-SELEX-experiments, except for Buf-2, was not assessed, as only modest enrichment was observed in both SELEX-experiments.

Results

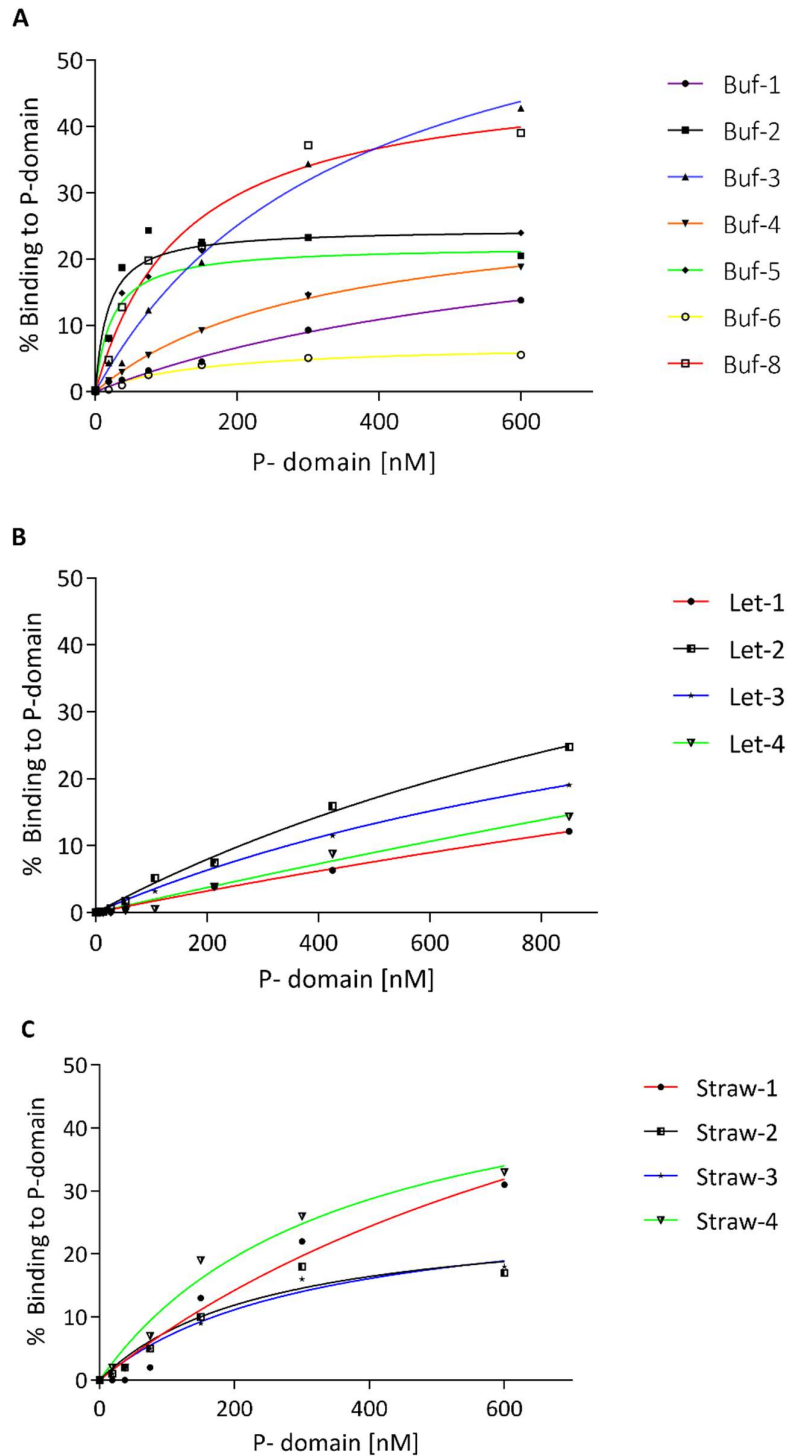


Figure 16. P-domain binding curves of oligonucleotides enriched in the buffer-, lettuce- and strawberry-SELEX-experiments. The binding curves shown, were generated with approximately 1 nM ^{32}P labeled aptamer candidate and 0-600 nM P-domain for the candidates of the buffer- and strawberry-SELEX-experiments, and 0-800 nM P-domain for the candidates of the lettuce-SELEX-experiment. (A) Binding graphs of oligonucleotides Buf-1 through Buf-6 and Buf-8. (B) Binding graphs of oligonucleotides Let-1 through Let-4. (C) Binding graphs of oligonucleotides Straw-1 through Straw-4.

Results

Oligonucleotides Buf-2, Buf-5, and Buf-8 each exhibited a low K_d value of 20 nM, 24 nM and 130 nM, respectively (Figure 16 (A)). The binding curves of oligonucleotides Buf-1, Buf-3 and Buf-4 exhibited a linear character which is reflected in the higher determined K_d values of 700 nM, 360 nM, and 314 nM, respectively (Figure 16 (A)). The binding curves of oligonucleotides Let-1 through Let-4 also appeared linear (Figure 16 (B)), resulting in higher K_d values in the low micromolar range of 4.7 μ M, 1.6 μ M, 1.4 μ M, and 7.1 μ M for Let-1, Let-2, Let-3 and Let-4, respectively. Oligonucleotides enriched during the strawberry-SELEX-experiment, exhibited K_d values in the high nanomolar range. For oligonucleotides Straw-1, Straw-2, Straw-3 and Straw-4 K_d values of 970 nM, 250 nM, 320 nM and 350 nM were determined, respectively (Figure 16 (C)).

3.4 Characterization of Aptamer Candidates

3.4.1 Determination of Aptamer-Target Selectivity, Affinity and Specificity

The selectivity of aptamer candidates Buf-1, Buf-2, and Buf-8 was tested in duplicate by FRA using the P-domain, BSA, lysozyme, and thrombin proteins (the promising results obtained in first FRA experiments for Buf-5 were not reproducible and the candidate therefore not further characterized). The proteins were chosen based on in house availability. The maximum protein binding of each oligonucleotide at protein concentration of 250 nM was normalized to 100 % and binding to the other proteins calculated relative to the maximum binding (see Figure 17).

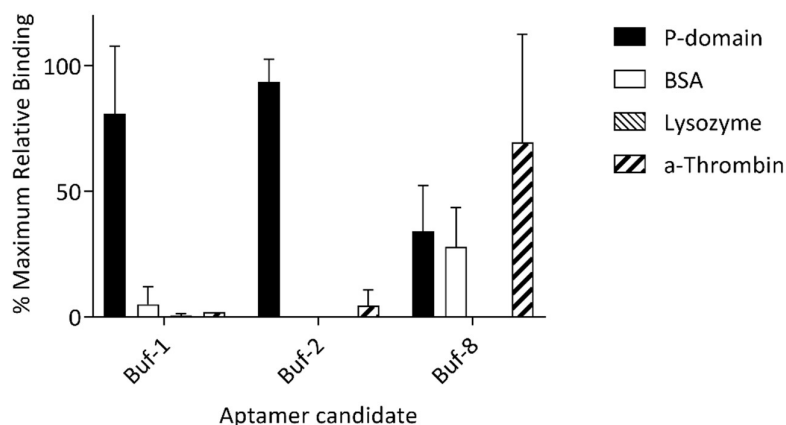


Figure 17. Binding of aptamer candidates to different proteins. Aptamer candidates are shown on the x-axes and aptamer protein binding on the y-axes. Aptamer selectivity was determined by FRA using 500 nM of purified P-domain, BSA, lysozyme and thrombin. Studies were conducted in duplicate and maximum protein binding (for Buf-1 and Buf-2 maximum protein binding was observed for the P-domain, for Buf-8 maximum binding was observed to thrombin) of each candidate normalized to 100 %.

Both oligonucleotides Buf-1 and Buf-2 exhibited the highest binding to the P-domain and only minor binding to BSA, lysozyme, and thrombin (maximum binding to P-domain was normalized to 100 %). Oligonucleotide Buf-8 exhibited the highest binding affinity to thrombin and bound BSA with a similar affinity as it did the P-domain (maximum binding to thrombin was normalized

Results

to 100 %). As Buf-8 did not bind the target with high selectivity, this aptamer candidate was not investigated further.

FRAs were completed in triplicate to determine the K_d values for target interaction of Buf-1 and Buf-2 in the molar range of 0-600 nM P-domain (Figure 18). For candidates Buf-1 and Buf-2 K_d values of 560 ± 144 nM (R^2 : 0.90) and 17 ± 7 nM (R^2 : 0.79) and were assessed, respectively.

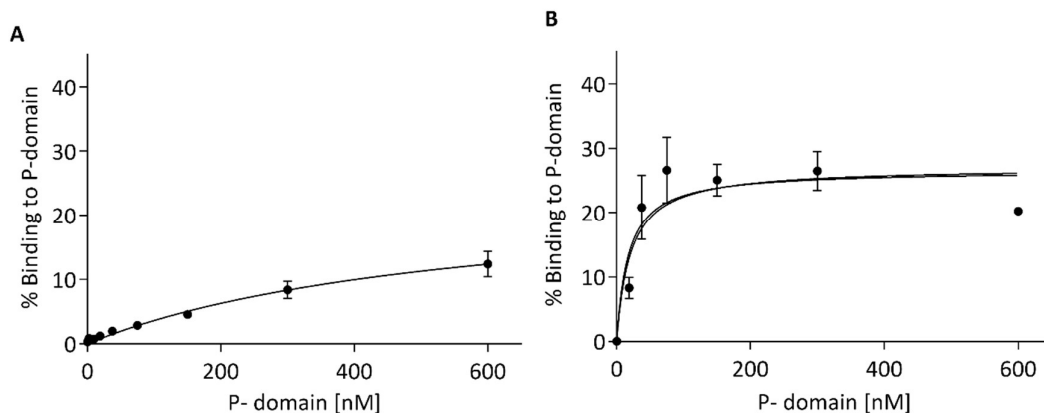


Figure 18. Affinities of oligonucleotides Buf-1 and Buf-2 for the P-domain. Binding studies were completed by FRA. (A) Determination of K_d value for candidate Buf-1 by FRA using a P-domain concentration range of 0-600 nM in a triplicate. (B) Determination of K_d value for candidate Buf-2 by FRA using a P-domain concentration range of 0-600 nM in a triplicate.

The P-domain binding specificity of oligonucleotides Buf-1 and Buf-2 was assessed by adding the unlabeled oligonucleotides Buf-1 and Buf-2 (specific competitor) and unlabeled thrombin aptamer (non-specific competitor) to the (labeled) aptamer-P-domain binding reaction (Figure 19 (A)). Average binding of the labeled aptamer candidate was determined at the P-domain concentration of 250 nM in presence of specific competitor, non-specific competitor and absence of competitor. Based on the resulting mean values of P-domain binding under these three conditions, the relative inhibition caused by the competitors was calculated. In presence of the specific competitor P-domain binding of Buf-1 and Buf-2 was inhibited by 99 % and 92 %, respectively. In presence of the non-specific competitor, Buf-1 and Buf-2 were inhibited by approximately 92 % and 11 %, respectively.

Additionally, target binding of Buf-1 and Buf-2 in presence of dextran sulfate was assessed (Figure 19 (B)). P-domain binding of aptamer candidates Buf-1 and Buf-2 was inhibited in presence of dextran sulfate by approximately 83 % and 47 %, respectively.

Results

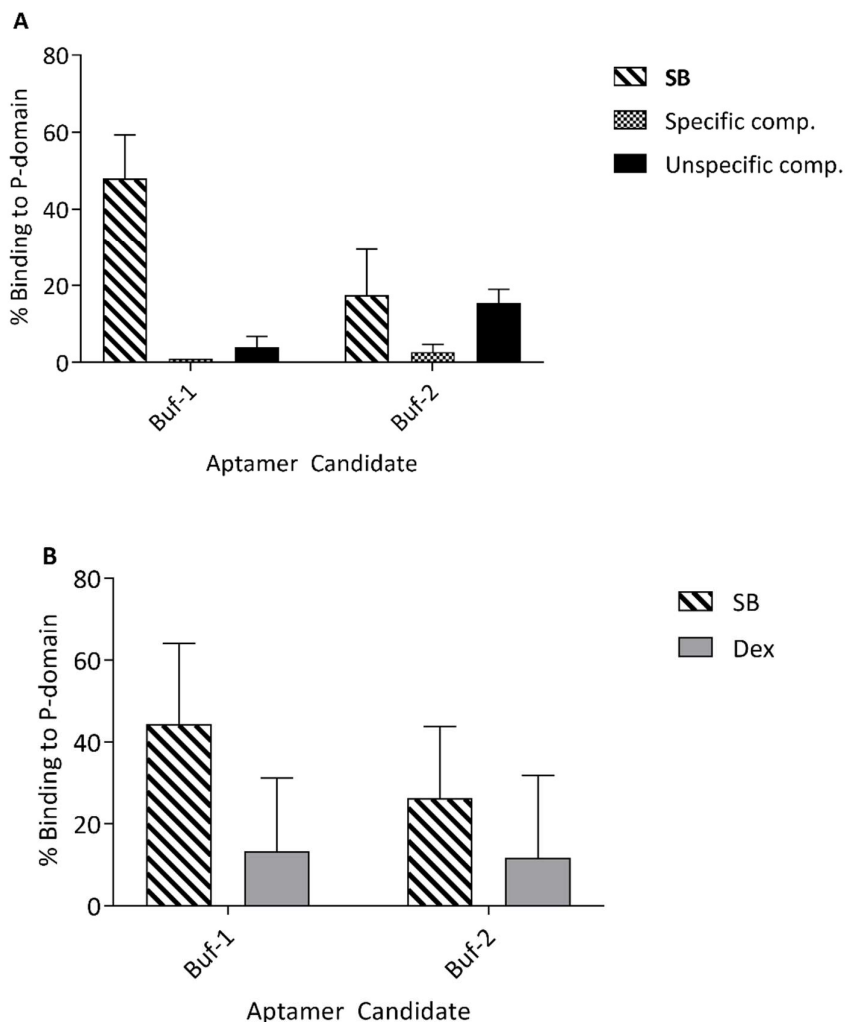


Figure 19. P-domain binding of Buf-1 and Buf-2 in presence of different competitors. (A) Binding of candidates Buf-1 and Buf-2 in presence of selection buffer (SB) and a 50-fold excess of each unlabeled aptamer candidate (specific comp.) and 50-fold excess of unlabeled TBA aptamer (nonspecific comp.). (B) Binding of Buf-1 and Buf-2 to the P-domain in presence of 5% dextran sulfate. The binding to the P-domain was determined by FRA using a final concentration of purified P-domain of 250 nM in a triplicate.

3.4.2 Structure Analysis of Aptamer Buf-2

The sequence of aptamer Buf-2 (Table 4) shows a high G content (40%). In addition, a motif was observed consisting of 20 nts following the ensuing pattern: 5'-GGGY₃GGGY₃GGGY₂GGG-3' with Y representing the nucleotides of C and T. Different DNA structures can be distinguished based on CD spectroscopy. To investigate the global three-dimensional structure of the oligonucleotide Buf-2, CD spectra were measured of the full length 40 nt oligonucleotide Buf-2, the 20 nt motif without the 3'-end (Buf-2 variant 1), the 20 nt motif without the 5'-end (Buf-2 variant 2), and the 20 nt motif by itself (Buf-2 variant 3) (Table 5).

Results

Table 5. Names and sequences of Buf-2 variants investigated by CD spectroscopy

Name	Sequence 5'-3'
Buf-2	GAAATTGGGTTCCGGGTTGGGTTGGGATTACTTAGCGATG
Buf-2 variant 1	GAAATTGGGTTCCGGGTTGGGTTGGG
Buf-2 variant 2	GGGTTCCGGGTTGGGTTGGGATTACTTAGCGATG
Buf-2 variant 3	GGGTTCCGGGTTGGGTTGGG

The commonly used online tool 'mfold'¹⁹² was not used to predict aptamer folding in this case, as quadruplex structures cannot be treated using this software application. Therefore, CD spectroscopy was used to estimate oligonucleotide structure of the four Buf-2 variants (Figure 20). The CD spectra of the different oligonucleotides showed that each oligonucleotide exhibited a different absorbance pattern in spectral region of 220 nm to 340 nm.

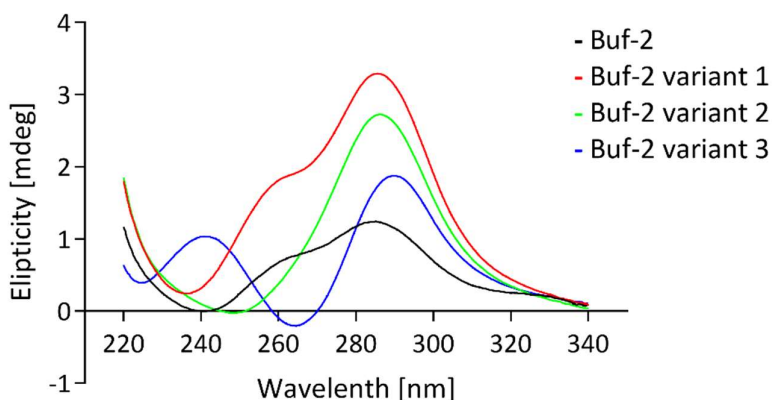


Figure 20. CD spectra of different oligonucleotides derived from aptamer Buf-2 to investigate Buf-2 structure. CD spectra of oligonucleotides were recorded in SB. The curves shown in the spectra were smoothed using the LOWESS function in GraphPad Prism.

Oligonucleotide Buf-2 exhibited two maxima at 288 nm and 265 nm, but no clear minimum between the peaks. For oligonucleotide Buf-2 variant 1 a similar pattern was observed with two maxima at 288 nm and 261 nm without a clear minimum between the peaks. However, an increased intensity of the amplitude compared with the Buf-2 curve was apparent for Buf-2 variant 1. The CD curve of oligonucleotide Buf-2 variant 2 showed only one maximum at 289 nm and a minimum at 252 nm. The curve of Buf-2 variant 3 showed two distinct maxima at 289 nm and 243 nm as well as a minimum at 265 nm.

In efforts to determine the P-domain binding motif and to truncate the 40 nt aptamer, the P-domain affinity of the different Buf-2 variants was investigated via FRA. The detected

Results

autoradiography signal for the different oligonucleotides is shown in Figure 21 (A), studies were conducted in duplicate. Maximum protein binding of oligonucleotide Buf-2 was normalized to 100 % and P-domain binding of the Buf-2 variants was calculated in relation. The binding curves are shown in Figure 21 (B).

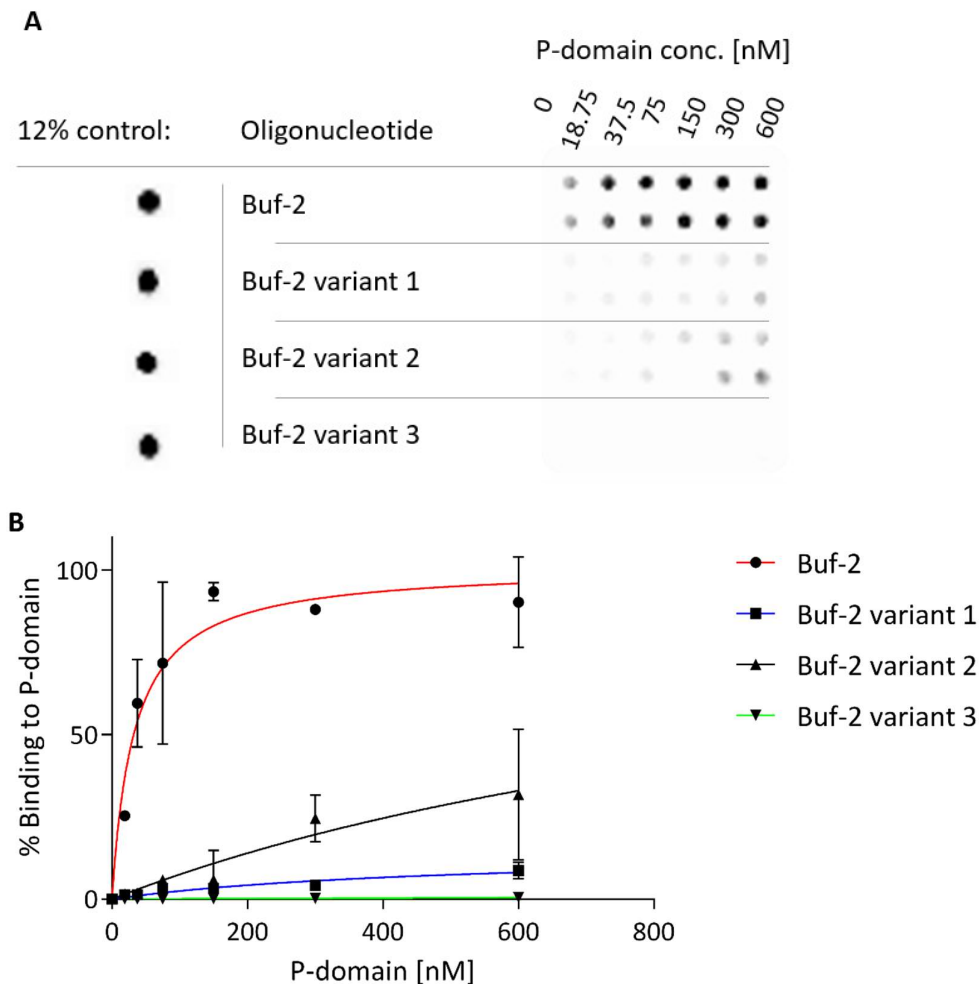


Figure 21. P-domain binding curves of different oligonucleotide variants derived from aptamer Buf-2. The binding of the different Buf-2 variants was tested via FRA. (A) Image of autoradiography signals after a FRA. The positive control, equaling 12 % of the labeled oligonucleotide in the filtrate is shown to the left. FRA were completed in a duplicate per variant and for a P-domain concentration range of 0-600nM. (B) The graph shows the matching blotted curves of the FRA.

The FRA studies show that none of the Buf-2 variants exhibited P-domain binding. As structure analysis was not the focus of this work, further regarding analysis was not conducted. However, results of the binding studies assessing the affinity of Buf-2 and the Buf-2 variants for the P-domain revealed, that the aptamer Buf-2 could not be truncated without loss of its P-domain affinity.

3.5 Aptamer P-domain Binding in Presence of Food Matrices

Representative oligonucleotides from the buffer-, lettuce-, and strawberry-SELEX-experiments were chosen based on their P-domain affinities assessed in previous binding studies (see section 3.3.2). Their P-domain binding in presence of food matrices was tested by adding food matrix-extracts and -suspensions to the oligonucleotide-target binding step prior to the filtration step of the FRA as described in section 6.10.3. The mean binding percentage of each oligonucleotide was calculated for the P-domain after background subtraction at the concentration of 250 nM (Figure 22). The P-domain affinity of candidate Straw-4 was marginal in these repeated studies; therefore, results for Straw-4 are not shown.

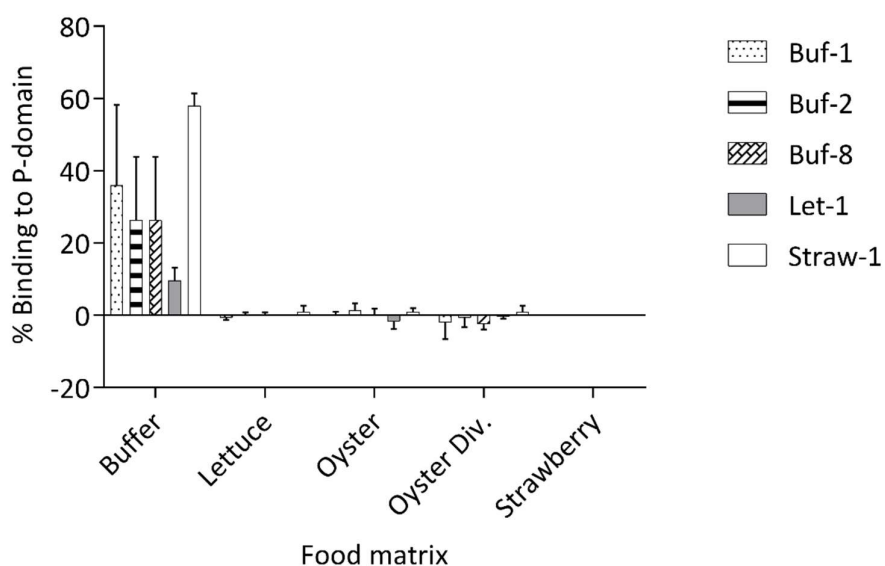


Figure 22. P-domain binding of aptamer candidates Buf-1, Buf-2 and Buf-8, Let-1 and Straw-1 in presence of food matrices. The oligonucleotide-P-domain binding in presence of the different food matrices was calculated for the P-domain concentration of 250 nM.

P-domain binding of the tested oligonucleotides (Buf-1, Buf-2, Buf-8, Let-1, and Straw-1) in presence of food matrices was not observed using the FRA method. However, since aptamer Buf-2 was highly enriched in the buffer-SELEX-experiment and in the oyster- and oyster div.-SELEX-experiments, the P-domain binding of this particular oligonucleotide in presence of oyster matrices was further investigated. As described in section 1.1.6 there are different types of oysters that enter the retail market. Therefore, an oyster-suspension and an oyster-preparation were generated from locally harvested fresh oysters from Cedar Point, Alabama (CP) as well as from locally purchased individually quick-frozen oysters (IQF). Using CP and IQF oysters, 10 % suspensions were prepared in SB using oyster homogenate (see section 6.10.3). Additionally, CP and IQF oyster homogenate was suspended in SB and further purified as described in section 6.10.3, to generate CP and IQF ‘preparations’. To compare target binding in presence of the

Results

different oyster matrices, P-domain binding of Buf-2 in SB was normalized to 100 % and P-domain binding curves in presence of undiluted CP and IQF suspensions and CP and IQF preparations shown relative to the binding curve of aptamer Buf-2 in SB (Figure 23).

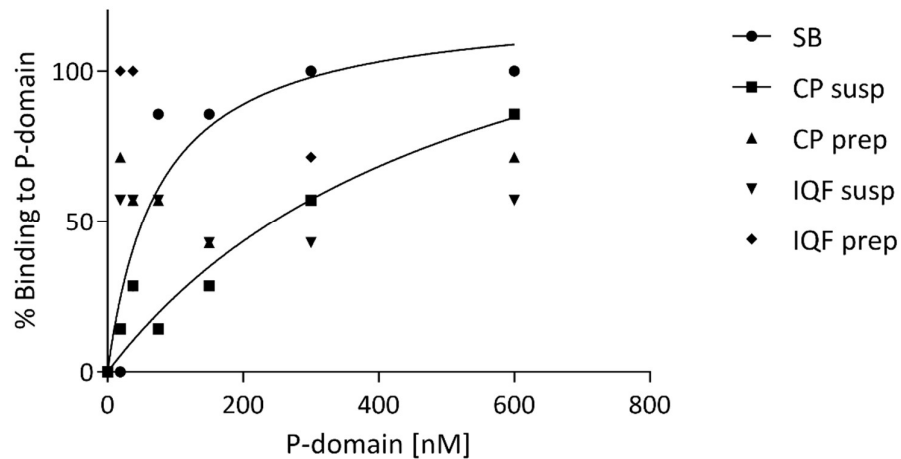


Figure 23. P-domain binding of aptamer Buf-2 in presence selection buffer (SB) and CP and IQF oyster preparations (CP and IQF prep) and suspensions (CP and IQF susp). Saturation binding curves were assessed for Buf-2 and the P-domain in a molar range of 0-600 nM. Curves were blotted for the Buf-2-P-domain binding in SB and in CP-oyster-suspension (CP susp).

Data points obtained to assess the P-domain binding of Buf-2 in presence of the IQF suspension and the IQF preparation as well as data points obtained for Buf-2 binding the P-domain in presence of the CP preparation did not fit the typical saturation binding model. However, P-domain binding data obtained in presence of CP suspension allowed the plotting of a saturation binding curve. The resulting curve appeared more linear compared to the Buf-2 binding curve in SB, which is reflected in the K_d values assessed in both binding scenarios. The determined K_d value for the P-domain and aptamer Buf-2 in SB in this experiment was 76 nM, the K_d value determined for the two ligands in the presence of CP suspension was 545 nM. This confirms previous results, that binding in undiluted food matrices proves difficult. Therefore, the P-domain binding of Buf-2 was investigated in a tenfold dilution of both the IQF and CP suspensions and the IQF and CP preparations. Results are presented with the P-domain binding of Buf-2 in SB normalized to 100 %. (Figure 24).

Results

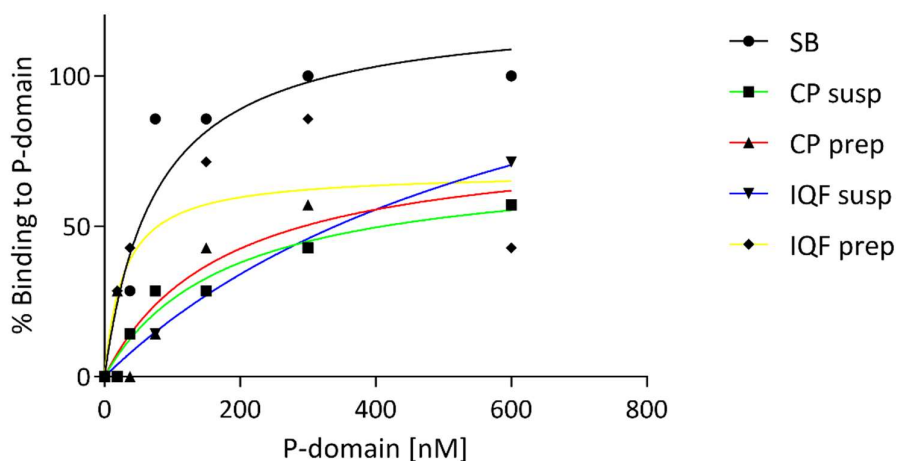


Figure 24. Binding of aptamer Buf-2 in presence selection buffer (SB) and of tenfold diluted CP and IQF oyster preparations (CP and IQF prep) and suspensions (CP and IQF susp). Saturation binding curves were determined for Buf-2 and the P-domain in a molar range of 0-600 nM.

Binding data obtained for the CP-suspension and the CP preparation, as well as for the IQF preparation resulted in data, allowing the blotting of saturation binding curves. A K_d value for Buf-2-P-domain binding was assessed in presence of tenfold diluted CP preparation, CP suspension, and IQF preparation of 179 nM, 176 nM, and 28 nM, respectively. However, Buf-2-P-domain binding in the presence of IQF suspension resulted in a rather linear binding curve, with a resulting K_d value of 688 nM. The binding curves obtained for the P-domain and Buf-2 in tenfold dilutions of the oyster-suspensions and oyster-preparations show that aptamer-target binding can be facilitated using less concentrated oyster matrices.

3.6 NoV Aptamers in Comparison

3.6.1 Motif Search Between Published Sequences

Prior to performing binding studies, a motif search was conducted to discover whether oligonucleotides enriched throughout all published SELEX efforts for the selection of aptamers for the NoV surface shared a common sequence motif. For this purpose, oligonucleotide sequences were compared using the online tool open software MEME suite¹⁹³. The abbreviation MEME describes the search parameters and stands for Multiple expectation maximization for Motif Elicitation.

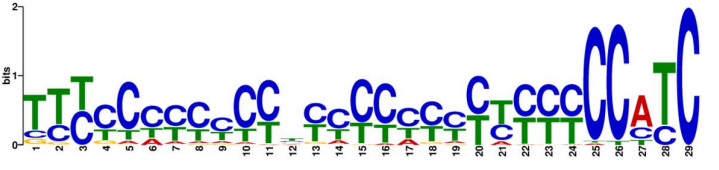
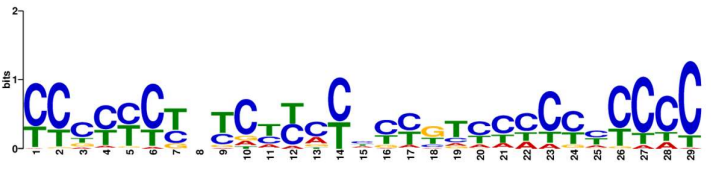
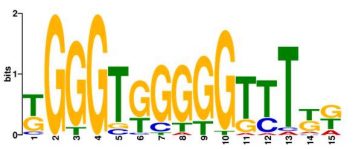
Common sequence motifs among oligonucleotides enriched in different SELEX experiments could suggest motifs that bind to the same site of the NoV surface protein. In this MEME search all sequences obtained for the five SELEX-experiments conducted in this work were included (shown in Table 40 to Table 44). Additionally, sequences published in previous efforts to select aptamers

Results

for NoV were included, as given in the studies described hereafter. In a 2015 study, 34 sequences obtained after cloning of the PCR product of SELEX-rounds 4, 7, and 9 during *in vitro* selection for NoV were published¹⁹⁰. Moore et al.¹⁸⁹ published six sequences, Giamberardino et al.¹⁸⁸ published three sequences, and Beier et al.¹⁸⁷ published one sequence.

For each motif search, the open software MEME calculates an E-Value and suggests that motifs discovered with an E-Value higher than 0.05 are not statistically relevant. Of 12 motifs discovered in this work, as per conditions selected for the motif search, only three motifs had an E-Value lower than 0.05 and thus were statistically significant. The three motifs are displayed below (Table 6). In cases where nucleotides between the different sequences were not identical, multiple nucleotides are shown staggered on top of one another.

Table 6. Relevant motifs detected in sequences of oligonucleotides enriched in SELEX efforts to select an aptamer for the NoV surface.

Motif Name	Discovered Motif	Sites*	Width [nt]
Motif 1		50	29
Motif 2		50	29
Motif 3		22	15

* the term 'site' is used by meme to describe the number of sequences in the search that match the particular motif

The first motif consisted of 29 nucleotides with high representation of Cs and Ts. 23, 21, and 5 oligonucleotide sequences matching motif 1 were identified in the enriched oligonucleotide pools of the oyster-, oyster div.-, and the strawberry-SELEX-experiment, respectively. Additionally, one oligonucleotide with motif 1 matching sequence was discovered by Escudero-Abarca et al. and named SMV 20.

As observed for motif 1, Cs and Ts were also highly represented in motif 2. Among motif 2 matching oligonucleotide sequences 14, 17, and 15 oligonucleotides were identified in the last

Results

SELEX-round's oligonucleotide pools of the oyster-, oyster div.-, and strawberry-SELEX-experiments, respectively. Two oligonucleotide sequences published by each Escudero-Abarca et al⁵⁶ (not given a name in the original publication) and Moore et al¹⁸⁹ (M 5, M 132) matched motif 2 as well.

It is noticeable that the motifs 1 and 2, even though identified by MEME suite as statistically significant, showed a high variability amongst the 29 nucleotides. This is depicted by multiple nucleotide representing letters shown at the same position (see Table 6). Additionally, it was observed, that oligonucleotides matching the motif's sequences were not noticeably enriched during SELEX-experiments conducted in this work. Among the oligonucleotide sequences matching motif 2 were those of oligonucleotides Straw-2, and Straw-3 (Table 7). The P-domain binding of these aptamer candidates was previously studied (section 3.3.2) and did not exhibit good binding to the P-domain.

Table 7. Selected oligonucleotides which sequences included the motif site.

Name	Matching motif	3'end	Motif (3'-5')	5'end
Straw-2*	2	CATAA	CCTTCCTTCCATCCCTCCTCCCCACTT	GCTGTC
Straw-3*	2		CCCTTCTCTGTCCCCCTTCTTCGACCCCT	GTTTAACCGC
Buf-4*	3	GG	TGGGTGGGGGTTGG	-
Buf-2*	3	GAAAT	TGGGTTGGGGTTGG	GTTGGGATTA
Straw-1*	3	ACTTGAGGTAAAA AGCGTTTGGGTC	GGTGGCGGGGTTGG	
SMV 19	3	CACCAG	TGTGTTGAGGTTGA	GCACACTGAT
Buf-6*	3	C	TGGGTTGGGGCTTA	TTTAATTCT

* Affinity for P-domain of these oligonucleotides has been studied previously (Figure 16)

The sequence of the third statistically significant motif discovered through MEME consisted mainly of Gs. Eleven oligonucleotides with sequences matching the motif were identified in the enriched oligonucleotide pool of the strawberry-SELEX-experiment, including the sequence of oligonucleotide Straw-1. Additionally, two oligonucleotides with corresponding sequences were identified in each of the enriched oligonucleotide pools of the lettuce- and oyster- div.- SELEX experiments, and three oligonucleotides with corresponding sequences were identified in the enriched oligonucleotide pools of the buffer- and oyster-SELEX-experiments. Among these

oligonucleotides were Buf-2, Buf-4 and Buf-6 as well as the oligonucleotide SMV-19. Oligonucleotide SMV-19 was selected and further characterized by Escudero-Abarca et al⁵⁶. The possible role of this motif will be further discussed in section 4.4.1.

3.6.2 Aptamer Affinity for a Variety of NoV VLPs

To investigate the binding of published NoV aptamers to various NoV VLPs, binding studies were completed using FRA with VLPs of NoV genotypes GI.1, GI.7, GII.3 and GII.4 Sydney and New Orleans. The VLPs were generously provided by Dr. Robert Atmar of the Baylor College of Medicine, Houston TX. The aptamer affinity to VLPs of five NoV genotypes was evaluated using FRA. The aptamer AG3 without primer annealing sites was not included in this study, as VLP amounts were limited. The aptamer AG3 was used including its primer annealing sites in its originally published application, and was therefore also used including its primer annealing sites in this work to stay consistent with previously published data¹⁸⁸.

The VLP concentrations for the FRA ranged from 0-1500 nM. VLP amounts available were sufficient to perform FRA binding studies in triplicate for seven aptamers. The selected aptamers are shown in Table 1 in the theoretical section. The aptamer-VLP binding curves are shown below. Each graph shows the binding of one aptamer to VLPs of the five NoV genotypes GI.1, GI.7, GII.3 and GII.4 Sydney and GII.4 New Orleans. VLP binding of aptamers Buf-2, Beier, AG3, SMV 19, SMV 21, M 1, and M 6-2 are shown in Figure 25, Figure 26, Figure 27, Figure 28, Figure 29, Figure 30, and Figure 31, respectively. All figures are shown with the y-axes indicating bound DNA to target protein from 0-80 %, to allow uniform evaluation of the graphs.

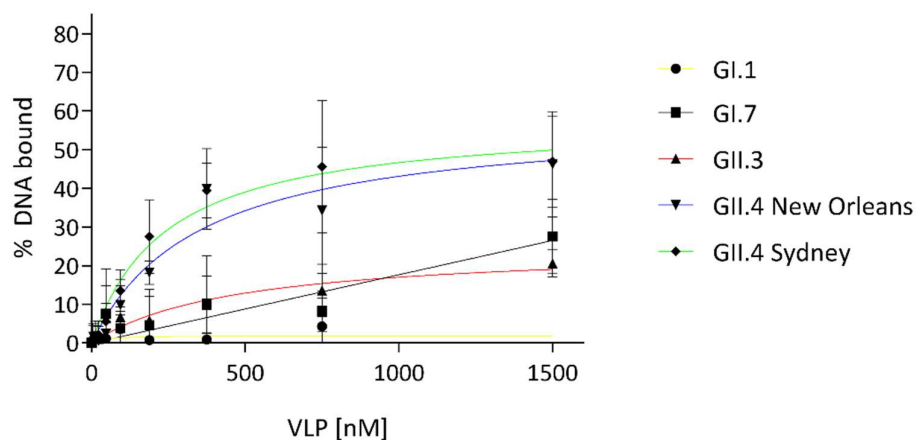


Figure 25. Binding of the aptamer Buf-2 and VLPs of NoV genotypes GI.1, GI.7, GII.3, GII.4 New Orleans, and GII.4 Sydney

Results

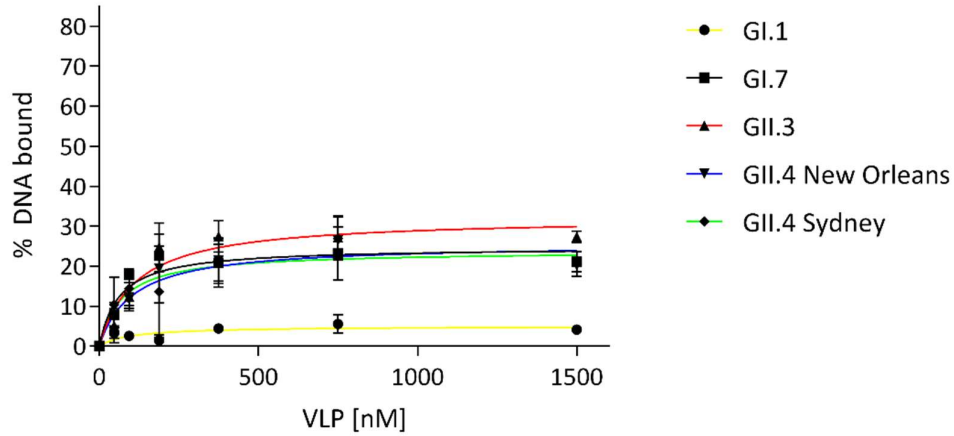


Figure 26. Binding of the aptamer Beier and VLPs of NoV genotypes GI.1, GI.7, GII.3, GII.4 New Orleans, and GII.4 Sydney

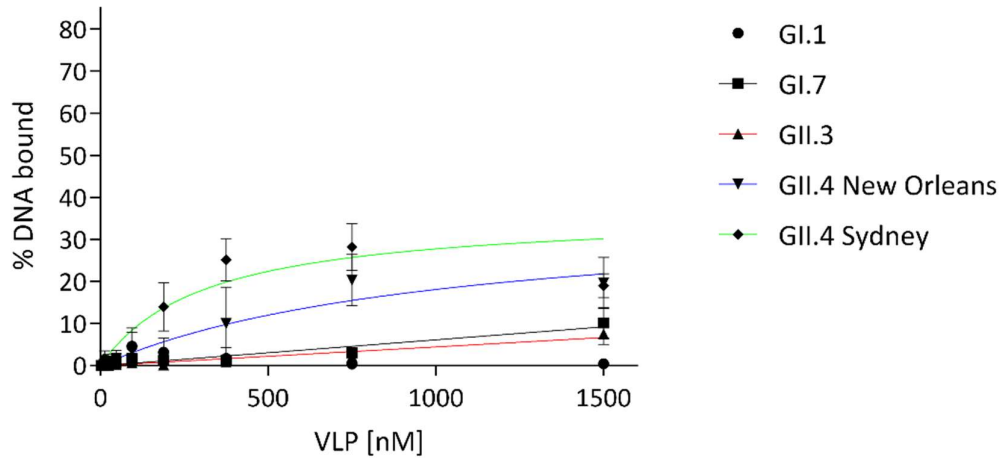


Figure 27. Binding of the aptamer AG3 and VLPs of NoV genotypes GI.1, GI.7, GII.3, GII.4 New Orleans, and GII.4 Sydney.

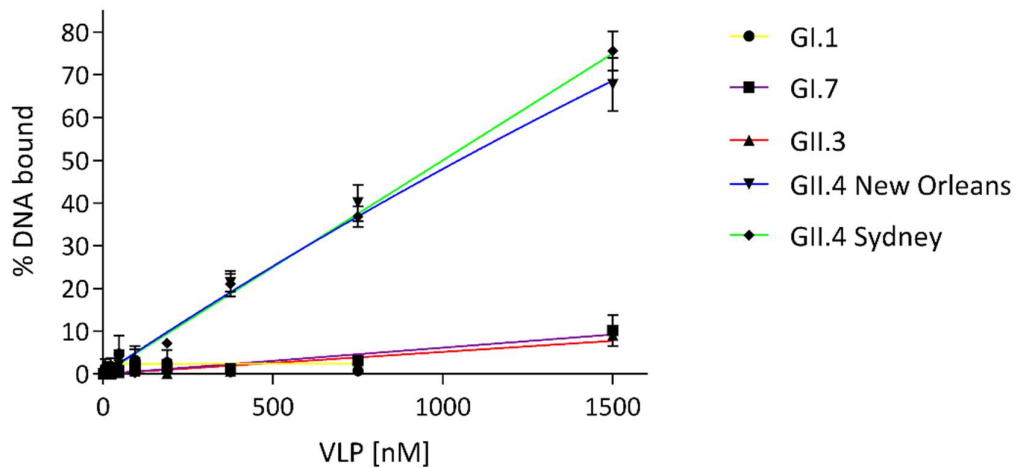


Figure 28. Binding of the aptamer SMV-19 and VLPs of NoV genotypes GI.1, GI.7, GII.3, GII.4 New Orleans, and GII.4 Sydney.

Results

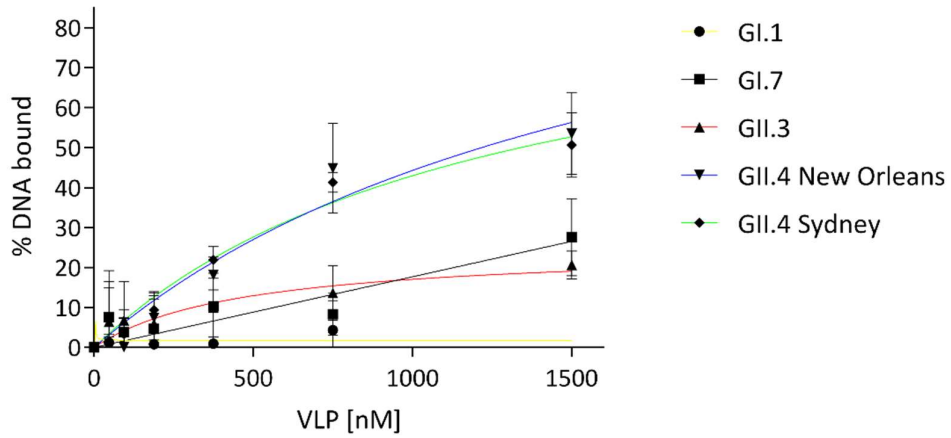


Figure 29. Binding of the aptamer SMV-21 and VLPs of NoV genotypes GI.1, GI.7, GII.3, GII.4 New Orleans, and GII.4 Sydney.

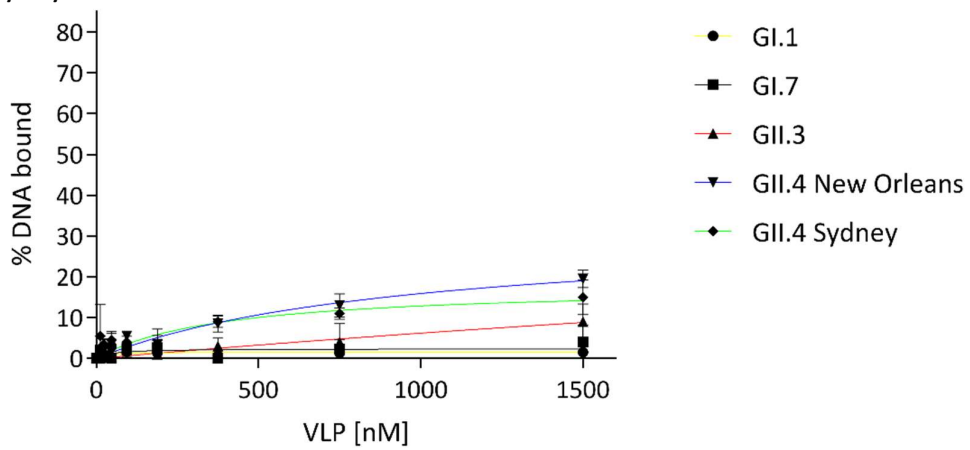


Figure 30. Binding of the aptamer M 1 and VLPs of NoV genotypes GI.1, GI.7, GII.3, GII.4 New Orleans, and GII.4 Sydney.

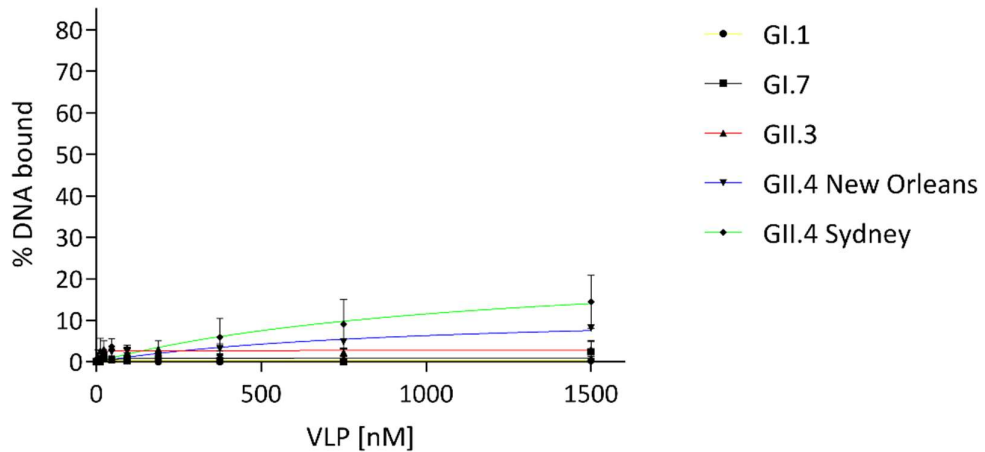


Figure 31. Binding of the aptamer M 6-2 and VLPs of NoV genotypes GI.1, GI.7, GII.3, GII.4 New Orleans, and GII.4 Sydney.

Results

Binding curves displaying VLP binding of aptamers SMV 19 and M 6-2 with VLPs of all genotypes exhibit linear character. However, the overall VLP binding of SMV 19 was high with approximately 76 % maximum binding to GII.4 Sydney VLPs at a concentration of 1500 nM. The overall VLP binding of M 6-2 was comparatively lower, with the maximal VLP binding observed for genotype GII.4 Sydney of approximately 14 % at a VLP concentration of 1500 nM.

Aptamers SMV 21, and M 1 showed the highest binding affinities to VLPs of genotype GII.4 New Orleans and GII.4 Sydney. SMV 21 showed a higher overall binding to the VLPs of approximately 50 % for the GII.4 genotypes compared to the overall VLP binding of M 1 of approximately 15-20 % for the same genotypes. Only moderate affinity to VLPs of GII.3 were observed for both SMV 21 and M 1. Binding affinities of these two aptamers for NoV genotypes GI.7 and GI.1 were marginal.

Buf-2 and AG3, showed highest binding affinities to VLPs of genotype GII.4 Sydney. Buf-2 showed an equally high affinity for GII. 4 New Orleans, but only low affinity for GII.3 and GI.7, as the binding curves to VLPs of the latter genotypes exhibited a linear character. A similar affinity pattern was observed for AG3 with lower binding affinities throughout. The binding affinities of both aptamers AG3 and Buf-2 to GI.1 were marginal.

Aptamer Beier showed the highest affinity to VLPs of genotype GII.3, but similar affinities were observed to VLPs of the GII.4 genotypes and GI.7. The affinity of Beier for GI.1 was marginal.

The determination of a K_d is only reasonable for those aptamer VLP interactions that resulted in a saturation binding curve. For aptamer SMV 19 a K_d was assessed for GII.4 New Orleans. For candidates M 1, M 6-2, SMV 21, and AG3 a K_d was each determined for binding to the NoV genotypes GII.4 New Orleans and Sydney. The aptamer Beier showed a broad binding affinity throughout the NoV genotypes, with the plotted binding curve reaching the plateau phase visibly at VLP concentrations below 400 nM. This is reflected in the K_d values determined for each NoV genotype, except for GI.1 as overall binding of Beier to VLPs of this genotype was marginal. The K_d values determined using the data shown in Figure 25 to Figure 31 are depicted in Table 8.

Results

Table 8. K_d values determined for selected NoV aptamers and VLPs of five different genotypes.

Aptamers	K_d for GI.1 [nM]	K_d for GI.7 [nM]	K_d for GII.3 [nM]	K_d for GII.4 New Orleans [nM]	K_d for GII.4 Sydney [nM]
M 1	-	-	-	963±348	388±238
M 6-2	-	-	-	928±425	1130±7895
SMV 19	-	-	-	9342±7491	-
SMV 21	-	-	-	1777±1021	1247±372
Buf-2	-	-	464.8±370.4	351±89	241±50
Beier	-	62.98±28.11	114.9±34.4	105±47	71±38
AG3	-	-	-	1033±433	313±81

3.6.3 Structure Analysis of Biotinylated and Non-Biotinylated Oligonucleotides Using Circular Dichroism Spectroscopy

After binding of selected NoV aptamers to NoV VLPs of different genotypes was assessed, the selected DNA aptamers were investigated by CD spectroscopy. One of the objectives of this study was to use NoV aptamers in a pull-down and dot-blot setting. Both applications rely on the use of biotinylated aptamers. However, sufficient amounts of NoV VLPs to test VLP binding of aptamers and their biotinylated counterparts were not available. Therefore, CD spectra of the biotinylated- and non-biotinylated-aptamers were measured and resulting spectra compared. It was assumed, that analogous CD-spectra of an aptamer and the according biotinylated aptamer could indicate, that the biotin-tag has no influence on the structure of the target-binding domain of the aptamer. The CD spectra of NoV biotinylated and non-biotinylated aptamers (Buf-2, Beier, AG3, SMV 19, SMV 21, M 1, and M 6-2) were measured in the according selection buffer present during each aptamer's SELEX-experiment (Table 13) and are shown in Figure 32.

Results

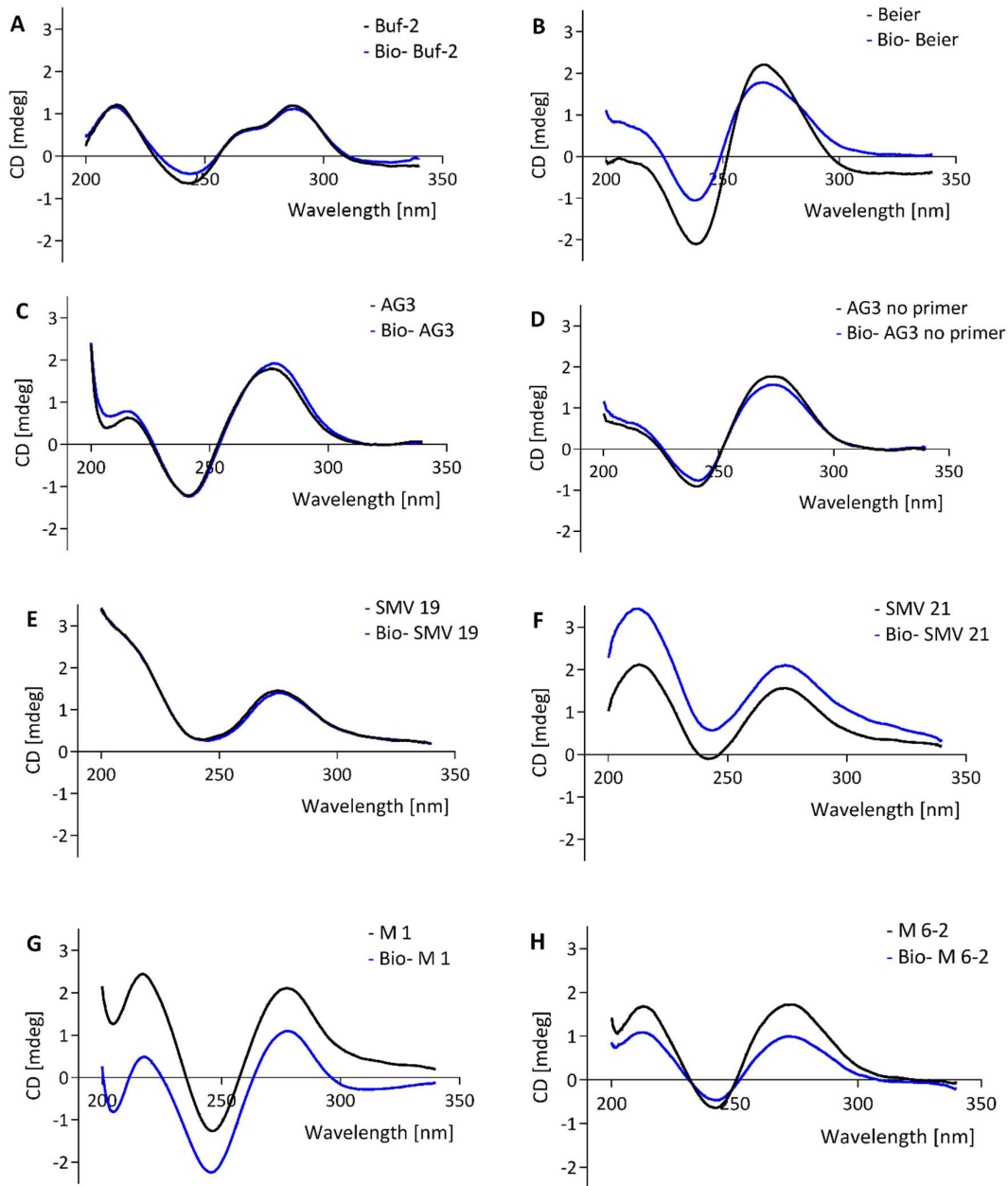


Figure 32. CD spectra of norovirus aptamers with and without 3'- end biotin tag. CD spectra of aptamer candidates Buf-2, Beier, AG3, AG3 without primer annealing site, SMV 19, SMV 21, M 1 and M 6-2 and their biotinylated counterparts are shown in A through H, respectively.

The CD-spectra obtained for the different aptamers show no difference in curve shape in correlation with absence or presence of a biotin tag. However, slight differences in curve amplitude was observed for certain oligonucleotides, notably SMV21, M 1 and M 6-2 (Figure 32 (F), (G) and (H)).

3.7 Aptamer-mediated Dot-Blot for the Detection of NoV VLPs

For the dot-blot application, multiple dilutions of NoV VLPs were blotted on a nitrocellulose membrane. The dried membrane was then blocked in 1 % BSA solution at 4°C overnight and prepared for the aptamer binding step. After the binding step, the aptamer target complex on the membrane was washed and aptamers cross linked to the membrane by UV light. Biotinylated aptamers were detected by alkaline phosphatase-linked streptavidin. For the negative control the dot-blot procedure was completed as described without using aptamers (for detailed methodology, please refer to section 6.12). Table 9 gives an overview of the aptamer-mediated dot-blot data using the NoV aptamers Buf-2, Beier, AG3, SMV 19, SMV 21, M 1, and M 6-2. However, the differences in spot intensity are only visible in the dot-blots shown in Figure 33.

Table 9. Results of aptamer mediated dot-blot. The detected VLP genotypes are indicated by an X in the according aptamer column and the lowest VLP concentration detected is given underneath the X in brackets.

NoV VLP genotype	Aptamers							
	negative	M 1	M 6-2	SMV 19	SMV 21	Buf-2	Beier	AG3
GI.1	-	-	-	-	-	-	-	-
GI.7	-	-	-	-	-	-	X (375 nM)	X (750 nM)
GII.3	-	-	-	-	-	-	X (750 nM)	X (1500 nM)
GII.4 New Orleans	-	X (375 nM)	-	X (750 nM)	X (750 nM)	X (188 nM)	X (94 nM)	X (375 nM)
GII.4 Sydney	-	X (1500 nM)	-	-	-	X (750 nM)	X (188 nM)	X (750 nM)

The dot-blot negative control showed no spots on the membrane, as expected. Using aptamer Buf-2 the detection of genotype GII.4 VLPs was accomplished, with spots for genotype GII.4 New Orleans exhibiting highest intensity. The lowest GII.4 New Orleans VLP concentration being detected in the Buf-2-mediated dot-blot, was 188 nM. A similar detection pattern as described for Buf-2 was observed for aptamer M 1. Using the M 1 aptamer-mediated dot-blot, the lowest concentration of GII.4 New Orleans VLPs detected, was 375 nM. With aptamer M 6-2, none of the tested NoV VLP genotypes were detected. Using aptamers SMV 19 and SMV 21, VLPs of Norovirus GII.4 New Orleans and GII.4 Sydney were detected. For both SMV 19 and SMV 21, the lowest concentration of GII.4 New Orleans detected was 750 nM. Using AG3 and Beier in the aptamer-mediated dot-blot resulted in a more comprehensive detection throughout the different NoV genotypes, as VLPs of genotypes GI.7, GII.3, GII.4 New Orleans and GII.4 Sydney were detected.

Results

Using the aptamer Beier in the aptamer-mediated dot-blot lead to the detection of the lowest concentration of GII.4 New Orleans VLPs of 94 nM.

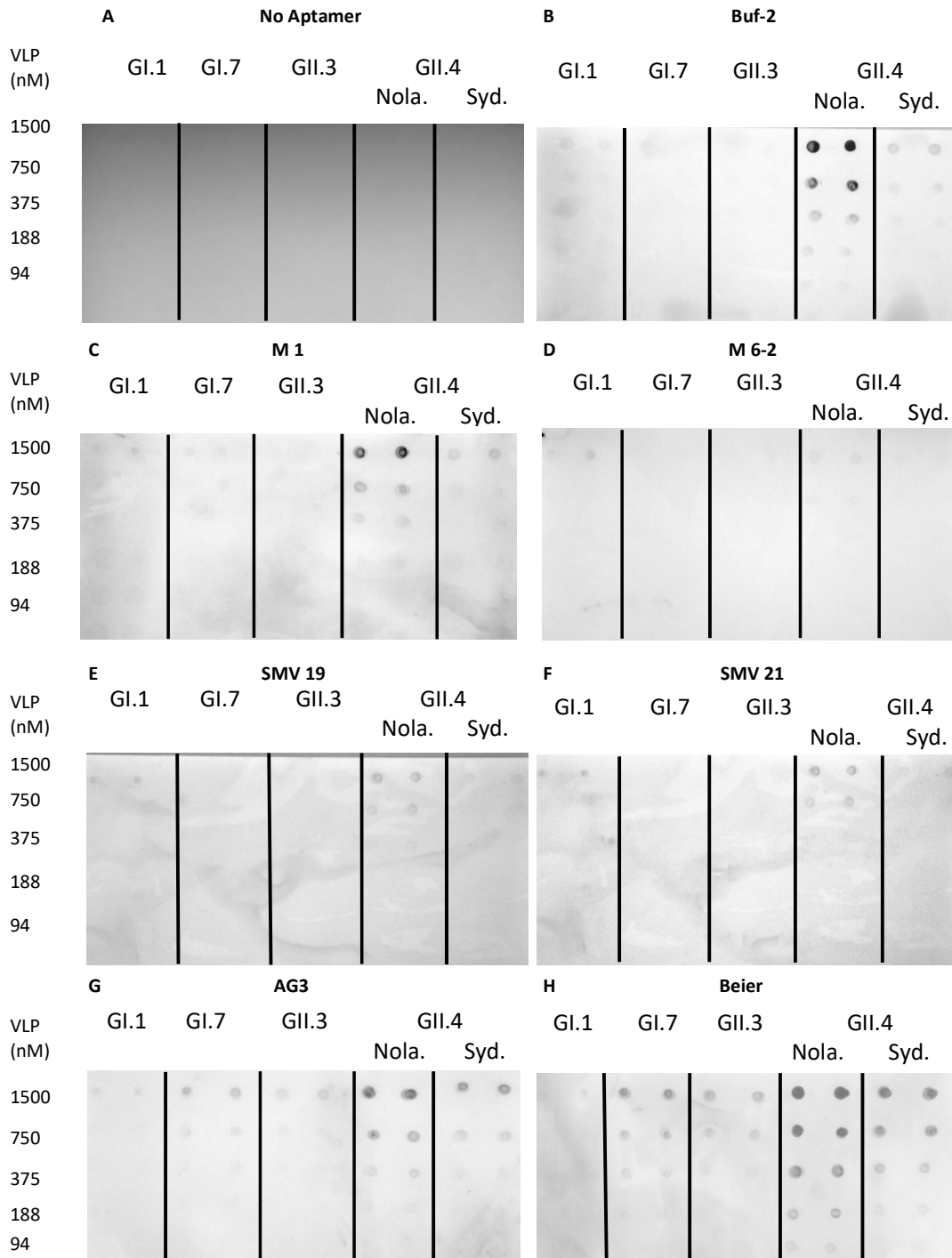


Figure 33. Aptamer mediated dot-blot using selected aptamers and five different genotypes of VLPs. The dot-blot of the negative control without aptamers is depicted in A; dot-blot with Aptamers Buf-2, M 1, M 6-2, SMV 19, SMV 21, AG3, and Beier are depicted in B through H, respectively. The concentration of the different VLP solutions applied to the nitrocellulose membrane (0-1500 nM) are indicated on the left side of each row. The different NoV genotypes used, are indicated by the abbreviations GI.1, GI.7, GII.3, and GII.4 Sydney (Syd.) and New Orleans (Nola.).

3.8 Aptamer-mediated NoV Pull-down

3.8.1 Aptamer-mediated Pull-down for the Extraction of NoV From Buffer

For the aptamer-mediated NoV pull-down, NoV of genotype GII.4 Den Haag was partially purified from stool sample (chosen based on availability) and diluted in the selection buffer used during selection of each aptamer tested in this study (compositions of the individual buffers are given in Table 16). For the pull-down (for experimental details, refer to section 6.13) biotinylated aptamers were transferred to the virus suspension, and after 1 h streptavidin beads added to collect aptamer bound viruses via the aptamer's biotin-tag. Streptavidin beads alone were used as negative control, and added to the virus suspension, without previously adding aptamers. The virus extracted from suspension by the pull-down was detected by RT-qPCR (section 6.5.4). During the first attempts of the aptamer-mediated NoV pull-down, a difference between presence and absence of aptamers during the pull-down could not be detected by RT-qPCR (data not shown). Thus, indicating non-specific binding of NoV to streptavidin beads.

In order to block non-specific binding of the viruses to the paramagnetic beads, the paramagnetic streptavidin beads were prepared in SB supplemented with 1 % BSA. The pull-down was then completed in three variations without the use of aptamers to determine non-specific binding to the paramagnetic beads: without the use of BSA; with BSA not continuously present in the pull-down protocol after the initial blocking step; and with BSA present in all steps of the pull-down protocol, including the virus binding step and all consecutive washing steps. All experiments were completed in a double-determination. After the pull-down was completed using the partially purified stool suspension, containing NoV of genotype GII.4 Den Haag, extracted virus was detected by RT-qPCR. To determine whether the differences in Ct-values obtained between the different variations were significant, a one-way ANOVA was completed followed by multiple comparison Dunnett's test, as previously described¹⁹⁴. In this case, normality of the data was assumed, as the data set was too small to perform normality testing. The calculated p-values indicate whether the different variations completed, resulted in a statistically significant reduction of non-specific NoV binding to the paramagnetic beads. The obtained Ct-values for the three variations are shown in a bar graph (Figure 34). Significance of difference between the aptamer-mediated pull-down variations completed with BSA blocking and the aptamer-mediated NoV pull-down performed without the BSA blocking are indicated by asterisks above the bars, each representing one blocking variation.

Results

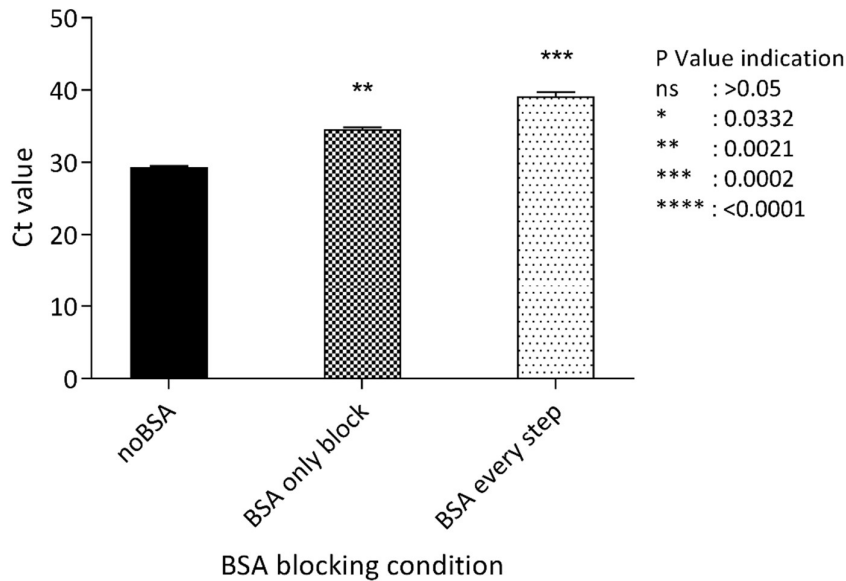


Figure 34. Ct values depicted in a bar graph, to compare blocking of streptavidin beads using 1 % BSA solution. Each bar represents the average Ct value obtained after NoV pull-down using one of the three blocking variations, which each differ in the way the paramagnetic beads were prepared for the pull down. The left bar shows the average Ct value obtained after NoV pull-down without blocking the beads with BSA (noBSA). The middle bar represents the average Ct value obtained after NoV pull-down using paramagnetic beads which were blocked with BSA prior to use, but without using BSA in subsequent steps in the pull-down protocol (BSA only block). The right bar shows the average Ct value obtained after NoV pull-down using paramagnetic beads which were blocked with BSA prior to use and in which 1 % BSA solution was used consecutively in every step of the pull-down protocol.

Results showed that non-specific binding of virus to the paramagnetic streptavidin beads could not be prevented completely. However, a statistically significant reduction was accomplished with both BSA-blocking variations. The variation employing BSA only during the blocking step led to a 100-fold decrease in pulled-down virus, whereas the variation implementing BSA in every step accomplished over a 1000-fold reduction of pulled-down virus. This was also reflected in the obtained p-values of 0.0021 for the variation using BSA only for the initial block, and 0.0002 for the variation including BSA in every step of the pull-down protocol.

As blocking of non-specific virus binding to the streptavidin beads was accomplished, an aptamer-mediated NoV pull-down was completed using two different dilutions (100- and 1000-fold) of partially purified NoV positive stool suspension, each in a triple determination. The NoV titer of the partially purified stool suspension was assessed by RT-qPCR post viral RNA extraction as described in the experimental section (see section 6.1.2 and 6.5.4) and a Ct value of approximately 22 determined.

NoV extraction by aptamer-mediated pull-down was completed using the aptamers Buf-2, Beier, AG3, SMV 19, SMV 21, M 1, and M 6-2 and the extracted virus quantity assessed by RT-qPCR. The results expressed as Ct values are shown in Figure 35 A and B for the 100- and 1000- fold dilutions

Results

of the partially purified stool suspension, respectively. The Ct values obtained after pull-down using aptamers were each compared to the Ct values of the negative control (JB=Just beads) by the multiple comparison Dunnett's test after a one-way ANOVA as previously described¹⁹⁴. Significance of differences to the negative control are indicated by asterisks above the bars, each representing the aptamer used for the pull-down. Using aptamer AG3 for the NoV pull-down did not show a statistically significant difference compared to the negative control. For all other aptamers, results showed a statistically significant difference between aptamer pull-down and negative control for both dilutions of the partially purified stool suspension. For the 1000-fold dilution no virus was recovered with the negative control and with AG3, indicated by the missing bar in Figure 35 B.

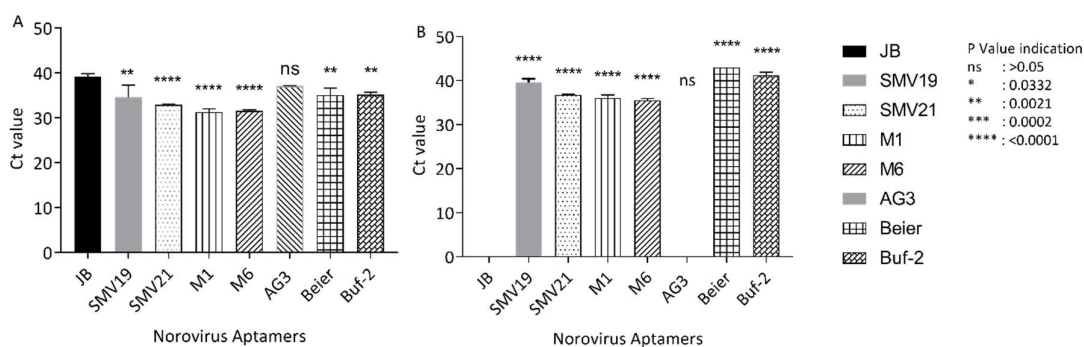


Figure 35. Aptamer-mediated NoV pull-down from stool suspension using different aptamers. The Ct values are shown on the y-axis, and each bar on the x-axis represents the aptamer used during the pull-down. Statistically significant differences in comparison to the negative control, without aptamer (just beads= JB) are indicated with asterisks above each bar. The aptamer mediated pull-downs were completed for each aptamer in a triplicate from a 100-fold dilution from partially purified stool (A) and 1000-fold dilution of the same preparation (B). In (B) no Ct values were obtained for JB and AG3.

3.8.2 Aptamer-mediated Pull-down for the Extraction of NoV From Oyster

After aptamers were successfully applied to extract NoV from a partially purified stool suspension, an aptamer-mediated NoV pull-down was tested from the food matrix: oyster div. For that purpose, oyster div. homogenate was supplemented with partially purified NoV GII.4 Den Haag stool suspension and utilized to compare the existing FDA-shellfish method to the aptamer-mediated pull-down, as described in section 6.1.1, and 6.13, respectively. The aptamer-mediated pull-down protocols were completed using the aptamers Buf-2, Beier, SMV 19, SMV 21, M 1, and M 6-2 and each aptamer's selection buffer (Table 13). Due to the results obtained in 3.8.1, the aptamer AG3 was not included in this study.

To be able to calculate the number of viruses extracted, the virus suspension used to supplement the oyster div. homogenate was serially diluted and virus number estimated by endpoint dilution RT-qPCR. Ct values were determined for the different dilutions, and standard errors for

Results

the triplicate assessed as shown below (Table 10). Ct values were plotted against the logarithm (log) value of the viral number. The resulting linear regression line including the corresponding equation and R² values are shown in Figure 36.

Table 10. Ct values and log values for Nov endpoint titration.

Y Ct value	Y Std- Err Ct Value	X Log (viral number)
21.41	0.16	5.69897
23.98	0.20	5
24.54	1.03	4.69897
27.00	0.17	4
28.28	0.14	3.69897
30.54	0.24	3
31.81	0.33	2.69897
33.22	0.46	2
35.03	0.14	1.69897
40.14 ^a	1.745	1

^a this data point was not included in the standard curve

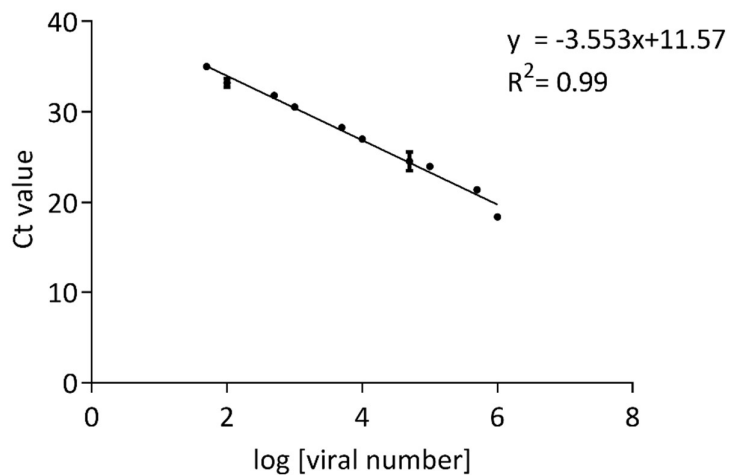


Figure 36. Graph of linear regression from NoV endpoint titration. In the regression, Ct values are plotted against log values of the estimated viral numbers (one virus contains one genomic copy number).

Results

The PCR efficiency for this assay was assessed as 91.2 % and the regression showed high linearity in range of Ct values 21.41 ± 0.16 and 35.03 ± 0.14 , as reflected in the R^2 of 0.99.

Using the equation from the linear regression of the endpoint dilution, viral numbers recovered by the FDA-shellfish method and the aptamer mediated pull down from oyster-div. were calculated per 3 μ L PCR template and per 4 g oyster homogenate (one sample size), since the pull-down was completed using only a subset of the sample (Table 11). The results show that the negative control for the aptamer pull-down (JB) recovered the highest virus numbers, compared to the aptamer mediated pull-downs. A comparison between the aptamer pull-down method and the FDA-shellfish method can therefore not be made until a suitable blocking method is provided. This issue will be addressed further in the discussion section 4.6.

Table 11. Viral numbers recovered using the FDA-shellfish method and with aptamer-mediated pull-down, using selected NoV aptamers. Calculated values are presented as mean values with the according standard deviation (StdDev).

Method/aptamer	Ct value	Log Viral number	Viral number/3 μ L		Viral number/ 4 g	
	Mean	Mean	Mean	StdDev	Mean	StdDev
FDA	23.78	4.9	$8.8 * 10^4$	$2.1 * 10^4$	$2.4 * 10^7$	$2.9 * 10^5$
FDA neg	-	-	-	-	-	-
JB	33.82	2.1	114	21	$3.5 * 10^3$	$6.4 * 10^3$
M 1^a	36.37	1.3	22	3	$6.7 * 10^3$	795
SMV 21	35.07	1.7	52	2	$1.6 * 10^4$	$4.4 * 10^3$
Beier^a	35.46	1.6	39	3	$1.2 * 10^4$	928
Buf-2	35.11	1.7	49	21	$1.5 * 10^4$	$2.1 * 10^3$

^a qPCR results for this candidate were outside of the linear range of the regression, data does not allow accurate quantification

4 Discussion

4.1 Aptamer Selection for the Norovirus P-domain

4.1.1 Negative Selection and Target Suitability

One of the goals of this study was to select and identify aptamers for the norovirus capsid with the intention of using these aptamers to extract NoV from food matrices. The P-domain, the most protruding protein domain on the NoV surface, was chosen as aptamer target, as it is not only the most accessible protein on the virus capsid, but also a unique NoV protein and therefore a good target for aptamers with intended application as extraction tool. Moreover, the P-domain had previously been produced using a pET expression system in *E. coli*¹⁹⁵. A protein production protocol was derived from published studies to generate the protein for SELEX and aptamer characterization. The target protein was expressed in a pET expression system in frame with a 6xHis-tag, benefiting from its advantages such as easy purification and immobilization to paramagnetic beads during SELEX. Nevertheless, it has been shown that His-tags can occasionally have an influence on folding for some proteins¹⁹⁶. Since the P-domain was produced with a His-tag, the immunogenic authenticity of the produced P-domain was tested prior to SELEX using NoV GII.4 antibodies. The antibody did indeed bind the P-domain in a dot-blot, indicating that the folding of immunogenic binding sites of the protein was not impacted by the presence of the His-tag. It was later confirmed that aptamer Buf-2, selected in this study using the P-domain as a target, bound to the virus-immunogenic and -morphologic identical NoV GII.4 VLPs. These findings indicate that the NoV GII.4 P-domain produced in *E. coli* is a suitable target for selection of aptamers for the NoV capsid. This also confirms previous findings which suggest the P-domain produced with a GST fusion tag to be an appropriate target for SELEX¹⁸⁹. However, to investigate this matter in its entirety, an advanced investigation using X-ray crystallography structure analysis would be required.

Compared to the native protein, the addition of the N-terminal His-tag added about 30 amino acids (approximately 3 kDa) to the produced protein (see vector map in section 9.10). To avoid the enrichment of oligonucleotides binding to this section of the recombinantly produced P-domain, a control protein with a His-tag was produced with the same expression vector and used for counter selection during SELEX. Binding tests with selected oligonucleotides enriched during the buffer-SELEX-experiment and both proteins showed that the tested oligonucleotides exhibited about 60 % to 95 % less binding affinity to the control protein. This indicates that enrichment of oligonucleotides targeting the 3 kDa added protein section was successfully circumvented by counter selection using the His-tagged control protein.

4.1.2 SELEX Strategy for Comparative Study

A comparative study including five parallel SELEX-experiments was accomplished during this work, studying the influence of food matrices on aptamer enrichment during SELEX. Each SELEX-experiment was completed in presence of a different food matrix or in presence of SB. For four SELEX-experiments, 16 rounds of SELEX were completed, for the strawberry-SELEX-experiment nine rounds of SELEX were completed. Negative selections were started in SELEX-round 3 and food matrices were introduced in SELEX-round 4. An oligonucleotide library with 40 nt random bases was chosen relative to the size of the target protein and the downstream application. A 40 nt oligonucleotide has an approximate molecular weight of 12.2 kDa. The estimated molecular weight of an entire VP1 protein is 58 kDa. Therefore, a 40 nt aptamer could interact with approximately a fifth of the VP1 protein, given that the entire oligonucleotide surface interacted with the VP1 protein. Considering that the viral capsid consists of 180 copies of the VP1 protein, this would allow aptamers to simultaneously interact with one VP1 protein on the viral capsid without sterically interfering each other.

In order to compare different SELEX-experiments, the oligonucleotide library was exposed to the SELEX target prior to introduction of food matrices to obtain a mildly enriched library which already contains multiple copies of target binding oligonucleotides. The intent was to start each SELEX-experiment with the exact same pool of oligonucleotides. The sequences obtained from the final SELEX-rounds of each SELEX-experiment revealed that the enriched oligonucleotides pools of the buffer- and the lettuce-SELEX-experiments as well as from the buffer-, oyster-, and oyster div.-SELEX-experiments shared oligonucleotides with common sequences. A cross-contamination of the parallel SELEX-experiments is unlikely, as the aliquot of SB used for each SELEX-round also was used in the negative control during the PCR amplification step of the same SELEX-round. As no contamination was detected throughout the SELEX-experiments, it was ensured that sample handling during SELEX and PCR did not lead to contamination of the parallel SELEX-experiments. The fact that identical oligonucleotides were identified between the different SELEX-experiments confirms that enrichment had taken place in the first SELEX-rounds, and that this approach taken to compare parallel SELEX-experiments, using common starting library, is feasible.

It is common knowledge in investigators of the aptamer development community, that a decrease in necessary PCR cycles to amplify target binding oligonucleotides during SELEX with increasing number of SELEX-rounds indicates enrichment of target binding oligonucleotides. This is due to the increasing stringency in every SELEX-round, which leads to a decrease of non-target-binding oligonucleotides and to an increase in the number of oligonucleotides eluted after the binding

Discussion

step which coincides with an increase of oligonucleotide template for the subsequent PCR. During this work, the number of PCR cycles needed, to amplify binding oligonucleotides stagnated or increased for all selections until SELEX-round nine, despite efforts to increase stringency such as an increase in washing steps and decrease of target protein. Hence, the amount of protein and beads used for the negative selection was doubled in SELEX-round nine and for the following SELEX-rounds. By doing so, a decrease in number of PCR cycles for the amplification of target binding oligonucleotides in the following SELEX-rounds was accomplished. This indicates that enrichment of target specific nucleic acid molecules was accomplished by removing non-target specific oligonucleotides by increasing the negative selection material. These findings suggest that a higher amount used for counter selections can favor the outcome of SELEX and confirms the importance of counter¹³⁰, and negative¹²⁹ selections during SELEX.

For the strawberry-SELEX-experiment, recovery of DNA after SELEX-round nine was not accomplished. This could have been due to the enrichment of non-target specific oligonucleotides during the strawberry-SELEX-experiment until SELEX-round 9. As a result, the doubling of the amount of counter selection material possibly leads to the elimination of these non-target specific molecules, resulting in the total loss of DNA in the eluate after the SELEX binding step. It is also possible, that the nature of the strawberry food matrix itself prevented the enrichment of target binding oligonucleotides. However, that would not explain, why no DNA was recovered after the doubling of the amount of counter selection material. If DNA enrichment had been prevented by the food matrix, a loss of DNA recovery would more likely have occurred after the introduction of the food matrices in SELEX-round 4.

The amount of oligonucleotide sequences analyzed from the last SELEX-round nucleic acid pool (Table 4) was limited to about 50 per each SELEX-experiment. Therefore, the results only give insight to a fraction of DNA molecules that prevailed in the last SELEX-round nucleic acid pools of the SELEX-experiments. NGS has proven useful in identifying enriched sequences and would have been a useful tool to investigate the diversity of the oligonucleotide pool throughout the SELEX experiment. There have been multiple reports of using NGS as a tool to identify enriched molecules by probing enriched nucleic acid pools during SELEX^{191, 197}. During a study published in 2011, all 10 completed SELEX-rounds were probed by NGS and 25 clones were identified by Sanger sequencing. It was shown that the same binding molecules were identified with Sanger sequencing after cloning and by NGS. Yet, binding molecules were identified as early as in SELEX-round two using NGS¹⁹¹. Since the cloning of the oligonucleotide pool usually only allows to look at a fraction of sequences, compared to the NGS technique, the method is less sensitive.

Molecules enriched in the first SELEX-rounds, might not even be detected by analyzing 50, or 100 clones. Therefore, to identify enrichment in an oligonucleotide pool by analyzing clones, the sequence-homogeneity of the pool must be rather pronounced, requiring the completion of more SELEX-rounds or the use of an extremely stringent SELEX-method e.g. capillary electrophoresis.

Nevertheless, the approach taken in this study, to compare the enrichment of oligonucleotides during SELEX by probing the last SELEX-round through cloning followed by sanger sequencing was practical, as oligonucleotide enrichment was observed for some SELEX-experiments. Regardless of which approach for sequences analysis is chosen, the sequence data obtained from a SELEX-experiment can only indicate the occurrence of oligonucleotide enrichment. Whether or not the enriched oligonucleotides specifically bind the target molecule must be determined in affinity studies.

4.1.3 SELEX in Presence of Food Matrices

Target affinity of enriched oligonucleotide pools of the five parallel SELEX-experiments was determined after SELEX-rounds 16 and 9, studying the P-domain affinity of the oligonucleotide pools of the final SELEX-rounds by FRA. Results showed that each of the oligonucleotide pools of the final SELEX-rounds exhibited higher binding to the P-domain compared to the unselected DNA library. The maximum binding to the P-domain was determined for the SELEX-round 16 oligonucleotide pool of the buffer-SELEX-experiment, which bound the P-domain 13 times stronger than the unselected library. The increased P-domain binding of all final SELEX-round oligonucleotide pools compared to the unselected library indicated, that enrichment of oligonucleotides with specific target affinity was facilitated in all conducted SELEX-experiments and that most stringent enrichment was accomplished during the buffer-SELEX-experiment. This was also confirmed by results obtained from sequencing the oligonucleotide pools of last SELEX-rounds from each SELEX-experiment. Here a correlation between the intensity of P-domain binding of the last round oligonucleotide pools and the decrease in sequence diversity was observed. Both the last round-oligonucleotide-pools of the lettuce and buffer-SELEX-experiment exhibited a comparatively high degree of sequence homogeneity, compare to the remaining SELEX-experiments and also showed highest overall P-domain binding in the FRA-experiment.

Both the binding study completed with the last round oligonucleotide pools of the last SELEX-rounds and the sequence data obtained, suggest that enrichment of oligonucleotides with high target affinity was accomplished in the buffer- and lettuce-SELEX-experiments. For the strawberry-, oyster-, and oyster div.-SELEX-experiments only modest enrichment of oligonucleotides specifically binding the P-domain was accomplished. P-domain binding studies

by FRA using selected oligonucleotides enriched during the strawberry- and lettuce-SELEX-experiments revealed, that oligonucleotides identified from these experiments did not exhibit specific P-domain affinity. The data collected at this point suggests that during the SELEX completed in this work (using paramagnetic particles as partitioning medium to separate target binding from non-target binding oligonucleotides), the presence of food matrices has a detrimental effect on enrichment of oligonucleotides with target specific affinities. Furthermore, the presence of food matrices during the SELEX binding step did not increase stringency as expected, since the strongest enrichment of target specific oligonucleotides was facilitated in the selection completed in an aqueous salt buffer (SB) in absence of food matrices. The idea of selecting aptamers *in vivo*, which is essentially the same idea as selecting aptamers in presence of food matrices to simulate assays conditions, has previously been tested in the field of therapeutics. In this application the goal was to select aptamers for colorectal cancer metastasis in an animal model. Enriched molecules were later identified to specifically bind to CT26 tumor proteins (K_d values of 30.8 nM and 68.9 nM) and used to specifically stain the tumor after *in vivo* injection¹³⁷. Hence, contrary to our findings, aptamer selection can be facilitated in a medium other than a salt buffer, although this was not accomplished during this work using food matrices. The *in vivo* selection was not compared to an *in vitro* selection for the same protein extract. It is therefore unknown whether an according *in vitro* SELEX-experiment would have yielded the same, or better result (while this knowledge would have been useful, given the ethical concerns of *in vivo* aptamer selections, as it involves the killing of animals).

4.1.4 PCR-Bias during SELEX

DNA molecules with complex structures, including stable stem constructs and molecules with CGG repetitions in the sequence led to decreased PCR efficiency and premature termination of the polymerase extension¹⁹⁸⁻²⁰⁰. This leads to a formation of PCR by-products, which can be detected as shorter fragments in the agarose gel. Additionally, decreased amplification efficiency can occur if template DNA fragments exhibit stem regions or G tetrads. This was suggested to be associated with an increased melting temperature in regions with high GC-abundance²⁰¹. During SELEX, a selection of stable molecules with complex structure is facilitated to yield specific interaction with the target. To enable amplification of these molecules of complex structure, the SELEX PCR assay used in this work was completed using an additive solution provided with the QiagenTM PCR Kit: the Q-solution. The Q-solution contains betaine, a common additive to improve amplification of PCR template with complex structure²⁰². Among the sequences identified from the last SELEX-round nucleic acid pools of the five selections were those with high abundance of GC. Of sequences identified from the lettuce and buffer-SELEX-experiments, 73 % and 79 % of the

Discussion

sequences exhibited a GC content higher than 50 %, respectively. An additional SELEX-experiment using a PCR assay without the addition of Q-solution was not completed. It can therefore not be confirmed whether the Q-solution contributed to the selection oligonucleotides with a high G and C content and thereby facilitated the selection of Buf-2, which proved to be a molecule with high affinity and selectivity for the P-domain. However, the use of DMSO and betaine to improve PCR amplification during SELEX has been suggested to improve aptamer selection, by enabling the enrichment of stable molecule structures which would otherwise not be amplified in PCR and thereby not be enriched during SELEX²⁰³.

In addition to PCR by-products caused by template DNA with complex structure, a different by-product formation has been reported: ladder type products, which extend far beyond the size of the oligonucleotide library. These products result from a base pairing mechanism resulting in distinct amplification patterns. In instances where this type of by-product formation was observed during SELEX, aptamer selection could not be accomplished. The issue was resolved by adequate primer design²⁰⁴. In this work, ladder type products were not observed during the PCR assay optimization, or during SELEX. Consequently, the oligonucleotide library used contained primer annealing sites which did not interfere with the PCR assay.

To avoid by-product formation during the PCR assay, the PCR amplification of the library was carefully optimized (data not shown) prior to the beginning of SELEX. This had previously been recommended to build the foundation of a successful aptamer selection²⁰⁵. In addition to optimizing the PCR assay, the DNA amplification was terminated before amplification reached the PCR plateau phase. For this purpose, the number of PCR cycles was determined for each SELEX-experiment and for every SELEX-round individually. However, a DNA fragment shorter than the nucleic acid library was observed in agarose gels after SELEX-round ten for the buffer-SELEX-experiment (data not shown). Efforts to prevent these fragments from reoccurring, by reducing the number of PCR cycles for amplification were not successful. Indeed, oligonucleotides Buf-3 and Buf-4 consisted of only about 20 nucleotides, whereas the majority of oligonucleotides identified from the oligonucleotide pool of the last SELEX-round of the parallel SELEX-experiments exhibited a length of about 40 nucleotides. It was noted that the sequence of Buf-3 is identical with part of the sequence of Buf-8. It is therefore likely that Buf-3 was indeed a PCR by-product, resulting from amplification problems of oligonucleotide Buf-8. This is supported by result obtained during the oligonucleotide screening, as only modest P-domain affinity was observed for Buf-3, and Buf-4, reflected in K_d values of 360 nM and 314 nM, respectively. The enrichment of these oligonucleotides as result of high target affinity is therefore unlikely. These findings allow

the assumption, that despite efforts to prevent the PCR bias, the enriched nucleic acid pool of the buffer-SELEX-experiment did suffer from by-product formation during PCR. This subject could have been investigated in more detail, if SELEX-rounds had been probed by NGS. Nevertheless, the buffer-SELEX-experiment did lead to the selection of Buf-2, which showed high P-domain affinity and selectivity, demonstrating that the SELEX did succeed, despite the presence of PCR by-product formation.

4.1.5 Aptamer Selection for the P-domain in Presence of Oyster Matrix

Enrichment of oligonucleotides was not noticeably achieved during the oyster- and oyster div.-SELEX-experiments, despite a mild enrichment of Buf-2. It is known that NoV VLPs bind the oyster diverticula and, depending on the NoV strain, can bind to oyster muscle tissue and glands^{55, 106}. NoV GI.1 VLPs bind oyster diverticula tissue through HBGA-A-like carbohydrate antigens¹⁰⁶. An additional study, characterizing the role of the P-domain interaction with HBGA, reported that the sole P-domain (produced in Sf9 cells) did bind to the HBGA, but that the sole shell domain did not⁴⁷. This indicates that the P-domain is responsible for the interaction with HBGA. Since the bond between NoV VLPs and oyster diverticular tissue was defined as HBGA A-like, we could assume that the P-domain bound to oyster tissue in the food matrix sample. The presence of oyster matrix during SELEX could have thereby prevented the binding of oligonucleotides to the P-domain, leading to the exclusion of P-domain binding oligonucleotides. However, it is not clear if the unassembled P-domain would bind oyster tissue in the same way as the assembled virus particles, or in the way the sole P-domain binds HBGAs.

4.2 Aptamer Identification and Characterization

4.2.1 Oligonucleotide Screening and Identification of Aptamer Candidates

The results of the sequencing of the last SELEX-round nucleic acid pools suggested that high enrichment was accomplished during the lettuce- and buffer-SELEX-experiments, but only modest enrichment during the strawberry-SELEX-experiment and little enrichment during the oyster- and the oyster div.-SELEX-experiments occurred. Single oligonucleotides were tested regarding target binding affinity and selected based on abundance in the last SELEX-round nucleic acid pool. As enrichment was not observed for the oyster- and the oyster div.-SELEX-experiments, target affinity of oligonucleotides identified in the last SELEX-round nucleic acid pools were not tested. The exception was oligonucleotide Buf-2, which was enriched in the buffer-SELEX-experiment and mildly enriched in the oyster- and the oyster div.-SELEX-experiments. Screening of enriched molecules by FRA revealed that oligonucleotides enriched during the buffer-SELEX-experiment exhibited high affinity target binding (interpretation of saturation binding FRA was completed

Discussion

according to a previously published guide¹³⁸). During the screening of enriched oligonucleotides, Buf-2, Buf-5, and Buf-8 were identified as aptamer candidates since they exhibited the highest affinity to the P-domain. However, repeated FRA results for Buf-5 were inconsistent for different P-domain concentrations and not reproducible within the triplicate tested (data not shown). Therefore, oligonucleotide Buf-5 was not further characterized. Oligonucleotide Buf-1 was also examined to understand why this candidate was enriched during the buffer- and the lettuce-SELEX-experiment, despite its merely moderate affinity to the P-domain. Aptamer selectivity was tested, by FRA with other proteins, chosen based on in-house availability. It was shown that candidates Buf-1 and Buf-2 were highly selective, based on the proteins tested in equimolar concentrations. However, Buf-8 did not bind exclusively to the P-domain, as determined in binding studies by FRA using the proteins BSA, lysozyme, and thrombin (Figure 17). Therefore, Buf-8 was not included in specificity and affinity studies.

The binding specificity of aptamer candidates Buf-1 and Buf-2 to the P-domain was assessed by adding unlabeled aptamer candidate (specific competitor) and unlabeled thrombin aptamer (non-specific competitor) to the aptamer-P-domain binding reaction. Aptamer candidate Buf-1 was inhibited by the non-specific competitor equally as it was by the specific competitor, indicating that P-domain binding of Buf-1 is not specific. This coincides with previous findings, showing that a high abundance of an oligonucleotide in the last SELEX-round does not necessarily correlate with strong binding characteristics¹⁹¹. However, P-domain binding of Buf-2 was not inhibited considerably in presence of non-specific competitor, confirming the specific P-domain affinity of this aptamer candidate.

Dextran sulfate has been used primarily as a polyanionic competitor in the development of SOMAmers (introduced in section 1.2.2) by presenting a kinetic challenge to promote the selection of aptamers with low K_{off} constants¹⁴⁸. Dextran sulfate has also been applied as an agent to reduce non-specific binding of DNA aptamers to their target²⁰⁶⁻²⁰⁷. It is likely that a low K_{off} is a beneficial property for an aptamer to be used in food matrices. The FRAs employed during our study did not give kinetic information and, therefore, no information about dissociation or association rates of the aptamer candidate-P-domain complex. Therefore, target binding behavior of different aptamer candidates in presence of dextran sulfate was investigated, to estimate possible kinetic binding characteristics. Although dextran sulfate was not included during the SELEX process, food matrices and increasing number of washing steps were introduced to favor aptamers with low dissociation rates. The P-domain binding of all candidates tested in the presence of dextran sulfate was inhibited by 47-82 % with candidate Buf-2, exhibiting the least inhibition by dextran sulfate.

These results indicate that Buf-2 could have most favorable kinetic properties of the aptamers tested. However, these observations would need to be confirmed using true kinetic techniques, such as ITC. Additionally, the role of the aptamer's kinetic properties in relation to its suitability for application in food analytical application should be further elucidated.

Buf-2 exhibited high affinity for the P-domain as indicated by its low K_d , it also exhibited selectivity, based on the proteins tested, and bound the P-domain specifically as indicated by the binding observed in presence of specific and non-specific competitors. Buf-2, therefore, fulfilled the criteria of an aptamer as it bound its target specifically and with high affinity.

4.2.2 Structure of Aptamer Buf-2

Aptamers can adopt G-quadruplex structures which form into four-stranded circular structures as a result of stacked G-quartet structures in presence of monovalent cations such as sodium or potassium ions, e.g. physiological buffer conditions^{157, 208-209}. G-quadruplexes result from inter- or intramolecular folding of one or multiple, molecules with high G abundance. The intramolecular folding of a G-quadruplex necessitates at least four G-tracts in one strand²¹⁰. This is the case for the potassium aptamer with the sequence: 5'-GGGTTAGGGTTAGGGTAGGG-3'²¹¹. During this work, aptamer Buf-2 exhibited a 20 nt motif with repeated occurrence of a G triplicate. Among G-quadruplex aptamers, the most common nucleotides found between the Gs are Ts, with As and Cs only being found in between the G tracts sporadically¹²⁴. This was consistent with the identified 20 nt motif in Buf-2, as T was found with highest abundance within the motif. For 20 nt fragment of the Buf-2 oligonucleotide with the sequence: 5'-GGGTTTCGGGTTTGGGTTGGG-3' the highest likelihood for G-quadruplex formation was projected using the open software QGRS Mapper. The result predicted the contribution of all 12 Gs. The analyzed Buf-2 variants (section 3.4.2) were chosen based on this motif.

CD spectroscopy enables the distinction between different DNA structures, by measuring the difference in absorption of right- and left-handed circularly polarized light of chiral molecules, which is called circular dichroism²¹². CD spectroscopy was, therefore used to investigate the structure of Buf-2 and of three variants of Buf-2. In addition to CD spectroscopy investigation, FRA of the four molecules were completed to find the P-domain binding motif of Buf-2 and investigate the possibility of truncating the aptamer. The positive and negative peaks of the molecules' CD spectra were compared with recently published CD spectra of aptamers with parallel, antiparallel formation, and the B form of DNA²¹³ (Table 12).

Discussion

Table 12. Maxima and minima in CD spectra of different aptamer structures. The wavelength maxima and minima of aptamer structures are shown, as reported in a recent study²¹³ and the maxima and minima of the Buf-2 variants are shown as recorded during the CD analysis (section 3.6.3).

Structure/molecule	Positive Peak [nm]	Negative Peak [nm]
Antiparallel G-quadruplex	295 (bulge 240)	265
Parallel G-quadruplex	260	240
B-form DNA	270	240
Buf-2	285, 260	240
Buf-2 variant 1	285,260	235
Buf-2 variant 2	285	250
Buf-2 variant 3	290,240	265

The Buf-2 variant 3 showed the typical spectrum of an antiparallel G-quadruplex, which has also been observed for the thrombin binding aptamer TBA¹⁵⁴. However, the spectra of Buf-2 and Buf-2 variant 1 are not consistent with this spectrum. Both their CD spectra show identical bands, despite the difference in amplitude. The CD spectra of Buf-2, Buf-2 variant 1 and Buf-2 variant 2 shared a common positive peak at 285 nm, which matches neither maxima of the G-quadruplex structures, nor the B-form DNA. Negative peaks for the three molecules were observed at 235 nm, 240 nm, and 250 nm. CD-spectra of B-form DNA and the parallel G-quadruplex aptamers both typically show a trough in the CD spectrum at 240 nm; it is therefore not possible to make a distinction between the B-form DNA and the parallel G-quadruplex based on this negative peak. However, the CD spectra of Buf-2 and Buf-2 variant 1 each showed a shoulder peak in the CD spectrum at 260 nm. The combination of the positive peak at 260 nm and the negative peak at 240 nm indicated the presence of a parallel G-quadruplex structure. The additional peak observed in both spectra at 285 nm, and the fact that an antiparallel Q-quadruplex structure had already been identified for Buf-2 variant 3 (20 nt motif) leads to the conclusion that Buf-2 is a parallel/antiparallel G-quadruplex hybrid. G-quadruplex hybrids were first described for telomeric regions in 2006²¹⁴. The CD spectrum shown in the 2006 study (Figure 37 (B)) shows multiple CD spectra. The G-quadruplex hybrid was termed Tel26 and in presence of K⁺ shows a spectrum (shown in light pink) very similar to the Buf-2 CD spectrum. The Tel26 spectrum exhibits the same maximum peak around 290nm, the shoulder peak around 265 nm, and a trough at 240 nm.

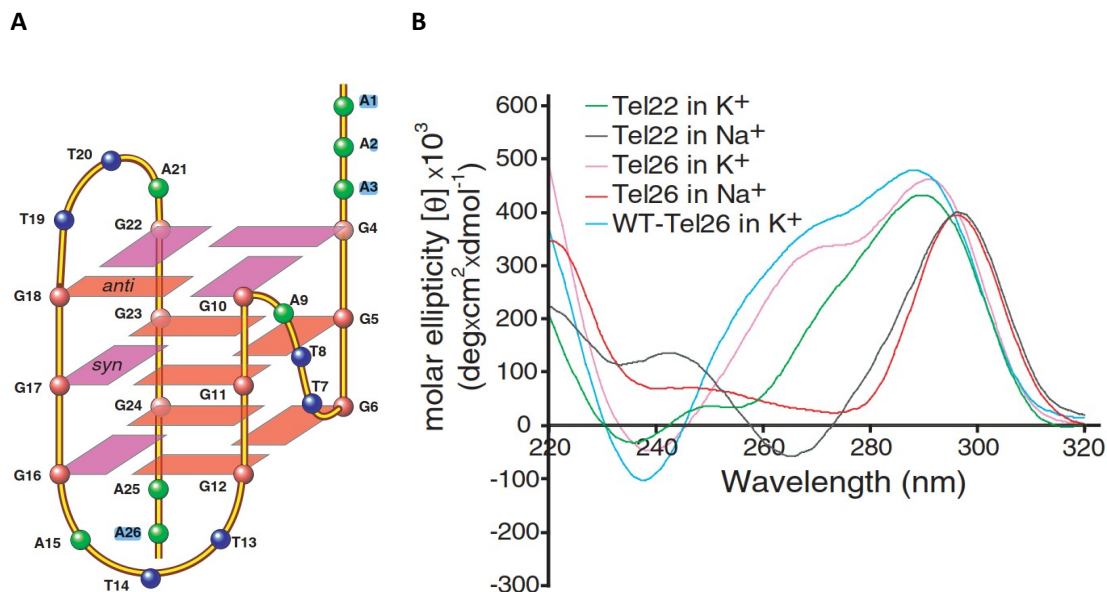


Figure 37. Proposed folding and CD spectrum of parallel/antiparallel G-quadruplex as described previously. (A) Schematic diagram of the folding topology of the unimolecular human telomeric hybrid G-quadruplex in potassium solution. Red ball: guanine, Red box (anti) guanine, magenta box: (syn) guanidine, green ball: adenine, blue ball: thymidine. (B) CD spectra of multiple telomeric molecules in 100 mM Na⁺, or K⁺ solutions at 25 °C. For Tel26, a parallel/antiparallel hybrid structure was proposed in K⁺ solution. The according CD spectrum is shown in a light pink line²¹⁴ (this figure has been used for the thesis in agreement with Oxford University Press and Copyright Clearance Center).

The formation of the hybrid G-quadruplex described in the study by Ambrus et al. 2006 is induced by the presence of potassium ions, as shown in Figure 37 (A)²¹⁴. In the case of Buf-2 however, the hybrid formation seems to be related to the presence of the 5'- end, as the shoulder peak at 260nm is only visible in the Buf-2 and the Buf-2 variant 1 CD spectra (Figure 20).

The FRA of the Buf-2 and its three molecule variants revealed that only the 40 nt Buf-2 molecule bound the P-domain. This could signify two things. One possibility is the binding motif is located within the 5'- or 3'- end of the molecule, but both need to be present to form the required structure to bind the P-domain. Secondly, it is possible that the molecule adopts an unpredicted structure upon target binding (induced fit). Such an induced fit upon target binding has been proposed other for aptamers, among these is the OTA binding aptamer, which folds into an antiparallel G-quadruplex upon binding to OTA²¹⁵.

The actual confirmation of Buf-2, as well as the aptamer structure when bound to the target molecule, would need to be assessed in further studies using NMR and UV thermal denaturation. Additionally, the P-domain binding of Buf-2 under different buffer conditions, focusing on the K⁺ and Na⁺ concentration could be assessed using CD spectroscopy to investigate the ion-dependency of the aptamer structure.

4.3 Aptamer P-domain Binding in the Presence of Food Matrices

The results from sequencing and binding studies of the last SELEX-round nucleic acid pools showed highest P-domain binding of oligonucleotides enriched during the buffer-SELEX-experiment and most successful enrichment of oligonucleotides in the buffer- and lettuce-SELEX-experiments. The P-domain binding of single oligonucleotides, enriched in the buffer-, lettuce-, and strawberry-SELEX-experiments was evaluated by FRA (See section 3.3.2). Results showed that P-domain binding of molecules enriched during the buffer-SELEX-experiment exhibited the highest target affinity with a K_d in the low nanomolar range, as determined for Buf-2 (17.42 ± 6.97 nM). This coincides with the K_d -range reported for other DNA aptamers with application in food matrices. Among those is the aptamer for the mycotoxin OTA, which exhibits a K_d of 360 nM and has been used in a variety of food matrices such as wheat, cereal, and coffee^{159, 184}. A DNA aptamer developed for enterotoxin C1, which was used in diluted milk matrix, exhibited a K_d of 65 nM²¹⁶. Based on the previous studies of aptamers developed for application in food, the affinity of DNA aptamers selected for the NoV P-domain should be sufficient to test the application in food matrices.

In order to investigate oligonucleotide-target binding in the presence of food matrices, P-domain binding of not only Buf-2, but also of oligonucleotides enriched in the lettuce- and strawberry-SELEX-experiments was analyzed in presence of the food matrices: strawberry, oyster, and lettuce. The results (see section 3.5) show, that none of the oligonucleotides exhibited P-domain binding in presence of the food matrices. Additionally, a difference in target binding between oligonucleotides with high P-domain affinity, like Buf-2, and oligonucleotides with low affinity for the P-domain, like Let-1 and Straw-1 in the presence of food matrices was not observed. This suggests, that the presence of food matrices during aptamer enrichment did not contribute to selecting aptamers with favorable target-binding properties in the according inherent application conditions.

The aptamer Buf-2 was enriched in the buffer-SELEX-experiment, but also present in the enriched oligonucleotide pools of both oyster- and the oyster div.-SELEX-experiments. As enrichment of Buf-2 in presence of oyster matrices did occur, additional studies were conducted with commercially available IQF oysters and manually harvested oysters from Cedar Point in Alabama, USA. Oyster samples were prepared in multiple ways. Whole oysters were blended and suspended in SB to a final concentration of 10 %, and additionally oyster samples were partially purified as described in section 6.10.3. P-domain binding of Buf-2 was tested in presence of these oyster preparations and in presence of a tenfold dilution of these preparations. In the undiluted oyster

Discussion

preparations, aptamer target binding was only observed in presence of undiluted CP oyster-suspension. In presence of diluted oyster preparations, aptamer target binding was observed for all oyster preparations. However, compared to the Buf-2-P-domain binding in SB, binding intensity in the presence of oyster-preparations was reduced by about 50 %. The data suggest that aptamer-target binding was inhibited by the presence of undiluted oyster matrices. In addition to this observation, it was noted that aptamer-target-binding in CP oyster-suspension was facilitated, when binding in IQF oyster-suspension was not observed. The food matrix present during SELEX was also prepared with oysters from CP (with a different batch of oysters). It is possible, that the aptamer bound its target in presence of the CP oysters, as these were the same kind of oysters (harvested in the same geographical location), which were also present during SELEX. This could be an issue for aptamer applicability, as oyster composition exhibits seasonal variability. Furthermore, oyster composition is depending on available feed and other environmental conditions. Therefore, variations in oyster composition between harvest areas can be expected. The idea to conduct a comparative study assessing the influence of food matrices was inspired by the fact that SELEX allows the choice of the selection conditions based on inherent application conditions. However, if the inherent conditions are not defined, the choice of selection conditions cannot be defined either, making the design of an according SELEX experiment difficult. As this problem is not limited to oysters, but applies to a variety of food with additional variables, such as level of ripeness of fruit and vegetable, geographical differences in foods and the high variability of ready-to-eat foods, these challenges need to be addressed in further studies.

While completing FRA in the presence of food matrix preparations, the background signal for binding studies in presence of oyster matrices was as high as the signal detected for the entire P-domain dilution series. In addition, a slower flow-through rate was observed during the FRA experiment in presence of oyster matrices. This raises the question whether FRA is a good analytical method to assess the aptamer binding in food matrices, as specific binding cannot be detected if it is lower than the background signal. An alternative for FRA would be sensor applications, which have been vastly promoted. Indeed, aptamers have been used in sensor or extraction applications from food. The protocol for these applications usually involves sample preparation and matrix dilution prior to aptamer application. This is also the case for the well-studied aptamer for OTA, which has been used in a variety of food matrices. The binding of the OTA aptamer to its target has been predicted as an induced fit upon target binding²¹⁵. This could be advantageous over aptamers that bind their target due to an intramolecular-stabilized complex structure, which could attract more non-specific targets in food matrices. The application described for the OTA aptamer required pre-extraction as well as four fold dilution of a 10 %

Discussion

oyster-suspension in SB¹⁸⁴. The food matrices used in this study were partly pre-extracted as described in the experimental section. However, efforts were taken to omit a dilution step since extraction or screening methods for foodborne viruses require high sample quantities, as the number of viral particles compared to the number of bacteria found in foods can be low, due to the lack of virus replication outside of the host organism. It was shown that the P-domain was detected by FRA in presence of 10-fold diluted oyster matrices. This 10-fold dilution of a sample during virus extraction, would however translate in 10-fold increase of extract volume, to be able to process the entire sample. This would result in an unfeasible sample volume for downstream applications such as high throughput applications. This problem does not necessarily apply to extraction or detection methods for bacteria. This is due to the bacterial replication in the contaminated food, contributing to a much higher number of bacteria in foods compared to viruses. Moreover, most bacteria can be cultured after successful recovery from a food source, increasing the overall likelihood of detection. Still, problems have also been reported with aptamer application in food matrices for the detection of bacteria. Aptamers for *Campylobacter* detection in chicken juice among other food matrices have recently been described in a sensor application¹⁷². However, the limit of detection for bacteria detected in buffer (2.5 bacteria/mL) was considerably lower than in chicken juice (100 bacteria/mL). That study stimulated a discussion about the usefulness of aptamers to distinguish viable from non-viable organisms, which would be of pronounced interest for the food industry. This is especially important in instances where viable organisms cannot be cultured or where the culture or propagation require high copy numbers, as is the case for NoV²¹⁷.

Despite the issue of the food matrix interfering with sample preparation and analytical assays in general it is noteworthy, that the aptamers for OTA and *Salmonella* have been used successfully in a multitude of food analytical assays (see section 1.2.4). As mentioned above, the OTA aptamer interacts with its target based on an induced fit mechanism. Further studies to explore the role of the target fit mechanism and whether the mechanism of target interaction determines an aptamers suitability in food matrices are yet to be completed. Aptamer Buf-2 binds the P-domain with high specificity and selectively, still the utility of the aptamer in undiluted food matrix samples could not be confirmed by FRA. Based on this context, the target specificity and its selective binding characteristics, do not determine, whether the aptamer can be used in food analytical application.

4.4 NoV Aptamers in Comparison

4.4.1 Motif Search Among Published Norovirus Aptamer Candidates

As previously shown for streptavidin, multiple SELEX attempts can lead to the selection of the same conserved binding motif for one SELEX target²¹⁸. Therefore, a motif search was completed, using the open software MEME suite, including all sequences published in studies related to aptamer selection for NoV. Of the three statistically relevant motifs identified in the search, two motifs mostly matched sequences which were not noticeably enriched during SELEX and had been identified in the nucleic acid pools of the last SELEX-rounds of the oyster- and strawberry-SELEX-experiments. Motif 2 occurred in the oligonucleotides Straw-2 and Straw-3 which had both been tested during the oligonucleotide screening. Both oligonucleotides exhibited only modest binding to the P-domain, and their binding characteristics could not compete with those of Buf-2. Consequently, they were not further characterized. The third motif showed a 15 nt sequence, which mainly constituted of G. Among sequences matching this motif were those of oligonucleotides Buf-2, Buf-4, Buf-6, and Straw-1, which had been tested during the oligonucleotide screening. The oligonucleotides Straw-1, Buf-4, and Buf-6 showed either marginal or non-specific P-domain binding, unlike Buf-2 which did bind the P-domain with high affinity. The third motif also matched the previously published aptamer SMV 19. Binding studies with SMV 19 and NoV VLPs which were completed during this work suggested a non-specific interaction between NoV GII.4 VLPs (see section 3.6.2). Motif 3 matching oligonucleotides exhibited both good binding characteristics, and non-specific binding to the P-domain or NoV VLPs. The existence of motif 3 in oligonucleotide sequences did therefore not correlate with high binding affinity. Although a motif search using MEME suite identified potential target binding motifs before¹⁹⁷, the empirical results of this study do not support these motifs as essential for binding.

4.4.2 Aptamer Affinity for a Variety of NoV VLPs

The binding of designated NoV aptamers to an assortment of NoV VLPs was tested by FRA. The purpose was to determine affinity and cross reactivity of the aptamer Buf-2 selected during this work and aptamers previously published for NoV (Table 1). The VLP concentration used during FRAs (0-1500 nM) was dependent upon protein amounts available. To compare aptamer VLP interaction, K_d values were calculated based on the estimated molecular weight of the VP1 protein (58 kDa). The VP1 protein is present 180 times on the viral capsid.

The VLP binding of SMV 19 to NoV genotypes GI.1, GI.7 and GII.3 was below 10 % at a concentration of 1500 nM VLP. However, for the GII.4 genotypes New Orleans and Sydney, average maximum target binding of 68 %, and 75 % was determined at a VP1 concentration of

Discussion

1500 nM, respectively. All five of the blotted curves appear linear. Thus, they did not reach saturation binding, indicating non-specific target binding. The VLPs were provided as purified, assembled capsids. Additionally, the samples were dialyzed against the buffer, which was used during each individual aptamer selection to simulate binding conditions during SELEX. Non-specific binding due to a contamination in the VLP solution is therefore unlikely. Instead, SMV 19 could have bound to multiple sites on the NoV VLP capsids, leading to the linear binding curve.

Aptamers SMV 19, SMV 21, M 1 and M 6-2 bound VLPs of GII.4 genotypes with highest affinity. The SMV 19 and SMV 21 aptamers had originally been selected for NoV GII.2⁵⁶. Using this genotype, K_d values of 191 nM and 101 nM were determined for SMV 19 and SMV 21, respectively. In the same study, binding to other NoV genotypes was assessed based on absorbance ratios between negative and positive NoV VLP samples at one VLP concentration, not blotting a binding curve. The ratios indicated that SMV 21 exhibited strong binding to GII.4 genotype Houston, good binding to GII.3, mild binding to GI.7, and marginal binding to GI.1. The results of binding studies completed in this work are consistent with these results, as far as binding was observed. However, as the binding curves did not reach saturation, and the K_d values determined by FRA indicate low affinity for the NoV genotypes tested in this work. These findings demonstrate the importance of determining binding curves to characterize aptamer ligand binding.

Aptamers generated by Moore et al., M 1 and M 6-2 had been tested with the same method as described for the SMV 19 and SMV 21, using absorbance ratios^{56, 189}. Using that method, strong binding to the capsid of GII.4 Houston and GII.2 had been determined for both aptamers M 1 and M 6-2; low binding was determined to the GI.1 capsid, and moderate binding to the capsid of genotypes GI.7 and GII.3. The studies completed during this dissertation confirm the binding pattern previously described, as affinity to the GII.4 genotypes were observed for these aptamers, with the highest affinity assessed for M 1 and GII.4 Sydney ($K_d \sim 390$ nM). Yet, K_d values were not assessed for GI.1, GI.7, and GII.3, as binding affinity was marginal. Overall, M 1 and M 6-2 aptamers exhibited low binding to the NoV VLPs. As high binding to the capsid protein was observed for other aptamers tested, it can be expected that VLPs interact sufficiently with the nitrocellulose membrane to produce high aptamer signal. It can therefore be assumed, that the low target binding exhibited by M 1 and M 6-2 is due to a high amount of “inactive” aptamer molecules, which could possibly be denatured, insufficiently, or incorrectly folded, prohibiting target binding.

Discussion

Aptamer AG3 also showed its highest affinity for NoV GII.4 among the tested genotypes. AG3 had been selected for an entirely different NoV genogroup, the MNV. A K_d for AG3 and MNV in the low picomolar range was determined previously (a specific K_d was not provided in the study). However, binding to human pathogenic NoV GII.3 VLPs had been confirmed using fluorescence anisotropy. The recombinant GII.3 capsid protein was detected in concentrations as low as 240 fM¹⁸⁸. The FRA completed during this study revealed that AG3 exhibited the highest affinity to GII.4 Sydney ($K_d \sim 313$ nM), and showed only modest to no affinity to the remaining four genotypes tested.

Aptamer Buf-2 bound VLPs of the GII.4 genotypes Sydney, and New Orleans specifically, reflected by the mid nanomolar range K_d values of 241 nM, and 351 nM, respectively. The K_d values were calculated using the molecular weight of the capsid protein, which is represented 180 times on the NoV capsid. Marginal binding of Buf-2 to VLPs of genotype GI.1, and modest binding to VLPs of genotype GI.7 and GII.3 were observed, as it was the case for the aptamers already discussed.

The difference in binding affinity of the aptamers for the different NoV genotypes is to be expected, since NoVs are divided into genotypes based on the genomic heterogeneity of the capsid region. This is reflected in heterogenic capsid proteins between the genotypes. To visualize the heterogeneity between the VLP genotypes used in the binding study, a phylogenetic tree was built using the Maximum-Likelihood method²¹⁹ with MEGA 7.2²²⁰. The capsid sequences were downloaded from GenBank and the accession numbers are shown in the tree (Figure 38).

Despite the fact, that the capsid region is the most variable region on the NoV genome, studies have shown that antibodies with cross reactive epitopes for NoV GI/GII capsids can be generated. An antibody binding each of four GI and GII genotypes has previously been identified²²¹⁻²²².

Discussion

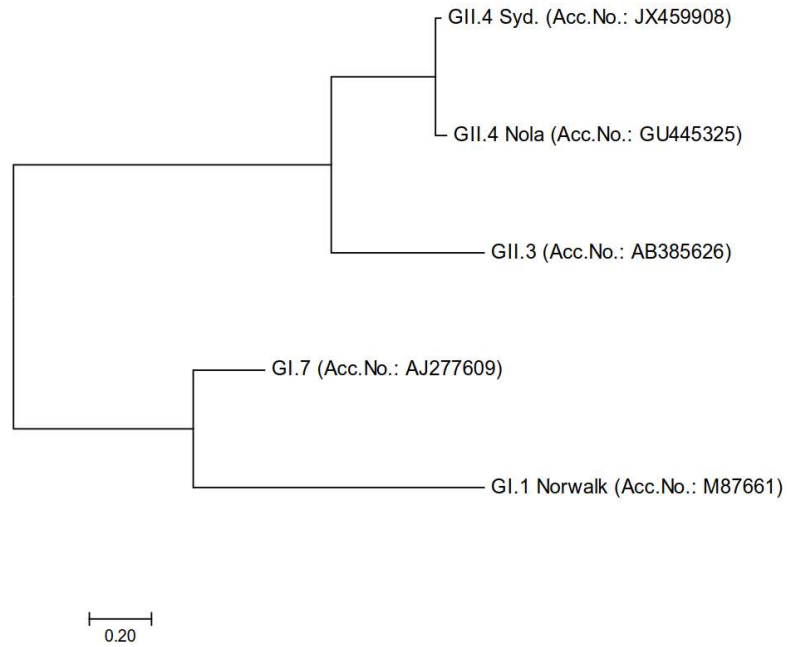


Figure 38. Phylogenetic tree generated with the sequences of NoV capsid protein of the five genotypes GI.1, GI.7, GII.3, GII.4 New Orleans (Nola), and GII.4 Sydney (Syd.). The scale bar represents the number of base substitutions per site.

Aptamer Beier showed broad affinity to VLPs of genotypes GI.7, GII.3, and the GII.4 genotypes New Orleans and Sydney. Additionally, the K_d values determined for Beier and the four genotypes were in the low to mid nanomolar range, between 63nM to 105 nM, indicating high target affinity. The binding to GI.1 was marginal, which indicates the absence of the aptamer binding motif in NoV genotype GI.1. Beier was generated by SELEX using an *E. coli* produced GII.4 VP1 protein, and chosen based on highest abundance in the twelfth SELEX-round nucleic acid pool¹⁸⁷. The aptamer VP1 protein binding complex was not previously characterized, but simulation predicted the aptamer to bind the shell region, and the hinge region between shell and protruding domain (Figure 39). Considering the broad NoV genotype affinity of Beier, the predicted VP1 binding makes sense as the genomic region for the shell domain is more conserved among the genotypes compared to the P-domain.

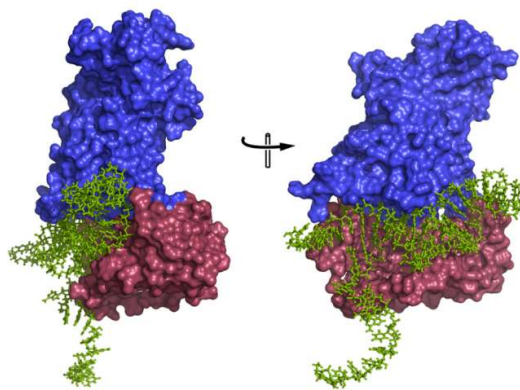


Figure 39. Simulated complex of aptamer Beier binding the NoV VP1 protein. The aptamer is shown in green, the shell domain is shown in red, and the protruding domain is shown in blue¹⁸⁷ (the reuse of this figure is in agreement with Oxford University Press and Copyright Clearance Center).

One major difference in the FRA of Beier in comparison to the remaining aptamer binding studies was the pH of the selection buffer. Beier was selected, and therefore FRA conducted, in a buffer with a pH of 6. It is known, that the NoV capsid changes adsorption/desorption behavior depending on pH in relation to the isoelectric point (pI) of a given virus⁵⁴. The pI values of VLPs of multiple NoV genotypes have been estimated to be around 6²²³. Therefore, the question remains whether the broad reactivity of the aptamer is due to a change in the net charge of the capsid at its pI.

4.4.3 Aptamer Structure Investigation Using Circular Dichroism Spectroscopy

For dot-blot and pull-down applications, aptamers were synthesized with a 5'-biotin tag. The biotin tag was spaced from the aptamer by a 12-hydrocarbon linker molecule, to prevent biotin-induced aptamer structure changes or steric hindrance in the target binding step. It has previously been determined that an aptamer tagged with a 12 hydrocarbon linker-biotin did not result in disruption of aptamers target binding domain²²⁴. Yet, the aptamers M 1 and M 6-2 had been selected using a biotinylated DNA library, to guarantee identical folding in inherent pull-down applications¹⁸⁹. Planning the SELEX experiment including future oligonucleotide modification could be beneficial, as aptamer labeling can lead to a decrease of aptamer target affinity, as any modification could lead to a change in aptamer folding²²⁵⁻²²⁶. Although biotin is a small molecule and was attached to the aptamer using a carbon spacer, to prevent structural influence, it was important to confirm that conformational integrity of the aptamer was not impaired by the biotin tag.

In order to investigate the aptamer structure with and without the biotin tag, CD spectra were recorded for each aptamer and its biotinylated counterpart. For none of the aptamers the wavelength of peak occurrences changed in presence of the biotin tag. For M 1 and SMV 21, the

spectra of the biotinylated, and non-biotinylated aptamer were shifted, however, the distance between positive and negative peaks remained the same, and no change in spectra amplitude was observed. This conveys that the biotinylated and non-biotinylated aptamers had a similar structure. However, for the aptamer M 6-2 and Beier a slight change in amplitude of biotinylated versus non-biotinylated spectra was observed. The spectrum of biotinylated M 6-2 aptamer exhibits a slightly decreased amplitude, compared to the non-biotinylated aptamer, indicating a higher degree of unfolded structures. Contrary, the biotinylated Beier aptamer showed a decreased amplitude compared to the spectrum of non-biotinylated aptamer. The spectra of biotinylated and non-biotinylated aptamer for Buf-2, AG3, and SMV 19 appeared aligned, indicating no influence of biotin tag on the structure of these molecules.

Other than Buf-2, all remaining tested aptamers show a positive band around 270-280 nm and a negative band around 245 nm. This is consistent with the absorbance of DNA B-forms, which characteristically show a positive band between 260 nm and 280 nm and a negative band around 245 nm²¹².

4.5 Aptamer-mediated Dot-blot

In order to show that aptamers can be used in a variety of applications, a dot-blot was developed as proof-of-concept. Assay optimization was not possible, due to the limited amount of VLPs available. A dot-blot application was chosen as it allows the use of food matrices with little sample clean-up efforts. The results confirm that the aptamer-mediated dot-blot using aptamers to detect a target protein is achievable. No spots were detected using the negative control, confirming that streptavidin did not cross react with NoV capsid proteins. It appeared that none of the aptamers bound to BSA, as blotted spots could be distinguished sharply from the background. BSA was used as a blocking agent and therefore present on each membrane; a binding to BSA would have resulted in a dark background. However, some blots appear slightly lined, likely from the oxidation of BCIP after alkaline phosphatase dephosphorylation resulting in a precipitating dye. Alkaline phosphatase-tagged streptavidin was chosen as detection agent, based on in-house availability of BCIP/NBT substrate. The mode of detection could be changed to obtain dot-blot with a more defined background.

Although the dot-blot results do not provide quantitative data, it was noted that aptamers showed similar binding characteristics as observed during the FRA comparative study. For aptamer Beier, a broad interaction among genotypes was observed, except for GI.1, which is consistent with the FRA studies. AG3 also showed FRA results consistent with dot-blot results, reflected in high spot intensities for the GII.4 genotypes, and weak intensity spots for GII.3 and GI.7. The M 6-2 mediated

Discussion

dot-blot did not result in the detection of NoV VLPs, which is consistent with FRA results, where only low overall binding to the VLPs was observed as well. The dot-blot of aptamers Buf-2, M 1, SMV 19, and SMV 21 showed strong binding to VLPs of genotype GII.4 New Orleans, which were detected in concentrations as low as 188 nM, 375 nM, 750 nM, and 750 nM for Buf-2, M 1, SMV 19, and SMV 21, respectively. However, it was notable that these four aptamers showed weaker binding to GII.4 Sydney during the dot-blot as compared to the FRAs. The dot-blot was completed using biotinylated aptamers, and the FRA assay using non-biotinylated aptamers. The overall similar binding characteristics of aptamer-target interactions by both methods indicated that there was no difference in target binding between biotinylated and non-biotinylated aptamers. This coincides with the CD-spectra results generated for aptamers with and without biotin tag.

The data collected confirms that an aptamer-mediated detection method like a dot-blot is feasible. This method could be used for the detection of pathogens from multiple food items. The food matrix effects that are observed in a multitude of analytical methods should be minor using a dot-blot, as most of the non-membrane binding matrix is rinsed off prior to the binding step in the process of the dot-blot method. This makes the dot-blot an attractive method for pathogen screening. An aptamer-mediated dot-blot developed for the detection of thrombin using the DNAzyme-labeled TBA aptamer in combination with TMB H₂O₂ substrate has been described²²⁷. The detection of lowest thrombin concentration of 600 nM was achieved, blotting 3 μ L sample, which equals about 1.2 pmol of thrombin protein per spot. With the Beier candidate, NoV GII.4 concentrations as low as 94 nM were detected, using a blotting volume of 2 μ L. This equals about 0.19 pmol per spot and is about ten times more sensitive than the TBA mediated thrombin dot-blot assay. The detection limit could be lowered by using fluorescent or chemiluminescent detection methods and by optimizing the aptamer concentration for detection. This would be necessary for NoV detection in food, as levels in contaminated foods and infectious dose are low. Considering that 2 μ L of a sample contain an infectious dose of 18 particles, this would translate into about 0.3 atto grams of viral capsid protein. It is obvious that a dot-blot assay for virus detection in foods would have to be considerably more sensitive. Nevertheless, this technique would be applicable in a clinical setting that analyses stool specimens, which contain a substantially higher viral titer. A dot-blot assay optimization could therefore be pursued, with the goal of to develop a clinical screening method for NoV.

4.6 Aptamer-mediated Norovirus Pull-Down

One of the objectives of this thesis was the development and discovery of a NoV aptamer to be used as an extraction tool. Therefore, the application of NoV aptamers in an aptamer-mediated pull-down assay to extract NoV from foods was investigated. Although previous studies using the FRA method showed that the aptamer-target binding might be impaired by the presence of food matrices, it was also discussed that the FRA method was not the ideal method to make this determination (see section 4.3). Therefore, all selected aptamers were tested in a pull-down assay (see section 3.8). The initial pull-down showed that the paramagnetic beads without aptamers (just beads=JB), which were used as a negative control in the virus pull-down, recovered virus from stool suspension. To be able to assess the pull-down abilities of the different aptamers, the beads needed to be blocked. Consequently, BSA blocking of the beads was implemented in the pull-down protocol, leading to a significant reduction (up to 1000-fold) of non-specific virus pull-down of the beads without aptamers. Using the BSA blocking method, a NoV pull-down was tested with aptamers SMV 19, SMV 21, M 1, M 6-2, AG3, Beier, and Buf-2. The virus recoveries were compared to the negative control, by multiple comparison test. P-values were calculated indicating significant differences compared to the negative control. The pull-down was completed using partially purified stool suspension, containing GII.4 genotype Den Haag in two dilutions (100-fold and 1000-fold).

For both dilutions, significantly more virus was recovered by aptamer-mediated pull-down, using aptamers SMV 19, SMV 21, M 1, M 6-2, Beier, and Buf-2, compared to the blocked paramagnetic beads. AG3 showed no significant difference to the negative control, of just the paramagnetic streptavidin beads. Results of the aptamer-mediated pull-down from the 100-fold dilution showed best virus recoveries, using aptamers M 1, and M 6-2, and SMV 21, reflected in the P-values of <0,0001 compared to the negative control. SMV 19, Beier and Buf-2 mediated pull-downs completed from the 100-fold stool dilution, recovered less virus compared to aptamers M 1, M 6-2 and SMV 21, reflected in higher Ct values and a higher P-value of 0.0021. Completing the pull-down from a 1000-fold stool dilution, no virus was recovered using the negative control and aptamer-mediated pull-down with AG3. The remaining aptamers tested, showed significantly higher recovery than the negative control. Overall, a similar NoV recovery pattern as observed for the 100-fold stool dilution was observed, completing pull-downs from a 1000-fold stool dilution.

Aptamer-mediated pull-downs using M 6-2, M 1, and SMV 21 showed the highest virus recovery, in descending order. The good results accomplished using aptamers M 1 and M 6-2 were not expected, as these aptamers did not show good binding characteristic in the FRA and dot-blot

Discussion

methods. The pull-down studies were completed using a different NoV GII.4 Den Haag (based on availability), a different genotype than used during the FRA binding studies. All aptamers showed genotype dependent differences in VLP binding, during FRA and dot-blot studies. Therefore, results observed during the pull-down differing from the previous studies could be due to genotype-specific binding of the aptamers. Hence, aptamers M 1, M 6-2, and SMV 19 could exhibit good binding characteristics for NoV GII.4 Den Haag.

Using the aptamers Beier, Buf-2 and M 1, M 6-2, SMV 19 and SMV 21, a NoV pull-down was completed from an artificially contaminated oyster sample and data from the pull-down compared to the existing FDA-shellfish method for NoV extraction from oysters. Results demonstrated the FDA-shellfish method had over 1000-fold better recovery than the best aptamer pull-down, accomplished with the SMV 21 aptamer. More importantly, it was shown that the blocking protocol developed using the BSA in every step of the pull-down, did not show the same efficiency in presence of the oyster matrix compared to the efficiency in buffer. The true potential of the aptamer-mediated pull-down can therefore not certainly be estimated.

Non-specific binding of viruses to paramagnetic beads are not a single occurrence. In a 2008 study an immunomagnetic approach to pull-down virus using antibodies was described, determining that monoclonal antibodies accomplished better NoV recovery than polyclonal antibodies²²⁸. However, a negative control employing beads without antibodies was not conducted. In a previous study investigating immunomagnetic pull-downs of enteric viruses it was noted that non-specific binding of viruses to paramagnetic beads was observed, but did not impair the limit of detection of the assay²²⁹. This makes sense for assays which follow the pull-down step with a subsequent specific detection step, like RT-qPCR, as commonly used for enteric RNA viruses. However, the blocking of the virus's non-specific binding to paramagnetic beads was imperative to determining the specificity of aptamer-mediated virus pull-downs. Additionally, it is noteworthy that the non-specific binding to paramagnetic beads is most probably not limited to only enteric viruses. Non-specific binding in pull-down assays could lead to the co-extraction of sample contaminants and PCR inhibitors, contradicting the idea of using a pull-down assay as purifying method in the first place.

M 1, and M 6-2 aptamers were previously studied in a pull-down application using BSA blocked paramagnetic streptavidin beads¹⁸⁹. However, in this study the negative control, using just the streptavidin beads was not prepared in skim milk, which was used as a blocking agent for aptamer-mediated pull-downs. Instead, the paramagnetic beads for the negative control were blocked with a commercial solution (Superblock T20, by Thermo Fisher Scientific). The results showed

Discussion

significantly better recoveries, compared to the negative control, during the pull-down for both aptamers in two of four stool dilutions tested. However, since the negative control did not represent the assay conditions, it is questionable whether these outcomes are truly a result of the aptamer pull-down or a result of non-specific binding to the skim milk blocked beads.

The results of the aptamer-mediated NoV pull-down from oysters suggest that the chemistry of the paramagnetic beads is not compatible with BSA blocking, which has also recently been noted by the manufacturer²³⁰. It is therefore necessary, to identify a suitable blocking agent before the aptamer-mediated pull-down can be further assessed. Additionally, the pull-down could be improved using an assortment of multiple NoV specific aptamers, increasing the cross reactivity and allow a more broad NoV detection, as suggested previously²³¹.

A further issue with the pull-down targeting the capsid protein, and using a genome-based detection method, is the fundamental occurrence of the virus and viral protein in clinical samples and the environment. It is well established for NoV and other enteric viruses that the presence of genomic viral RNA does not indicate whether the viral particle is intact⁷⁸; this is a problem as it suggests the presence of unassembled virus capsid in the sample. The pull-down depends on the retention of the entire viral particle on the paramagnetic bead to detect the capsid enclosed genome. The presence of unassembled capsid protein in stool samples would occupy aptamers and make them unavailable to bind an intact viral particle. Hence, potentially impairing the detection of NoV, as unassembled capsid protein is extracted but not identified by the detection method. This could be resolved by using an excess of aptamer and magnetic beads for the pull-down.

5 Conclusion and Outlook

The primary goal of this work, selecting and characterizing an aptamer for the NoV surface, was accomplished. The aptamer Buf-2 was discovered by SELEX and exhibited specific affinity for the NoV P-domain with a K_d of 17.42 ± 6.97 nM. Furthermore, a comparative study was conducted, investigating the influence of food matrices on aptamer enrichment during SELEX. The findings provided new insights into the SELEX process, and elucidated the importance of continuing the optimization of the SELEX method. It was demonstrated that food matrices had variable effects on the enrichment of aptamers during the *in vitro* selection. The introduction of food matrices to SELEX was either detrimental to the enrichment of oligonucleotides with target-specific binding (e.g., both oyster- and the oyster div.-SELEX-experiments), or facilitated the enrichment of non-target-specific oligonucleotides (e.g., the strawberry- and lettuce-SELEX-experiments). However, it was observed that completing parallel *in vitro* selections, branching from the same pre-enriched nucleic acid library can help identify oligonucleotides with target-specific binding properties. This was the case with the selected aptamer Buf-2, which was enriched during the buffer-SELEX-experiment, but was also mildly enriched during the oyster- and the oyster div.-SELEX-experiments. Buf-2 exhibited the most promising binding characteristics to the NoV P-domain, compared to other oligonucleotides enriched during the parallel SELEX-experiments.

The comparative study was based on the hypothesis, that the parallel SELEX-experiments conducted in presence of different food matrices would lead to the enrichment of aptamers that can be used as an analytical tool in the food matrices in which presence they were selected. It was further anticipated that successful aptamer target binding will depend on the presence of the food matrix used during the SELEX-experiment, as it was expected, that the different food matrices will influence aptamer folding and its ability to interact with its target. In contrast to this hypothesis, the empirical results revealed that the introduction of food matrices to SELEX neither facilitated the successful selection of aptamers that bound their target in undiluted food samples, nor increased stringency during SELEX. This suggests that a pathogen-specific aptamer with application in food matrix does not need to be selected in presence of the food matrices. Furthermore, superior target binding of aptamers like Buf-2 over oligonucleotides that did not exhibit specific binding to the target, like Buf-8, in the presence of food matrices was not observed. This indicates that aptamers may require properties beyond high affinity and selectivity to be applied for pathogen extraction and detection in undiluted food matrices. Recently, the selection of aptamers with low dissociation constants has been promoted and a new class of chemically modified aptamers has been introduced in the field of proteomics: the *SOMAmers*¹⁴⁸. It is likely that the use of aptamers with low dissociation constants is advantageous for aptamers to be used

Conclusion and Outlook

in food matrices as well. Hence, the use of *SOMAmers* and the significance of aptamer-target dissociation constants needs to be evaluated regarding aptamer-target binding in presence of food matrices. Additionally, previous aptamers which were utilized in food analytical assays (OTA aptamer) were identified to bind their target through an induced fit mechanism. As the utility of Buf-2 in undiluted food matrices could not be confirmed, despite the aptamer's verified high and specific target affinity, it seems that additional characteristics defining an aptamer determine its utility in food matrices. The target binding mechanism could be one of these characteristics and therefore the dependency of target binding mechanism and the utility of an aptamer in the presence of food matrices should be evaluated.

At this point, the utility of aptamers in applications involving undiluted food remains uncertain. Nonetheless, aptamers still present a valuable tool in food analytical chemistry and can be used for detection and quantification of foodborne pathogens. The emerging use of aptamers as analytic tools to distinguish viable from non-viable organisms, as well as the need to extract intact viral particles and bacteria for downstream applications (e.g. whole genome sequencing and tissue culture), emphasizes the usefulness of aptamers in food analytical methods.

This investigative study on the influence of food matrices in aptamer enrichment underlines the importance of not only selecting aptamers for foodborne pathogens but also for conducting focused research that investigates the selection and binding of aptamers in the presence of food matrices. These studies should include investigations focusing on the role of the aptamer 'fit' and kinetic characteristics of aptamers with intended application in food and implement new developments in the aptamer field. Additionally, the adaption of the SELEX process to facilitate aptamers that can be used in food matrices needs to be investigated further. Ultimately, the discovery of structural and kinetic attributes that an aptamer needs, in order to bind to its target in undiluted food matrices, is imperative to establish aptamers as reliable extraction and detection tools in food chemistry and to be established as valuable analytic tools in regulatory research.

In addition to investigating the role of food matrices in the SELEX process, binding properties of NoV aptamers published in the years 2013-2015 and the aptamer selected during this work and published in 2018 were characterized. This was accomplished by conducting binding studies with selected aptamers and NoV VLP of the genotypes GI.1, GI.7, GII.3 and two strains of NoV genotype GII.4. It was shown that the majority of aptamers bound the NoV capsid proteins, with K_d values determined in the low nanomolar to low micromolar range, depending on the aptamer and NoV VLP genotype. Aptamer Buf-2 bound VLPs of the genotypes GII.3 and to the VLPs of the two GII.4 strains, with determined K_d s values of 351 ± 89 nM and 241 ± 50 nM for genotypes GII.4 New

Conclusion and Outlook

Orleans and GII.4 Sydney, respectively. The majority of the aptamers bound to the VLPs of NoV GII.4 exclusively. However, the aptamer Beier showed broad reactivity among genotypes investigated, except to NoV VLPs of genotype GI.1, with K_{ds} of 62.98 ± 28.11 nM, 114.9 ± 34.4 nM, 105 ± 47 nM and 71 ± 38 nM for VLPs of the genotypes GI.1, GII.3, GII.4 New Orleans, and GII.4 Sydney, respectively. Nevertheless, broad reactivity of the aptamer Beier against a variety of proteins must be determined to confirm aptamer selectivity for NoV. Further efforts to generate broadly reactive NoV aptamers could exploit the SELEX variant, toggle SELEX²³². During toggle SELEX, the oligonucleotide library is exposed to two targets consecutively in alternating SELEX-rounds. Thereby, aptamers are selected which bind to a common binding motif between the two targets. In addition to using a broadly reactive aptamer, binding to a broad spectrum of NoV genotypes could also be accomplished by using a panel of aptamers that bind to certain NoV genotypes specifically.

The tested aptamers were eventually applied in two analytical systems: an aptamer-mediated dot-blot and pull-down assay. It was shown, that the use of aptamers as detection- and extraction-tool can be facilitated but requires further optimization. This was especially true for the aptamer-mediated pull-down assays. One major aspect that requires addressing to improve the pull-down assay, is the need of a suitable blocking agent for paramagnetic beads. Additionally, the aptamer concentration used for the pull-down requires optimization. The NoV pull-down efficiency could also be increased by using a mixture of different NoV aptamers; this could provide a broader assay application in regard to the different NoV genotypes. However, the results obtained offer useful information for the additional studies related to NoV aptamers and offer a foundation for future aptamer-mediated assays for the detection and extraction of NoV.

6 Experimental Section

All instruments used in this work are listed in Table 32 including the manufacturer and the place of manufacturing, if available. Additionally, oligonucleotides, chemicals, enzymes and other materials used during this work, as well as buffer compositions are listed in the material section (section 7; Table 14-Table 31).

6.1 Virus Concentration and Extraction

6.1.1 Virus Concentration and Extraction from Shellfish including Viral RNA Extraction: FDA-Shellfish Method

For virus extraction from shellfish, FDA work instructions were followed. After the virus was extracted and concentrated, viral RNA was extracted using Qiagen RNeasy Mini Kit with modifications as described in the following protocol. The methods have been referred to in this work as FDA-shellfish method.

For virus concentration and extraction, 6 to 10 whole oysters were shucked and the digestive diverticula removed to obtain a 4 g sample. After adding 100 μ L extraction control (murine NoV with concentration of 103 plaque forming units per g) and 40 mL MilliQ Water, the suspension was gently mixed, transferred to a warring blender and homogenized by blending for 30 s. The resulting homogenate was transferred into a 50-mL conical tube and virus adsorption to oyster tissue accomplished by pH adjustment to values between 4.0 and 5.0 using 3 M HCl (the pH measurement was accomplished by transferring a small aliquot from the suspension to a petri-dish and measuring the pH of the removed aliquot using a handheld pH-meter). After centrifugation for 15 min at 4°C with 2000 x g, the supernatant was discarded and the pellet vigorously suspended with 40 mL glycine buffer (composition: Table 15) using a vortex. The pH of the suspension was then adjusted to 7.5-7.8 using 5 M NaOH to facilitate desorption of viral particles into the supernatant. The suspension was separated again by centrifugation for 15 min at 4°C with 5000 x g. The supernatant was then transferred into an ultracentrifuge tube and the pellet extracted again in 20 mL threonine buffer (composition: Table 15), as described for the first desorption step. The supernatant was combined with the previously decanted supernatant in the ultracentrifuge tube and virus concentrated by 1 h ultracentrifugation at 170,000 x g. The supernatant was discarded and the pellet suspended in 5 mL PBS buffer (composition: Table 15) and transferred to a 50-mL conical tube. Five mL chloroform were added to the pellet suspension, the tube tightly closed and the two phases mixed by vortexing for 30 s. After centrifugation at 1700 x g at 4°C for 15 min, the aqueous layer was transferred to a new ultracentrifuge tube. The

Experimental Section

chloroform phase was extracted again using 5 mL threonine buffer as described above and the aqueous phases combined in the ultracentrifuge tube and virus concentrated by ultracentrifugation at 170,000 g for 1 h at 4°C. After centrifugation, the supernatant was discarded and the virus pellet suspended with 400 µL PBS. The suspension was distributed evenly between two 1.5-mL microcentrifuge tubes. The virus concentrate was either used for RNA extraction immediately or stored at -70 °C until further use.

RNA was extracted from concentrates using Qiagen's RNeasy Mini Kit (Qiagen, Valencia, CA) per manufacturer's recommendations as described in the following, with the exception of the lysis solution. Centrifugation conditions for all steps if not otherwise noted were completed at 10,000 x g for 1 min using a benchtop centrifuge.

An aliquot of 500 µL guanidiniumisothiocyanate solution (6 M) was added to one virus concentrate (200 µL). After mixing using a vortex 700 µL 50 % ethanol (diluted from 200 proof ethanol) solution were added and the tube inverted three times. The sample was then forced through an RNeasy mini spin-column by centrifugation in two steps or until the entire sample volume passed through the column. The column bed was subsequently washed with RW1 buffer. This washing step included a 15-min incubation period of the buffer on the column bed, after which the buffer was forced through the column by centrifugation. After the first washing step, the column was placed into a new collection tube and the column bed washed three times with 500 µL RPE buffer, including a 15-min incubation period for the first two washes. For the last RPE washing step, the centrifugation was completed at 16,000 x g for 2 min. The column bed was then dried after the column was transferred into a new collection tube by centrifuging at 16,000 x g for 1 min. RNA was subsequently eluted in two steps, using 35 µL and 25 µL TE-buffer. The eluted RNA was either immediately analyzed by RT-q-PCR (see section 6.5.4) or stored at -70°C.

6.1.2 Virus Extraction and RNA Extraction from Clinical Stool Samples

The Gulf Coast Seafood Laboratory maintains a wide collection of clinical stool samples, collected from different hospitals. These samples have previously been analyzed regarding their NoV content. For samples that tested positive for NoV, the genogroup and genotype had been identified.

A 10 % suspension of 1.5 ± 0.5 g of NoV positive stool was prepared using PBS. Samples were mixed using a vortex followed by the addition of 5 mL chloroform. The phases were mixed by vortexing for 30 s and separated by centrifugation at 4°C for 10 min at 2000 x g. The aqueous phase was transferred into a new 50-mL conical tube, and chloroform extraction repeated using

additional 5 mL chloroform. Subsequently, the aqueous phase was transferred to a new 50-mL conical tube and filter sterilized using a low protein binding filter (Table 27). The filtrate was used as purified stool suspension for multiple applications. After virus extraction and purification from stool, viral RNA was extracted using the Qiagen Viral RNA extraction Mini Kit as instructed by the manufacturer.

6.2 Purification of DNA, RNA, and Oligonucleotides Using Commercial Kits

Commonly, nucleic acid purification kits revolve around a silica column. In presence of chaotropic salts, silica specifically binds nucleic acids, which can be eluted of the column after multiple washing steps, using nuclease free water or TE-buffer.

6.2.1 DNA Isolation from Agarose Gels

The DNA fragment to be extracted was excised from the agarose gel under UV light using a scalpel and DNA extracted using the Qiagen Gel Extraction Kit as per manufacturer's instructions.

6.2.2 Purification of PCR Products

Excess primers and nucleotides were removed from PCR products using the Qiagen PCR product MiniElute Kit as per manufacturer's instructions.

6.2.3 Purification of Oligonucleotides

Radiolabeled DNA was purified using the Zymo Oligo Clean&Concentrator™ Kit, as per manufacturer's instructions. Radiolabeled oligonucleotides were eluted with 15 µL nuclease free water and then 15 µL of twofold concentrated SB added to the eluate to obtain radiolabeled aptamer candidate in SB with the salt concentration used throughout this project. The names and compositions of the different buffers used are shown in Table 13 and Table 16.

6.2.4 Purification of Single-Stranded Nucleic Acid

Single-stranded DNA was purified with BioRad G30 mikro-spin columns using the buffer exchange protocol, as per manufacturer's instructions.

6.2.5 Purification of DNA Post-Cycle-Sequencing Reaction

After the sequencing reaction, incorporating dNTPs and ddNTPs, DNA was purified using the Zymo ZR DNA Sequencing Clean-Up Kit™, as per manufacturer's instructions.

6.2.6 Purification of Plasmids from Overnight Culture

For the plasmid extraction, Qiagen Plasmid Extraction Kit was used with a modified protocol, described in the following. A single colony was transferred into 3 mL LB media supplemented with 100 µg/mL Ampicillin and incubated overnight at 37°C on a shaking incubator. Next day the cells

of 2 mL of the overnight culture were collected at the bottom of a 2-mL microcentrifuge tube by centrifugation for 5 min at 5000 x g at room temperature and the supernatant discarded. The cells were suspended in 300 µL Qiagen buffer P1 by mixing, using a vortex and 300 µL Qiagen buffer P2 added and the gently mixed. After 5 min incubation 300 µL of Qiagen buffer N3 was added and the mixture gently agitated by inverting the tube and placed on ice for 5-10 min for complete precipitation of proteins and genomic DNA. The precipitate was then separated from solution by centrifugation for 1 min at 10,000 x g at room temperature. The supernatant was transferred to a clean microcentrifuge tube containing 800 µL isopropanol and the mixture inverted multiple times. After 2 h at room temperature or overnight at -20°C, the precipitate was collected at the bottom of the tube by centrifugation at 4°C for 15 min at 16,000 x g. The supernatant was removed by gentle suction and the pellet washed with 70 % ethanol solution twice. The pellet was then air dried under a fume hood and suspended in either water or TE-buffer, based on downstream application.

6.3 Nucleic Acid Separation and Detection

6.3.1 Agarose Gel Electrophoresis and In-Gel Nucleic Acid Detection with Ethidium Bromide

Agarose gel electrophoresis is an established method for separation of DNA molecules in an electric field, based on size and charge. Post electrophoresis, separated DNA fragments of different sizes appear as bands in the gel and are compared to a DNA standard containing DNA fragments of defined sizes. DNA is commonly detected by ethidium bromide, an intercalating fluorescent dye that binds to the DNA-helix without apparent sequence preference²³³. Ethidium bromide absorbs UV light of 310-350 nm and reemits this energy as yellow/orange light.

Agarose gels are prepared by boiling agarose in 200 mL 1 x TAE buffer using a microwave. After cooling (to about 65°C), ethidium bromide solution was added to a final concentration of 0.002 µg/mL agarose gel solution. The agarose solution is then poured into a gel cast and a comb placed on the cast rim to yield sample wells. The amount of agarose was adjusted to obtain the gel percentage needed, which is related to the size of DNA molecules to be analyzed. In this work 1-3 % agarose gels were used and electrophoresis completed at 110 V.

In this work ethidium bromide was a gel component. In order to monitor the progress of molecule separation during electrophoresis, the gel was placed in the Gel Documentation System Gel DOC™ XR+ and DNA bands detected under UV light in the gel documentation unit, taking advantage of

ethidium bromide's properties described above. Gel Images were taken, using the Software Image Lab (BioRad, freeware).

6.3.2 Nucleic Acid Detection Using Autoradiography

Commercially available phosphor storage screens are composed of BaFBr:Eu²⁺ in an organic binder²³⁴. High energy radiation, such as beta particles emitted by ³²P, excite the Eu²⁺ ion into the conduction band. As a result, the electron is trapped in the 'F-center' of the BaFBr- complex crystal and Eu²⁺ is oxidized to Eu³⁺. By exposing the excited complex to light from helium-neon laser at 633 nm, the electrons are liberated and move back to the conduction band, reducing Eu³⁺ to Eu^{2+*}. Eu^{2+*} then releases a photon at 390 nm and returns into ground state²³⁵⁻²³⁶. The light emitted from the phosphor screen upon laser stimulation is proportional to the amount of radioactivity and can be detected by the phosphor imager.

Radiolabeled DNA detection of samples on filter paper (wrapped in polyethylene food wrap to avoid contamination of the phosphor screen) was accomplished by overnight exposure of the filter to the phosphor screen. The phosphor screen was subsequently scanned using the phosphor imager at pixel size 50 µm in the phosphor imaging mode. Autoradiography data was analyzed using the Image Quant software, by GE Healthcare and exported to GraphPad Prism 7 for subsequent analysis. The screen was then erased for the next use by light exposure using the BioRad Screen Eraser K.

6.4 Nucleic Acid Quantification

6.4.1 Nucleic Acid Quantification using the NanoDrop

The NanoDrop measures the absorbance of solutions at wavelengths 260 nm and 280 nm. DNA is quantified using conversion factors, supplementing the molar extinction coefficient (as per Beer's law). The conversion factors are 50 µg/OD₂₆₀ for double stranded DNA, approximately 40 µg/OD₂₆₀ for single-stranded RNA, and approximately 33 µg/OD₂₆₀ for single-stranded DNA. The Nano Drop spectrophotometer requires only 1 µL of sample.

6.4.2 Nucleic Acid Quantification using the Qubit[®]-Fluorometer.

The Qubit fluorometer was used to quantify DNA. It works in combination with a fluorescence-based assay kit. Each kit contains a fluorophore reagent selectively binding the analyte to generate an external standard curve. To determine double stranded DNA concentration and single-stranded DNA concentrations the Kits Qubit dsDNA BR Assay Kit and Qubit ssDNA Assay Kit were used according to manufacturer's instructions, respectively.

6.5 Nucleic Acid Amplification, Modification, and Sequencing

Primers, probes, and other oligonucleotides, as well as other materials used for nucleic acid amplification, modification and sequencing are shown in section 7.5 in Table 19.

6.5.1 Amplification of VP1 Gene by Reverse Transcriptase PCR

A clinical stool sample positive for NoV genogroup II was partially purified by chloroform extraction, and viral RNA was extracted (see section 6.1.2). The VP1 gene was amplified from genomic RNA by reverse transcriptase (RT)-PCR in a nested two-step reaction using two different sets of primers as follows. The first set of primers consisted of GSK G2 forward primer and ORF 3 reversed primer, both previously described^{111, 237}. This primer set was applied to generated cDNA of NoV's ORF 2 and 3 using Superscript II RT as per manufacturer's instructions. Briefly, the primers (2 pmol/reaction each), dNTPs (1 μ L of dNTP mix containing 10mM each nucleotide), nuclease free water and template RNA were combined and the mixture incubated at 65°C for 5 min and immediately chilled on ice for 2 min. Keeping the reaction on ice, 5x First-strand Buffer (5xFSB), RNAsin (20 U/ μ L), DTT (0.1 M) and Superscript-Reverse Transcriptase II (2 U/ μ L) were combined and added to the mixture. The RT-reaction was incubated for 50 min at 42°C followed by an enzyme inactivation step at 70°C for 15 min. An RNase H treatment was completed subsequent to the inactivation of the RT-enzyme adding 1 μ L (2U) for 20 min at 37 C in a water bath.

Of the RT- reaction, 20 % (4 μ L) was used as template to amplify the VP1 gene using Platinum Taq[®] polymerase and previously described VLP primers¹⁹⁵ (cycling conditions: 94°C for 180 s, 35 cycles of: 94°C for 30 s, 66.6°C for 30 s, 68°C for 90 s, final extension: 72°C 240 s). The master mix pipetting scheme is shown in the annex (Table 33).

6.5.2 Amplification of P-domain Gene by PCR

The P-domain gene was amplified from the recombinant VP1 gene, using DNA polymerase Platinum Pfx[®] polymerase to generate a blunt end PCR product (cycling conditions: 94°C for 300 s, 35 cycles of: 94°C for 30 s, 60.0°C for 30 s, 68°C for 90 s, final extension: 72°C 420 s) with previously described P-domain primers¹⁹⁵. The master mix pipetting scheme is shown in the annex (Table 34).

The VP1 gene which served as template for the P-domain PCR, was obtained by double restriction digestion of the recombinant TOPO plasmid using Eco RI and Bam HI restriction enzymes, as the two restriction sites were included in the primer sites. The restriction digestion was completed as per recommendations of new England Biolabs (NEB), using the NEB 2.1 buffer. The resulting DNA fragment was purified by agarose gel electrophoresis and subsequently extracted from the agarose gel.

6.5.3 Amplification of Nucleic Acid Library During SELEX

The 40 nt random DNA library was flanked by primer annealing sites at either side of the random region. Primers for library amplification were used as previously described²³⁸, with the exception of the reverse primer, which was not biotinylated but phosphorylated to enable post PCR complementary strand separation by exonuclease digestion.

To allow amplification of nucleic acid molecules with complex structures, Q-Solution™ provided through Qiagen One-step RT-PCR Kit™ was added to the master mix as instructed by the manufacturer. DNA amplification was optimized regarding magnesium, primer and polymerase concentration. The optimal master mix pipetting scheme is shown in the annex (Table 35). The DNA library amplification was optimized and amplified with cycling conditions of 94 °C for 3 min, followed 9-25 cycles of: 94°C for 15 s, 55 °C for 10 s and 72°C for 15 s, without final extension step.

6.5.4 Multiplex Reverse Transcriptase Real Time PCR Assay for Norovirus

Norovirus RNA was detected by a RT-qPCR assay as previously described¹¹³. Briefly, the assay is designed as a multiplex assay, detecting NoV GI and GII simultaneously using degenerated cog primers for GI and GII¹¹⁷. Two Cy5 probes were used for GI and one Cy3 probe for GII. Additionally, the PCR master mix includes primers and one TxRed probe for an internal control referred to as internal amplification control (IAC) primers and probe. The master mix pipetting scheme is shown in the annex (Table 36). The RNA was reverse transcribed and immediately amplified by a hot start DNA polymerase in a one tube reaction with the Qiagen OneStep RT-PCR Kit using optimized cycling conditions (50°C for 50 min and 95°C for 15 min followed by 50 cycles of 95°C for 10 s, 53°C for 25 s, and 62°C for 70 s). Fluorescence was read at the end of the 62°C elongation step. All RT-qPCR reactions were completed using SmartCycler II (Cepheid) using default analysis parameters, except that the manual threshold fluorescence units were set to 10.

6.5.5 Amplification of plasmid DNA from Bacterial Colony by PCR

The colony PCR is an easy analysis tool to screen colonies for successful ligation of the DNA-insert into the vector. For colony PCR, a master mix is prepared using gene specific primers or primers flanking the multiple cloning site on the plasmid. Instead of template DNA, a colony from an agar plate is transferred and suspended into the master mix. In case of a positive ligation and depending on the choice of primers the PCR will result in a DNA fragment of a known size. Depending on the nature of the plasmid used, these primer regions flanking the multiple cloning site can vary. The primer sets flanking the multiple cloning sites of the different vectors used in this work are named T7 and M13 and the primer sequences are shown in section 7.5 (Table 20). The pipetting scheme of the master mix is summarized in the annex (Table 35) and the PCR was

completed using cycling conditions as per manufacturer's instructions (cycling conditions: 94°C for 2 min followed by 25 cycles of 94°C for 60s, 55°C for 60 s, and 72°C for 60s, final extension: 72°C 420 s).

6.5.6 Sequencing of VP1 gene PCR product

In this work DNA sequences were obtained using the dye terminator sequencing method, a variant of Sanger Sequencing²³⁹. The VP1 and the P-domain genes were sequenced on the CEQ 8000-Sequencer with the dye terminator cycle sequencing (DTCS) method, using the Genome Lab DTCS Quick Start Kit with optimized cycling conditions (30 cycles of 96°C for 20 s, 50.0°C for 20 s, 60°C for 4 min). For sequencing, primers were designed to anneal to complementary annealing sites located on the VP1 genome to obtain 400 bp fragments (all primers are listed in Table 19), sequencing the 1.6 kb fragment in multiple pieces with subsequent alignment. The primer sites were chosen to produce overlapping fragments, to allow optimal alignment of the resulting sequences. Alignment of the obtained sequences was achieved using the software BioEdit. The sequences were then used to identify the NoV genotype with the database 'Calicinet'²⁴⁰.

6.5.7 Generation of Single-Stranded Nucleic Acid by Lambda Exonuclease Digestion

Lambda exonuclease is an enzyme catalyzing the removal of 5' mononucleotides from DNA, in this work from PCR product. The preferred substrate of lambda exonuclease is 5'-phosphorylated double stranded DNA. The digestion of only the reverse strand of the PCR product, leaving the single-stranded forward strand was accomplished by using a phosphorylated reverse primer during the amplification of the oligonucleotide library.

For exonuclease digestion purified PCR product (see section 6.2.2) amplified with phosphorylated reverse primer was subjected to lambda exonuclease digestion at 37°C for 50 min with 25 U lambda exonuclease (New England Biolabs, Ipswich MA, USA) in a 50 µL reaction, followed by enzyme inactivation at 70°C for 10 min. Complete exonuclease digestions was monitored by agarose gel electrophoresis, and single-stranded nucleic acid purified as described in section 6.2.4.

6.5.8 Radionuclide End-Labeling of Oligonucleotides

The 5'-end of DNA-oligonucleotides and PCR products generated with a 'conventional', synthesized primer can be directly labeled with γ -phosphate of ATP in a kinase phosphorylation reaction, catalyzed by the polynucleotide kinase (PNK). The direct phosphorylation is possible due to the 5'-hydroxylated-end of synthesized oligonucleotides.

Single-stranded nucleic acids were labeled with [γ - ^{32}P]-ATP (Perkin Elmer, Meridan CT, USA) using the Promega T4 Polynucleotide Kinase (Madison WI, USA) according to manufacturer's instructions. Unincorporated nucleotides were removed as described in section 6.2.3.

6.6 Molecular Cloning and Transformation

6.6.1 Cloning and Transformation Using the Champion™ pET Directional TOPO® Kit

The concept of molecular cloning has first been described in 1972²⁴¹. During molecular cloning a DNA fragment is inserted into a vector, which is consequently used for transformation of host cells. The kind of vector used during this work is a plasmid.

The pET Directional TOPO®-cloning reaction was performed following instructions provided by the manufacturer using fresh blunt-end PCR-product (see section 6.5.2). The recombinant vector was used for transformation of *E. coli* One Shot®TOP10 cells for amplification- and maintenance purposes as per manufacturer's recommendations using the chemical transformation protocol.

For protein production, recombinant vector was purified (section 6.2.6) and transformation of *E. coli* cells BL21 Star™(DE3) OneShot® accomplished, as per manufacturer's recommendations using the chemical transformation protocol.

6.6.2 Cloning of PCR Products and Transformation

PCR products were cloned using the pCR™4-TOPO® vector as described in the TOPO™ TA Cloning Kit for Sequencing. Transformation was completed using *E. coli* One Shot™TOP 10, supplied with the Kit as per manufacturers recommendations using the chemical transformation protocol.

6.6.3 Identification of Colonies Carrying the Recombinant Vector

Colonies resulting from the pCR™4-TOPO® were identified by Blue and White Screening and positive clones further analyzed by colony PCR (section 6.5.5).

The pET100/D-TOPO® vector is inapplicable for blue and white screening; hence 50 colonies were analyzed by Colony PCR using T7 primers (section 6.5.5). The construct between the T7 primers, which flank the multiple cloning site on the vector, was sequenced (section 6.5.6) to confirm that the gene is in frame with the 6xHis-tag.

6.7 Protein Analytical Methods

6.7.1 Protein Separation Techniques

Proteins are commonly separated based on size, using SDS PAGE, first described by Laemmli²⁴². SDS is an anionic detergent, denaturing the proteins three-dimensional structure and coating the

protein's individual charge with its own anionic charge. Negatively charged proteins are subsequently separated based on their retardation in the polyacrylamide gel in the electric field, where small molecules move faster through the porous gel. Proteins of different molecular masses appear as bands in the gel after completed electrophoresis and are visualized in gel using a coomassie dye and are compared to a protein standard.

6.7.2 Protein Separation by SDS PAGE and Subsequent In-Gel Detection

Protein denaturation with SDS was completed adding an equal volume of 2x SDS buffer (see Table 14) to the protein sample and boiling of the mixture for 5 min in a heat block (the tube lids were sealed with a clip to avoid the opening of the tube during boiling).

Each 8 μ L sample and 8 μ L protein SDS PAGE molecular weight standard (Table 25) were used for analysis on a 10 % SDS PAGE gel (pipetting schemes for stacking and running gels are shown in annex Table 38 and Table 39). After completed electrophoresis at 200 V for approximately 45 min, separated proteins were visualized in the gel with Biosafe™ Coomassie-dye as per manufacturer's instructions.

6.7.3 Protein Separation Using the 2200 Tape Stations

The Agilent 2200 Tape Station system is a tape-based platform for small scale electrophoresis applications. The separation chemistry is based on the basic principle of SDS-PAGE. In this work the P200 Screen Tape and P200 reagents were used. The Agilent supplies and reagents are designed for analysis of proteins with sizes of 10-200 kDa. The Tape Station analysis-software enables the comparison of band intensities. This tool can be used to calculate percentages of protein fractions in one sample.

The P200 Screen Tape and P200 reagents were used and sample preparation completed as per manufacturer's recommendations.

6.7.4 Dot-blot for Protein Identification

The identity of the produced P-domain was confirmed with NoV antibodies 167024 and 97046 (Abcam, Cambridge, MA, USA) by dot-blot. Norovirus mouse monoclonal VLP GII.4-2002 antibody (antibody 167024) was used to recognize the produced P-domain. The mouse antibody was subsequently detected using Rabbit Anti-Mouse IgG H&L conjugated with horse radish peroxidase (HPR) (antibody 97046). The oxidation of 3,5,3'5'-tetramethylbenzidine by horse HPR in presence of H₂O₂ results in a blue product. NoV positive stool samples were used as positive control, and NoV negative stool samples were used as negative control. All wash steps were completed using 30 mL buffer. Compositions of buffers used in this protocol are shown in Table 15. The dot-blot

was completed as follows, and the protocol derived from exemplary protocol given on the abcam website.

Of the protein samples 2 μ L were blotted on a nitrocellulose membrane, the membrane washed three times for 5 min in TBS buffer and left for drying. It was then blocked overnight in TBST-BSA buffer at 4 °C. Next day, the membrane was removed from blocking buffer and washed three times for 5 min using TBST buffer. The membrane was then submerged in 30 mL of the primary antibody diluted in TBST. The primary antibody concentration was optimized to a final concentration of 0.28 μ g/mL TBST. After 2 h at room temperature under mild horizontal rotation the membrane was washed five times for 5 min using TBST and 60 mL of the second antibody dilution added in a final concentration of 50 ng/mL TBST. The membrane was subsequently washed five times for five minutes in TBST, once in TBS and then equilibrated in Citrate Buffer. The membrane was transferred to a petri dish and 25 mL TMB color reagent added. The membrane was developed for 5 min, rinsed with water and a picture taken using Image Lab software and Gel Documentation System Gel DOC™ XR+. Dark blue spots on the membrane indicated a positive sample.

6.7.5 Protein Identification After In-Gel Trypsin Digestion by LC MS

The produced, purified protein band was excised from an SDS-PAGE-Gel. An in-gel digestion using trypsin was performed and the peptide-fragments resulting from the digestion extracted from the gel by sonication. The sample preparation and analysis were kindly provided by the working group of Dr. Lewis Pannell of the Mitchell Cancer Institute in Mobile AL, USA by LC-ESI-MS/MS, using an orbitrap. The resulting peptide sequence was identified using the search engine “Mascot” by Matrix Science.

6.7.6 Protein Quantification Using the Qubit Fluorometer

Proteins have traditionally been quantified using the Bradford²⁴³ or Lowry²⁴⁴ method. However, in this work protein concentration was determined using the Qubit Fluorometer (section 6.4.2). The fluorometer is used in combination with a fluorescence-based assay kits, supplying a fluorophore reagent selectively binding the analyte, and reagents to generate an external standard curve. Protein concentrations were determined using Qubit Protein Assay-Kit as per manufacturer’s instruction.

6.8 Protein Production and Purification

6.8.1 Production of P-domain in *E. coli*

The pET expression system used in this work, the Champion™ pET100/ Directional TOPO® Expression Kit allows expression of a recombinant protein with an N-terminal 6x- HisTag and is

Experimental Section

based on bacteriophage T7 elements, commonly used for protein production in *E. coli*. Proteins produced in this work were expressed in frame with a His-tag, taking advantage of the histidine affinity to Co^{2+} , and Ni^{2+} for protein purification via metal affinity chromatography²⁴⁵.

Blunt end PCR product of the P-domain gene was cloned into the expression vector pET100/D-TOPO[®] of the Champion™ pET100/ Directional TOPO[®] Expression Kit (section 6.6.1) and subsequently sequenced (section 6.5.6). For the production of the P-domain gene the recombinant pET100/D-TOPO[®] vector was used for transformation of *E. coli* host BL21 Star™(DE3). The P-domain was produced as previously described¹⁹⁵, with modifications after optimization as follows. Expression for the P-domain was induced at OD600: 0.6 with IPTG at a final concentration of 0.1 mM at 16 °C. Cells were harvested after 18 h shaking incubation at 16°C. Cells were harvested by centrifugation at room temperature for 15 min at 12000 x g at and cell pellets frozen overnight.

6.8.2 Production of Control Protein

The control protein of the *Champion™ pET* Directional TOPO[®] Expression Kit, the β -galactosidase was produced per manufacturer's instruction.

6.8.3 Cell Lysis and Protein Purification

The cell pellet was washed twice with 10 mL 1xPBS-buffer and subsequently suspended in 4 mL lysis-buffer (Table 15) per 1 g wet pellet weight by mixing with a vortex. After suspension of the pellet the protease inhibitor PMSF was added to a final concentration of 1 mM, lysozyme was added to a final concentration of 0.25 mg/mL, and 2 μL Benzonase/50 mL lysate was added. The suspension was incubated at 37°C for 20 min, followed by a freezing step at -20 °C. The freeze and thaw process was completed three times. After lysis the soluble protein-fraction was separated from the insoluble fraction by centrifugation at 30,000 x g for 30 min. Both fractions were analyzed by SDS PAGE.

6.8.4 Purification of Recombinant Protein

After cell lysis, recombinant protein was isolated via affinity chromatography using the cobalt resin HisPur™ by Thermo Fisher Scientific (Rockford IL, USA). The procedure was completed by gravity flow column, packing a plastic column with 400 μL resin suspension to purify recombinant protein from the soluble fraction of the lysate of 3 L bacterial culture. The sample was applied to the resin bed twice and kept on ice during the entire process. Column equilibration and washes were completed as per manufacturer's instructions, the optimized conditions are presented in the results section.

6.8.5 Protein Dialysis

Purified protein was dialyzed overnight at 4 °C and again at room temperature (temp range 19-21 °C) with fresh buffer for 4 h using SnakeSkin™ dialysis tubing 10 K MWCO. The tubing was the opened by cutting with a sterile pair of scissors and the sample transferred to a fresh tube.

6.9 *In vitro* Selection of Aptamers for the Norovirus P-domain Produced in *E. coli*

6.9.1 Preparations of Food Matrices for SELEX

To prepare the whole oyster (*Crassostrea virginica*) matrix, ten 10 locally harvested oysters (Fowl River, AL, USA) were homogenized using a warring blender. For oyster div. matrices, the diverticula of about 40 oysters were dissected and homogenized using a warring blender. Frozen strawberries were purchased from a local supermarket and 40 g homogenized by blending. Using the food homogenates, 10 % suspensions (4 g in 40 mL) were prepared in SB. The pH of the suspensions was adjusted to 7.4, as needed. To prepare the lettuce matrix, romaine lettuce was torn in uniform pieces by hand (diameter: 0.5”), and 50 g of lettuce rinsed with 50 mL of SB, by orbital shaking at 50 rpm for 15 min in a Whirl-Pak® sampling bag (6” x 9”). The rinse solution was transferred to a new container and used as lettuce matrix. The pH of the lettuce matrix was tested but did not require adjustment. The absence of NoV in food matrix preparations was confirmed by RT-qPCR as previously described¹¹³. Matrix preparations were aliquoted and frozen until further use.

6.9.2 Protein Immobilization on Paramagnetic Particles

For SELEX, target binding oligonucleotides must be separated from non-target binding oligonucleotides. In this work this was accomplished by immobilizing the target protein, the P-domain, on paramagnetic beads, taking advantage of the His-tag of the recombinant protein. The purified dialyzed P-domain and control protein (for counter selections) was immobilized on Dynabeads® His-Tag Isolation & Pulldown (Fisher Scientific, Suwanee GA, USA), using 500-750 µL protein solution (average concentration 68 µg/mL) and 25-50 µL bead suspension (1-2 mg beads) as described by the manufacturer with small variations. Briefly, for each SELEX-round, beads were freshly prepared and incubated with protein solution for 15 min, washed twice with wash buffer (as directed by the manufacturer, but without Tween®-20), and twice with SB. Washed beads were suspended in 50 µL SB. The protein concentration was measured before and after immobilization using the Qubit® (section 6.7.6). The difference in protein concentration pre and post immobilization was presumed to be the protein amount successfully immobilized on the beads. This value was then used to calculate the amount of protein per µL based on the suspension volume of 50 µL.

6.9.3 SELEX

The SELEX was started with 2.5 nmol oligonucleotide library divided in five microcentrifuge tubes each containing 500 pmol oligonucleotide library. Prior to each SELEX-round the library was heated in 500 μ L SB for 5 min at 95°C, and immediately cooled on ice for 15 min. BSA stock solution (10 mg/L BSA in SB) was added to a final concentration of 0.01 % BSA. The P-domain coated Dynabeads® suspension was then added to the library. The P-domain amount for the first SELEX-round was 390 pmol per 500 pmol library, in a final volume of 700 μ L SB. The amount of target protein was gradually reduced to 55 pmol, with increasing number of SELEX-rounds. The aptamer-P-domain binding-step was completed after 30 min incubation at room temperature under tilt rotation on setting 4.5 using the Bellco Roller Drum by Bellco Glass Inc. (Vineland, New Jersey, USA). Subsequently the P-domain binding oligonucleotides were retrieved by bead collection using a magnet rack. The supernatant was aspirated and thereby non-binding oligonucleotides removed. The collected beads were washed with 500 μ L SB. For the washing step, beads were completely suspended in SB and inverted by hand for 1 min, the beads were collected using a magnetic rack and the supernatant aspirated. Binding molecules were immediately heat-eluted from the beads at 80°C for 5 min in 55 μ L nuclease-free water.

The eluted oligonucleotides were directly amplified by PCR as described in section 6.5.3 and 15 μ L eluted oligonucleotides retained and frozen at -70°C. PCR-product formation was monitored after each SELEX-round after electrophoresis on ethidium bromide stained 3 % agarose gel (section 6.3.1) to determine the optimal number of PCR-cycles for each SELEX-round to prevent by-product formation, as previously described²⁴⁶. For this purpose, an aliquot of 5 μ L eluate for each selection was tested by PCR. The test-PCR-reaction was paused in an interval of two cycles, starting with a cycle number based on the expected DNA amount (e.g. in cycle 8, 10, 12, and 14), and an aliquot of 10 μ L removed. The amplified DNA in the resulting five 10 μ L-aliquots per SELEX-experiment was subsequently detected on a 3 % agarose gel with ethidium bromide after separation by electrophoresis as described in section 6.3.1. The remaining eluted oligonucleotides were amplified using the lowest number of PCR cycles for which a band of desired size was detected in the agarose gel.

Single-strand generation for the next SELEX-round was achieved by exonuclease digestion (section 6.5.7) from purified PCR product. The exonuclease digestion was confirmed on ethidium bromide stained 3 % agarose gel (section 6.3.1). The DNA single-strands were purified and eluted in SB with G30 BioSpin columns (section 6.2.4) using the buffer exchange protocol. Single-stranded DNA library in SB was prepared for the next SELEX-round as described above for the first SELEX-round.

Experimental Section

In order to ensure selection of aptamers binding specifically to the P-domain, negative selection was included in the SELEX process using the *Champion™ pET Directional TOPO® Expression Kit* His-tagged control protein. For this purpose, the control protein immobilized on the His-Tag Isolation & Pulldown Dynabeads® was exposed to the nucleic acid library of round three for 15 min. After magnetic collection of the control protein-beads, the supernatant was carefully aspirated and introduced to the P-domain binding step.

In SELEX-round four, the pre-enriched single-stranded nucleic acid library was divided in five equal parts and each introduced to the P-domain after negative selection. Subsequently, food matrices were introduced by washing the oligonucleotide-target complex after the binding step with each one of the four different food matrices or SB in five parallel selections (buffer, lettuce, strawberry, oyster and oyster div.). Each washing step included the collection of paramagnetic particles using a magnetic rack, a full suspension in 500 µL SB or food matrix suspension, and an incubation for 1 min. Immediately after, the beads were collected again and a washing step repeated, or nucleic acids eluted after aspiration of the supernatant as described above. The number of food matrix washing steps was increased from one to five in subsequent SELEX-rounds and the amount of beads for the negative selection was doubled in SELEX-round nine. Throughout the experiment, each selection was treated equally regarding target amount and counter selections, as well as washing steps with the food matrix.

After the five parallel *in vitro* selections were completed, final oligonucleotide pools were cloned (section 6.6.2). Each 50 clones per selection, a total of 250 clones, were randomly chosen for sequencing of the DNA insert of the recombinant vector. The colonies were isolated and transferred to a fresh LB agar plate supplemented with ampicillin (see Table 15), incubated overnight at 37°C and then sent to company Genewiz (NJ, USA), where the sequencing of the vector insert was completed using the T3 primer.

6.10 Identification and Characterization of Aptamers and Oligonucleotides

6.10.1 Sequence Abundance and Motif Search

Identical sequences among those obtained for the different selections were counted and the abundance of each sequence calculated in relation to the total number of sequences obtained per selection. The sequences of all selections are summarized in annex Table 40 to Table 44. Additionally, oligonucleotide sequences were investigated regarding shared nucleotide motifs using the meme-suite freeware¹⁹³.

6.10.2 FRAs to Investigate DNA Protein Interaction

The concept of the FRA is based on the observation, that proteins interact with the nitrocellulose membrane, whereas oligonucleotides do not, or to a significantly lower amount. Protein and radiolabeled oligonucleotides are collectively filtered through a nitrocellulose membrane, the protein binds to the membrane and radiolabeled DNA can only be detected if bound to the protein.

Protein-DNA interactions were investigated via FRAs on 0.45 μm nitrocellulose membranes. The assay was adapted from established practices²⁴⁷⁻²⁴⁸, using the Bio-Dot® SF Microfiltration Apparatus. For the FRA, nitrocellulose membranes were treated with 0.4 M NaOH for 10 min, washed three times in water and then equilibrated in SB. Radiolabeled single-stranded oligonucleotides or an oligonucleotide pool (1 nM final DNA concentration) and multiple target protein dilutions (typically 0-600 nM protein) were incubated for 60 min in SB and 20 μL of the reaction applied to the nitrocellulose membrane under suction. The nitrocellulose membrane was washed immediately, pre- and post-sample application, with 600 μL SB. Retained DNA was detected by autoradiography and relative binding to the target protein calculated through known amount of labeled DNA which was blotted directly to the membrane. DNA binding to the membrane was corrected by background subtraction for each protein dilution series applying a 20 μL sample which did not contain protein.

FRA data were fitted with the GraphPad Prism® program (version 7.02) and K_d values determined using the one site-specific binding equation, as given in the following, where T is the target concentration.

$$\text{Bound Aptamer} = \frac{B_{\text{max}}[T]}{K_d + [T]}$$

6.10.3 FRAs to Investigate DNA Protein Interaction in Presence of Food Matrices

The FRA was also used to determine aptamer-target binding in food matrices. For that purpose, the ³²P labeled oligonucleotides were diluted directly into the food suspension and subsequently added to the P-domain dilutions, resulting in a final concentration of 4.5 % food homogenate suspension for the strawberry-, oyster-, and oyster div.-SELEX-experiments. For the lettuce-SELEX-experiment the dilution corresponded to 22.5 g lettuce rinsed solution with 50 mL SB. To prevent clogging of the filters during the study, the strawberry, lettuce, and oyster matrix preparations (see section 6.9.1) were clarified by centrifugation for 1 min at 2000 x g to remove debris.

Experimental Section

Aptamer-P-domain binding in presence of oyster matrices was assessed by FRA, preparing two oyster matrix preparations, using two different types of oysters both of the species *Crassostrea virginica*. Oysters from Cedar Point (CP) in Alabama, USA, were freshly harvested and not further treated, before shucking. The individually quick-frozen oysters (IQF) are commercially available oysters, which were presented on a half shell, sprayed with a salt solution and individually, quickly frozen. From both oysters a 10 % suspension was prepared by blending the whole oyster in SB. Additionally, oyster diverticular were dissected of both oyster types and the FDA-shellfish method completed until the first ultracentrifugation step (section 6.1.1), but ended before the first ultracentrifugation step. The preparation was then further purified by chloroform extraction in a 1:1 ratio as described in the FDA-shellfish method (section 6.1.1). The absence of NoV for all food matrices was confirmed by RT-qPCR (section 6.5.4).

6.10.4 FRAs to Investigate DNA Protein Interaction in Presence of Competitors

For competition studies, selected radiolabeled aptamer candidates were incubated with the P-domain and 50-fold molar excess of the same non-radiolabeled aptamer (specific competitor) as well as in presence of 50-fold excess of the non-radiolabeled aptamer for α -thrombin termed TBA (non-specific competitor)²⁴⁹. To determine specificity of selected candidates, the FRA was completed using BSA, lysozyme, and thrombin as described for the P-domain.

6.10.5 FRAs to Investigate Target Binding of Selected NoV Aptamers

Aptamer's binding to five genotypes of NoV VLPs was tested in a molar range of 0-1500 nM. NoV VLPs of genotypes GI.1, GI.7, GII.3, GII.4 New Orleans, and GII.4 Sydney were kindly provided by Robert Atmar of Baylor College of Medicine, Houston TX. The binding reactions were prepared as described in section 6.10.2. However, each aptamer's individual buffer present during its selection was used and VLPs therefore dialyzed against the appropriate buffer for each aptamer. The buffers used for the tested aptamers are shown in Table 13.

Experimental Section

Table 13. Buffers present during SELEX of each aptamer with the corresponding literature reference.

Aptamer	Buffer	Literature
SMV 19	Gibco tc PBS	56
SMV 21		
M 1		189
M 6		
AG3	Giamb. Buffer	188
Beier	Beier Buffer	187
Buf-2	Selection Buffer	250

6.11 Analysis of Oligonucleotides Using Circular Dichroism Spectroscopy

The difference in absorption of right- and left-handed circularly polarized light by chiral molecules is called circular dichroism. CD is described by ellipticity (Θ), expressed in degrees. CD can be used to provide structural molecule information²¹². In this work it was used to investigate whether or not a biotin tag has an influence on molecular folding of the target binding domain of an aptamer by comparing CD spectra of the same oligonucleotide with and without biotin tag. Additionally, different variants of the oligonucleotide Buf-2 were investigated by CD-spectroscopy. For both studies, the CD spectra were recorded as described hereafter.

Oligonucleotides and their biotinylated counterparts were diluted in their corresponding selection buffer (Table 13) to achieve a final aptamer concentration of 10 μ M. The diluted aptamers were prepared by heat denaturation, for 5 min at 95°C, and immediately cooled on ice for 15 min and transferred to a glass cuvette with 0.1 cm pathway. CD spectra were obtained in 1 nm steps in the wavelength range of 200 nm to 320 nm, using the CD-Spectrometer Jasco 810 (the use of the instrument was kindly granted by the University of South Alabama, Chemistry Department in agreement with Dr. Allyn Scheffler and Prof. Dr. David Forbes).

For each oligonucleotide, three scans were averaged to create a spectrum. The buffer signals were each subtracted and the data were exported to excel and blotted in GraphPad Prism[®] program (version 7.02). To smooth the curves, spectra are depicted using the LOWESS function in GraphPad Prism[®] default settings.

6.12 Aptamer-mediated Dot-blot Detecting Norovirus Virus Like Particles

It is commonly known in molecular biology, that biotin and streptavidin share the strongest non-covalent interaction known. This has widely been taken advantage of in molecular biology in a vast variety of applications. In this work biotinylated aptamers were used in combination with streptavidin in a pull-down application using streptavidin coated paramagnetic beads, and in a dot-blot application. For the dot-blot, biotinylated aptamers were used to bind their target norovirus, which was blotted on a membrane. The biotinylated aptamers were then crosslinked to the membrane, where biotin was available to be bound by streptavidin. The streptavidin used for this application was linked to an alkaline phosphatase, which enabled visualization of the streptavidin bound to the biotinylated aptamer. Alkaline phosphatase is an enzyme, taken advantage of in multiple detection systems. In this work the phosphatase was used to catalyze the dephosphorylating of 5-Bromo-4-chloro-3-indolyl phosphate (BCIP), which is oxidized by nitro blue tetrazolium chloride (NBT) to a dark blue precipitating dye.

A duplicate of 2 μL of the NoV VLP solutions of different concentrations were blotted on a nitrocellulose membrane (0,45 μm pore size). After 15 min, to let the protein solutions dry on the membrane, the membranes were submerged in 50 mL blocking solution (PBS supplemented with 5% BSA) and incubated overnight at 4°C in a closed container. The following day aptamers were prepared by diluting 30 μL of a 100 μM aptamer solution in 900 μL of each aptamer's SB. The dilution was heated to 85 °C for 5 min and, immediately cooled on ice for 10 min, and finally equilibrated at room temperature for 20 min. In parallel the membrane was removed from the blocking solution, placed in a new container and washed five times for 5 min with each 40 mL SB (depending on which aptamer used, see Table 13). The prepared aptamer solution was diluted in 20 mL SB and added to the washed membrane for 1 h. The membrane was then washed three times for 5 min with each 35 mL SB. DNA was immediately crosslinked to the membrane using the auto function in the UV cross linker for 60 s. Subsequently, the membrane was dried and aptamers either immediately detected or stored in a dry environment at approximately 18 °C for no longer than seven days. As negative control, proteins were blotted on a membrane and the dot-blot protocol completed without the use of aptamers.

For aptamer detection, the dried membrane was equilibrated in 40 mL PBS for 15 min. In parallel 6 μL alkaline phosphatase linked streptavidin was diluted in 30 mL PBS. After the equilibration buffer was decanted, the diluted streptavidin solution was added, and incubated with the membrane for 30 min. The membrane was then washed four times with PBS for 5 min. All steps were completed at room temperature. The substrate solution for the alkaline phosphatase was

prepared by dissolving a NBT/BCIP Ready-to-Use tablet in 10 mL MilliQ water and was added to the membrane, which had been blotted dry on a paper towel and placed on a petri dish. After 40 min incubation in the dark and under mild rotation, the reaction was stopped by rinsing the membrane in MilliQ water. The developed membrane was then photographed, using the Gel Documentation System Gel DOC™ with the white light function.

6.13 Aptamer-mediated Pull-down of Norovirus GII.4

6.13.1 Preparation of the Paramagnetic Beads.

As described in section 6.12, the strong interaction between biotin and streptavidin is taken advantage of by many molecular techniques. For the aptamer-mediated pull-down, biotinylated aptamers are added to a virus containing solution. After allowing the aptamer to bind its target, the aptamer virus complex is pulled to streptavidin coated paramagnetic beads mediated by the aptamer's biotin tag.

For the aptamer-mediated pull-down, Dynabeads My One Streptavidin® were used. For each pull-down 50 µL beads were used to recover 200 pmol biotinylated oligonucleotide, as per manufacturer's instructions (Fisher Scientific).

6.13.2 Preparation of BSA-Blocked Streptavidin Coated Paramagnetic Beads.

Paramagnetic beads were equilibrated at room temperature, and mixed vigorously using a vortex for 30 s, to accomplish a homogenous suspension. Subsequently, an adequate amount was removed from the storage vessel and transferred to a fresh tube. Beads were then washed twice using twice the bead volume with SB supplemented with 1 % BSA (BSA-SB). Each washing step implemented removing storage or wash buffer after collection of beads using a magnet rack. Followed by fully suspending the beads in fresh wash buffer using a vortex for mixing and aspirating the wash buffer again after collecting beads using the magnet rack. Washed beads were suspended in twice the bead-volume using BSA-SB, placed in a vial spin carousel and incubated overnight at 4 °C with circular rotation for blocking. Next day beads were again washed twice with twice the bead volume using BSA-SB. The beads were then suspended in one bead volume BSA-SB until being used within 1 h.

6.13.3 Preparation of Aptamers

The biotinylated aptamers were prepared to obtain in 200 pmol oligonucleotide in 50 µL SB. The aptamer solution was then kept at 85°C for 6 min using a heat block, immediately cooled on ice for 10 min and finally equilibrate to room temperature for 20 min.

6.13.4 Aptamer-mediated Virus Pull-down From Buffer

For the pull-down, 50 μ L aptamer solution was added to the prepared virus suspension aliquot of 1 mL. After 1 h with tilt rotation at room temperature, 50 μ L blocked beads (section 6.13.2) were added to the mixture to facilitate a pull-down of biotinylated aptamer-NoV binding complexes under tilt rotation. After an additional 30 min at room temperature, the beads were collected and supernatant discarded. The beads were washed four times with 500 μ L BSA-SB and finally suspended in 140 μ L PBS. For the pull-down without BSA blocking, all steps were carried out identically, without the use of BSA.

6.13.5 Aptamer-mediated Virus Pull-Down in Presence of Oyster Food Matrix

The virus pull-down from oyster was based on the existing method for virus extraction from shellfish¹⁰⁹. Oysters were shucked and digestive glands dissected and homogenized using a warring blender. Three times 4 g were removed from the homogenate and processed as negative control using the FDA-shellfish method (section 6.1.1). To the remaining digestive gland homogenate 100 μ L of NoV positive purified stool suspension was added and the mixture again blended to achieve equal distribution of NoV in the digestive gland homogenate. Of this homogenate, 4 g samples were transferred to each one 50 mL conical tube. Three sample aliquots of 4 g were processed using the FDA-shellfish method (section 6.1.1) and each three times 4 g oyster samples were used to complete an aptamer pull-down. For the pull-down, the oyster digestive gland was suspended vigorously in 40 mL SB using a vortex and the pH adjusted to 4.0-5.0 using 1 M HCl. After centrifugation for 15 min at 4°C at 2000 x g the supernatant was discarded and the pellet vigorously suspended with 10 mL SB using a vortex. The pH of the suspension was then adjusted to 7.5-7.8 using 1 M NaOH. The suspension was centrifuged for 15 min at 4°C at 5000 x g. Of the supernatant 1.5 mL were transferred to a 2 mL microcentrifuge tube and 200 pmol aptamer (see section 6.13.3) added. The NoV pull-down was completed as described in section 6.13.4.

6.13.6 NoV RNA Extraction and Detection Post Pull-Down

The sample volume needed for the viral RNA extraction (section 6.1.1, 6.1.2) is 140 μ L. The 140 μ L bead suspension from the pull-down were therefore directly used for viral RNA extraction. Manufacturer's directions were followed with minor alterations, as described in the following. After viral lysis, and prior to the column loading step, the microcentrifuge tubes containing the beads suspension were placed on a magnet rack and the supernatant, containing the virus lysate, transferred to the spin column. The viral RNA extraction protocol was then resumed.

Experimental Section

The RNA eluent was either immediately used for detection with RT-qPCR (section 6.5.4) in two 3 μ L reactions per extract or stored at -70 until further use.

7 Experiment Materials

7.1 Chemicals

For list of hazardous chemicals, please refer to list in annex (section 9.3, Table 29). The list also includes chemicals that were classified hazardous by Harmonized System of Classification and Labelling of Chemicals. All chemicals were purchased from Fisher Scientific or Sigma Aldrich, based on availability.

7.2 Buffers, Solutions and Media

Buffers were sterilized by filter sterilization using a vacuum-based bottle top filtration device (pore size 0.2 μm). Media was sterilized using the autoclave.

Table 14. Buffers and solutions used for electrophoresis.

Buffer Name	Buffer components/Manufacturer
30 % Acrylamide/Bis Solution	Bio-Rad, Hercules CA, USA
Biosafe™ Coomassie-stain	
TEMED Solution	
Ethidium bromide solution (10 mg/mL)	Fisher Scientific, Suwanee GA, USA
TAE Buffer (50x concentrate)	
Loading Dye (6x) for Agarose gel electrophoresis	Qiagen, Valencia CA, USA
10 % APS	Sigma-Aldrich, St. Louis, MO, USA
10X SDS PAGE Running Buffer	3 % Tris base, 14.4 % Glycine, 1 % SDS, Water
2x SDS sample buffer	0.1 M Tris HCl (pH: 6.8), 20 % Glycerol, 3.6 M 2-Mercaptoethanol, 4% SDS, 0.05 % bromphenol blue
Resolving Gel Buffer	250 mL 1.5 M Tris base (pH: 8.8), 10 mL 10 % SDS, 400 mL dH ₂ O
Stacking Gel Buffer	62.5 mL 1 M Tris base (pH: 6.8), 5 mL 10 % SDS, 340 mL dH ₂ O

Experiment Materials

Table 15. Buffers used for aptamer mediated dot-blot, pull-down, and FDA-shellfish method, and buffers and media used during purification of recombinant protein.

Buffer Name	Buffer components/Manufacturer
Detection buffer dot-blot	1 M Tris Base, 100 mM NaCl
TBS Buffer	20 mM Tris HCl, 150 mM NaCl, pH 7.5
TBST Buffer	20 mM Tris HCl, 150 mM NaCl, 0.05 % Tween®-20 pH 7.5
TBST Buffer with BSA	0.1 % BSA, TBS-T
Citrate Buffer	50 mM C ₆ H ₈ O ₇ , 100 mM Na ₂ HPO ₄ , pH 5
TMB color reagent	5 mg TMB, 3 mL CH ₃ OH, 25 mL Citrate Buffer
Glycine Buffer	0.75 M glycine, 0.15 M NaCl, pH:7.6
Threonine Buffer	0.5 M Threonine, 0.15 M NaCl, pH 7.5
TE-buffer (Primer TE)	10 mM Tris, 0.1 mM EDTA
Lysis Buffer	50 mM Na ₂ HPO ₄ , 300 mM NaCl, 10 mM imidazole, pH:7.5
Protein Wash Buffer*	50 mM Na ₂ HPO ₄ , 300 mM NaCl, 25-75 mM imidazole*, pH:7.5
Protein Elution buffer*	50 mM Na ₂ HPO ₄ , 30 mM NaCl, 100-250 mM imidazole*, pH:7.5
Blocking Buffer	5 % BSA in PBS
LB Media	10 g tryptone, 5 g yeast extract, 10 g NaCl, per 1 L dl H ₂ O
LB Media Amp	10 g tryptone, 5 g yeast extract, 10 g NaCl, 100 mg Ampicillin, per 1 L dl H ₂ O
LB Agar	10 g tryptone, 5 g yeast extract, 10 g NaCl, 100 mg Ampicillin, 15 g bacto agar per 1 L dl H ₂ O

*Protein wash buffers were made with different imidazole concentrations, as indicated in the experimental section

Experiment Materials

Table 16. Buffers used during SELEX and aptamer characterization.

Buffer Name	Buffer components/Manufacturer
Selection buffer used for SELEX in this work	2 mM KCl, 1 mM MgCl ₂ , 1 mM CaCl ₂ 10 mM Tris Base, 100 mM NaCl, pH 7.4
Beier buffer	5 mM KCl, 2 mM MgCl ₂ ·6H ₂ O, 1 mM CaCl ₂ , 3 mM KH ₂ PO ₄ 17 mM Na ₂ HPO ₄ , 100 mM NaCl, pH 6
Giamb. buffer	5 mM KCl, 5 mM MgCl ₂ ·6H ₂ O, 20 mM Tris Base, 50 mM NaCl, pH 7.4
HisTag beads wash buffer	Na ₂ HPO ₄ 50 mM, NaCl 300 mM, Tween 20 [®] 0.01 %
PBS	Gibco, purchased through Fisher Scientific, Suwanee GA, USA

7.3 Commercial Kits

Table 17. Commercial Kits used during this work.

Name	Manufacturer
Genome Lab DTCS Quick Start Kit	Beckman Coulter, Brea CA USA
Champion™ pET Directional TOPO® Expression Kit by	Fisher Scientific, Suwanee GA, USA
Qubit dsDNA BR Assay Kit	
Qubit Protein Assay Kit	
Qubit ssDNA Assay Kit	
Qubit Protein Assay Kit	
Gel extraction Kit	Qiagen, Valencia CA, USA
One Step RT-PCR Kit	
PCR product MinElute Kit	
Plasmid Extraction Kit	
RNeasy Mini Kit	
Sensiscript RT Kit	Qiagen, Valencia CA, USA
Viral RNA extraction Kit	
Oligo Clean&Concentrator™ Kit	Zymo, Irvine CA, USA
ZR DNA Sequencing Clean-up Kit™	

Experiment Materials

7.4 Nucleotides and Radionuclides

Table 18. List of nucleotides and radionuclides used for binding studies and filter retention assays.

Name	Manufacturer
dNTPs	Qiagen, Valencia CA, USA
[γ - ³² P]-ATP	Perkin Elmer (Meridan CT, USA)

7.5 Oligonucleotides and Nucleic Acid Library

All oligonucleotides were ordered from integrated DNA technologies, Inc (IDT), Coralville Iowa, USA.

Table 19. Sequence list of primers and other oligonucleotides used during this work except aptmers, which are listed in the results section.

Name	Oligonucleotide Sequence (5'-3')	Literature
GI cog F	CGYTGGATGCGNTTYCATGA	117
GI cog R	CTTAGACGCCATCATCATTYAC	
GI probe I	Cy5-AGATYCGGATCYCCTGTCCA-IBRQ	
GI probe II	Cy5-AGATCGGGTCTCCTGTCCA-IBRQ	
GII cog F	CARGARBCNATGTTYAGRTGGATGAG	
GII cog R	TCGACGCCATCTTCATTCACA	
GII probe	Cy3-TGGGAGGGCGATCGCAATCT-IBRQ	
IAC Fw (46)	GACATCGATATGGGTGCCG	113
IAC Rev (194)	AATATTCGCGAGACGATGCAG	
IAC Probe	TxRed-TCTCATGCGTCTCCCTGGTGAATGTG-IBRQ	113
G2SK F	CNT GGG AGG GCG ATC GCA A	111
G2SK R	CCRCCNGCATRHCRTTRTACAT	
ORF 3	AAAGACACTAAAGAAAGGAAAGAT	237
GII VLP F	CACAGGATCCATGAAGATGGCGTCGAATGAC	195
GII VLP R	CTCTGAATTCTTATAATGCACGTCTACGCCCGCTCCA	
GII P-domain F	CACCATGAAACCATTACCGTCCCAATCTTAACTG	

Experiment Materials

Name	Oligonucleotide Sequence (5'-3')	Literature
GII P-domain F	TTATAATGCACGTCTACGCCCCGCTCCA	
Library F	GGTATTGAGGGTCGCATC	238
Library R	Phospho. -AGAGGAGAGTTAGAGCCATC	
GII 5466 F	TTTCCAACCTGAAGGCTTGAG	
GII 5485 R	CTCAAGCCTTCAGTTGGAAA	
GII 5976 F	GATTATACAATGAATTTGGC	
GII 5995 R	GCGAAATTCATTGTATAATC	
GII 6484b F	CACAATCTGATGTGGCTCTG	
GII 6503b R	CAGAGCCACATCAGATTGTG	

Table 20. List of primers used for colony PCR and for the different vectors used.

Vector	Application	Primer name	Primer Sequence (5'-3')
pCR™4-TOPO	Maintenance, sequencing	M13 F	GTAAAACGACGGCCAGT
		M13 R	CAGGAAACAGCTATGAC
pET100/D-TOPO®	P-domain production	T7 F	TAATACGACTCACTATAGGG
		T7 R	TAGTTATTGCTCAGCGGTGG

7.6 Enzymes and Enzyme Reagents

Table 21. List of enzymes used during this work.

Name	Manufacturer
Benzonase	Fisher Scientific, Suwanee GA, USA
Platinum Pfx DNA Polymerase	
Platinum Taq DNA Polymerase	
Superscript II	
Bam HI	New England Biolabs, Ipswich MA, USA
Eco RI	
U Lambda Exonuclease	

Experiment Materials

Name	Manufacturer
T4 Polynucleotide Kinase	Promega, (Madison WI, USA)
RNAse H	Qiagen, Valencia CA, USA

Table 22. Enzyme reagents and PCR reagents.

Name	Manufacturer
10x Buffer for Master Mix	Fisher Scientific, Suwanee GA, USA
5x Buffer for Master Mix	
MgCl ₂ Solution	
N3 Buffer	Qiagen, Valencia CA, USA
P1 buffer	Qiagen, Valencia CA, USA
P2 Buffer	
Q-Solution	

7.7 Plasmids and Bacteria

Plasmids used were each provided with commercial Kits (section 7.3). For cloning and maintenance, plasmid pCR™4-TOPO was used in combination with TOP10 competent *E. coli* cells. For protein production the pET100/D-TOPO® vector was used and propagated in TOP10 competent *E. coli* for maintenance purposes. For protein production the vector was transformed into the *E. coli* expression cell line BL21 Star™(DE3).

7.8 Viruses and Virus Like Particles (VLPs)

The murine norovirus was produced in house by Dr. Jacqueline Woods using tissue culture with the macrophage cell line RAW. After infection, newly generated virus was purified and titer determined by plaque assay. The virus was stored at -70 °C until use.

Norovirus VLPs of five genotypes were kindly provided by Dr. Robert Atmar through Baylor College of Medicine (Houston TX, USA), with permission of Prof Dr. LeeAnn Jaykus.

7.9 Antibodies and Other Proteins

Table 23. Antibodies and other proteins used during this work.

Name	Manufacturer
Anti- norovirus GII.4 Antibody [2002-5G] (167024)	Abcam, Cambridge, MA, USA
Rabbit-anti-Mouse Antibody HPR (97046)	
BSA	Sigma-Aldrich, St. Louis, MO, USA
Lysozyme	
Thrombin	
Alkaline phosphatase linked Streptavidin	Fisher Scientific, Suwanee GA, USA

7.10 Other Materials

Table 24. Magnetic beads, and spin columns used for SELEX and other aptamer applications.

Name	Manufacturer
Dynabeads™ His-Tag Isolation & Pull-down	Fisher Scientific, Suwanee GA, USA
Dynabeads Streptavidin	
G30 BioSpin columns	Bio-Rad, Hercules CA, USA

Table 25. Material used for protein purification and analysis.

Name	Manufacturer
HisPur™	Fisher Scientific, Suwanee GA, USA
Snake Skin™, Dialysis Tubing, 10 K MWCO	Fisher Scientific, Suwanee GA, USA
SDS PAGE Molecular Weight Standards, Low Range	Bio-Rad, Hercules CA, USA
Agilent P200 Tape	Agilent, Santa Clara CA, USA
Agilent P200 Reagents	Agilent, Santa Clara CA, USA

Table 26. Material used during filter retention assays.

Name	Manufacturer
0.45µm nitrocellulose membranes	Fisher Scientific, Suwanee GA, USA
Biorad filter paper	Bio-Rad, Hercules CA, USA

Experiment Materials

Table 27. Laboratory ware commonly used during this work.

Name	Manufacturer
50 mL Conical Tubes	Fisher Scientific, Suwanee GA, USA
Nonstick, RNase-free Microfuge Tubes	Fisher Scientific, Suwanee GA, USA
Smart cycler tubes	Cepheid, Sunnyvale CA, USA
PCR Tubes	Fisher Scientific, Suwanee GA, USA
Corning Low Protein Binding Filter (0.2µm)	Corning, purchased through Fisher Scientific, Suwanee GA, USA
Sterilisation syringe filter (0.45 µm)	Fisher Scientific, Suwanee GA, USA
NBT/BCIP Ready-to-Use Tablets	Roche, purchased through: Sigma-Aldrich, St. Louis, MO, USA

7.11 List of Software

Table 28. List of software used during this work.

Name	Manufacturer
BioEdit (5)	mbio
EndNote 8.0	EndNote
Image Lab	BioRad (freeware)
Image Quant	GE Healthcare
MEGA 7	MEGA
MEME Suite¹⁹³	Web based open software
Office	Microsoft
Prism 7.02	GraphPad
Tape Station Analysis Software	Agilent

8 Literature

1. Kapikian, A. Z.; Wyatt, R. G.; Dolin, R.; Thornhill, T. S.; Kalica, A. R.; Chanock, R. M., Visualization by Immune Electron Microscopy of a 27-nm Particle Associated with Acute Infectious Nonbacterial Gastroenteritis. *Journal of Virology* **1972**, *10* (5), 1075-1081.
2. Adler, J. L.; Zickl, R., Winter Vomiting Disease. *Journal of Infectious Diseases* **1969**, *119* (6), 668-673.
3. Koo, H. L.; Ajami, N.; Atmar, R. L.; DuPont, H. L., Noroviruses: The Principal Cause of Foodborne Disease Worldwide. *Discovery medicine* **2010**, *10* (50), 61-70.
4. Scallan, E.; Hoekstra, R. M.; Angulo, F. J.; Tauxe, R. V.; Widdowson, M.-A.; Roy, S. L.; Jones, J. L.; Griffin, P. M., Foodborne Illness Acquired in the United States—Major Pathogens. *Emerging Infectious Diseases* **2011**, *17* (1), 7-15.
5. Mayo, M. A. *Virus Taxonomy*; International Committee on Taxonomy of Viruses: Houston, 2002; pp 1071-1076.
6. Van Regenmortel, M. H. V., Fauquet, C.M., Bishop, D.H.L., Carstens, E.B.,; Estes, M. K., Lemon, S.M., Maniloff, J., Mayo, M.A., McGeoch, D.J.,; Pringle, C. R., Wickner, R.B., , Virus Taxonomy: Seventh Report of the International Committee on Taxonomy of Viruses. **2000**.
7. Green, J.; Vinje, J.; Gallimore, C. I.; Koopmans, M.; Hale, A.; Brown, D. W. G., Capsid Protein Diversity among Norwalk-like Viruses. *Virus Genes* **2000**, *20* (3), 227-236.
8. Wang, Q.-H.; Han, M. G.; Cheetham, S.; Souza, M.; Funk, J. A.; Saif, L. J., Porcine Noroviruses Related to Human Noroviruses. *Emerging Infectious Diseases* **2005**, *11* (12), 1874-1881.
9. Sugieda, M.; Nakajima, S., Viruses detected in the caecum contents of healthy pigs representing a new genetic cluster in genogroup II of the genus 'Norwalk-like viruses'. *Virus Research* **2002**, *87* (2), 165-172.
10. Oliver, S. L.; Wood, E.; Asobayire, E.; Wathes, D. C.; Brickell, J. S.; Elschner, M.; Otto, P.; Lambden, P. R.; Clarke, I. N.; Bridger, J. C., Serotype 1 and 2 Bovine Noroviruses Are Endemic in Cattle in the United Kingdom and Germany. *Journal of Clinical Microbiology* **2007**, *45* (9), 3050-3052.
11. Wolf, S.; Williamson, W.; Hewitt, J.; Lin, S.; Rivera-Aban, M.; Ball, A.; Scholes, P.; Savill, M.; Greening, G. E., Molecular detection of norovirus in sheep and pigs in New Zealand farms. *Veterinary Microbiology* **2009**, *133* (1), 184-189.
12. Karst, S. M.; Wobus, C. E.; Lay, M.; Davidson, J.; Virgin, H. W., STAT1-Dependent Innate Immunity to a Norwalk-Like Virus. *Science* **2003**, *299* (5612), 1575-1578.
13. Martella, V.; Lorusso, E.; Decaro, N.; Elia, G.; Radogna, A.; D'Abramo, M.; Desario, C.; Cavalli, A.; Corrente, M.; Camero, M.; Germinario, C. A.; Bányai, K.; Di Martino, B.; Marsilio, F.; Carmichael, L. E.; Buonavoglia, C., Detection and Molecular Characterization of a Canine Norovirus. *Emerging Infectious Diseases* **2008**, *14* (8), 1306-1308.
14. Pinto, P.; Wang, Q.; Chen, N.; Dubovi, E. J.; Daniels, J. B.; Millward, L. M.; Buonavoglia, C.; Martella, V.; Saif, L. J., Discovery and Genomic Characterization of Noroviruses from a Gastroenteritis Outbreak in Domestic Cats in the US. *PLoS ONE* **2012**, *7* (2), e32739.
15. de Graaf, M.; van Beek, J.; Koopmans, M. P. G., Human norovirus transmission and evolution in a changing world. *Nature Reviews Microbiology* **2016**, *14*, 421.
16. Mattison, K.; Shukla, A.; Cook, A.; Pollari, F.; Friendship, R.; Kelton, D.; Bidawid, S.; Farber, J. M., Human Noroviruses in Swine and Cattle. *Emerging Infectious Diseases* **2007**, *13* (8), 1184-1188.
17. Summa, M.; von Bonsdorff, C.-H.; Maunula, L., Pet dogs—A transmission route for human noroviruses? *Journal of Clinical Virology* **2012**, *53* (3), 244-247.
18. Caddy, S. L.; de Rougemont, A.; Emmott, E.; El-Attar, L.; Mitchell, J. A.; Hollinshead, M.; Belliot, G.; Brownlie, J.; Le Pendu, J.; Goodfellow, I., Evidence for Human Norovirus Infection of Dogs in the United Kingdom. *Journal of Clinical Microbiology* **2015**, *53* (6), 1873-1883.

Literature

19. Harris, J. P.; Edmunds, W. J.; Pebody, R.; Brown, D. W.; Lopman, B. A., Deaths from Norovirus among the Elderly, England and Wales. *Emerging Infectious Diseases* **2008**, *14* (10), 1546-1552.
20. Trivedi, T. K.; Desai, R.; Hall, A. J.; Patel, M.; Parashar, U. D.; Lopman, B. A., Clinical characteristics of norovirus-associated deaths: A systematic literature review. *American Journal of Infection Control* **41** (7), 654-657.
21. Murata, T.; Katsushima, N.; Mizuta, K.; Muraki, Y.; Hongo, S.; Matsuzaki, Y., Prolonged Norovirus Shedding in Infants ≤ 6 Months of Age With Gastroenteritis. *The Pediatric Infectious Disease Journal* **2007**, *26* (1), 46-49.
22. Robert, L. A.; Antone, R. O.; Mark, A. G.; Mary, K. E.; Sue, E. C.; Frederick, H. N.; David, Y. G., Norwalk Virus Shedding after Experimental Human Infection. *Emerging Infectious Disease Journal* **2008**, *14* (10), 1553.
23. Teunis, P. F. M.; Moe, C. L.; Liu, P.; E. Miller, S.; Lindesmith, L.; Baric, R. S.; Le Pendu, J.; Calderon, R. L., Norwalk virus: How infectious is it? *Journal of Medical Virology* **2008**, *80* (8), 1468-1476.
24. Atmar, R. L.; Opekun, A. R.; Gilger, M. A.; Estes, M. K.; Crawford, S. E.; Neill, F. H.; Ramani, S.; Hill, H.; Ferreira, J.; Graham, D. Y., Determination of the 50% Human Infectious Dose for Norwalk Virus. *The Journal of Infectious Diseases* **2014**, *209* (7), 1016-1022.
25. Hutson, A. M.; Atmar, R. L.; Graham, D. Y.; Estes, M. K., Norwalk Virus Infection and Disease Is Associated with ABO Histo-Blood Group Type. *The Journal of Infectious Diseases* **2002**, *185* (9), 1335-1337.
26. Thorven, M.; Grahn, A.; Hedlund, K.-O.; Johansson, H.; Wahlfrid, C.; Larson, G.; Svensson, L., A Homozygous Nonsense Mutation (428G→A) in the Human Secretor (FUT2) Gene Provides Resistance to Symptomatic Norovirus (GGII) Infections. *Journal of Virology* **2005**, *79* (24), 15351-15355.
27. Lindesmith, L.; Moe, C.; Marionneau, S.; Ruvoen, N.; Jiang, X.; Lindblad, L.; Stewart, P.; LePendou, J.; Baric, R., Human susceptibility and resistance to Norwalk virus infection. *Nature Medicine* **2003**, *9*, 548.
28. Ettayebi, K.; Crawford, S. E.; Murakami, K.; Broughman, J. R.; Karandikar, U.; Tenge, V. R.; Neill, F. H.; Blutt, S. E.; Zeng, X.-L.; Qu, L.; Kou, B.; Opekun, A. R.; Burrin, D.; Graham, D. Y.; Ramani, S.; Atmar, R. L.; Estes, M. K., Replication of Human Noroviruses in Stem Cell-Derived Human Enteroids. *Science (New York, N.Y.)* **2016**, *353* (6306), 1387-1393.
29. Duizer, E.; Schwab, K. J.; Neill, F. H.; Atmar, R. L.; Koopmans, M. P. G.; Estes, M. K., Laboratory efforts to cultivate noroviruses. *Journal of General Virology* **2004**, *85* (1), 79-87.
30. Lay, M. K.; Atmar, R. L.; Guix, S.; Bharadwaj, U.; He, H.; Neill, F. H.; Sastry, J. K.; Yao, Q.; Estes, M. K., Norwalk Virus Does Not Replicate in Human Macrophages or Dendritic Cells Derived from the Peripheral Blood of Susceptible Humans. *Virology* **2010**, *406* (1), 1-11.
31. Wobus, C. E.; Karst, S. M.; Thackray, L. B.; Chang, K.-O.; Sosnovtsev, S. V.; Belliot, G.; Krug, A.; Mackenzie, J. M.; Green, K. Y.; Virgin, H. W., Replication of Norovirus in Cell Culture Reveals a Tropism for Dendritic Cells and Macrophages. *PLoS Biology* **2004**, *2* (12), e432.
32. Taube, S.; Kolawole, A. O.; Höhne, M.; Wilkinson, J. E.; Handley, S. A.; Perry, J. W.; Thackray, L. B.; Akkina, R.; Wobus, C. E., A Mouse Model for Human Norovirus. *mBio* **2013**, *4* (4), e00450-13.
33. Bok, K.; Parra, G. I.; Mitra, T.; Abente, E.; Shaver, C. K.; Boon, D.; Engle, R.; Yu, C.; Kapikian, A. Z.; Sosnovtsev, S. V.; Purcell, R. H.; Green, K. Y., Chimpanzees as an animal model for human norovirus infection and vaccine development. *Proceedings of the National Academy of Sciences of the United States of America* **2011**, *108* (1), 325-330.
34. Cheetham, S.; Souza, M.; Meulia, T.; Grimes, S.; Han, M. G.; Saif, L. J., Pathogenesis of a Genogroup II Human Norovirus in Gnotobiotic Pigs. *Journal of Virology* **2006**, *80* (21), 10372-10381.

35. Jiang, X.; Graham, D.; Wang, K.; Estes, M., Norwalk virus genome cloning and characterization. *Science* **1990**, *250* (4987), 1580-1583.
36. Jiang, X.; Wang, M.; Graham, D. Y.; Estes, M. K., Expression, self-assembly, and antigenicity of the Norwalk virus capsid protein. *Journal of Virology* **1992**, *66* (11), 6527-6532.
37. Jiang, X.; Wang, M.; Wang, K.; Estes, M. K., Sequence and Genomic Organization of Norwalk Virus. *Virology* **1993**, *195* (1), 51-61.
38. Thorne, L. G.; Goodfellow, I. G., Norovirus gene expression and replication. *Journal of General Virology* **2014**, *95* (2), 278-291.
39. Glass, P. J.; White, L. J.; Ball, J. M.; Leparco-Goffart, I.; Hardy, M. E.; Estes, M. K., Norwalk Virus Open Reading Frame 3 Encodes a Minor Structural Protein. *Journal of Virology* **2000**, *74* (14), 6581-6591.
40. Vongpunsawad, S.; Venkataram Prasad, B. V.; Estes, M. K., Norwalk Virus Minor Capsid Protein VP2 Associates within the VP1 Shell Domain. *Journal of Virology* **2013**, *87* (9), 4818-4825.
41. Prasad, B. V. V.; Hardy, M. E.; Dokland, T.; Bella, J.; Rossmann, M. G.; Estes, M. K., X-ray Crystallographic Structure of the Norwalk Virus Capsid. *Science* **1999**, *286* (5438), 287.
42. Glass, R. I.; Parashar, U. D.; Estes, M. K., Norovirus Gastroenteritis. *The New England journal of medicine* **2009**, *361* (18), 10.1056/NEJMra0804575.
43. Jiang, X.; Wilton, N.; Zhong, W. M.; Farkas, T.; Huang, P. W.; Barrett, E.; Guerrero, M.; Ruiz-Palacios, G.; Green, K. Y.; Green, J.; Hale, A. D.; Estes, M. K.; Pickering, L. K.; Matson, D. O., Diagnosis of Human Caliciviruses by Use of Enzyme Immunoassays. *The Journal of Infectious Diseases* **2000**, *181* (Supplement_2), S349-S359.
44. Harrington, P. R.; Lindesmith, L.; Yount, B.; Moe, C. L.; Baric, R. S., Binding of Norwalk Virus-Like Particles to ABH Histo-Blood Group Antigens Is Blocked by Antisera from Infected Human Volunteers or Experimentally Vaccinated Mice. *Journal of Virology* **2002**, *76* (23), 12335-12343.
45. White, L. J.; Hardy, M. E.; Estes, M. K., Biochemical characterization of a smaller form of recombinant Norwalk virus capsids assembled in insect cells. *Journal of Virology* **1997**, *71* (10), 8066-72.
46. Bertolotti-Ciarlet, A.; White, L. J.; Chen, R.; Prasad, B. V. V.; Estes, M. K., Structural Requirements for the Assembly of Norwalk Virus-Like Particles. *Journal of Virology* **2002**, *76* (8), 4044-4055.
47. Tan, M.; Hegde, R. S.; Jiang, X., The P Domain of Norovirus Capsid Protein Forms Dimer and Binds to Histo-Blood Group Antigen Receptors. *Journal of Virology* **2004**, *78* (12), 6233-6242.
48. Tan, M.; Huang, P.; Meller, J.; Zhong, W.; Farkas, T.; Jiang, X., Mutations within the P2 domain of norovirus capsid affect binding to human histo-blood group antigens: evidence for a binding pocket. *J Virol* **2003**, *77* (23), 12562-12571.
49. Tan, M.; Fang, P.-A.; Xia, M.; Chachiyo, T.; Jiang, W.; Jiang, X., Terminal modifications of norovirus P domain resulted in a new type of subviral particles, the small P particles. *Virology* **2011**, *410* (2), 345-352.
50. Tan, M.; Huang, P.; Xia, M.; Fang, P.-A.; Zhong, W.; McNeal, M.; Wei, C.; Jiang, W.; Jiang, X., Norovirus P Particle, a Novel Platform for Vaccine Development and Antibody Production. *Journal of Virology* **2011**, *85* (2), 753-764.
51. Ming, X.; Tibor, F.; Xi, J., Norovirus capsid protein expressed in yeast forms virus-like particles and stimulates systemic and mucosal immunity in mice following an oral administration of raw yeast extracts. *Journal of Medical Virology* **2007**, *79* (1), 74-83.
52. Taube, S.; Kurth, A.; Schreier, E., Generation of recombinant Norovirus-like particles (VLP) in the human endothelial kidney cell line 293T. *Archives of Virology* **2005**, *150* (7), 1425-1431.
53. Santi, L.; Batchelor, L.; Huang, Z.; Hjelm, B.; Kilbourne, J.; Arntzen, C. J.; Chen, Q.; Mason, H. S., An efficient plant viral expression system generating orally immunogenic Norwalk virus-like particles. *Vaccine* **2008**, *26* (15), 1846-1854.

54. Da Silva, A. K.; Kavanagh, O. V.; Estes, M. K.; Elimelech, M., Adsorption and Aggregation Properties of Norovirus GI and GII Virus-like Particles Demonstrate Differing Responses to Solution Chemistry. *Environmental science & technology* **2011**, *45* (2), 520-526.
55. Le Guyader, F. S.; Loisy, F.; Atmar, R. L.; Hutson, A. M.; Estes, M. K.; Ruvoën-Clouet, N.; Pommepuy, M.; Le Pendu, J., Norwalk Virus-specific Binding to Oyster Digestive Tissues. *Emerging Infectious Diseases* **2006**, *12* (6), 931-936.
56. Escudero-Abarca, B. I.; Suh, S. H.; Moore, M. D.; Dwivedi, H. P.; Jaykus, L. A., Selection, characterization and application of nucleic acid aptamers for the capture and detection of human norovirus strains. *PLoS One* **2014**, *9* (9), e106805.
57. Green, K., *Caliciviridae: The noroviruses*. 2013; Vol. 1, p 582-608.
58. Vinjé, J., Advances in Laboratory Methods for Detection and Typing of Norovirus. *Journal of Clinical Microbiology* **2015**, *53* (2), 373-381.
59. Ahmed, S. M.; Hall, A. J.; Robinson, A. E.; Verhoef, L.; Premkumar, P.; Parashar, U. D.; Koopmans, M.; Lopman, B. A., Global prevalence of norovirus in cases of gastroenteritis: a systematic review and meta-analysis. *The Lancet Infectious Diseases* **2014**, *14* (8), 725-730.
60. Fankhauser, R. L.; Monroe, S. S.; Noel, J. S.; Humphrey, C. D.; Bresee, J. S.; Parashar, U. D.; Ando, T.; Glass, R. I., Epidemiologic and Molecular Trends of "Norwalk-like Viruses" Associated with Outbreaks of Gastroenteritis in the United States. *The Journal of Infectious Diseases* **2002**, *186* (1), 1-7.
61. Lopman, B.; Reacher, M.; van Duynhoven, Y.; Hanon, F.-X.; Brown, D.; Koopmans, M., Viral Gastroenteritis Outbreaks in Europe, 1995–2000. *Emerging Infectious Diseases* **2003**, *9* (1), 90-96.
62. Atmar, R. L.; Estes, M. K., The Epidemiologic and Clinical Importance of Norovirus Infection. *Gastroenterology Clinics of North America* **2006**, *35* (2), 275-290.
63. Lanata, C. F.; Fischer-Walker, C. L.; Olascoaga, A. C.; Torres, C. X.; Aryee, M. J.; Black, R. E.; for the Child Health Epidemiology Reference Group of the World Health, O.; Unicef, Global Causes of Diarrheal Disease Mortality in Children <5 Years of Age: A Systematic Review. *PLOS ONE* **2013**, *8* (9), e72788.
64. Bartsch, S. M.; Lopman, B. A.; Ozawa, S.; Hall, A. J.; Lee, B. Y., Global Economic Burden of Norovirus Gastroenteritis. *PLOS ONE* **2016**, *11* (4), e0151219.
65. Ahmed, S. M.; Hall, A. J.; Robinson, A. E.; Verhoef, L.; Premkumar, P.; Parashar, U. D.; Koopmans, M.; Lopman, B. A., Global prevalence of norovirus in cases of gastroenteritis: a systematic review and meta-analysis. *Lancet Infect Dis* **2014**, *14* (8), 725-30.
66. Sukhrie, F. H. A.; Siebenga, J. J.; Beersma, M. F. C.; Koopmans, M., Chronic Shedders as Reservoir for Nosocomial Transmission of Norovirus. *Journal of Clinical Microbiology* **2010**, *48* (11), 4303-4305.
67. Milbrath, M. O.; Spicknall, I. H.; Zelner, J. L.; Moe, C. L.; Eisenberg, J. N. S., Heterogeneity in norovirus shedding duration affects community risk. *Epidemiology and Infection* **2013**, *141* (8), 1572-1584.
68. Verhoef, L.; Hewitt, J.; Barclay, L.; Ahmed, S.; Lake, R.; Hall, A., J.; Lopman, B.; Kroneman, A.; Vennema, H.; Vinjé, J.; Koopmans, M., Norovirus Genotype Profiles Associated with Foodborne Transmission, 1999–2012. *Emerging Infectious Disease journal* **2015**, *21* (4), 592.
69. Hall, A. J.; Wikswo, M. E.; Pringle, K.; Gould, L. H.; Parashar, U. D., Vital signs: foodborne norovirus outbreaks - United States, 2009-2012. *MMWR Morb Mortal Wkly Rep* **2014**, *63* (22), 491-5.
70. Vega, E.; Barclay, L.; Gregoricus, N.; Shirley, S. H.; Lee, D.; Vinjé, J., Genotypic and Epidemiologic Trends of Norovirus Outbreaks in the United States, 2009 to 2013. *Journal of Clinical Microbiology* **2014**, *52* (1), 147-155.
71. Lysén, M.; Thorhagen, M.; Brytting, M.; Hjertqvist, M.; Andersson, Y.; Hedlund, K.-O., Genetic Diversity among Food-Borne and Waterborne Norovirus Strains Causing Outbreaks in Sweden. *Journal of Clinical Microbiology* **2009**, *47* (8), 2411-2418.

72. de Graaf, M.; van Beek, J.; Vennema, H.; Podkolzin, A. T.; Hewitt, J.; Bucardo, F.; Templeton, K.; Mans, J.; Nordgren, J.; Reuter, G.; Lynch, M.; Rasmussen, L. D.; Iritani, N.; Chan, M. C.; Martella, V.; Ambert-Balay, K.; Vinjé, J.; White, P. A.; Koopmans, M. P., Emergence of a novel GII.17 norovirus – End of the GII.4 era? *Eurosurveillance* **2015**, *20* (26), 21178.
73. Siebenga, J. J.; Vennema, H.; Zheng, D.-P.; Vinjé, J.; Lee, B. E.; Pang, X.-L.; Ho, E. C. M.; Lim, W.; Choudekar, A.; Broor, S.; Halperin, T.; Rasool, N. B. G.; Hewitt, J.; Greening, G. E.; Jin, M.; Duan, Z.-J.; Lucero, Y.; O’Ryan, M.; Hoehne, M.; Schreier, E.; Ratcliff, R. M.; White, P. A.; Iritani, N.; Reuter, G.; Koopmans, M., Norovirus Illness Is a Global Problem: Emergence and Spread of Norovirus GII.4 Variants, 2001–2007. *The Journal of Infectious Diseases* **2009**, *200* (5), 802-812.
74. Raphael, D.; Neil, R. B.; Herbert, D.; Robert, F. B.; Richard, G. W.; Julius, A. K.; Richard, H.; Robert, M. C., Biological Properties of Norwalk Agent of Acute Infectious Nonbacterial Gastroenteritis. *Proceedings of the Society for Experimental Biology and Medicine* **1972**, *140* (2), 578-583.
75. Seitz, S. R.; Leon, J. S.; Schwab, K. J.; Lyon, G. M.; Dowd, M.; McDaniels, M.; Abdulhafid, G.; Fernandez, M. L.; Lindesmith, L. C.; Baric, R. S.; Moe, C. L., Norovirus Infectivity in Humans and Persistence in Water. *Applied and Environmental Microbiology* **2011**, *77* (19), 6884-6888.
76. Charles, K. J.; Shore, J.; Sellwood, J.; Laverick, M.; Hart, A.; Pedley, S., Assessment of the stability of human viruses and coliphage in groundwater by PCR and infectivity methods. *Journal of Applied Microbiology* **2009**, *106* (6), 1827-1837.
77. Espinosa, A. C.; Mazari-Hiriart, M.; Espinosa, R.; Maruri-Avidal, L.; Méndez, E.; Arias, C. F., Infectivity and genome persistence of rotavirus and astrovirus in groundwater and surface water. *Water Research* **2008**, *42* (10), 2618-2628.
78. Richards, G. P.; Watson, M. A.; Meade, G. K.; Hovan, G. L.; Kingsley, D. H., Resilience of Norovirus GII.4 to Freezing and Thawing: Implications for Virus Infectivity. *Food and Environmental Virology* **2012**, *4* (4), 192-197.
79. Cheesbrough, J. S.; Barkess-Jones, L.; Brown, D. W., Possible prolonged environmental survival of small round structured viruses. *Journal of Hospital Infection* **1997**, *35* (4), 325-326.
80. Park, G. W.; Barclay, L.; Macinga, D.; Charbonneau, D.; Pettigrew, C. A.; Vinjé, J., Comparative Efficacy of Seven Hand Sanitizers against Murine Norovirus, Feline Calicivirus, and GII.4 Norovirus. *J Food Prot* **2010**, *73* (12), 2232-2238.
81. Gall, A. M.; Mariñas, B. J.; Lu, Y.; Shisler, J. L., Waterborne Viruses: A Barrier to Safe Drinking Water. *PLOS Pathogens* **2015**, *11* (6), e1004867.
82. Carter, M. J., Enterically infecting viruses: pathogenicity, transmission and significance for food and waterborne infection. *Journal of Applied Microbiology* **2005**, *98* (6), 1354-1380.
83. Rodríguez-Lázaro, D.; Cook, N.; Ruggeri, F. M.; Sellwood, J.; Nasser, A.; Nascimento, M. S. J.; D’Agostino, M.; Santos, R.; Saiz, J. C.; Rzeżutka, A.; Bosch, A.; Gironés, R.; Carducci, A.; Muscillo, M.; Kovač, K.; Diez-Valcarce, M.; Vantarakis, A.; von Bonsdorff, C.-H.; de Roda Husman, A. M.; Hernández, M.; van der Poel, W. H. M., Virus hazards from food, water and other contaminated environments. *FEMS Microbiology Reviews* **2012**, *36* (4), 786-814.
84. Marks, P. J.; Vipond, I. B.; Carlisle, D.; Deakin, D.; Fey, R. E.; Caul, E. O., Evidence for airborne transmission of Norwalk-like virus (NLV) in a hotel restaurant. *Epidemiology and Infection* **2000**, *124* (3), 481-487.
85. Daniels, N. A.; Bergmire-Sweat, D. A.; Schwab, K. J.; Hendricks, K. A.; Reddy, S.; Rowe, S. M.; Fankhauser, R. L.; Monroe, S. S.; Atmar, R. L.; Glass, R. I.; Mead, P., A Foodborne Outbreak of Gastroenteritis Associated with Norwalk-like Viruses: First Molecular Traceback to Deli Sandwiches Contaminated during Preparation. *The Journal of Infectious Diseases* **2000**, *181* (4), 1467-1470.
86. Patterson, T.; Hutchings, P.; Palmer, S., Outbreak of SRSV gastroenteritis at an international conference traced to food handled by a post-symptomatic caterer. *Epidemiology and Infection* **1993**, *111* (1), 157-162.

87. Chen, M.-Y.; Chen, W.-C.; Chen, P.-C.; Hsu, S.-W.; Lo, Y.-C., An outbreak of norovirus gastroenteritis associated with asymptomatic food handlers in Kinmen, Taiwan. *BMC Public Health* **2016**, *16*, 372.
88. WHO, W. H. O., WHO Estimates of the Global burden of Foodborne Diseases. **2015**, (ISBN:978 92 4 156516 5), 255.
89. Le Guyader, F. S.; Mittelholzer, C.; Haugarreau, L.; Hedlund, K.-O.; Alsterlund, R.; Pommepuy, M.; Svensson, L., Detection of noroviruses in raspberries associated with a gastroenteritis outbreak. *International Journal of Food Microbiology* **2004**, *97* (2), 179-186.
90. Mäde, D.; Trübner, K.; Neubert, E.; Höhne, M.; Johne, R., Detection and Typing of Norovirus from Frozen Strawberries Involved in a Large-Scale Gastroenteritis Outbreak in Germany. *Food and Environmental Virology* **2013**, *5* (3), 162-168.
91. PÖNKÄ, A.; Maunula, L.; von Bonsdorff, C. H.; Lyytikäinen, O., An outbreak of calicivirus associated with consumption of frozen raspberries. *Epidemiology and Infection* **1999**, *123* (3), 469-474.
92. Sarvikivi, E.; Roivainen, M.; Maunula, L.; Niskanen, T.; Korhonen, T.; Lappalainen, M.; Kuusi, M., Multiple norovirus outbreaks linked to imported frozen raspberries. *Epidemiology and Infection* **2012**, *140* (2), 260-267.
93. Müller, L.; Rasmussen, L. D.; Jensen, T.; Schultz, A. C.; Kjelsø, C.; Barnadas, C.; Sigsgaard, K.; Larsen, A. R.; Widstrup Jensen, C.; Jeppesen, S.; Uhrbrand, K.; Hove, N.; Mølbak, K.; Ethelberg, S., Series of Norovirus Outbreaks Caused by Consumption of Green Coral Lettuce, Denmark, April 2016. *PLoS Currents* **2016**, *8*.
94. Costantini, V.; Loisy, F.; Joens, L.; Le Guyader, F. S.; Saif, L. J., Human and Animal Enteric Caliciviruses in Oysters from Different Coastal Regions of the United States. *Applied and Environmental Microbiology* **2006**, *72* (3), 1800-1809.
95. Le Guyader, F. S.; Bon, F.; DeMedici, D.; Parnaudeau, S.; Bertone, A.; Crudeli, S.; Doyle, A.; Zidane, M.; Suffredini, E.; Kohli, E.; Maddalo, F.; Monini, M.; Gallay, A.; Pommepuy, M.; Pothier, P.; Ruggeri, F. M., Detection of Multiple Noroviruses Associated with an International Gastroenteritis Outbreak Linked to Oyster Consumption. *Journal of Clinical Microbiology* **2006**, *44* (11), 3878-3882.
96. Loury, P.; Le Guyader, F. S.; Le Saux, J. C.; Ambert-Balay, K.; Parrot, P.; Hubert, B., A norovirus oyster-related outbreak in a nursing home in France, January 2012. *Epidemiology and Infection* **2015**, *143* (12), 2486-2493.
97. Schaeffer, J.; Le Saux, J.-C.; Lora, M.; Atmar, R. L.; Le Guyader, F. S., Norovirus contamination on French marketed oysters. *International Journal of Food Microbiology* **2013**, *166* (2), 244-248.
98. Iwamoto, M.; Ayers, T.; Mahon, B. E.; Swerdlow, D. L., Epidemiology of Seafood-Associated Infections in the United States. *Clinical Microbiology Reviews* **2010**, *23* (2), 399-411.
99. Ehrich, M. K.; Harris, L. A., A review of existing eastern oyster filtration rate models. *Ecological Modelling* **2015**, *297*, 201-212.
100. Mason, J. O.; McLean, W. R., INFECTIOUS HEPATITIS TRACED TO THE CONSUMPTION OF RAW OYSTERS: AN EPIDEMIOLOGIC STUDY. *American Journal of Epidemiology* **1962**, *75* (1), 90-111.
101. Metcalf, T. G., Viruses on shellfish-growing waters. *Environment International* **1982**, *7* (1), 21-27.
102. Atmar, R. L.; Neill, F. H.; Romalde, J. L.; Le Guyader, F.; Woodley, C. M.; Metcalf, T. G.; Estes, M. K., Detection of Norwalk virus and hepatitis A virus in shellfish tissues with the PCR. *Applied and Environmental Microbiology* **1995**, *61* (8), 3014-8.
103. Le Guyader, F.; Haugarreau, L.; Miossec, L.; Dubois, E.; Pommepuy, M., Three-Year Study To Assess Human Enteric Viruses in Shellfish. *Applied and Environmental Microbiology* **2000**, *66* (8), 3241-3248.

104. Miossec, L.; Le Guyader, F.; Haugarreau, L.; Comps, M. A.; Pommepuy, M., *Possible relation between winter epidemic of acute gastroenteritis in France and viral contamination of shellfish*. 1998; Vol. 17, p 1661-1664.
105. SCHWAB, K. J.; NEILL, F. H.; ESTES, M. K.; METCALF, T. G.; ATMAR, R. L., Distribution of Norwalk Virus within Shellfish Following Bioaccumulation and Subsequent Depuration by Detection Using RT-PCR. *Journal of Food Protection* **1998**, *61* (12), 1674-1680.
106. Tian, P.; Bates, A. H.; Jensen, H. M.; Mandrell, R. E., Norovirus binds to blood group A-like antigens in oyster gastrointestinal cells. *Letters in Applied Microbiology* **2006**, *43* (6), 645-651.
107. Maalouf, H.; Zakhour, M.; Le Pendu, J.; Le Saux, J.-C.; Atmar, R. L.; Le Guyader, F. S., Distribution in Tissue and Seasonal Variation of Norovirus Genogroup I and II Ligands in Oysters. *Applied and Environmental Microbiology* **2010**, *76* (16), 5621-5630.
108. Le Guyader, F. S.; Atmar, R. L.; Le Pendu, J., Transmission of viruses through shellfish : when specific ligands come into play. *Current opinion in virology* **2012**, *2* (1), 10.1016/j.coviro.2011.10.029.
109. Woods, J. W.; Calci, K. R.; Marchant-Tambone, J. G.; Burkhardt Iii, W., Detection and molecular characterization of norovirus from oysters implicated in outbreaks in the US. *Food Microbiology* **2016**, *59*, 76-84.
110. Eden, J.-S.; Tanaka, M. M.; Boni, M. F.; Rawlinson, W. D.; White, P. A., Recombination within the Pandemic Norovirus GII.4 Lineage. *Journal of Virology* **2013**, *87* (11), 6270-6282.
111. Kojima, S.; Kageyama, T.; Fukushi, S.; Hoshino, F. B.; Shinohara, M.; Uchida, K.; Natori, K.; Takeda, N.; Katayama, K., Genogroup-specific PCR primers for detection of Norwalk-like viruses. *Journal of Virological Methods* **2002**, *100* (1-2), 107-114.
112. Katayama, K.; Shirato-Horikoshi, H.; Kojima, S.; Kageyama, T.; Oka, T.; Hoshino, F. B.; Fukushi, S.; Shinohara, M.; Uchida, K.; Suzuki, Y.; Gojobori, T.; Takeda, N., Phylogenetic Analysis of the Complete Genome of 18 Norwalk-like Viruses. *Virology* **2002**, *299* (2), 225-239.
113. DePaola, A.; Jones, J. L.; Woods, J.; Burkhardt, W.; Calci, K. R.; Krantz, J. A.; Bowers, J. C.; Kasturi, K.; Byars, R. H.; Jacobs, E.; Williams-Hill, D.; Nabe, K., Bacterial and Viral Pathogens in Live Oysters: 2007 United States Market Survey. *Applied and Environmental Microbiology* **2010**, *76* (9), 2754-2768.
114. Rolfe, K. J.; Parmar, S.; Mururi, D.; Wreghitt, T. G.; Jalal, H.; Zhang, H.; Curran, M. D., An internally controlled, one-step, real-time RT-PCR assay for norovirus detection and genogrouping. *Journal of Clinical Virology* **2007**, *39* (4), 318-321.
115. Miura, T.; Parnaudeau, S.; Grodzki, M.; Okabe, S.; Atmar, R. L.; Le Guyader, F. S., Environmental Detection of Genogroup I, II, and IV Noroviruses by Using a Generic Real-Time Reverse Transcription-PCR Assay. *Applied and Environmental Microbiology* **2013**, *79* (21), 6585-6592.
116. Mattison, K.; Grudeski, E.; Auk, B.; Charest, H.; Drews, S. J.; Fritzinger, A.; Gregoricus, N.; Hayward, S.; Houde, A.; Lee, B. E.; Pang, X. L.; Wong, J.; Booth, T. F.; Vinjé, J., Multicenter Comparison of Two Norovirus ORF2-Based Genotyping Protocols. *Journal of Clinical Microbiology* **2009**, *47* (12), 3927-3932.
117. Kageyama, T.; Kojima, S.; Shinohara, M.; Uchida, K.; Fukushi, S.; Hoshino, F. B.; Takeda, N.; Katayama, K., Broadly Reactive and Highly Sensitive Assay for Norwalk-Like Viruses Based on Real-Time Quantitative Reverse Transcription-PCR. *Journal of Clinical Microbiology* **2003**, *41* (4), 1548-1557.
118. Lewis, G. D.; Metcalf, T. G., Polyethylene glycol precipitation for recovery of pathogenic viruses, including hepatitis A virus and human rotavirus, from oyster, water, and sediment samples. *Applied and Environmental Microbiology* **1988**, *54* (8), 1983-1988.
119. Atmar, R. L.; Neill, F. H.; Woodley, C. M.; Manger, R.; Fout, G. S.; Burkhardt, W.; Leja, L.; McGovern, E. R.; Le Guyader, F.; Metcalf, T. G.; Estes, M. K., Collaborative evaluation of a method for the detection of Norwalk virus in shellfish tissues by PCR. *Applied and Environmental Microbiology* **1996**, *62* (1), 254-8.

120. Rutjes, S. A.; Lodder-Verschoor, F.; Poel, W. H. M. v. d.; Duijnhoven, Y. H. P. v.; Husman, A. M. d. R., Detection of Noroviruses in Foods: A Study on Virus Extraction Procedures in Foods Implicated in Outbreaks of Human Gastroenteritis. *Journal of Food Protection* **2006**, *69* (8), 1949-1956.
121. Ellington, A. D.; Szostak, J. W., In vitro selection of RNA molecules that bind specific ligands. *Nature* **1990**, *346* (6287), 818-22.
122. Tuerk, C.; Gold, L., Systematic evolution of ligands by exponential enrichment: RNA ligands to bacteriophage T4 DNA polymerase. *Science* **1990**, *249* (4968), 505-10.
123. Robertson, D. L.; Joyce, G. F., Selection in vitro of an RNA enzyme that specifically cleaves single-stranded DNA. *Nature* **1990**, *344*, 467.
124. Tucker, W. O.; Shum, K. T.; Tanner, J. A., G-quadruplex DNA Aptamers and their Ligands: Structure, Function and Application. *Current Pharmaceutical Design* **2012**, *18* (14), 2014-2026.
125. Bock, L. C.; Griffin, L. C.; Latham, J. A.; Vermaas, E. H.; Toole, J. J., Selection of single-stranded DNA molecules that bind and inhibit human thrombin. *Nature* **1992**, *355*, 564.
126. Colas, P.; Cohen, B.; Jessen, T.; Grishina, I.; McCoy, J.; Brent, R., Genetic selection of peptide aptamers that recognize and inhibit cyclin-dependent kinase 2. *Nature* **1996**, *380*, 548.
127. U.S. National Institutes of Health digital archive of biomedical and life science journal literature, P. C., PMC Advanced Search for the Keyword 'Aptamer's. <https://www.ncbi.nlm.nih.gov/pmc/?term=Aptamer> **2018**.
128. Aquino-Jarquín, G.; Toscano-Garibay, J. D., RNA Aptamer Evolution: Two Decades of SELECTION. *International Journal of Molecular Sciences* **2011**, *12* (12), 9155-9171.
129. Ellington, A. D.; Szostak, J. W., Selection in vitro of single-stranded DNA molecules that fold into specific ligand-binding structures. *Nature* **1992**, *355*, 850.
130. Jenison, R. D.; Gill, S. C.; Pardi, A.; Polisky, B., High-resolution molecular discrimination by RNA. *Science* **1994**, *263* (5152), 1425.
131. Mendonsa, S. D.; Bowser, M. T., In Vitro Evolution of Functional DNA Using Capillary Electrophoresis. *Journal of the American Chemical Society* **2004**, *126* (1), 20-21.
132. Mendonsa, S. D.; Bowser, M. T., In Vitro Selection of High-Affinity DNA Ligands for Human IgE Using Capillary Electrophoresis. *Analytical Chemistry* **2004**, *76* (18), 5387-5392.
133. Hybarger, G.; Bynum, J.; Williams, R. F.; Valdes, J. J.; Chambers, J. P., A microfluidic SELEX prototype. *Analytical and Bioanalytical Chemistry* **2006**, *384* (1), 191-198.
134. Cho, M.; Xiao, Y.; Nie, J.; Stewart, R.; Csordas, A. T.; Oh, S. S.; Thomson, J. A.; Soh, H. T., Quantitative selection of DNA aptamers through microfluidic selection and high-throughput sequencing. *Proceedings of the National Academy of Sciences* **2010**, *107* (35), 15373-15378.
135. Nguyen Quang, N.; Perret, G.; Ducongé, F., Applications of High-Throughput Sequencing for In Vitro Selection and Characterization of Aptamers. *Pharmaceuticals* **2016**, *9* (4), 76.
136. Daniels, D. A.; Chen, H.; Hicke, B. J.; Swiderek, K. M.; Gold, L., A tenascin-C aptamer identified by tumor cell SELEX: Systematic evolution of ligands by exponential enrichment. *Proceedings of the National Academy of Sciences of the United States of America* **2003**, *100* (26), 15416-15421.
137. Mi, J.; Liu, Y.; Rabbani, Z. N.; Yang, Z.; Urban, J. H.; Sullenger, B. A.; Clary, B. M., In vivo selection of tumor-targeting RNA motifs. *Nature Chemical Biology* **2009**, *6*, 22.
138. Pollard, T. D., A Guide to Simple and Informative Binding Assays. *Molecular Biology of the Cell* **2010**, *21* (23), 4061-4067.
139. Ruckman, J.; Green, L. S.; Beeson, J.; Waugh, S.; Gillette, W. L.; Henninger, D. D.; Claesson-Welsh, L.; Janjic, N., 2'-Fluoropyrimidine RNA-based Aptamers to the 165-Amino Acid Form of Vascular Endothelial Growth Factor (VEGF165): INHIBITION OF RECEPTOR BINDING AND VEGF-INDUCED VASCULAR PERMEABILITY THROUGH INTERACTIONS REQUIRING THE EXON 7-ENCODED DOMAIN. *Journal of Biological Chemistry* **1998**, *273* (32), 20556-20567.
140. Huizenga, D. E.; Szostak, J. W., A DNA Aptamer That Binds Adenosine and ATP. *Biochemistry* **1995**, *34* (2), 656-665.

141. Keefe, A. D.; Cload, S. T., SELEX with modified nucleotides. *Current Opinion in Chemical Biology* **2008**, *12* (4), 448-456.
142. Imanishi, T.; Obika, S., BNAs: novel nucleic acid analogs with a bridged sugar moiety. *Chemical Communications* **2002**, (16), 1653-1659.
143. Schmidt, K. S.; Borkowski, S.; Kurreck, J.; Stephens, A. W.; Bald, R.; Hecht, M.; Friebe, M.; Dinkelborg, L.; Erdmann, V. A., Application of locked nucleic acids to improve aptamer in vivo stability and targeting function. *Nucleic Acids Research* **2004**, *32* (19), 5757-5765.
144. Peng, C. G.; Damha, M. J., G-quadruplex induced stabilization by 2'-deoxy-2'-fluoro-d-arabinonucleic acids (2'-F-ANA). *Nucleic Acids Research* **2007**, *35* (15), 4977-4988.
145. Klußmann, S.; Nolte, A.; Bald, R.; Erdmann, V. A.; Fürste, J. P., Mirror-image RNA that binds D-adenosine. *Nature Biotechnology* **1996**, *14*, 1112.
146. Vater, A.; Sell, S.; Kaczmarek, P.; Maasch, C.; Buchner, K.; Pruszyńska-Oszmalek, E.; Kolodziejcki, P.; Purschke, W. G.; Nowak, K. W.; Strowski, M. Z.; Klusmann, S., A Mixed Mirror-image DNA/RNA Aptamer Inhibits Glucagon and Acutely Improves Glucose Tolerance in Models of Type 1 and Type 2 Diabetes. *Journal of Biological Chemistry* **2013**, *288* (29), 21136-21147.
147. Ozer, A.; Pagano, J. M.; Lis, J. T., New Technologies Provide Quantum Changes in the Scale, Speed, and Success of SELEX Methods and Aptamer Characterization. *Molecular Therapy. Nucleic Acids* **2014**, *3* (8), e183.
148. Gold, L.; Ayers, D.; Bertino, J.; Bock, C.; Bock, A.; Brody, E. N.; Carter, J.; Dalby, A. B.; Eaton, B. E.; Fitzwater, T.; Flather, D.; Forbes, A.; Foreman, T.; Fowler, C.; Gawande, B.; Goss, M.; Gunn, M.; Gupta, S.; Halladay, D.; Heil, J.; Heilig, J.; Hicke, B.; Husar, G.; Janjic, N.; Jarvis, T.; Jennings, S.; Katilius, E.; Keeney, T. R.; Kim, N.; Koch, T. H.; Kraemer, S.; Kroiss, L.; Le, N.; Levine, D.; Lindsey, W.; Lollo, B.; Mayfield, W.; Mehan, M.; Mehler, R.; Nelson, S. K.; Nelson, M.; Nieuwlandt, D.; Nikrad, M.; Ochsner, U.; Ostroff, R. M.; Otis, M.; Parker, T.; Pietrasiewicz, S.; Resnicow, D. I.; Rohloff, J.; Sanders, G.; Sattin, S.; Schneider, D.; Singer, B.; Stanton, M.; Sterkel, A.; Stewart, A.; Stratford, S.; Vaught, J. D.; Vrkljan, M.; Walker, J. J.; Watrobka, M.; Waugh, S.; Weiss, A.; Wilcox, S. K.; Wolfson, A.; Wolk, S. K.; Zhang, C.; Zichi, D., Aptamer-Based Multiplexed Proteomic Technology for Biomarker Discovery. *PLoS ONE* **2010**, *5* (12), e15004.
149. Watson, J. D.; Crick, F. H. C., Molecular Structure of Nucleic Acids: A Structure for Deoxyribose Nucleic Acid. *Nature* **1953**, *171*, 737.
150. Zimmermann, G. R.; Wick, C. L.; Shields, T. P.; Jenison, R. D.; Pardi, A., Molecular interactions and metal binding in the theophylline-binding core of an RNA aptamer. *RNA* **2000**, *6* (5), 659-667.
151. Wilson, C.; Nix, J.; Szostak, J., Functional Requirements for Specific Ligand Recognition by a Biotin-Binding RNA Pseudoknot. *Biochemistry* **1998**, *37* (41), 14410-14419.
152. Tuerk, C.; MacDougall, S.; Gold, L., RNA pseudoknots that inhibit human immunodeficiency virus type 1 reverse transcriptase. *Proceedings of the National Academy of Sciences of the United States of America* **1992**, *89* (15), 6988-6992.
153. Boiziau, C.; Dausse, E.; Yurchenko, L.; Toulmé, J.-J., DNA Aptamers Selected Against the HIV-1trans-Activation-responsive RNA Element Form RNA-DNA Kissing Complexes. *Journal of Biological Chemistry* **1999**, *274* (18), 12730-12737.
154. Macaya, R. F.; Schultze, P.; Smith, F. W.; Roe, J. A.; Feigon, J., Thrombin-binding DNA aptamer forms a unimolecular quadruplex structure in solution. *Proceedings of the National Academy of Sciences of the United States of America* **1993**, *90* (8), 3745-3749.
155. Tasset, D. M.; Kubik, M. F.; Steiner, W., Oligonucleotide inhibitors of human thrombin that bind distinct epitopes. *Journal of Molecular Biology* **1997**, *272* (5), 688-698.
156. Hermann, T.; Patel, D. J., Adaptive Recognition by Nucleic Acid Aptamers. *Science* **2000**, *287* (5454), 820-825.
157. Gellert, M.; Lipsett, M. N.; Davies, D. R., HELIX FORMATION BY GUANYLIC ACID. *Proceedings of the National Academy of Sciences of the United States of America* **1962**, *48* (12), 2013-2018.

158. Wang, K. Y.; McCurdy, S.; Shea, R. G.; Swaminathan, S.; Bolton, P. H., A DNA aptamer which binds to and inhibits thrombin exhibits a new structural motif for DNA. *Biochemistry* **1993**, *32* (8), 1899-1904.
159. Cruz-Aguado, J. A.; Penner, G., Determination of Ochratoxin A with a DNA Aptamer. *Journal of Agricultural and Food Chemistry* **2008**, *56* (22), 10456-10461.
160. Gatto, B.; Palumbo, M.; Sissi, C., Nucleic Acid Aptamers Based on the G-Quadruplex Structure: Therapeutic and Diagnostic Potential. *Current Medicinal Chemistry* **2009**, *16* (10), 1248-1265.
161. Đapić, V.; Abdomerović, V.; Marrington, R.; Peberdy, J.; Rodger, A.; Trent, J. O.; Bates, P. J., Biophysical and biological properties of quadruplex oligodeoxyribonucleotides. *Nucleic Acids Research* **2003**, *31* (8), 2097-2107.
162. Đapić, V.; Bates, P. J.; Trent, J. O.; Rodger, A.; Thomas, S. D.; Miller, D. M., Antiproliferative Activity of G-Quartet-Forming Oligonucleotides with Backbone and Sugar Modifications. *Biochemistry* **2002**, *41* (11), 3676-3685.
163. Zhou, J.; Rossi, J., Aptamers as targeted therapeutics: current potential and challenges. *Nature Reviews Drug Discovery* **2016**, *16*, 181.
164. Zhuo, Z.; Yu, Y.; Wang, M.; Li, J.; Zhang, Z.; Liu, J.; Wu, X.; Lu, A.; Zhang, G.; Zhang, B., Recent Advances in SELEX Technology and Aptamer Applications in Biomedicine. *International Journal of Molecular Sciences* **2017**, *18* (10), 2142.
165. Deyev, S. M.; Lebedenko, E. N., Modern Technologies for Creating Synthetic Antibodies for Clinical application. *Acta Naturae* **2009**, *1* (1), 32-50.
166. Ng, E. W. M.; Shima, D. T.; Calias, P.; Cunningham Jr, E. T.; Guyer, D. R.; Adamis, A. P., Pegaptanib, a targeted anti-VEGF aptamer for ocular vascular disease. *Nature Reviews Drug Discovery* **2006**, *5*, 123.
167. Ferrara, N.; Adamis, A. P., Ten years of anti-vascular endothelial growth factor therapy. *Nature Reviews Drug Discovery* **2016**, *15*, 385.
168. Mousa, S. A.; Mousa, S. S., Current Status of Vascular Endothelial Growth Factor Inhibition in Age-Related Macular Degeneration. *BioDrugs* **2010**, *24* (3), 183-194.
169. Jayasena, S. D., Aptamers: An Emerging Class of Molecules That Rival Antibodies in Diagnostics. *Clinical Chemistry* **1999**, *45* (9), 1628-1650.
170. Liu, X.; Zhang, X., Aptamer-Based Technology for Food Analysis. *Applied Biochemistry and Biotechnology* **2015**, *175* (1), 603-624.
171. Lee, H.-J.; Kim, B. C.; Kim, K.-W.; Kim, Y. K.; Kim, J.; Oh, M.-K., A sensitive method to detect Escherichia coli based on immunomagnetic separation and real-time PCR amplification of aptamers. *Biosensors and Bioelectronics* **2009**, *24* (12), 3550-3555.
172. Bruno, J. G.; Phillips, T.; Carrillo, M. P.; Crowell, R., Plastic-Adherent DNA Aptamer-Magnetic Bead and Quantum Dot Sandwich Assay for Campylobacter Detection. *Journal of Fluorescence* **2008**, *19* (3), 427.
173. Joshi, R.; Janagama, H.; Dwivedi, H. P.; Senthil Kumar, T. M. A.; Jaykus, L.-A.; Schefers, J.; Sreevatsan, S., Selection, characterization, and application of DNA aptamers for the capture and detection of Salmonella enterica serovars. *Molecular and Cellular Probes* **2009**, *23* (1), 20-28.
174. Ohk, S. H.; Koo, O. K.; Sen, T.; Yamamoto, C. M.; Bhunia, A. K., Antibody-aptamer functionalized fibre-optic biosensor for specific detection of Listeria monocytogenes from food. *Journal of Applied Microbiology* **2010**, *109* (3), 808-817.
175. Kirby, R.; Cho, E. J.; Gehrke, B.; Bayer, T.; Park, Y. S.; Neikirk, D. P.; McDevitt, J. T.; Ellington, A. D., Aptamer-Based Sensor Arrays for the Detection and Quantitation of Proteins. *Analytical Chemistry* **2004**, *76* (14), 4066-4075.
176. Chen, J.; Fang, Z.; Liu, J.; Zeng, L., A simple and rapid biosensor for ochratoxin A based on a structure-switching signaling aptamer. *Food Control* **2012**, *25* (2), 555-560.

177. Pang, S.; Labuza, T. P.; He, L., Development of a single aptamer-based surface enhanced Raman scattering method for rapid detection of multiple pesticides. *Analytist* **2014**, *139* (8), 1895-1901.
178. Svobodova, M.; Mairal, T.; Nadal, P.; Bermudo, M. C.; O'Sullivan, C. K., Ultrasensitive aptamer based detection of β -conglutin food allergen. *Food Chemistry* **2014**, *165*, 419-423.
179. Li, L.; Li, B.; Qi, Y.; Jin, Y., Label-free aptamer-based colorimetric detection of mercury ions in aqueous media using unmodified gold nanoparticles as colorimetric probe. *Analytical and Bioanalytical Chemistry* **2009**, *393* (8), 2051-2057.
180. Huang, S.; Gan, N.; Liu, H.; Zhou, Y.; Chen, Y.; Cao, Y., Simultaneous and specific enrichment of several amphenicol antibiotics residues in food based on novel aptamer functionalized magnetic adsorbents using HPLC-DAD. *Journal of Chromatography B* **2017**, *1060*, 247-254.
181. Amaya-González, S.; de-los-Santos-Álvarez, N.; Miranda-Ordieres, A. J.; Lobo-Castañón, M. J., Aptamer Binding to Celiac Disease-Triggering Hydrophobic Proteins: A Sensitive Gluten Detection Approach. *Analytical Chemistry* **2014**, *86* (5), 2733-2739.
182. Golub, E.; Pelosof, G.; Freeman, R.; Zhang, H.; Willner, I., Electrochemical, Photoelectrochemical, and Surface Plasmon Resonance Detection of Cocaine Using Supramolecular Aptamer Complexes and Metallic or Semiconductor Nanoparticles. *Analytical Chemistry* **2009**, *81* (22), 9291-9298.
183. Lamont, E. A.; He, L.; Warriner, K.; Labuza, T. P.; Sreevatsan, S., A single DNA aptamer functions as a biosensor for ricin. *Analytist* **2011**, *136* (19), 3884-3895.
184. Wu, X.; Hu, J.; Zhu, B.; Lu, L.; Huang, X.; Pang, D., Aptamer-targeted magnetic nanospheres as a solid-phase extraction sorbent for determination of ochratoxin A in food samples. *Journal of Chromatography A* **2011**, *1218* (41), 7341-7346.
185. Hyeon, J.-Y.; Chon, J.-W.; Choi, I.-S.; Park, C.; Kim, D.-E.; Seo, K.-H., Development of RNA aptamers for detection of Salmonella Enteritidis. *Journal of Microbiological Methods* **2012**, *89* (1), 79-82.
186. Singh, P. K.; Jairath, G.; Ahlawat, S. S.; Pathera, A.; Singh, P., Biosensor: an emerging safety tool for meat industry. *Journal of Food Science and Technology* **2016**, *53* (4), 1759-1765.
187. Beier, R.; Pahlke, C.; Quenzel, P.; Henseleit, A.; Boschke, E.; Cuniberti, G.; Labudde, D., Selection of a DNA aptamer against norovirus capsid protein VP1. *FEMS Microbiology Letters* **2014**, *351* (2), 162-169.
188. Giamberardino, A.; Labib, M.; Hassan, E. M.; Tetro, J. A.; Springthorpe, S.; Sattar, S. A.; Berezovski, M. V.; DeRosa, M. C., Ultrasensitive Norovirus Detection Using DNA Aptasensor Technology. *PLoS ONE* **2013**, *8* (11), e79087.
189. Moore, M. D.; Escudero-Abarca, B. I.; Suh, S. H.; Jaykus, L. A., Generation and characterization of nucleic acid aptamers targeting the capsid P domain of a human norovirus GII.4 strain. *J Biotechnol* **2015**, *209*, 41-9.
190. Escudero-Abarca, B. I.; Suh, S. H.; Moore, M. D.; Dwivedi, H. P.; Jaykus, L.-A., Selection, Characterization and Application of Nucleic Acid Aptamers for the Capture and Detection of Human Norovirus Strains. *PLoS ONE* **2014**, *9* (9), e106805.
191. Schütze, T.; Wilhelm, B.; Greiner, N.; Braun, H.; Peter, F.; Mörl, M.; Erdmann, V. A.; Lehrach, H.; Konthur, Z.; Menger, M.; Arndt, P. F.; Glökler, J., Probing the SELEX Process with Next-Generation Sequencing. *PLoS One* **2011**, *6* (12), e29604.
192. Zuker, M., Mfold web server for nucleic acid folding and hybridization prediction. *Nucleic Acids Research* **2003**, *31* (13), 3406-3415.
193. Bailey, T. L.; Boden, M.; Buske, F. A.; Frith, M.; Grant, C. E.; Clementi, L.; Ren, J.; Li, W. W.; Noble, W. S., MEME Suite: tools for motif discovery and searching. *Nucleic Acids Research* **2009**, *37* (suppl_2), W202-W208.

194. Bourhy, P.; Bremont, S.; Zinini, F.; Giry, C.; Picardeau, M., Comparison of Real-Time PCR Assays for Detection of Pathogenic *Leptospira* spp. in Blood and Identification of Variations in Target Sequences. *Journal of Clinical Microbiology* **2011**, *49* (6), 2154-2160.
195. Koho, T.; Huhti, L.; Blazevic, V.; Nurminen, K.; Butcher, S. J.; Laurinmäki, P.; Kalkkinen, N.; Rönholm, G.; Vesikari, T.; Hytönen, V. P.; Kulomaa, M. S., Production and characterization of virus-like particles and the P domain protein of GII.4 norovirus. *Journal of Virological Methods* **2012**, *179* (1), 1-7.
196. Carson, M.; Johnson, D. H.; McDonald, H.; Brouillette, C.; DeLucas, L. J., His-tag impact on structure. *Acta Crystallographica Section D* **2007**, *63* (3), 295-301.
197. Dupont, D. M.; Larsen, N.; Jensen, J. K.; Andreasen, P. A.; Kjems, J., Characterisation of aptamer–target interactions by branched selection and high-throughput sequencing of SELEX pools. *Nucleic Acids Research* **2015**, *43* (21), e139-e139.
198. Pallansch, L.; Beswick, H.; Talian, J.; Zelenka, P., Use of an RNA folding algorithm to choose regions for amplification by the polymerase chain reaction. *Analytical Biochemistry* **1990**, *185* (1), 57-62.
199. Usdin, K.; Woodford, K. J., CGG repeats associated with DNA instability and chromosome fragility form structures that block DNA synthesis in vitro. *Nucleic Acids Research* **1995**, *23* (20), 4202-4209.
200. Sahdev, S.; Saini, S.; Tiwari, P.; Saxena, S.; Singh Saini, K., Amplification of GC-rich genes by following a combination strategy of primer design, enhancers and modified PCR cycle conditions. *Molecular and Cellular Probes* **2007**, *21* (4), 303-307.
201. McDowell, D. G.; Burns, N. A.; Parkes, H. C., Localised sequence regions possessing high melting temperatures prevent the amplification of a DNA mimic in competitive PCR. *Nucleic Acids Research* **1998**, *26* (14), 3340-3347.
202. Frackman S, K. G., Simpson D, Storts D, Betaine and DMSO: Enhancing Agents for PCR. *Promega Notes* **1998**, 27.
203. Kang, J.; Soog Lee, M.; Gorenstein, D. G., The enhancement of PCR amplification of a random sequence DNA library by DMSO and betaine: Application to in vitro combinatorial selection of aptamers. *Journal of Biochemical and Biophysical Methods* **2005**, *64* (2), 147-151.
204. Tolle, F.; Wilke, J.; Wengel, J.; Mayer, G., By-Product Formation in Repetitive PCR Amplification of DNA Libraries during SELEX. *PLoS ONE* **2014**, *9* (12), e114693.
205. Musheev, M. U.; Krylov, S. N., Selection of aptamers by systematic evolution of ligands by exponential enrichment: Addressing the polymerase chain reaction issue. *Anal Chim Acta* **2006**, *564* (1), 91-96.
206. Kim, K.; Lee, S.; Ryu, S.; Han, D., Efficient isolation and elution of cellular proteins using aptamer-mediated protein precipitation assay. *Biochem Biophys Res Commun* **2014**, *448* (1), 114-119.
207. Yoon, J. W.; Jang, I. H.; Heo, S. C.; Kwon, Y. W.; Choi, E. J.; Bae, K.-H.; Suh, D.-S.; Kim, S.-C.; Han, S.; Haam, S.; Jung, J.; Kim, K.; Ryu, S. H.; Kim, J. H., Isolation of Foreign Material-Free Endothelial Progenitor Cells Using CD31 Aptamer and Therapeutic Application for Ischemic Injury. *PLoS ONE* **2015**, *10* (7), e0131785.
208. Sen, D.; Gilbert, W., Formation of parallel four-stranded complexes by guanine-rich motifs in DNA and its implications for meiosis. *Nature* **1988**, *334*, 364.
209. Rhodes, D.; Lipps, H. J., G-quadruplexes and their regulatory roles in biology. *Nucleic Acids Research* **2015**, *43* (18), 8627-8637.
210. Phan, A. T., Human telomeric G-quadruplex: structures of DNA and RNA sequences. *FEBS Journal* **2010**, *277* (5), 1107-1117.
211. Ueyama, H.; Takagi, M.; Takenaka, S., A Novel Potassium Sensing in Aqueous Media with a Synthetic Oligonucleotide Derivative. Fluorescence Resonance Energy Transfer Associated with Guanine Quartet–Potassium Ion Complex Formation. *Journal of the American Chemical Society* **2002**, *124* (48), 14286-14287.

212. Kypr, J.; Kejnovská, I.; Renčíuk, D.; Vorlíčková, M., Circular dichroism and conformational polymorphism of DNA. *Nucleic Acids Research* **2009**, *37* (6), 1713-1725.
213. Lai, Y.-T.; DeStefano, J. J., DNA Aptamers to Human Immunodeficiency Virus Reverse Transcriptase Selected by a Primer-Free SELEX Method: Characterization and Comparison with Other Aptamers. *Nucleic Acid Therapeutics* **2012**, *22* (3), 162-176.
214. Ambrus, A.; Chen, D.; Dai, J.; Bialis, T.; Jones, R. A.; Yang, D., Human telomeric sequence forms a hybrid-type intramolecular G-quadruplex structure with mixed parallel/antiparallel strands in potassium solution. *Nucleic Acids Research* **2006**, *34* (9), 2723-2735.
215. Yang, C.; Wang, Y.; Marty, J.-L.; Yang, X., Aptamer-based colorimetric biosensing of Ochratoxin A using unmodified gold nanoparticles indicator. *Biosensors and Bioelectronics* **2011**, *26* (5), 2724-2727.
216. Huang, Y.; Chen, X.; Duan, N.; Wu, S.; Wang, Z.; Wei, X.; Wang, Y., Selection and characterization of DNA aptamers against Staphylococcus aureus enterotoxin C1. *Food Chemistry* **2015**, *166*, 623-629.
217. Ettayebi, K.; Crawford, S. E.; Murakami, K.; Broughman, J. R.; Karandikar, U.; Tenge, V. R.; Neill, F. H.; Blutt, S. E.; Zeng, X.-L.; Qu, L.; Kou, B.; Opekun, A. R.; Burrin, D.; Graham, D. Y.; Ramani, S.; Atmar, R. L.; Estes, M. K., Replication of human noroviruses in stem cell-derived human enteroids. *Science* **2016**, *353* (6306), 1387-1393.
218. Bing, T.; Yang, X.; Mei, H.; Cao, Z.; Shangguan, D., Conservative secondary structure motif of streptavidin-binding aptamers generated by different laboratories. *Bioorganic & Medicinal Chemistry* **2010**, *18* (5), 1798-1805.
219. Tamura, K.; Nei, M., Estimation of the number of nucleotide substitutions in the control region of mitochondrial DNA in humans and chimpanzees. *Molecular Biology and Evolution* **1993**, *10* (3), 512-526.
220. Kumar, S.; Stecher, G.; Tamura, K., MEGA7: Molecular Evolutionary Genetics Analysis Version 7.0 for Bigger Datasets. *Molecular Biology and Evolution* **2016**, *33* (7), 1870-1874.
221. Shiota, T.; Okame, M.; Takanashi, S.; Khamrin, P.; Takagi, M.; Satou, K.; Masuoka, Y.; Yagyū, F.; Shimizu, Y.; Kohno, H.; Mizuguchi, M.; Okitsu, S.; Ushijima, H., Characterization of a Broadly Reactive Monoclonal Antibody against Norovirus Genogroups I and II: Recognition of a Novel Conformational Epitope. *Journal of Virology* **2007**, *81* (22), 12298-12306.
222. Lindesmith, L. C.; Ferris, M. T.; Mullan, C. W.; Ferreira, J.; Debbink, K.; Swanstrom, J.; Richardson, C.; Goodwin, R. R.; Baehner, F.; Mendelman, P. M.; Bargatze, R. F.; Baric, R. S., Broad Blockade Antibody Responses in Human Volunteers after Immunization with a Multivalent Norovirus VLP Candidate Vaccine: Immunological Analyses from a Phase I Clinical Trial. *PLOS Medicine* **2015**, *12* (3), e1001807.
223. Goodridge, L.; Goodridge, C.; Wu, J.; Griffiths, M.; Pawliszyn, J., Isoelectric Point Determination of Norovirus Virus-like Particles by Capillary Isoelectric Focusing with Whole Column Imaging Detection. *Analytical Chemistry* **2004**, *76* (1), 48-52.
224. Nagarkatti, R.; Bist, V.; Sun, S.; Fortes de Araujo, F.; Nakhasi, H. L.; Debrabant, A., Development of an Aptamer-Based Concentration Method for the Detection of Trypanosoma cruzi in Blood. *PLOS ONE* **2012**, *7* (8), e43533.
225. Li, B.; Wei, H.; Dong, S., Sensitive detection of protein by an aptamer-based label-free fluorescing molecular switch. *Chemical Communications* **2007**, (1), 73-75.
226. Sobic, A.; Meneghello, A.; Cretaio, E.; Gatto, B., Human Thrombin Detection Through a Sandwich Aptamer Microarray: Interaction Analysis in Solution and in Solid Phase. *Sensors (Basel, Switzerland)* **2011**, *11* (10), 9426-9441.
227. Zhu, J.; Li, T.; Hu, J.; Wang, E., A novel dot-blot DNazyme-linked aptamer assay for protein detection. *Analytical and Bioanalytical Chemistry* **2010**, *397* (7), 2923-2927.
228. Yao, L.; Wu, Q.; Wang, D.; Kou, X.; Zhang, J., Development of monoclonal antibody-coated immunomagnetic beads for separation and detection of norovirus (genogroup II) in faecal extract samples. *Letters in Applied Microbiology* **2009**, *49* (2), 173-178.

229. Gilpatrick, S. G.; Schwab, K. J.; Estes, M. K.; Atmar, R. L., Development of an immunomagnetic capture reverse transcription-PCR assay for the detection of Norwalk virus. *Journal of Virological Methods* **2000**, *90* (1), 69-78.
230. ThermoFisher Dynabeads® MyOne™ Streptavidin C1, Retrieved from: <https://www.thermofisher.com/de/de/home/references/protocols/proteins-expression-isolation-and-analysis/protein-isolation-protocol/dynabeads-myone-streptavidin-c1.html#top> February 6. **2018**.
231. Kim, Y. S.; Chung, J.; Song, M. Y.; Jurng, J.; Kim, B. C., Aptamer cocktails: Enhancement of sensing signals compared to single use of aptamers for detection of bacteria. *Biosensors and Bioelectronics* **2014**, *54*, 195-198.
232. White, R.; Rusconi, C.; Scardino, E.; Wolberg, A.; Lawson, J.; Hoffman, M.; Sullenger, B., Generation of Species Cross-reactive Aptamers Using Toggle SELEX. *Molecular Therapy* **4** (6), 567-573.
233. Farrell, R. E. P. D., *RNA Methodologies*. 4th ed.; Elsevier: 2010; Vol. 4, p 744.
234. Amemiya, Y.; Miyahara, J., Imaging plate illuminates many fields. *Nature* **1988**, *336*, 89.
235. Takahashi, K.; Miyahara, J.; Shibahara, Y., Photostimulated Luminescence (PSL) and Color Centers in BaFX : Eu²⁺ (X = Cl, Br, I) Phosphors. *Journal of The Electrochemical Society* **1985**, *132* (6), 1492-1494.
236. Sonoda, M.; Takano, M.; Miyahara, J.; Kato, H., Computed radiography utilizing scanning laser stimulated luminescence. *Radiology* **1983**, *148* (3), 833-838.
237. Park, J.-W.; Lee, S.-G.; Lee, Y.-M.; Jheong, W.-H.; Ryu, S.; Paik, S.-Y., Full sequence analysis and characterization of the South Korean Norovirus GII-4 variant CUK-3. *Virology Journal* **2011**, *8* (1), 1-5.
238. Murphy, M. B.; Fuller, S. T.; Richardson, P. M.; Doyle, S. A., An improved method for the in vitro evolution of aptamers and applications in protein detection and purification. *Nucleic Acids Res* **2003**, *31* (18), e110.
239. Sanger, F.; Nicklen, S.; Coulson, A. R., DNA sequencing with chain-terminating inhibitors. *Proceedings of the National Academy of Sciences of the United States of America* **1977**, *74* (12), 5463-5467.
240. Vega, E.; Barclay, L.; Gregoricus, N.; Williams, K.; Lee, D.; Vinjé, J., Novel Surveillance Network for Norovirus Gastroenteritis Outbreaks, United States. *Emerging Infectious Diseases* **2011**, *17* (8), 1389-1395.
241. Jackson, D. A.; Symons, R. H.; Berg, P., Biochemical Method for Inserting New Genetic Information into DNA of Simian Virus 40: Circular SV40 DNA Molecules Containing Lambda Phage Genes and the Galactose Operon of Escherichia coli. *Proceedings of the National Academy of Sciences of the United States of America* **1972**, *69* (10), 2904-2909.
242. Laemmli, U. K., Cleavage of Structural Proteins during the Assembly of the Head of Bacteriophage T4. *Nature* **1970**, *227*, 680.
243. Bradford, M. M., A rapid and sensitive method for the quantitation of microgram quantities of protein utilizing the principle of protein-dye binding. *Analytical Biochemistry* **1976**, *72* (1), 248-254.
244. Lowry, O. H.; Rosebrough, N. J.; Farr, A. L.; Randall, R. J., PROTEIN MEASUREMENT WITH THE FOLIN PHENOL REAGENT. *Journal of Biological Chemistry* **1951**, *193* (1), 265-275.
245. Lilius, G.; Persson, M.; BüLow, L.; Mosbach, K., Metal affinity precipitation of proteins carrying genetically attached polyhistidine affinity tails. *European Journal of Biochemistry* **1991**, *198* (2), 499-504.
246. Sefah, K. S., Dihua; Xiong, Xiangling; O'Donoghue, Meghan, B.; Tan, Weihong, Development of DNA aptamers using Cell-SELEX. *Nature Protocols* **2010**, *5*, 1169-1185.
247. Hall, K. B.; Kranz, J. K., Nitrocellulose Filter Binding for Determination of Dissociation Constants. In *RNA-Protein Interaction Protocols*, Haynes, S. R., Ed. Humana Press: Totowa, NJ, 1999; pp 105-114.

Literature

248. Papoulas, O., Rapid Separation of Protein-Bound DNA from Free DNA Using Nitrocellulose Filters. In *Current Protocols in Molecular Biology*, John Wiley & Sons, Inc.: 2001.
249. Bock, L. C.; Griffin, L. C.; Latham, J. A.; Vermaas, E. H.; Toole, J. J., Selection of single-stranded DNA molecules that bind and inhibit human thrombin. *Nature* **1992**, 355 (6360), 564-566.
250. Schilling, K. B.; DeGrasse, J.; Woods, J. W., The influence of food matrices on aptamer selection by SELEX (systematic evolution of ligands by exponential enrichment) targeting the norovirus P-Domain. *Food Chemistry* **2018**, 258, 129-136.

9 Annex

9.1 Register of Figures

Figure 1. An electron microscopic picture of NoV particles from stool filtrate in PBS buffer ¹	1
Figure 2. The organization of the norovirus genome, which is divided in three ORFs.	3
Figure 3. The structure of the NoV surface.....	4
Figure 4. Structural surface models of five particles as resulting from assembly of VP1 protein or truncated VP1 proteins.	5
Figure 5. Phylogenetic tree, based on the NoV major capsid protein sequences.	6
Figure 6. Routes of environmental virus transmission.	9
Figure 7. Schematic depiction of virus extraction methods for different food matrices used at the FDA laboratories.	13
Figure 8. Schematic depiction of SELEX process using paramagnetic beads as immobilization medium to separate target binding from non-binding oligonucleotides.	16
Figure 9. Examples for aptamer secondary and tertiary structures.	19
Figure 10. SDS Page Gels (10%) showing protein fractions collected during P-domain and control protein purification.	27
Figure 11. Tape Station 2200 Image of purified control protein and P-domain after electrophoresis.	28
Figure 12. Outline to investigate the influence of food matrix on aptamer enrichment during SELEX.....	29
Figure 13. Agarose gel (3%) showing PCR amplicons to determine number of PCR cycles of SELEX-round 7.....	31
Figure 14. P-domain binding of enriched nucleic acid pools of the final round of each SELEX-experiment.....	34
Figure 15. Binding of selected enriched oligonucleotides to the P-domain and the control protein.	37
Figure 16. P-domain binding curves of oligonucleotides enriched in the buffer-, lettuce- and strawberry-SELEX-experiments.....	38
Figure 17. Binding of aptamer candidates to different proteins. Aptamer candidates are shown on the x-axes and aptamer protein binding on the y-axes.	39
Figure 18. Affinities of oligonucleotides Buf-1 and Buf-2 for the P-domain. Binding studies were completed by FRA.	40
Figure 19. P-domain binding of Buf-1 and Buf-2 in presence of different competitors.	41

Figure 20. CD spectra of different oligonucleotides derived from aptamer Buf-2 to investigate Buf-2 structure.	42
Figure 21. P-domain binding curves of different oligonucleotide variants derived from aptamer Buf-2.	43
Figure 22. P-domain binding of aptamer candidates Buf-1, Buf-2 and Buf-8, Let-1 and Straw-1 in presence of food matrices.....	44
Figure 23. P-domain binding of aptamer Buf-2 in presence selection buffer (SB) and CP and IQF oyster preparations (CP and IQF prep) and suspensions (CP and IQF susp).	45
Figure 24. Binding of aptamer Buf-2 in presence selection buffer (SB) and of tenfold diluted CP and IQF oyster preparations (CP and IQF prep) and suspensions (CP and IQF susp).....	46
Figure 25. Binding of the aptamer Buf-2 and VLPs of NoV genotypes GI.1, GI.7, GII.3, GII.4 New Orleans, and GII.4 Sydney	49
Figure 26. Binding of the aptamer Beier and VLPs of NoV genotypes GI.1, GI.7, GII.3, GII.4 New Orleans, and GII.4 Sydney	50
Figure 27. Binding of the aptamer AG3 and VLPs of NoV genotypes GI.1, GI.7, GII.3, GII.4 New Orleans, and GII.4 Sydney.	50
Figure 28. Binding of the aptamer SMV-19 and VLPs of NoV genotypes GI.1, GI.7, GII.3, GII.4 New Orleans, and GII.4 Sydney.	50
Figure 29. Binding of the aptamer SMV-21 and VLPs of NoV genotypes GI.1, GI.7, GII.3, GII.4 New Orleans, and GII.4 Sydney.....	51
Figure 30. Binding of the aptamer M 1 and VLPs of NoV genotypes GI.1, GI.7, GII.3, GII.4 New Orleans, and GII.4 Sydney.	51
Figure 31. Binding of the aptamer M 6-2 and VLPs of NoV genotypes GI.1, GI.7, GII.3, GII.4 New Orleans, and GII.4 Sydney.	51
Figure 32. CD spectra of norovirus aptamers with and without 3'- end biotin tag.	54
Figure 33. Aptamer mediated dot-blot using selected aptamers and five different genotypes of VLPs.	56
Figure 34. Ct values depicted in a bar graph, to compare blocking of streptavidin beads using 1 % BSA solution. T.....	58
Figure 35. Aptamer-mediated NoV pull-down from stool suspension using different aptamers.	59
Figure 36. Graph of linear regression from NoV endpoint titration.	60
Figure 37. Proposed folding and CD spectrum of parallel/antiparallel G-quadruplex as described previously.	72

Figure 38. Phylogenetic tree generated with the sequences of NoV capsid protein of the five genotypes GI.1, GI.7, GII.3, GII.4 New Orleans (Nola), and GII.4 Sydney (Syd.).	79
Figure 39. Simulated complex of aptamer Beier binding the NoV VP1 protein.	80
Figure 40. Figure shows the map of the expression plasmid used in this work:pET 100/D-TOPO	165

9.2 Register of Tables

Table 1. Summary of selected, previously published NoV aptamers, their SELEX target and determined K_d .	23
Table 2. Optimal conditions of P-domain production in BL21 Star™(DE3).	26
Table 3. Conditions of individual SELEX-rounds including protein amounts, number, and volume of washing steps and PCR cycles for the five parallel SELEX-experiments.	32
Table 4. Oligonucleotides enriched during the parallel SELEX-experiments with their relative abundances in each oligonucleotide pool of the last SELEX-round.	35
Table 5. Names and sequences of Buf-2 variants investigated by CD spectroscopy.	42
Table 6. Relevant motifs detected in sequences of oligonucleotides enriched in SELEX efforts to select an aptamer for the NoV surface.	47
Table 7. Selected oligonucleotides which sequences included the motif site.	48
Table 8. K_d values determined for selected NoV aptamers and VLPs of five different genotypes.	53
Table 9. Results of aptamer mediated dot-blot.	55
Table 10. Ct values and log values for Nov endpoint titration.	60
Table 11. Viral numbers recovered using the FDA-shellfish method and with aptamer-mediated pull-down, using selected NoV aptamers.	61
Table 12. Maxima and minima in CD spectra of different aptamer structures.	71
Table 13. Buffers present during SELEX of each aptamer with the corresponding literature reference.	106
Table 14. Buffers and solutions used for electrophoresis.	111
Table 15. Buffers used for aptamer mediated dot-blot, pull-down, and FDA-shellfish method, and buffers and media used during purification of recombinant protein.	112
Table 16. Buffers used during SELEX and aptamer characterization.	113
Table 17. Commercial Kits used during this work.	113
Table 18. List of nucleotides and radionuclides used for binding studies and filter retention assays.	114

Table 19. Sequence list of primers and other oligonucleotides used during this work except aptmers, which are listed in the results section.	114
Table 20. List of primers used for colony PCR and for the different vectors used.....	115
Table 21. List of enzymes used during this work.....	115
Table 22. Enzyme reagents and PCR reagents.	116
Table 23. Antibodies and other proteins used during this work.....	117
Table 24. Magnetic beads, and spin columns used for SELEX and other aptamer applications. .	117
Table 25. Material used for protein purification and analysis.	117
Table 26. Material used during filter retention assays.	117
Table 27. Laboratory ware commonly used during this work.....	118
Table 28. List of software used during this work.	118
Table 29. List of hazardous materials in accordance with GHS.....	138
Table 30. List of pictograms including their names, according signal word and described danger	140
Table 31. List of Chemicals classified as CMR substances.....	151
Table 32. List of instruments used during this work	151
Table 33. Pipetting Scheme for VP1 amplification (section 6.5.1)	154
Table 34. Pipetting Scheme for P-Domain amplification (section 6.5.2)	154
Table 35. Pipetting Scheme for amplification of SELEX nucleic acid library (section 6.5.3).....	154
Table 36. Pipetting Scheme for RT-qPCR multiplex assay for the detection of NoV GI and GII (section 6.5.4).....	155
Table 37. Pipetting Scheme for Colony PCR (section 6.5.5)	156
Table 38. Pipetting Scheme to obtain 10 mL of stacking gel, for a 10 %SDS PAGE gel	156
Table 39. Pipetting Scheme to obtain 20 mL of separating gel, for a 10 %SDS PAGE gel	156
Table 40. List of sequences obtained from 50 clones, after cloning of the last SELEX-round of the buffer-SELEX-experiment	158
Table 41. List of sequences obtained from 50 clones, after cloning of the last SELEX-round of the lettuce-SELEX-experiment	158
Table 42. List of sequences obtained from 50 clones, after cloning of the last SELEX-round of the strawberry-SELEX-experiment.....	159
Table 43. List of sequences obtained from 50 clones, after cloning of the last SELEX-round of the oyster-SELEX-experiment	160
Table 44. List of sequences obtained from 50 clones, after cloning of the last SELEX-round of the oyster diverticular selection.....	162

9.3 List of Hazardous Components in Accordance with GHS

Following Table 29, hazard statements (H phrases) and precaution statements (P-phrases) form part of the Globally Harmonized System of Classification and Labelling of Chemicals (GHS) are listed.

Table 29. List of hazardous materials in accordance with GHS

Chemical	Pictogram	H-Sentence	P-Sentence
2-Mercaptoethanol	GHS05, GHS06, GHS08, GHS09	301+331-310- 315-317-318- 373-410	261-280-301+310+330- 302+352+310- 305+351+338+310-403+233
30% Acrylamide/Bis Solution 37.5:1	GHS07, GHS08	302+312-315- 319-317-340- 350-361-382	260-280-305+351+338-405- 501
Ammoniumpersulfate (APS)	GHS03, GHS07, GHS08	272-302-315- 317-319-334-335	220-261-280-305+351+338- 342+311
Ampicillin	GHS08	317-334	261-280-284-304+340- 342+311
BCIP (5-bromo-4-chloro-3-indolyl- phosphate, 4-toluidine salt)	GHS07	312-315-319-335	261-280-302-352+312- 304+340+312-337+313- 403+233
Chloroform	GHS06, GHS08	302-315-319- 331-336-351- 361d-372	261-281-305+351+338-311
Citric Acid	GHS07	319	280-305+351+338-337+313
Ethanol, 200 proof anhydrous	GHS02, GHS07	225-319	210-240-305+351+338- 403+233
Ethidium bromide 10mg/mL	GHS06, GHS08	331-341	261-281-311
Guanidinium isothiocyanate (98%, and 6M solution)	GHS05, GHS07	302+312+332- 314-412	260-280-301+312+330- 303+361+353-304+340+310- 305+351+338

Annex

Chemical	Pictogram	H-Sentence	P-Sentence
Hydrochloric acid	GHS05, GHS07	290-314-335	260-280-303+361+353- 304+340+310-305+351+338
Hydrogenperoxide (30% solution)	GHS05, GHS07	302-318-142	280-301+312+330- 305+351+338+310-
Imidazole	GHS05, GHS07, GHS08	302-314-360D	201-260-280-303+361+353- 305+351+338-308+313
Isopropanol	GHS02, GHS07	225-319-336	210-233-280-302+352- 309+310
Methanol	GHS02, GHS06, GHS08	225- 301+311+331- 370	210-280-302+352+312- 304+340+311-370+378- 403+235
NBT (3,3'-[3,3'-Dimethoxy(1,1'- biphenyl)-4,4'-diyl]bis[2-(4- nitrophenyl)-5-phenyl-2H- tetrazoliumdichloride)	GHS08	315-319-335-371	305+351+338-304+340- 302+352-332+313-309+311- 260-280-264-270-271- 403+233-501-405-362
Phenylmethanesulfonyl fluoride (PMSF)	GHS05, GHS06	301-314	280-301+310+330- 303+361+353-304+340+310- 305+351+338
Sodium hydroxide	GHS05	290-314	280-301+330+331- 305+351+338-308+310
Sodiumdodecyl sulfate	GHS02, GHS05, GHS07		
TEMED	GHS02, GHS05, GHS07	225-302-314-332	210-280-305+351+338-310

9.3.1 Pictogram description in accordance with the GHS

Pictograms, their names with the associated signal word and the described type of danger are shown in Table 30.

The signal word indicates the degree of danger. The word danger is used for the higher level, and the word warning is used for the lower degrees of danger. Toxicity categories are based on levels of LD₅₀ and on the type of exposure: dermal or oral.

Table 30. List of pictograms including their names, according signal word and described danger

Pictogram	Naming of the pictograms	Signal word	Danger
	GHS01 Explosive Bomb	Danger	Unstable, Explosive
	GHS02 Flame	Danger or Warning	Flammable
	GHS03 Flame over circle	Danger or Warning	Oxidising
	GHS04 Gas cylinder	Warning	Compressed Gas

Annex

Pictogram	Naming of the pictograms	Signal word	Danger
	<p>GHS05 Corrosion</p>	<p>Danger or Warning</p>	<p>Corrosive Category 1</p>
	<p>GHS06 Skull and crossbones</p>	<p>Danger</p>	<p>Toxic Category 1-3</p>
	<p>GHS07 Exclamation mark</p>	<p>Warning</p>	<p>Toxic category 4, Irritant category 2 or 3 Lower systemic health hazard</p>
	<p>GHS08 Health hazard</p>	<p>Danger or Warning</p>	<p>Systemic health hazards</p>
	<p>GHS09 Environment</p>	<p>Warning (for category 1, for category 2 no signal word)</p>	<p>Environment</p>

9.3.2 Lists of P and H phrases in accordance with the GHS

Physical Hazards

H200	Unstable explosive	H241	Heating may cause a fire or explosion
H201	Explosive; mass explosion hazard	H242	Heating may cause a fire
H202	Explosive; severe projection hazard	H250	Catches fire spontaneously if exposed to air
H203	Explosive; fire, blast or projection hazard	H251	Self-heating; may catch fire
H204	Fire or projection hazard	H252	Self-heating in large quantities; may catch fire
H205	May mass explode in fire	H260	In contact with water releases flammable gases which may ignite spontaneously
H220	Extremely flammable gas		
H221	Flammable gas		
H222	Extremely flammable material	H261	In contact with water releases flammable gas
H223	Flammable material	H270	May cause or intensify fire; oxidizer
H224	Extremely flammable liquid and vapour	H271	May cause fire or explosion; strong oxidizer
H225	Highly flammable liquid and vapour	H272	May intensify fire; oxidizer
H226	Flammable liquid and vapour	H280	Contains gas under pressure; may explode if heated
H227	Combustible liquid		
H228	Flammable solid	H281	Contains refrigerated gas; may cause cryogenic burns or injury
H240	Heating may cause an explosion	H290	May be corrosive to metals

Health Hazards

H301	Toxic if swallowed	H332	Harmful if inhaled
H302	Harmful if swallowed	H333	May be harmful if inhaled
H303	May be harmful if swallowed	H334	May cause allergy or asthma symptoms or breathing difficulties if inhaled
H304	May be fatal if swallowed and enters airways	H335	May cause respiratory irritation
H305	May be harmful if swallowed and enters airways	H336	May cause drowsiness or dizziness
H310	Fatal in contact with skin	H340	May cause genetic defects
H311	Toxic in contact with skin	H341	Suspected of causing genetic defects
H312	Harmful in contact with skin	H350	May cause cancer
H313	May be harmful in contact with skin	H351	Suspected of causing cancer
H314	Causes severe skin burns and eye damage	H360	May damage fertility or the unborn child
H315	Causes skin irritation	H361	Suspected of damaging fertility or the unborn child
H316	Causes mild skin irritation	H362	May cause harm to breast- fed children
H317	May cause an allergic skin reaction	H370	Causes damage to organs
H318	Causes serious eye damage	H371	May cause damage to organs
H319	Causes serious eye irritation		
H320	Causes eye irritation		
H330	Fatal if inhaled		
H331	Toxic if inhaled		

Annex

H372	Causes damage to organs through prolonged or repeated exposure	H373	May cause damage to organs through prolonged or repeated exposure
------	--	------	---

Environmental Hazards

H400	Very toxic to aquatic life	H412	Harmful to aquatic life with long lasting effects
H401	Toxic to aquatic life		
H402	Harmful to aquatic life	H413	May cause long lasting harmful effects to aquatic life
H410	Very toxic to aquatic life with long lasting effects		
H411	Toxic to aquatic life with long lasting effects		

General Precaution statements

P101	If medical advice is needed, have product container or label at hand	P102	Keep out of reach of children
		P103	Read label before use

Prevention Precaution statements

P201	Obtain special instructions before use	P220	Keep/Store away from clothing/.../combustible materials
P202	Do not handle until all safety precautions have been read and understood	P221	Take any precaution to avoid mixing with combustibles
P210	Keep away from heat/sparks/open flames/hot surfaces – No smoking	P222	Do not allow contact with air
P211	Do not spray on an open flame or other ignition source	P223	Keep away from any possible contact with water, because of violent reaction and possible flash fire

Annex

P230	Keep wetted with ...	P261	Avoid breathing dust/fume/gas/mist/vapour s/spray
P231	Handle under inert gas		
P232	Protect from moisture	P262	Do not get in eyes, on skin, or on clothing
P233	Keep container tightly closed	P263	Avoid contact during pregnancy/while nursing
P234	Keep only in original container	P264	Wash ... thoroughly after handling
P235	Keep cool		
P240	Ground/bond container and receiving equipment	P270	Do not eat, drink or smoke when using this product
P241	Use explosion-proof electrical/ventilating/light/ .../equipment	P271	Use only outdoors or in a well-ventilated area
P242	Use only non-sparking tools	P272	Contaminated work clothing should not be allowed out of the workplace
P243	Take precautionary measures against static discharge	P273	Avoid release to the Environment
P244	Keep reduction valves free from grease and oil	P280	Wear protective gloves/protective clothing/eye protection/face protection
P250	Do not subject to grinding/shock/.../friction		
P251	Pressurized container – Do not pierce or burn, even after use	P281	Use personal protective equipment as required
P260	Do not breathe dust/fume/gas/mist/vapour s/spray	P282	Wear cold insulating gloves/face shield/eye protection

Annex

P283	Wear fire/flare resistant/retardant clothing	P231+232	Handle under inert gas. Protect from moisture
P284	Wear respiratory protection	P235+410	Keep cool. Protect from sunlight
P285	In case of inadequate ventilation wear respiratory protection		

Response precautionary statements

P301	IF SWALLOWED:	P314	Get Medical advice/attention if you feel unwell
P302	IF ON SKIN:		
P303	IF ON SKIN (or hair):	P315	Get immediate medical advice/attention
P304	IF INHALED:		
P305	IF IN EYES:	P320	Specific treatment is urgent (see ... on this label)
P306	IF ON CLOTHING:		
P307	IF exposed:	P321	Specific treatment (see ... on this label)
P308	IF exposed or concerned:	P322	Specific measures (see ... on this label)
P309	IF exposed or you feel unwell:	P330	Rinse mouth
P310	Immediately call a POISON CENTER or doctor/physician	P331	Do NOT induce vomiting
P311	Call a POISON CENTER or doctor/physician	P332	If skin irritation occurs:
P312	Call a POISON CENTER or doctor/physician if you feel unwell	P333	If skin irritation or a rash occurs:
P313	Get medical advice/attention	P334	Immerse in cool water/wrap in wet bandages
		P335	Brush off loose particles from skin

Annex

P336	Thaw frosted parts with lukewarm water. Do not rub affected areas	P361	Remove/Take off immediately all contaminated clothing
P337	If eye irritation persists:	P362	Take off contaminated clothing and wash before reuse
P338	Remove contact lenses if present and easy to do. continue rinsing	P363	Wash contaminated clothing before reuse
P340	Remove victim to fresh air and keep at rest in a position comfortable for breathing	P370	In case of fire:
P341	If breathing is difficult, remove victim to fresh air and keep at rest in a position comfortable for breathing	P371	In case of major fire and large quantities:
P342	If experiencing respiratory symptoms:	P372	Explosion risk in case of fire
P350	Gently wash with soap and water	P373	DO NOT fight fire when fire reaches explosives
P351	Rinse continuously with water for several minutes	P374	Fight fire with normal precautions from a reasonable distance
P352	Wash with soap and water	P375	Fight fire remotely due to the risk of explosion
P353	Rinse skin with water/shower	P376	Stop leak if safe to do so
P360	Rinse immediately contaminated clothing and skin with plenty of water before removing clothes	P377	Leaking gas fire – do not extinguish unless leak can be stopped safely
		P378	Use ... for extinction
		P380	Evacuate area
		P381	Eliminate all ignition sources if safe to do so

Annex

P390	Absorb spillage to prevent material damage	P304+340	IF INHALED: Remove victim to fresh air and keep at rest in a position comfortable for breathing
P391	Collect spillagee		
P301+310	IF SWALLOWED: Immediately call a POISON CENTER or doctor/physician	P304+341	IF INHALED: If breathing is difficult, remove victim to fresh air and keep at rest in a position comfortable for breathing
P301+312	IF SWALLOWED: Call a POISON CENTER or doctor/physician if you feel unwell		
P301+330+331	IF SWALLOWED: Rinse mouth. Do NOT induce vomiting	P305+351+338	IF IN EYES: Rinse continuously with water for several minutes. Remove contact lenses if present and easy to do – continue rinsing
P302+334	IF ON SKIN: Immerse in cool water/wrap in wet bandages	P306+360	IF ON CLOTHING: Rinse immediately contaminated clothing and skin with plenty of water before removing clothes
P302+350	IF ON SKIN: Gently wash with soap and water		
P302+352	IF ON SKIN: Wash with soap and water		
P303+361+353	IF ON SKIN (or hair): Remove/Take off immediately all contaminated clothing. Rinse skin with water/shower	P307+311	IF exposed: Call a POISON CENTER or doctor/physician
		P308+313	IF exposed or concerned: Get medical advice/attention
P304+312	IF INHALED: Call a POISON CENTER or doctor/physician if you feel unwell	P309+311	IF exposed or you feel unwell: Call a POISON CENTER or doctor/physician
		P332+313	IF skin irritation occurs: Get medical advice/attention

- P333+313 IF skin irritation or a rash occurs: Get medical advice/attention
- P335+334 Brush off loose particles from skin. Immerse in cool water/wrap in wet bandages
- P337+313 Get medical advice/attention
- P342+311 Call a POISON CENTER or doctor/physician
- P370+376 In case of fire: Stop leak if safe to do so
- P370+378 In case of fire: Use ... for extinction
- P370+380 In case of fire: Evacuate area
- P370+380+375 In case of fire: Evacuate area. Fight fire remotely due to the risk of explosion
- P371+380+375 In case of major fire and large quantities: Evacuate area. Fight fire remotely due to the risk of explosion

Storage precaution statements

P401	Store ...	P420	Store away from other materials
P402	Store in a dry place		
P403	Store in a well ventilated place	P422	Store contents under ...
P404	Store in a closed container	P402+404	Store in a dry place. Store in a closed container
P405	Store locked up	P403+233	Store in a well-ventilated place. Keep container tightly closed
P406	Store in a corrosive resistant/... container with a resistant inner liner	P403+235	Store in a well-ventilated place. Keep cool
P407	Maintain air gap between stacks/pallets	P410+403	Protect from sunlight. Store in a well ventilated place
P410	Protect from sunlight	P410+412	Protect from sunlight. Do not expose to temperatures exceeding 50 °C/122 °F
P411	Store at temperatures not exceeding ... °C/... °F		
P412	Do not expose to temperatures exceeding 50 °C/122 °F	P411+235	Store at temperatures not exceeding ... °C/... °F. Keep cool

Disposal Precaution Statement

P501 Dispose of contents/container to ...

9.4 List of Chemicals classified as CMR Substances

Table 31. List of Chemicals classified as CMR substances

Cas-Number	Chemical	Amount used	CMR Category
79-06-1	Acrylamide	30 % aqueous solution for polymerization	C:1B M:1B R2
56-65-5	$\gamma^{32}\text{P}$ -ATP	Radiolabeling of oligonucleotides	
1239-45-8	Ethidiumbromide	10mg/mL aqueous solution as intercalation dye for nucleic acid molecules	M:2

9.5 List of Instrumentation

Table 32. List of instruments used during this work

Instrument	Name	Manufacturer
Autoclave	amsco® Eagle® SG-2021 Scientific Gravity Sterilizer	Steris (Mentor Ohio, USA)
Benchtop Centrifuge with Cooling Unit	Centrifuge 5804 R	Eppendorf (Westbury, NY, USA)
Centrifuge rad room	Sorvall Legend Micro 21	Thermo Scientific (Waltham, MA, USA)
Centrifuge	Benchtop Centrifuge 5415 D	Eppendorf (Westbury, NY, USA)
Centrifuge floor-model	Sorvall TRC 6+ Centrifuge	Thermo Scientific (Waltham, MA, USA)
CD Spectrometer	CD Spectrometer Jasco 810	Jasco (Easton, MD, USA)
Drum Roller	Bellco Roller Drum	Bellco Glass Inc. (Vineland NJ, USA)

Annex

Instrument	Name	Manufacturer
Freezers	Fridgidaire	Fridgidaire (Charlotte, NC, USA)
Fridges	Fridge-Line® Frigid Cab TM	Lab Line Instruments, Inc. (Dubuque, IA, USA)
Liquid Scintillation Analyzer	TRI-CARB 2500 TR	Packard (Conroe, TX, USA)
Microfiltration device	Bio-Dot® SF Microfiltration Apparatus	BioRad (Hercules, CA, USA)
NanoDrop	NanoDrop® Spectrophotometer ND-1000	Thermo Scientific (Waltham, MA, USA)
Orbital Shaker	MaxQ 2000	Thermo Scientific (Waltham, MA, USA)
Orbital Shaker	Orbital Shaker	Bellco Biotechnology (Vineland NJ, USA)
PCR Hood	PCR Enclosure	Labcono (Kansas City, MO USA)
pH Electrode	accumet accuTupH®	Fisher Scientific (Suwanee GA, USA)
pH meter handheld	ExStik® waterproof pH Meter	Extech Instruments (Nashua, NH, USA)
pH Meter	accumet XL 500 Dual Chennel pH/mv/Ion/Conductivity	Fisher Scientific (Suwanee GA, USA)
PhosphorImager	Typhoon Fla 9000	GE Healthcare (Chicago, IL, USA)
Qubit	Qubit	Thermo Scientific (Waltham, MA, USA)
Quick Spin Centrifuge	My Fuge	Benchmark (Sayreville, NJ, USA)

Annex

Instrument	Name	Manufacturer
Real time instrument	Smart Cycler	Cepheid (Sunnyvale, CA, USA)
Scale	PB503-S/FACT	Mettler Toledo (Columbus, OH, USA)
Screen Easer	Screen Eraser K	BioRad (Hercules, CA, USA)
Shaking heatblock	Thermomixer R	Eppendorf (Westbury, NY, USA)
Shaking Incubator	Forma Orbital Shaker	Thermo Scientific (Waltham, MA, USA)
Thermocycler	PeqStar	peqlab® through VWR (Road Radnor, PA, USA)
Thermomixer	Thermomixer R 1.5 mL	Eppendorf (Westbury, NY, USA)
UV-Crosslinker	Sepctrolinker XL-1500 UV Crosslinker	Spectronics Cooperation (Westbury, NY, USA)
Vortex	Vortex Mixer	Fisher Scientific (Suwanee GA, USA)
Vortex	Vortexer 2 Vortex Genie 2	VWR (Road Radnor, PA, USA)
Vortex Mixer	Digital Vortex Mixer	VWR (Road Radnor, PA, USA)
Water bath	Lauda ecoline 003 E100	Lauda (Deran, NJ, USA)

9.6 Pipetting Schemes for PCR Master Mixes

Table 33. Pipetting Scheme for VP1 amplification (section 6.5.1)

Component	Volume[μ L]/ 50 μ L reaction
Nuclease-free Water	30.35
PCR-Buffer	2.5
MgCl ₂ (50mM)	1.6
dNTPs (10mM each nucleotide)	1.5
Forward Primer(10 mM)	1.5
Reversed Primer (10 mM)	1.5
Taq Polymerase (5U/ μ L)	0.3
Template	10.75

Table 34. Pipetting Scheme for P-Domain amplification (section 6.5.2)

Component	Volume[μ L]/ 50 μ L reaction
Nuclease-free Water	37.5
PCR-Buffer	5
MgCl ₂ (50mM)	1
dNTPs (10mM each nucleotide)	1.5
Forward Primer(10 mM)	1.5
Reversed Primer (10 mM)	1.5
Taq Polymerase (5U/ μ L)	0.5
Template	1.5

Table 35. Pipetting Scheme for amplification of SELEX nucleic acid library (section 6.5.3)

Component	Volume[μ L]/ 50 μ L reaction reaction
Nuclease free Water	21.1
PCR-Buffer	5
MgCl ₂ (50mM)	1.5
dNTPs (10mM each nucleotide)	1

Annex

Component	Volume[μ L]/ 50 μ L reaction reaction
Forward Primer(10 mM)	3
Reversed Primer (10 mM)	3
Q-Solution	10
Taq Polymerase (5U/ μ L)	0.4
Template	5

Table 36. Pipetting Scheme for RT-qPCR multiplex assay for the detection of NoV GI and GII (section 6.5.4)

Component	Volume[μ L]/25 μ L reaction
Nuclease free Water	5.8
PCR-Buffer	5
MgCl ₂ (50mM)	2
dNTPs (10mM each nucleotide)	0.75
GI cog Forward Primer(10 mM)	0.75
GI cog Reversed Primer (10 mM)	0.75
GII cog Forward Primer(10 mM)	0.75
GII cog Reversed Primer (10 mM)	0.75
IAC Forward Primer(10 mM)	0.187
IAC Reverse Primer(10 mM)	0.187
GI probe I (10mM)	0.25
GI probe I (10mM)	0.25
GII probe (10mM)	0.25
IAC probe (10mM)	0.375
Taq Polymerase (5U/ μ L)	1.25
Internal control template	0.2
Template	3

Table 37. Pipetting Scheme for Colony PCR (section 6.5.5)

Component	Volume[μ L]/ 50 μ L reaction
Nuclease free Water	40
PCR-Buffer	5
MgCl ₂ (50mM)	1
dNTPs (10mM each nucleotide)	1
Forward Primer(10 mM)	1
Reversed Primer (10 mM)	1
Taq Polymerase (5U/ μ L)	1
Template	Colony

9.7 Pipetting Schemes for 10 % SDS PAGE Gel

Table 38. Pipetting Scheme to obtain 10 mL of stacking gel, for a 10 %SDS PAGE gel

Component	Volume[mL]
dl Water	5.95
0.5 M Tri-HCl solution, pH 6.8	2.5
10 % SDS solution	0.1
30 % Acrylamide/Bis Solution	1.35
10 % Ammonuimpersulfat (APS)	0.1
TEMED	0.01

Table 39. Pipetting Scheme to obtain 20 mL of separating gel, for a 10 %SDS PAGE gel

Component	Volume[mL]
dl Water	7.6
1.5 M Tri-HCl solution, pH 8.8	5.2
10 % SDS solution	0.2
30 % Acrylamide/Bis Solution	6.8
10 %Ammonium persulfate (APS)	0.1
TEMED	0.01

9.8 Full Sequences of P-Domain, and VP1 Gene

9.8.1 Sequence P-Domain (5'-3')

CACCATGAAACCATTCACCGTCCCAATCTTAACTGTTGAAGAAATGACCAATTCAAGATTCGCCATTCCTTTGGAAAAAT
 TGTTACGGGTCCCAGCAGTGCCTTTGTTGTTCAACCACAAAATGGCAGATGCACGACTGATGGCGTGCCTTAGGCACC
 ACCAACTGTCTCCTGTCAACATCTGCACCTTCAGAGGGGATGTCACCCACATTGCCGGTTCTCGTAATTACACAATGAA
 TTTGGCCTCTCTAAATGGAAACAATTACGACCCAACAGAAGAAATCCCAGCCCTCTGGGAATCCAGATTTCTGGGAA
 AGATCCAAGGTGTGCTCACTCAAACCACAAAGGGAGATGGCTCGACCCGGGGCCATAAAGCTACAGTTTACTGAGGAGT
 GCCGACTTTACTCCAAAGATGGGCAGTGTTCATTTGCTACTGATACAGAAAATGATTTGAAACTCACCAAAACACAAA
 ATTCACCCAGTCGGTGTCAATTCAGGATGGTAGCACCACCACCGAAATGAACCCCAACAATGGGTGCTCCCAAGTTATT
 CAGGGTAGAAAATGTTCATAATGTACACCTAGCCCTGCTGTAGCCCCCAATTTCCGGGTGAACAACCTCTTTTCTTCAG
 GTCTACTATGCCGGATGCAGCGGGTATCCCAACATGGATTTGGATTGCCTACTCCCCAGGAGTGGGTACAGCACTTCT
 ATCAAGAGGCAGTCCAGCACAATCTGATGTGGCTCTATTGAGATTTGTAATCCAGACACGGGTAGGGTCTTGTGTTGAG
 TGCAAACTTCATAAATCAGGCTATGTCACAGTGGCTCACACCGGCCAACATGATTTGGTCATCCCCCAATGGTTATTT
 TAGGTTTGATTCTGGGTTAATCAATCTACACACTTGCCCCATGGGAAATGGAGCGGGGCGTAGACGTGCATTATAA

9.8.2 Sequence of the VLP gene (5'-3')

ATGGAGTCCGCAGCCAACCTCGTCCAGAGGTCAACAATGAGGTTATGGCTTTGGAGCCCGTTGTCCGGTCCCGCTATTGC
 GCGCCTGTAGCGGGCCAAACAAAATGTAATTGACCCCTGGATTAGAGATAAATTTGTACAAGCCCTGGTGGAGAGTTCA
 CAGTATCCCCTAGAAACGCTCCAGGTGAAATACTATGGAGCGCGCCCTTAGGCCCTGATTTGAATCCCCTACCTATCTCAT
 TTGGCCAGAATGTATAATGGTTATGCAGGCGGTTTTGAAGTGCAGGTGATCCTCGCGGAGAACGCGTTCACCGCCGGAAA
 AATTATATTTGCAGCAGTCCCACCAATTTTCCAACCTGAAGGCTTGAGTCCAGCCAGGTCACATGTTCCCCACATAA
 TAGTAGATGTTAGGCAATTTGGAACCTGTGTTGATCCCCCTACCTGATGTTAGGAATAACTTCTATCACTATAATCAGTCA
 AATGATTTCTACCATTAATTTGATAGCAATGCTGTACACACCACCTTAGGGCCAATAATGCCGGGATGATGTCTTACAGT
 CTCTTGTGAGTCTTACGAGGCCATCCCCTGATTTTGACTTCAATTTATGGTGCCACCCACAGTTGAGTCAAGAACTA
 AGCCATTTACTGTCCCAATCTTGACTGTTGAAGAAATGACCAATTCAAGATTCGCCATTCCTTTGGAAAAATGTTTCAG
 GGTCCCAGCAGTGCCTTTGTTGTTCAACCACAAAATGGCAGATGCACGACTGATGGCGTGCCTTAGGCACCACCCAACT
 GTCTCCTGTCAACATCTGCACCTTCAGAGGGGATGTCACCCACATTCGCGGTTCTCGTAATTACACAATGAATTTGGCCT
 CTCTAAATTTGGAACAATTACGACCCAACAGAAGAAATCCCAGCCCTCTGGGAATCCAGATTTCTGGGAAAGATCCAA
 GGTGTGCTCACTCAAACCACAAAGGAGATGGCTCGACCCGGGGCCATAAAGCTACAGTTTACTGAGGAGTGGGACTT
 TACTCCAAAGATGGGCAGTGTTCATTTGCTACTGATACAGAAAATGATTTTGAACCTCACCAAAACACAAAATTCACCC
 CAGTCGGTGTCAATCCAGGATGGTAGCACCACCACCGAAATGAACCCCAACAATGGGTGCTCCCAAGTTATTCAGGTAGA
 AATGTTCATAATGTACACCTAGCCCTGCTGTAGCCCCAATTTCCGGGTGAACAACCTCTTTTCTTCAGGTCTACTAT
 GCCCGGATGCAGCGGGTATCCCAACATGGATTTGGATTGCCTACTCCCCAGGAGTGGGTACAGCACTTCTATCAAGAGG
 CAGTCCAGCACAATCTGATGTGGCTCTATTGAGATTTGTAATCCAGACACGGGTAGGGTCTTGTGTTGAGTCAAACCTT
 CATAAATCAGGCTATGTCACAGTGGCTCACACCGGCCAACATGATTTGGTCATCCCCCAATGGTTATTTAGGTTTGA
 TTCTGGGTTAATCAAT

9.9 List of Sequences Identified in the Last SELEX-rounds of the five parallel SELEX-experiments

Table 40. List of sequences obtained from 50 clones, after cloning of the last SELEX-round of the buffer-SELEX-experiment

Oligonucleotide Name	Sequence 5'-3'	Number of sequence replication is final nucleic acid pool
Buf-1	GGGTTAGAACTAGGCTGTTAACCATGCCCCGACCGACGTA	25
Buf-2	GAAATTGGGTTTCGGGTTTGGGTTGGGATTACTTAGCGATG	6
Buf-3	TTTGGTTTGGTTGGTCTGGTATC	5
Buf-4	GGTGGGTGGGGGTTTGG	7
Buf-5	CATTTTTTAGGTTGGGTAGGTTGGTAAAAATTTGTCTCCT	1
Buf-6	CTGGGTTGGGGCTTATTTAATTTCTACTTTGGGGCGGGG	1
Buf-7	AAGGGCGAATTCGCCCT	1
Buf-8	GAGGGTCGCATCTTTGGTTTGGTTGGTCTGGTATG	1

Table 41. List of sequences obtained from 50 clones, after cloning of the last SELEX-round of the lettuce-SELEX-experiment

Oligonucleotide Name	Sequence 5'-3'	Number of sequence replication is final nucleic acid pool
Buf-1	GGGTTAGAACTAGGCTGTTAACCATGCCCCGACCGACGTA	15
Buf-4	GGTGGGTGGGGGTTTGG	1
Let-1	GGACCAACTGATAAATGTTGGCCCCGTCTGAAGGCTAC	8
Let-2	AACGTATAACGCATTGACGTTCTCTTGAAGCTCAGATCGG	7
Let-3	ATAGTCGCTTGACGAGCTTTTTGCCACGCATGCTTGGGTC	3
Let-4	CAACGGATTCTAAAATTGTAGTCCCTCCCCGTCTGAGGGTAGA	4
Let-5	GTCCGGTATCGTGGTGGCTTAGACCAAGCAGTAATGTCTCGA	1
Let-6	CGGGGTGGGGTCTTTTACTGTGCTGCTAATTGGGTGGGGGA	1

Annex

Table 42. List of sequences obtained from 50 clones, after cloning of the last SELEX-round of the strawberry-SELEX-experiment

Oligonucleotide Name	Sequence 5'-3'	Number of sequence replication in final nucleic acid pool
Straw-1	ACTTGAGGTAAAAAGCGTTTGGGTGCGTGGCGGGGTTTG	1
Straw-2	CATAACCTTCCTTCCATCCCTCCTCCCCACTTCCGCTGTC	2
Straw-3	CCCTTCTCTGTCCCCCTTCCTTCGACCCTGTTTAACCGCA	1
Straw-4	GGCGTGGTATTTTGTGTGTTTTCTGTGTAGTGTGTAAAT	2
Straw-5	CAACACACTTCCATTCCCGTTCGCCCTTCCCCTTTCATC	1
Straw-6	CACCCTGCACTCGTCCGCCCTCCCCTCGTCCCCTTGTCCC	1
Straw-7	CAGCCCTTCCCCCTTCGCCTCCCTCCTCCCACACCCCGACC	1
Straw-8	CATGGGGGGGGTCTTTCGTCTAGGTATCTCGGGGTGGGG	1
Straw-9	CCAACTTCCCCCGCTCCTCCCATCTTATTCTGTGCGTTC	1
Straw-10	CCAACTTCCATCTCCTGCCAGCCCTTTCCTTCCCCATC	1
Straw-11	CCACCGCCCTTTTGTCCCATCACACCAACCCCTCCCTTC	1
Straw-12	CCACCTTCCCCCACCATTTCCTGCATCCCCCTCCCCATC	2
Straw-13	CCAGTCATCCCGCCTCCTTCCCCCTACACCTCTACCGAC	1
Straw-14	CCCCCCCACCATCCTCCCCAACCTTCGCTCCCAGTCCATC	1
Straw-15	CCCCCCCATCCTGCACCGTTGCCTTCTACCTTCCCCCGCC	1
Straw-16	CCCCCCCCTTTCGTCCACAGCCCTTTTCCTCACCTCATC	1
Straw-17	CCCCCCGTACACACTCCCCCTCCATAATACGTTCCCCCCC	1
Straw-18	CCCCCGCCCTGTTTCCCCTCTTGCGGTTATTTCCCCATC	1
Straw-19	CCCCGTTACCTTGGCTCCTCCGTTTCCCCTCCCGAATCA	1
Straw-20	CCGCTACTTCTTCCCGCCTTCCCCACAGCTGCACCCCCCCC	1
Straw-21	CCTCCACTCGCCCTCCACCCAGCTCCTCTTCTCCCCATC	1
Straw-22	CGGGTGGGGTATTTTTACCGTATATCATATTGGGTGGGG	1

Annex

Oligonucleotide Name	Sequence 5'-3'	Number of sequence replication in final nucleic acid pool
Oy-4	CAACTGTTATCTCCGCCTCCCCCTACTCCTCTTTCCATC	1
Oy-5	CAACTTTCCTTTCCCGCTTCACATTTTCCCCTCCCCATC	1
Oy-6	CACCACAGTTCCTACCCCCCTCCCTTTTCTACCCCATC	1
Oy-7	CACCTTCCCCCGGTCTATCCTTCCCTCTCTCCCTCCATC	1
Oy-8	CACTAGTCTCGCCTTCCCCTTTCCCCCTTCTCCCCATC	1
Oy-9	CACTTTTCCCCCGTCTCTACTTCCCTCATTCCCCATC	1
Oy-10	CACTTTTGCTTCTTTACATTATTTCTCACAGTTTCCATC	1
Oy-11	CAGTTCGCTTTTTTCTTGTTTTATCCTTACCTCTCCAT	1
Oy-12	CATTCTTCTCCCGTCTTCCCCACTTACCCTTTTCCATC	1
Oy-13	CCACCTTCTCTCCTACTTAGTCCCACCCCTCCTCCCATC	1
Oy-14	CCAGCCTGTTTCCACCACCTCCTAACCCGTTCCTCCCATC	1
Oy-15	CCAGTCTTAACCACACACCCCGCCTATTACTTCTTCCATC	1
Oy-16	CCATCTTGCTTTTCCCCGTCCACCCTCCTTCTCCCATC	1
Oy-17	CCCCTTCTCTCCCACTGTA AACACCACCCCTCCCATC	1
Oy-18	CCCCTTTCACAGTCCACCTTCTCGCCCCCACTTCCCATC	1
Oy-19	CCCGGCTGTTTTTCCCCCCCCCTCCTTCTTCCCTCCATC	1
Oy-20	CCCTTCCGTTCAACTTCTGTATATTTCCACCCCCCATC	1
Oy-21	CCCTTCTCCCTACTCCCTCCTCCCCGTCTCTCACTCCATC	1
Oy-22	CCCTTTCCCTTTTTCGTTCCCCCTTCCCTCACCTACATC	1
Oy-23	CCCTTTTCTCCCCCTTCCCCTCCTCTTCCCTCACCCATC	1
Oy-24	CCGAATACCCCGCCGCTAACATTA ACTCAATACCCCATC	1
Oy-25	CCGCCTTGGTCGTTCTTCCACTTCCCCTCCTTCCCCATC	1
Oy-26	CCGCTACGTCTTATTCCACCTACTCCCGACCCCTCCATC	1
Oy-27	CCTTCTCCACTAGTTATTCCCCCGTTTCCCTCCCCCNCT	1

Annex

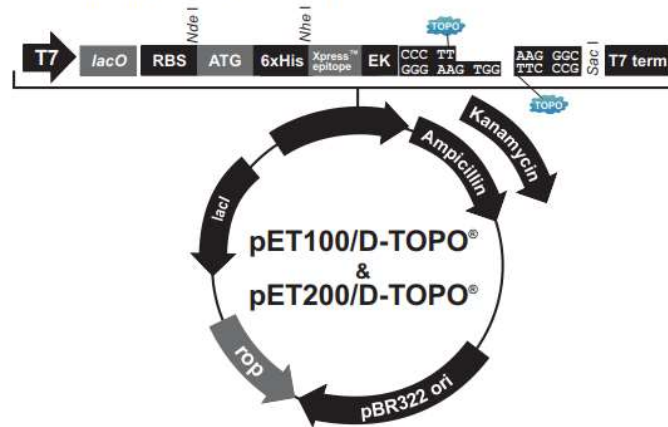
Oligonucleotide Name	Sequence 5'-3'	Number of sequence replication in final nucleic acid pool
Oydiv-2	ACACGCTTCTTCCCCGCCCCCCTTTCAACCTTCCCATC	1
Oydiv-3	CAACTGTTATCTCCGCCTCCCCCTACTCCTCTTTTCCATC	1
Oydiv-4	CAGTCCTTTCTCGCTTCCGTACTCCCCCGCCCCCCCATC	1
Oyster Div. 5	CATCCTCCTTTTTCTCCTCCCTTACCCGCACCTTCTCCAT	1
Oyster Div. 6	CATTCTTCTCCACTCCCCGCCCTTCTCACTTTCCCCATC	1
Oyster Div. 7	CCCATCTCCGCGTTCTCCTGTCTCACTTCCCCCTCCATC	1
Oyster Div. 8	CCCCCCACATCTCCCCACCTTACCTCAACTATTTCCATC	1
Oyster Div. 9	CCCCCCCCATGTCGCAGTAACTTCCCCCGCTTCCCCATC	1
Oydiv-10	CCCCCCCCCATCTCATATCCAGTTCCCCCACCTTCCCCATC	1
Oydiv-11	CCCCCCCCCGTTTCGCTCTCCATTCTCTACCCTTCCATC	1
Oydiv-12	CCCCGACCCAGACATGATGAAATAAAAAACCCCCACCCCG	1
Oydiv-13	CCCCTTCTCCCTCCTGCTGTCTCCGTCCCCACTTTCCATC	2
Oydiv-14	CCCGCTCTGTACGTTTCTTTATCCCTCCCTCCCCATC	2
Oydiv-15	CCCTGTCTCCTTCCCTCCGTCCTCACCCCTCCGCACATC	1
Oydiv-16	CCCTTTTCTCCCCCTTCCCCCTCCTTCTCCTTACCCCCATC	1
Oydiv-17	CCTTCTCCTTCCCCCTGTGTCCCCACCTTTTACCATC	1
Oydiv-18	CGTCTCTGAGTTCCCCCTCCCCGCTCTCCTTTCCCCATC	1
Oydiv-19	CTACTTCCCCTAGCTTTTGTACTCCCCTTTCCTCCCATC	1
Oydiv-20	CTAGTTCTCCATCCGCTTCTACTTCTCCCCCTCCCATC	1
Oydiv-21	CTGTTCTTCTTCCGCTCTTTGTCCCTGTCTCCTCCCCATC	1
Oydiv-22	CTTCTCACCTGTTCTCACCCCTCGCCCCCTTCCCATC	1
Oydiv-23	GATGAAAAGGAAAGGAGAAGGGGGGAACGAAGAACTG	1
Oydiv-24	GATGGGGGAAGGGGAGTAGAAAACGAAGGAAATAAAGACA	1

Annex

Oligonucleotide Name	Sequence 5'-3'	Number of sequence replication in final nucleic acid pool
Oydiv-25	TAATCTCCCTATCCCCACTTCCCCTCGTCCCTACCCATC	1
Oydiv-26	TCCACTCTTCTTCCCTCCCCCATTTCCCTTTCTCTCCATC	1
Oydiv-27	TCCCATTCTTCCACCTAGTTCCCTCCACTCCCCCATC	2
Oydiv-28	TCTCCCGTCCTTTCCCCCGTCCACCTTCCCCTCCCCATC	1
Oydiv-29	TGGTTTTTCCTTCTCTCGTATCTTCCTTTTCCCTCCCATC	1
Oydiv-30	TGTCTTGTCTCTTCCCTTCCCTTCCCTCTCACCCCATC	1
Oydiv-31	TGTTTTCCCCCATCTATCCTCCCGTGTTCCTCCATC	1
Oydiv-32	TGTTTTTCTCCTTCTTCCCCCATCCTTCCCTCTCCCCATC	1
Oydiv-33	TTCCACTTTTCCCTTCTAATGTCCACTTTCCACCTCCCATC	1
Oydiv-34	TTCCATCCTTTTCCGTCTCTTCCCGCCCACTTCTCCCATC	1
Oydiv-35	TTCTATCCCCGTTTCCCTCCCGCTGCATTTCTTTCCATC	1
Oydiv-36	TTTCTTCGCTCTGTCCAACCTTTCTACTGTTTCCCATC	1
Oydiv-37	TTTCTGTCCATTTTCCAGCTCTCCCCTCTCTTCTTCCATC	1
Oydiv-38	TTTTCACTTCTCTCCACCACCCCTTTCCCTCCCCCATC	1
Oydiv-39	TTTTCTTACTTCCGTGCTTATCTTATTCTTCTTCCCATC	1
Oydiv-40	TTTTTCTATCCACATCCCTGTCCCCTTTCTCCCCCATC	1
Oydiv-41	TTTTTCTATCCACATCCCTGTCCCCTTTCTCCCCCATC	1

9.10 Plasmid Map of Vector pET 100/D-TOPO

The figure below shows the features of the pET100/D-TOPO[®] (5764 bp) and pET200/D-TOPO[®] (5741 bp) vectors. The complete sequence of each vector is available for downloading from our Web site (www.invitrogen.com) or by contacting Technical Service (see page 56).



	<u>pET100/D-TOPO[®]</u>	<u>pET200/D-TOPO[®]</u>
T7 promoter	209-225	209-225
T7 promoter/priming site	209-228	209-228
<i>lac</i> operator (<i>lacO</i>)	228-252	228-252
Ribosome binding site (RBS)	282-288	282-288
Initiation ATG	297-299	297-299
Polyhistidine (6xHis) region	309-326	309-326
Xpress [™] epitope	366-389	366-389
EK recognition site	375-389	375-389
TOPO [®] Cloning site (directional)	396-409	396-409
T7 reverse priming site	466-485	466-485
T7 transcription termination region	427-555	427-555
<i>bla</i> promoter	856-954	856-954
Ampicillin (<i>bla</i>) resistance gene	955-1815	---
Kanamycin resistance gene	---	955-1749
pBR322 origin	2022-2757	1969-2610
<i>ROP</i> ORF (complementary strand)	3001-3192	2978-3169
<i>lacI</i> ORF (complementary strand)	4507-5595	4481-5572

Figure 40. Figure shows the map of the expression plasmid used in this work:pET 100/D-TOPO

10 Curriculum Vitae

Entfällt aus datenschutzrechtlichen Gründen.

Curriculum Vitae

11 Acknowledgements

I would like to express my appreciation to my professor **Ulrich Hahn** for agreeing to supervise my work overseas and for trusting me with my scientific efforts. I am particularly grateful for his thorough and patient review of my thesis document.

I would also like to thank Prof. Hahn's working group, especially **Dr. Katharina Redder** for welcoming me during visits in Germany and for the steady scientific exchange through Skype and email.

I wish to thank the entire staff of the US FDA GCS laboratory for the very friendly and supportive work environment. I very much appreciate to have been given the opportunity to work with such devoted and humble scientists and supportive staff. Thank you, **Dr. William Burkhardt III** and **Dr. Jessica Jones**, for being strong managers and for supporting me and my research throughout my thesis. Thank you, **Kevin Calci** and **George Doup** for making working in the laboratory a fun time. Thank you, my 'workbench-neighbor' **Dr. Kristin Butler**, for the continuous scientific exchange during my studies, your kind advice, and steady encouragement through my time at the FDA.

I am especially grateful for **Kathy ElSaid's** support in completing my work involving radioactive material. It would have not been possible without you.

Thank you, **Rachel Rodriguez**, for being a wonderful 'virus-colleague' and for being a caring friend.

My greatest thanks, however, goes to **Dr. Jackie Woods**, my adviser. She led me through my research with trust, encouragement, and her kind, positive spirit. I am grateful to have experienced the scientific world, especially virus research through your eyes.

Thank you, **Clara, Olga** and especially **Hermey** for the most pleasant student time and your lasting friendship and support.

The completion of this thesis would not have been possible without the patient support of **my loving family** and my fiancé **Christopher Loeffler**. I hereby extend my genuine thanks and gratitude to them.

Eidesstaatliche Erklärung

12 Eidesstaatliche Erklärung

Hiermit versichere ich an Eides statt, die vorliegende Dissertation selbst verfasst und keine anderen als die angegebenen Hilfsmittel benutzt zu haben. Die eingereichte schriftliche Fassung entspricht der auf dem elektronischen Speichermedium. Ich versichere, dass diese Dissertation nicht in einem früheren Promotionsverfahren eingereicht wurde.

Datum:

Unterschrift:

